UNIVERSITY OF SOUTHAMPTON

FACULTY OF ENGINEERING AND THE ENVIRONMENT

School of Civil Engineering and the Environment

MOISTURE RETENTION AND NEAR SATURATED FLOW IN MECHANICALLY BIOLOGICALLY TREATED (MBT) WASTE

by
Kiriaki Zardava

Thesis for the degree of Doctor of Philosophy
December 2012

UNIVERSITY OF SOUTHAMPTON
ABSTRACT
FACULTY OF ENGINEERING AND THE ENVIRONMENT
SCHOOL OF CIVIL ENGINEERING AND THE ENVIRONMENT
Doctor of Philosophy

MOISTURE RETENTION AND NEAR SATURATED FLOW INMECHANICALLY BIOLOGICALLY TREATED (MBT) WASTE

by Kiriaki Zardava

The aim of this research is to understand the interactions between liquid and gas flow at high degrees of saturation, as this could have a significant effect on the effectiveness of landfill remediation by flushing. Particular attention is paid to two key parametric functions that are believed to control the simultaneous flow of leachate and gas in waste materials. These are the relationship between capillary pressure or suction and the degree of leachate saturation or volumetric moisture content, known as the moisture retention characteristic; and the relationship between unsaturated hydraulic conductivity and moisture content.

The thesis starts with a review of previous work on moisture retention characteristic curves and relative permeability functions for waste materials. New data from a drainage column experiment, pressure plate apparatus and hanging water column tests on mechanically and biologically treated (MBT) waste specimens are then presented and compared. The results from the drainage experiments have been interpreted using the unsaturated flow model HYDRUS-1D (Šimůnek et al., 2005) and the University of Southampton Landfill Degradation and Transport model LDAT (White *et. al* 2004). These results give support to the modelling concepts and the integrity of the code for both models and highlight the capabilities of single and dual porosity models.

Use of the van Genuchten (1980) type curves to represent the moisture retention characteristics was found to be fruitful. The values of the parameters that control the shapes of these curves, and therefore the shape of the relationships between capillary pressure and moisture content and unsaturated hydraulic conductivity and moisture content, are reviewed using both results from the literature and results from the experimental work described in the thesis. The sensitivity of the shapes to the values of the parameters is examined as is the sensitivity of the results of numerical modelling that is based on the parameter values. The relationship of the parameter values to the material dry density is also explored. Whilst the flow in the

gas phase is not central to the subject of the thesis, it has been possible to make observations on the relationship between unsaturated gas permeability and moisture content.

The thesis draws attention to the fact that different experimental techniques can lead to significantly different estimates of the moisture retention characteristics. Hanging column tests show an apparently sensible variation of moisture retention curve with density and are self-consistent. However a partial or full interruption of the liquid phase within the specimen, or between the specimen and the hanging column porous plate will inhibit the drainage of liquid from the specimen, resulting in an increase in the retained moisture content at a given applied external suction. This has significant implications for the study of liquid movement in unsaturated wastes. A key recommendation from the work is that the moisture retention characteristic curve for a waste is perhaps better determined from direct measurements of suction and moisture content, as in the drainage column apparatus for the suction range 0-10 kPa. For higher suctions carefully set up pressure plate tests are advisable.

List of Contents

List of Figures

List of Tables

Academic Thesis: Declaration of Authorship

I,Kiriaki Zardava

declare that this thesis and the work presented in it are my own and has been generated by me as the result of my own original research.

'*Moisture retention and near saturated flow in mechanically biologically treated (MBT) waste*'

I confirm that:

1. This work was done wholly or mainly while in candidature for a research degree at this University;

2. Where any part of this thesis has previously been submitted for a degree or any other qualification at this University or any other institution, this has been clearly stated;

3. Where I have consulted the published work of others, this is always clearly attributed;

4. Where I have quoted from the work of others, the source is always given. With the exception of such quotations, this thesis is entirely my own work;

5. I have acknowledged all main sources of help;

6. Where the thesis is based on work done by myself jointly with others, I have made clear exactly what was done by others and what I have contributed myself;

7. Either none of this work has been published before submission, or parts of this work have been published as: [please list references below]:

Signed: ……Date: ……..

1. Zardava, K., Powrie, W. and White, J. (2012). Moisture retention characteristics of municipal solid wastes. Journal of Geotechnical and Geoenvironmental Engineering, American Society of Civil Engineers (in preparation).

2. Zardava, K., Powrie, W. and White, J. (2011). Laboratory experiments for measuring the moisture retention characteristics of MBT waste. Fourth International Workshop “Hydro-Physico-Mechanics of Landfills”, Santander, Spain; 27-28 April 2011.

3. Nayagum,D., White, J., Zardava, K. and Holmes, D. (2011).Investigating dynamic effects of capillary pressure-saturation relationships on unsaturated flow in waste materials. Fourth International Workshop “Hydro-Physico-Mechanics of Landfills”, Santander, Spain; 27-28 April 2011.

4. Beaven, R., Powrie, W. and Zardava, K. (2011). Hydraulic properties of MSW. Chapter 1 in Geotechnical characterization, field measurement and laboratory testing of municipal solid waste (ed D Zekkos). American Society of Civil Engineers Special Technical Publication no 209.

5. Nayagum,D., White, J., Zardava, K. and Beaven, R. (2010) The use of a numerical model to extrapolate laboratory scale results on waste to full scale landfill remediation applications. Global Waste Management Symposium, San Antonio, Texas, USA, October 3-6, 2010.

6. Zardava, K., Powrie, W. and White, J. (2009). The determination of the moisture retention characteristics of waste materials using vertical drainage experiments. Proceedings Sardinia 2009, 12th International Waste Management and Landfill Symposium, S.Margherita, Cagliari, Italy. 5-10 October 2009.

7. Zardava, K., Powrie, W. and White, J. (2009). The determination of the moisture retention characteristics of waste materials using vertical drainage experiments. Third International Workshop “Hydro-Physico-Mechanics of Landfills”, Braunschweig, Germany; 10 - 13 March 2009.

8. Nayagum,D., White, J., Rees-White, T., Holmes, D. and Zardava, K. (2009). Numerical modelling of air and leachate through waste material under vertical drainage and forced-air flow. Third International Workshop “Hydro-Physico-Mechanics of Landfills”, Braunschweig, Germany; 10 - 13 March 2009.

9. Beaven, Richard P., Powrie, William and Zardava, Kiriaki (2008) Hydraulic properties of MSW. 2008 International Symposium on Waste Mechanics, New Orleans, US, Reston, US, American Society of Civil Engineers.

Acknowledgements

I would like to express my deepest appreciation and thanks to all those who have helped me in preparing my PhD thesis.

Especially, I am grateful to my supervisors Prof. William Powrie and Prof. Jim White for their continued encouragement and guidance throughout my research work, which has been improved considerably as a result of their critical comments.

I would like to thank Dr. Ramen Nayagum for his contribution to this research by running the LDAT model for the experimental data. A special thanks to Mr. Harvey Skinner and Mr. Karl Scammel, the technicians, for their assistance in the lab. I am very grateful to my colleague David Holmes for his assistance in the set-up of the experiments and carrying heavy buckets of MBT waste into the laboratory. I will never forget the long hours we spent in the lab struggling to overcome technical problems. I would also like to thank everyone in the Waste Research Management Group for making me feel a member of the team and exchanging knowledge and experiences

The opportunity to undertake this research at the University of Southampton was possible through the funding of EPSRC.

Last but not least I would like to thank my family, my friends and Alex for their patience and emotional support during my student life.

Abbreviations

BES	2-bromoethanesulfonate
EC	Electrical Conductivity
LDAT	Landfill Degradation and Transport Model
MBT	Mechanical-Biological treatment
MRC	Moisture Retention Curve
MSE	Mean Square Error
MSW	Municipal Solid Waste
PSD	Particle Size Distribution
SLAM	Science and strategies for the Long-term management and remediation of landfills
SW1	Sample of fresh shredded domestic waste
SWCC	Soil-Water Characteristic Curve
SWRC	Soil-Water Retention Curve
TDR	Time Domain Reflectometry

Notations

This notation list contains the most used terms. Other terms which are used within this thesis are defined as they occur, within the section to which they are specifically applicable.

A	Cross-sectional area to flow (m^2)
A^G	Total flow area of the gas phase (m^2)
A^L	Total flow area of the liquid phase (m^2)
a,b	McKee and Bumb model fitting parameters
b	Shape factor depending on the geometry of the material
B	Clapp and Hornberger model parameters
Bo	Bond number
C_w	Slope of the SWCC
D	Medium-liquid diffusivity
d_1, d_2, d_3	Thickness of layers in Eq. 6.3
dT	Throat diameter in Eq. 4.1
e	Void ratio
g	Acceleration due to gravity (m/sec2)
G_s	Specific gravity
h	Hydraulic head
H	Distance between the centre of the specimen and the water level in the burette (hanging column technique)
K	Intrinsic permeability (m^2)
k(θ)	Unsaturated hydraulic conductivity
$k_{r,G}$	Relative permeability of the gas phase (m/sec)
$k_{r,L}$	Relative permeability of the liquid phase (m/sec)
k_s	Saturated hydraulic conductivity (m/sec)
k_α	Effective hydraulic conductivity at the interface between the two domains in dual-porosity system
k_{sm}, k_{sf}	Saturated hydraulic conductivity in matrix and fracture domain
l	Length over which the pressure drop is taking place in Eq. 2.6; length of the flow path in Eq. 2.16; van Genuchten-Mualem parameter for tortuosity and connectivity in Eq. 2.26
l_m, l_f	van Genuchten-Mualem parameter for tortuosity and connectivity in matrix and fracture domain
m	van Genuchten model fitting parameter

m_f	van Genuchten model fitting parameter in fracture domain
m_q	Number of different sets of measurements in Eq. 6.1
n	van Genuchten model fitting parameter
N	Number of data points in Eq. 7.1
n_f	van Genuchten model fitting parameter in fracture domain
n_{qj}	Number of measurements in a particular measurement set in Eq.6.1
p^G	Gas pressure relative to atmosphere (kN/m^2)
p^L	Liquid pressure relative to atmosphere (kN/m^2)
pc(θ) or ψ(θ)	Moisture retention function
Q	Total discharge, Q (m^3/s)
qj* (x,ti) and	
qj (x,ti,b):	Model predictions for the vector of optimized parameters in Eq. 6.1
R	Radius of the meniscus curvature
R^2	Correlation coefficient
R_c	Critical bubble cavity radius
R_{max}	Maximum bubble cavity radius
r_p	Characteristic length scale of the pore space (m)
S	Degree of saturation
Se_m	Effective fluid saturation of the mobile region
Se_{im}	Effective fluid saturation of the immobile region
u_a	Pore air pressures
u_w	Pore water pressure
v	Specific volume
V_w	Volume of liquid
V_{w-d}	Drainable volume of liquid
V_{w-r}	Retained volume of liquid
v_j, $w_{i,j}$	Weights associated with a particular measurement set or point inEq.6.1
w	Gravimetric moisture content
w_f	Volume of fracture domain divided by the total flow domain
y_i	Model simulated values in Eq. 7.1
Y_i	Data values in Eq. 7.1
z	Elevation above a vertical datum
z_{iF}	Volumetric fraction of component n in the liquid /gas phase (m^3/ m^3)
λ	Brooks & Corey model fitting parameter
θ	Volumetric moisture content
ψ_{aev}.	Air-entry value (kN/m^2 or KPa)
ρ^F	Density of fluid F (kg/m^3)

μ^F	Viscosity of fluid F (kg/m/sec)
ψ_Z	Gravimetric potential
ψ_m	Matric potential
Ψ_i	Inflection point of the moisture retention curve
φ	Porosity
α	van Genuchten model fitting parameter
γ	Surface tension in Eq. 2.3; Noble and Arnold model fitting parameter in Eq.2.31
θ_e	Effective saturation or normalised water content
θ_r	Residual moisture content
θ_s	Saturated moisture content
Λ	Ratio of the change in void volume (dV_v) that occurs when the volume of solids changes by an amount (dV_s)
ρ_{bulk}	Bulk density
ρ_{dry}	Dry density
ρ_g	Density of gas
ρ_s	Density of the solid particles
ρ_w	Density of water
φ_e	Drainable porosity
β	Contact angle of liquid with the solid particles
θ_{mo}	Liquid moisture content into mobile region
θ_{im}	Liquid moisture content into immobile region
θ_{wf}	Volume of liquid in the fracture domain divided by the fracture domain volume
θ_{wm}	Volume of liquid in the matrix domain divided by the matrix domain volume
Γ_w	Transfer rate for liquid from the inter- to the intra-aggregate pores
Γ_w	Mass exchange term describing the transfer of liquid between fracture and matrix domains (T^{-1});
θ_{im}	Matrix moisture content
χ_w	Empirical scaling factor in dual-porosity system
α	Effective diffusion path length, the distance from the center of the matrix to the fracture boundary
Φ	Objective function in Eq. 6.1 in HYDRUS 1D model
θ_{rf}	Residual moisture content
θ_{sf}	Saturated moisture content
α_f	van Genuchten model fitting parameter in fracture domain

CHAPTER 1 INTRODUCTION

1.1 Research Overview

Land disposal of solid waste has changed dramatically over the last ten years. It is widely recognised that the polluting potential of landfills will continue for centuries rather than decades. Landfills generate contaminated leachate and landfill gas as the waste degrades. The movement of these emissions into the surrounding environment is a serious concern. Alternative waste management methods like recycling, incineration and waste pre-treatment reduce contaminant levels but still require final disposal of a significant amount of residual wastes in landfills (Powrie and Dacombe, 2006). For existing landfills, in situ treatment is the only realistic option for bringing wastes into equilibrium with the surrounding environment within a reasonable timescale (e.g. Knox, 1990; Walker et al., 1997).For this to be achieved, it will be necessary to manage a landfill receiving wastes not of final storage quality to a stable and non-polluting state (known as "completion"), in chemical and hydraulic equilibrium with the surrounding environment, within a timescale of about 30 years (CIWM, 1999). Stabilization of landfills containing putrescible wastes must be achieved through a combination of biodegradation of the organic matter and flushing out of recalcitrant contaminants. Both of these require active leachate extraction, treatment and recirculation. It is now recognized that without active management, traditional landfills such as those which received raw municipal solid waste between about 1970 and 2010 in the UK and elsewhere may take hundreds of years to achieve completion (Hall et al, 2004).

The EU Landfill Directive (99/31/EC) requires that wastes are now treated to reduce their biodegradability prior to being landfilled: nonetheless, it is likely that 10-25% of the original biodegradability of a municipal solid waste (MSW) will remain (Siddiqui et al, 2009). Trials on the bio-mechanical treatment and its effect on the landfill behaviour show that the quality of the remaining organic fraction for landfilling should be considered because it is more relevant than the quantity of biodegradable waste, in terms of the level of gaseous emissions from landfill. In Germany since 2005 only treated wastes are allowed to be landfilled (Müller and Bulson, 2005). As more than 90 % of the thermally treated waste is going into road construction, almost only the material remaining from mechanical-biological

treatment is deposited. But in the UK and in other parts of Europe landfilling has been the predominant means of disposal of waste for the past decades (Figure 1.1), with currently 461 operational landfills and about 2120 closed landfills in the UK . With no leachate collection and treatment, the soil and groundwater may be polluted locally while the produced methane contributes to climate change on a global level (Ehrig, 1983; Beaven, 2001).

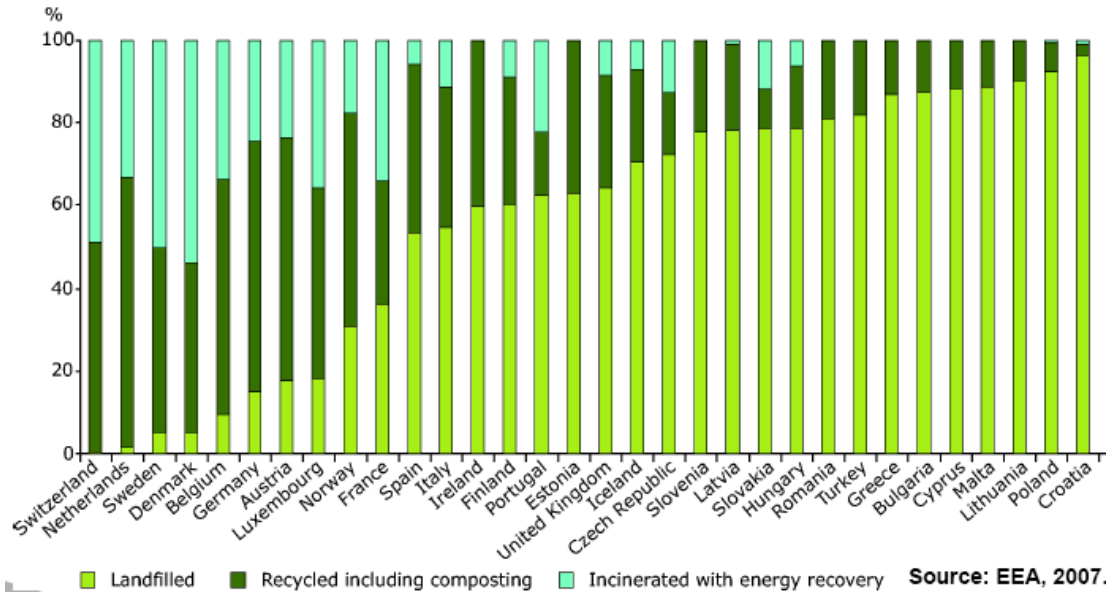

Figure 1.1 Treatment of Municipal Solid Waste in Europe in 2007

The stabilization of landfilled MSW, whether or not it has been pre-treated, will require active leachate management to encourage the biodegradation of putrescible materials and/or remove recalcitrant contaminants by flushing or leachate recirculation. Several studies on leachate recirculation methods are available for application to bioreactor landfills. Some of the popular methods include prewetting, surface spraying, surface ponds, vertical wells, and horizontal trenches (Reinhart, 1995). One of the main uncertainties concerning the practicality of operating a landfill in this way is the control of fluid flows in relation to the leachate and gas content of the waste. Moisture content and movement are major factors governing biodegradation and flushing; they also impact on the control of biogas emissions, gas collection and the extraction of residual trapped gas.

Modelling of unsaturated landfill flow processes is a potentially valuable tool for the prediction of leachate and gas discharge rates, the design of leachate and gas

control systems and the estimation of biodegradation and settlement in engineered landfills. For example (White et al, 2011) have proposed a simple 1D model for the management of leachate recirculation. However, successful modelling of moisture movement within a landfill is constrained by a lack of understanding of the unsaturated hydraulic properties of the landfilled waste. In landfilled waste, the particle and pore size distribution, heterogeneity of waste composition and leachate chemistry complicate the determination of moisture retention and hydraulic properties. Predicting the moisture distribution, leachate generation and flow in landfilled waste using unsaturated flow theory is dependent both on the validity of the flow theory and on the hydraulic properties of the landfilled waste. Unsaturated flow has been researched extensively in the fields of soil physics, hydrology, and geotechnical/petroleum engineering. However, there has beenvery limited evaluation in the context of landfilled waste and MBT waste (Korfiatis et al., 1984; Imam, 2003; Kazimoglu et al, 2005, 2006; Stoltz, 2007; Münich, 2009; Staub 2010; Breitmeyer, 2011, Tinet et al., 2011).

1.2 Research aims and objectives

This research was carried out to contribute to the Engineering and Physical Sciences Research Council Funded project *Science and strategies for the long-term management and remediation of landfills*.

The overall objectives of the proposed research were to develop:

- a better understanding of the role of landfill gas on flow and transport processes and the factors controlling the flow of air in landfills ;
- a better understanding of the processes involved in the flushing of contaminants from different types of wastes (including both current and future residual wastes) at a variety of scales;
- new techniques for characterising the contaminant transport behaviour of wastes at the field scale; and
- a toolkit of models that can be used to assess the effect of various post closure management techniques on completion time, improving the ability to predict and hence manage the long term behaviour of landfills.

A subsidiary objective was to design and undertake experiments at the laboratory scale to provide qualitative data on the generation and movement of gas within waste materials to aid the improvement of conceptual process models.

Thus the aim of this research is to understand the interactions between liquid and gas flow at high degrees of saturation, as this could have a significant effect on the effectiveness of landfill remediation by flushing. Particular attention is paid to a number of key parametric functions that are believed to control the simultaneous flow of leachate and gas in waste materials. These are the relationship between capillary pressure or suction and the degree of leachate saturation or volumetric moisture content in the active pore space of the material, and the hydraulic conductivity properties. For waste materials such relationships have not been fully established.

This research aims:

1. to evaluate the parameters of moisture retention functions of waste materials $p_C(\theta)$and of unsaturated hydraulic conductivity $k(\theta)$from drainage experiments of waste columns,pressure plate and hanging water column techniques.
2. to demonstrate the extent to which functional relationships may be derived between the physical properties of waste (density and structure) and the moisture content related properties (capillary pressure and permeability).

The objectives are:

1. to design (instrumentation and monitoring arrangements) and undertake free drainage, pressure plate and hanging column experiments in near saturated waste materials (degree of saturation: 0.8-1) to determine the relationships between the capillary pressure, $p_c(\theta)$ and relative permeability for the liquid phase, $k_{r,L}(\theta)$ and moisture content (θ)or degree of saturation (S).

2. to use the results from the drainage experiments as qualitative data on the liquid movement within waste materials, to validate or at least contribute to the improvement of the unsaturated flow algorithms in conceptual process models, like the University of Southampton Landfill Degradation And Transport model LDAT, (White et. al 2004).

3. to interpret the results from the drainage experiments using the unsaturated flow model HYDRUS-1D (Šimůnek et al., 2005).

The extent to which these aims and objectives have been met by the research will be discussed as part of the conclusions in Chapter 8.

1.3 Thesis outline

This thesis is divided into seven chapters. In this Introduction chapter (Chapter 1), a research overview has been given to highlight the context and purpose of this work, and the main objectives have been outlined (section 1.2). Chapter 2 provides a detailed literature survey on the characteristics of three-phase systems, fluid flow in the unsaturated zone and a review of previous work on moisture retention characteristic curves and unsaturated permeability functions for wastes.

Chapter 3 provides information on the waste sample tested and describes the different techniques (drainage, pressure plate and hanging water column) used for the determination of the moisture retention characteristics for MBT waste specimens.

In Chapter 4 the experimental results from the three techniques are presented and analysed. A comparison of the moisture retention curves (MRC) for the MBT specimens derived using the different techniques follows and technical recommendations are given. In Chapter 5 the unsaturated permeability is estimated from the drainage and pressure plate experiments and compared with existing empirical functions.

Chapter 6 describes the models Hydrus-1D and LDAT and their application to the data from the drainage experiments, and presents and analyses the model simulations.

In Chapter 7 an analysis of the sensitivity of the results to the model parameters is carried out.

Chapter 8 reviews the extent to which the aims and objectives of the research have been met, and presents the major conclusions that can be drawn from the research including recommendations for future work.

CHAPTER 2 LITERATURE REVIEW

2.1 Characterisation of three-phase systems

Sections 2.1.1 and 2.1.2 were taken from Chapter 1 of the ASCE Special Technical Publication Beaven R. P., Powrie W. and Zardava K. (2011). The author of this thesis played a significant role in the preparation of the Chapter and acknowledges the contribution made by her co-authors.

2.1.1 Definition of terms and phase relations

Landfilled waste is a porous medium with particulate solid material and pore space distributed throughout the volume. The pore space may be filled with liquid and/or gas. The porous medium most closely comparable to solid waste landfills in terms of structure, porosity and gas content is often considered to be unsaturated soil (McDougall et al., 2004). However, a waste is rather more complicated not least because of the potential for biological and chemical actions and interactions, and the fact that the solid phase comprises a wide range of different material types with vastly different mechanical and physical properties.

A porous medium is conventionally idealised as a solid structure with interconnected voids filled with a fluid (liquid and/or gas), as indicated in Figure 2.1 Each phase may consist of a number of components comprising of chemical compounds and species but they are assumed to be homogeneous within themselves and to form a physical continuum to which the mathematical methods of fluid mechanics can be applied. The same component may exist in more than one phase and also it is possible for all components to move. In the solid phase, the components move through settlement, in the liquid and gas phases they move by seepage flow and diffusion. The state of the porous medium is conventionally defined by the relationships between the phases (solid, liquid and gas), either by mass or by volume. Unfortunately, the same term is sometimes used (usually in different branches of science) to mean different things. An example of this is the water content, which may be defined by mass or by volume, and expressed as the ratio of the mass/volume of water to that of the whole or of the solids alone. Definitions of the phase relations most commonly used, and where appropriate the relationships between them, are summarised in Table 2.1. These originate mainly in the soil mechanics or soil science literature. An additional refinement that is

useful for wastes, but not normally needed with soils, is the distinction between retained and drainable water. In a waste, water may be retained through sorption into certain types of materials (e.g. paper, card and textiles), or by being trapped in a closed-ended container such as a bottle or a can. The phase relationships in Table 2.1 are derived from the basic masses and volumes of each element defined in Figure 2.2, with the volume of liquid V_w split into drainable (V_{w-d}) and retained (V_{w-r}) components. ρ_w is the density of water, ρ_g is the density of gas, and ρ_s is the density of the solid particles. The ratio ρ_s/ρ_w is the specific gravity, G_s. In wastes, ρ_s may vary considerably (for example, from 0.6 Mg/m^3 for dry wood to 7.8 Mg/m^3 for steel), and the choice of an appropriate particle density is both a challenge and a potential source of error.

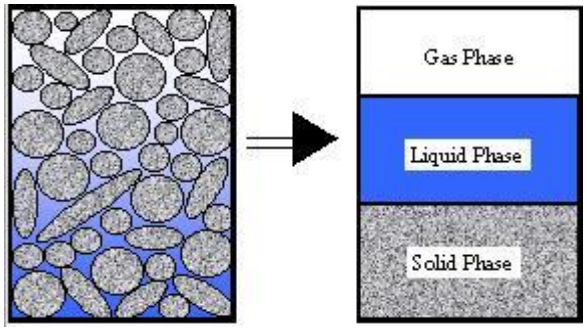

Figure 2.1 Three-phase porous medium

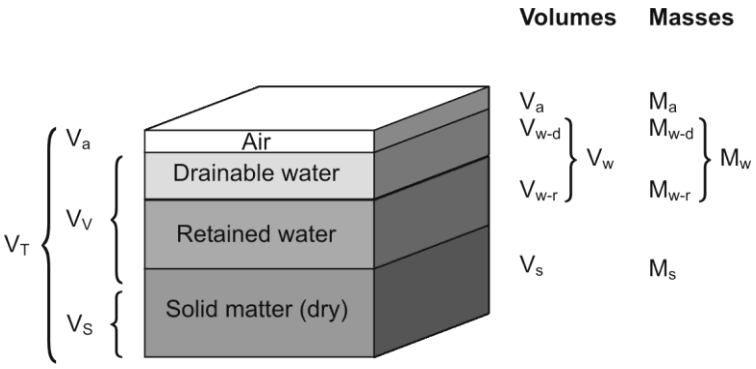

Figure 2.2. Volume-mass relationships

Table 2.1 Basic definitions and phase relations for porous media

Parameter and symbol	Definition	Equation and inter-relationships
void ratio, e	volume of voids/volume of solids	$e = V_v/V_s$
porosity, φ	volume of voids/total volume	$\varphi = V_v/V_t = e/(1+e)$
specific volume, v	total volume/volume of solids	$v = V_t/V_s = (1+e) = 1/(1-\phi)$
drainable or effective porosity,φ_e	volume of drainable water/total volume	$\varphi_e = V_{w\text{-}d}/V_t$
gravimetric water content, w	mass of water/mass of solids	$w = M_w/M_s$
volumetric water content, θ	volume of water/total volume	$\theta = V_w/V_t = w.Gs/(1+e)$
Degree of saturation, S	volume of water/volume of voids	$S = V_w/V_v = w.G_s/e$
Gas content, G	volume of gas/volume of voids	$G = V_g/V_v = 1\text{-}S$
Bulk density, ρ_{bulk}	total mass/total volume	$\rho_{bulk} = G_s.\ \rho_w.(1+w)/v$ $= (G_s+e).\ \rho_w/v$
Dry density, ρ_{dry}	the bulk density a waste would have at the same void ratio but dry (w = 0)	$\rho_{dry} = G_s.w/v$
Particle density, ρ_s	mass of the solid particles/ mass of water occupying the same volume as the given mass of solid particles	$\rho_s = M_s/V_s$

The different definitions of water content (mass of water /mass of dry solids; mass of water/total (wet) mass; and volume of water/total volume) commonly used in waste science can cause confusion, especially as not all authors make it clear which one they are using. The gravimetric water content by dry mass is arguably the most suitable measure: the problem with both of the other measures (gravimetric by wet mass and volumetric) is that the mass or volume of the water features in both the numerator and the denominator of the expression.

A further complication with waste is that the void ratio will in general change as degradation occurs. This may be quantified by the parameter Λ (McDougall et al. 2004 and McDougall 2007) defined as the ratio dV_v/dV_s where dV_v is the change in void volume that occurs when the volume of solids changes by an amount dV_s. If Λ = 0, the volume of voids does not change and the change in total volume is equal to the change in the volume of solids. If Λ = -1, the volume of voids increases by the same amount as the volume of solids lost and degradation takes place at constant total volume (leading to a more open structure and the potential for sudden collapse). If Λ = e (the void ratio), then the void ratio does not change as a consequence of degradation, and if Λ > e then the reduction in void volume exceeds the loss of solids, leading to densification and possible increase in strength.

2.1.2 Distribution of gas and liquid

The way in which gas and liquid are distributed within a waste, and the flow regimes of each, will depend primarily on the water content and degree of saturation. Single phase flow of liquid (if the porous medium is saturated: Figure 2.3a) is the most straightforward condition to analyse. If gas bubbles are small and uniformly distributed throughout the liquid, and do not move independently of it, flow might still reasonably be treated as single phase with a permeant fluid of reduced density. As a porous medium is drained or further gas generated, water is replaced or displaced by gas in the largest pores first. Initially the gas bubbles may be immobile (Figure 2.3b), but are able to move through the liquid in response to internal or external pressure differences (Figure 2.3c). As the degree of saturation decreases further, the bubbles expand and join together until a continuous gas phase is formed. At this point, liquid and gas may flow continuously and independently through the waste.

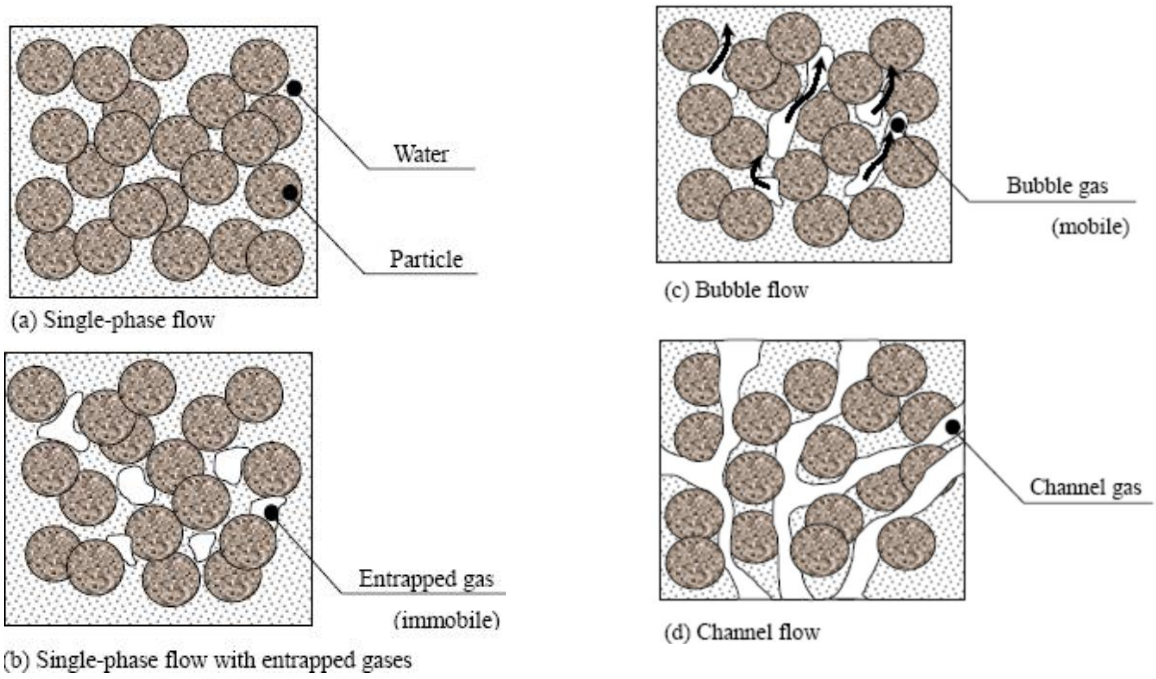

Figure 2.3 Schematic illustrations of fluids flow in porous media

The transition from bubble (Figure 2.3c) to channel (Figure 2.3d) flow in a porous medium is governed by the ratio of buoyancy forces driving upward flow to surface tension forces (see section 2.1.4) arising from the contact between the gas/liquid interface and the solid grains that tend to retard bubble flow, and is quantified by the Bond number, Bo: (Brooks et al., 1999):

$$Bo = \frac{\left(p^L - p^G\right) * g r_p^2}{\gamma} \qquad (2.1)$$

where r_p is a characteristic pore dimension (length) and γ is the surface tension of the interface. When Bo>1, buoyancy forces dominate indicating bubble flow. When Bo<1, capillary forces dominate indicating channel flow.

Sills et al (1991) stated that the gas pressure, p^G, influences the effect of large bubbles on the soil behaviour and it was therefore useful to consider the bounds on the possible values. Considering the interaction between the gas and the pore liquid, the gas pressure, p^G, is always greater than the pore liquid pressure, p^L , and surface tension effects limit the difference between p^G and p^L. Figure 2.4 shows the extreme conditions that can occur in respect of the curvature of the

menisci between gas and pore liquid. As the liquid is drained, liquid-gas interfaces (menisci) are being formed. Initially, the gas pressure is the smallest that can occur and the radius of meniscus curvature is at its maximum, which is given by the bubble cavity radius R_{max}, as shown in Figure 2.4a. Later as the gas pressure increases the minimum possible value for the radius is given by a critical value R_c, which corresponds to a meniscus that is just able to bridge the largest gap between the soil particles and the bubble boundary (Figure 2.4b).

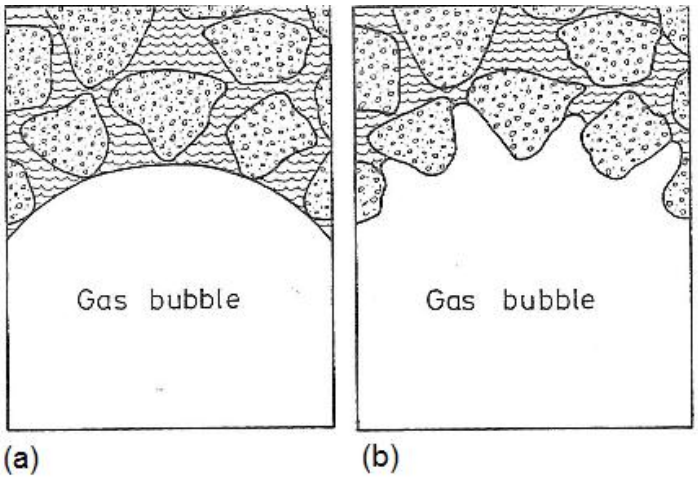

Figure 2.4 Extreme conditions of meniscus curvature: (a) $R=R_{max}$ and (b) $R=R_c$ (Sills et al, 1991)

The surface tension limits for gas pressure are given by:

$$p^L + \frac{2\gamma}{R_{\max}} < p^G < p^L + \frac{2\gamma}{R_c} \qquad (2.2)$$

The lower limit in equation 2 corresponds to the onset of 'bubble flooding'. If the value $p^G - p^L$ falls to $2\gamma/R_{max}$, the gas pressure is insufficient to maintain completely gas filled cavities against the restraint provided by surface tension and pore liquid from the surrounding saturated soil matrix drains into the bubble cavities.

2.1.3 Liquid and gas phase in landfills

A waste deposit in a landfill generally contains an unstable organic fraction that will degrade over time. As it degrades the organic fraction will produce gas, which will move through the body of the landfill and eventually discharge from the landfill.

The waste will normally contain a liquid phase known as leachate. The liquid arises from liquid that was either present in the waste material at the time it was deposited, or liquid that has been added later as the result of rainfall infiltration into the waste mass, or as artificial irrigation, or from decomposition of solid matter. Liquids, primarily in the form of volatile fatty acids, are also a product of degradation and these mix with other liquid in the material to form the leachate contained in the waste. The waste material will thus form a multi-phase material that consists of a solid matrix containing within its pore spaces a mixture of liquid and gas.

The liquid phase in a landfill plays a very important role in the bio-chemical processes taking place in the waste material contained in the landfill, and in the way in which a landfill reacts with its environment. At any location in a landfill the condition, properties and behaviour of the liquid phase is determined by the hydrology and fluid mechanics of the landfill material, topics that are not particularly well understood. The liquid phase influences the bio-chemical processes in the following ways (White and Beaven, 2008):

1. The liquid phase accommodates the chemical reactions that take place in a landfill, and those degrade and stabilise the waste material.
2. Water in the liquid phase acts as a solvent and provides the pathway for the solid phase to dissolve into the liquid phase and thus become available to take part in the chemical reactions.
3. Water in the liquid phase is an important reactant in many of the stabilising chemical reactions.
4. The liquid phase and its solutes can provide the means by which a landfill can contaminate its immediate environment in the event of unplanned releases of the liquid phase into the environment.
5. The liquid phase and its solutes also provide the opportunity to stabilise a landfill more rapidly by planned management of the liquid phase in flushing, treatment and leachate recirculation systems.
6. Through its involvement in the bio-degradation process the liquid phase influences the production of gas in a landfill. Through its presence in the pore spaces of the landfill the liquid phase has an impact on the transport of gas that has to take place through the same pore spaces.

Leachate is contained in the pore spaces of the solid waste material. Leachate may be collected from the waste using wells or drains. It can then either be treated

or removed, or be reintroduced into the waste material through an artificial recharge system. This latter process is known as leachate recirculation. The recirculation of landfill leachate within a landfill may be used to control the amount of leachate contained in the waste material in a landfill. Managing the leachate in this way can be used to optimise both gas generation and leachate treatment systems.

Landfill gas typically contains 40% to 60% methane and 40% to 60% carbon dioxide. It also includes small amounts of nitrogen, oxygen, ammonia, sulfides, hydrogen, carbon monoxide and non-methane organic compounds (Tchobanoglous et al, 1993). Most landfill gas is produced by bacterial decomposition, which occurs when organic waste is broken down by bacteria naturally present in the waste. Landfill gases can be also created when certain wastes, particularly organic compounds, change from a liquid or a solid into a vapour (volatilization). The third process is by the reactions of certain chemicals present in waste, i.e. chlorine bleach and ammonia.

The rate and volume of landfill gas produced at a specific site depend on the characteristics of the waste (e.g., composition and age of the refuse) and a number of environmental factors (e.g., the presence of oxygen in the landfill, moisture content, and temperature). The more organic waste present in a landfill, the more landfill gas is produced by the bacteria during decomposition. Most models of landfill gas production are based on first order exponential models, with half-lives (the time by which half the potential gas generation has been achieved) that range between 1 and 25 years, Cossu, R.et al. (1996). These models predict that the maximum gas generation occurs directly after waste is deposited, but within the context of landfilling and the continual placement of waste in new cells, peak gas production from a landfill will often be delayed, often by several years. The presence of moisture in a landfill increases gas production because it encourages bacterial decomposition. A moisture content of 40% or higher, based on wet weight, promotes maximum gas production. Waste compaction may slow gas production because it increases the density of the landfill waste, decreasing the permeability rate at which liquid can infiltrate the waste. Finally, as the landfill's temperature rises, bacterial activity increases, resulting in increased gas production (Crawford and Smith, 1985**).**

Gas may be contained in the pore space of waste either in the liquid phase

dissolved as a solute, or in the gas phase. The amount dissolved will depend on the chemistry of the gas, the presence of other solutes, and the ambient conditions as determined by pore pressure and temperature. Gas contained in this way will be transported by the combined processes of diffusion and dispersion within the liquid phase, and convection by the liquid. Where there are quantities of gas present in the pore spaces, as gas rather than as a solute, and these quantities are small in relation to the liquid phase, gas movement will be restrained by surface tension effects, and the gas will be present as small immobile pockets. Depending on the local gas generation conditions these small gas pockets will either dissolve and then be transported by the liquid phase, or grow and form fissures or channels along which gas can then flow.

White & Beaven (2008) concluded that the ways in which key landfill operational areas will benefit from a better understanding of the movement of landfill gas and leachate are:

1. The development of models for estimating the stabilisation times for the biodegradation of waste will be improved.
2. The long term emissions of gas and liquids from caps and liners will become more accurate.
3. Interpreting gas pressure and flow data from gas wells in order to assess landfill gas generation rates will become a possibility.
4. The assessment of pressure heads on liners and at internal points in landfills to confirm slope stability will become more reliable.
5. The relationship between liquid flow, density changes, and waste settlement will become clearer.

2.1.4 Surface tension and capillarity

Surface tension arises from the attraction that molecules of the liquid have for each other. As a result, the fluid interface behaves almost as if it were an elastic membrane. This force per unit length is called the surface tension (γ) with units N/m. At equilibrium for a spherical bubble of liquid and gas, it can be shown from a consideration of balance of forces on a small element of interface (Figure 2.5) that:

$$p^G - p^L = \frac{2\gamma}{R}\cos\beta \qquad (2.3)$$

Where p^G and p^L are the gas and pore liquid pressures and R is the radius of curvature of the menisci at the bubble boundary. The angle β is the angle of contact of the meniscus with the solid particle.

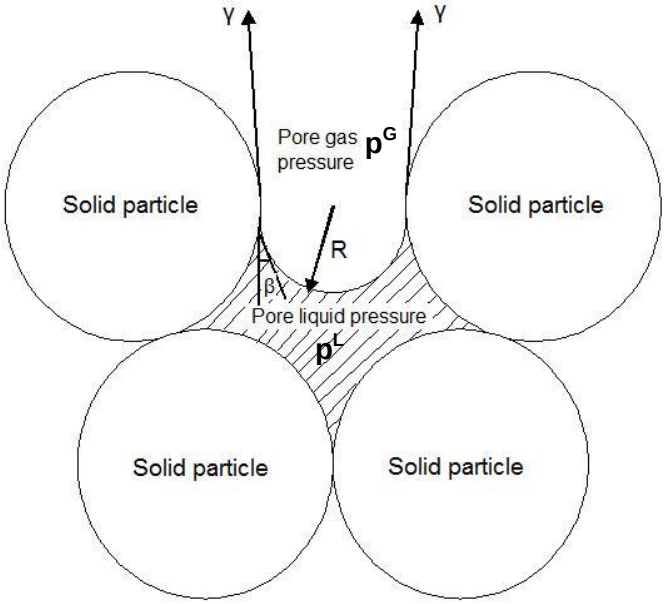

Figure 2.5 Surface tension forces on a spherical bubble

The most important phenomenon observed in natural soils as a result of surface tension is capillarity, the difference in pressure between the gas and liquid phases. Capillary action describes the attraction of liquid molecules to solid particles. Capillary action is responsible for moving liquid from wet areas of the porous medium to dry areas. It results from the surface tension of liquid and its contact angle (β) with the solid particles. If a tube is sufficiently narrow and the liquid adhesion to its walls is sufficiently strong, surface tension can draw liquid up the tube (Sears, and Zemanski, 1995). The height the column is lifted is given by:

$$h = \frac{2\gamma \cos \beta}{\rho g R} \tag{2.4}$$

where: *h* is the height the liquid is lifted, *γ* is the liquid-gas surface tension, *ρ* is the density of the liquid, *r* is the radius of the capillary, *g* is the acceleration due to gravity, *β* is the angle of contact described above.

If the pressure potential in a pore is higher than the air-entry value (the critical suction value, such that when it is exceeded the largest pore begins to empty), both cohesive (between liquid molecules) and adhesive (between liquid molecules

and substrate) forces cannot hold the liquid any longer. This will result in liquid draining until the pressure potential at the gas-liquid interface is equal to the air-entry value (ψ_{aev}).The process of drainage takes place through the bottom, while gas is introduced from the top. As the liquid is being drained, liquid-gas interfaces (menisci) are being formed. A capillary pressure (p_c) is set up across the meniscus interface between the liquid and gas. This creates a difference between the pressures in the liquid (p^L) and gas (p^G) phases. This difference is expressed in terms of the capillary pressure (p_c) which is assumed to be a function of the degree of saturation (S) or volumetric moisture content (θ), where $\theta = \phi S$. The main theoretical and practical tool currently used to quantify the capillary pressure function is a relationship between capillary pressure and saturation (S) or volumetric moisture content (θ) at equilibrium (Bear and Verruijt, 1992):

$$p_c = p^G - p^L \tag{2.5}$$

The exact form of this function in the case of waste materials is presently unknown and is the subject of the research project. When the gas pressure is zero relative to atmospheric pressure, $p^L = -p_C$ and negative. This negative capillary pressure is also called the matric potential, tension or suction.

2.2 Fluid flow in unsaturated zone

2.2.1 Governing liquid flow equations

Single porosity models assume a vertical uniform liquid movement in a partially saturated rigid porous medium. This is described by Richard's equation (Richards, 1931) using the assumptions that the gas phase plays an insignificant role in the liquid flow process and that liquid flow due to thermal gradients can be neglected. Applying conservation of water mass and assuming Darcy's law (Equation 2.6) is valid, Richards' equation (Equation 2.7) can be derived to describe liquid flow in unsaturated refuse.

$$Q = (-k_s A/\mu)(\partial p/\partial l) \tag{2.6}$$

$$\partial\theta/\partial t = \partial/\partial z\left[k(\theta)\left(\partial\psi/\partial z + 1\right)\right] \tag{2.7}$$

where θ is the volumetric moisture content at given suction (ψ) and k(θ) is the unsaturated hydraulic conductivity. To solve Equation 2.7 the constitutive relations between suction and hydraulic conductivity with volumetric moisture content must be defined (Sections 2.3.2 and 2.3.4). The derivation of Richard's equation (Equation 2.7) for one phase 1D flow is described in Appendix A.

Dual-porosity models assume that liquid flow is restricted to the fractures (or inter-aggregate pores and macro-pores), and that liquid in the matrix (intra-aggregate pores or the rock matrix) does not move at all. Thus, intra-aggregate pores represent immobile pockets that can exchange, retain and store liquid, but do not permit convective flow. This conceptualization leads to two-domain, dual-porosity type flow and transport models (Philip, 1968; van Genuchten and Wierenga, 1976) that divide the liquid phase into mobile (flowing, inter-aggregate), θ_{mo}, and immobile (inactive, intra-aggregate), θ_{im}, regions and $\theta = \theta_{mo} + \theta_{im}$.

The dual-porosity formulation for liquid flow is based on a mixed formulation, which uses Richards equation to describe liquid flow in the fractures (macro-pores), and a simple mass balance equation to describe moisture dynamics in the matrix as follows (Šimůnek et al., 2003):

$$\partial\theta_{mo} / \partial t = \partial / \partial x\left[k(\theta)\left(\partial\psi / \partial z + 1\right)\right] - \Gamma_w \tag{2.8}$$

$$\partial\theta_{im} / \partial t = \Gamma_w \tag{2.9}$$

Where Γ_w is the transfer rate for liquid from the inter- to the intra-aggregate pores.

The mass transfer rate, Γ_w, for liquid between the fracture and matrix regions in several dual-porosity studies (e.g. Phillip, 1968; Šimunek et al., 2001) has been assumed to be proportional to the difference in effective water contents of the two regions using the first-order rate equation:

$$\Gamma_w = \partial\theta_{im} / \partial t = w(S_e^{\,m} - S_e^{\,im}) \tag{2.10}$$

where θ_{im} is the matrix moisture content, w is a first-order rate coefficient (T^{-1}), and $S_e^{\,m}$ and $S_e^{\,im}$ are effective fluid saturations of the mobile (fracture) and immobile (matrix) regions, respectively.

While dual-porosity models assume that liquid in the matrix is inactive, dual permeability models allow for liquid flow in the matrix as well. The dual-permeability model assumes that pores can be divided into a fracture or macro-pore domain and a matrix domain. Here, liquid flows through each domain separately with mass exchange permitted between the two domains. For the dual-permeability model, Richards' equation (Equation 2.7) is written for the fracture and matrix domain. The flow equations for the macro-pore or fracture (subscript *f*) and matrix (subscript *m*) pore systems in this approach are given by:

$$\partial\theta_{wf} / \partial t = \partial / \partial z\left[k_{wf}(\theta_{wf})\left(\partial\psi_f / \partial z + 1\right)\right] - \Gamma_w / w_f \tag{2.11}$$

$$\partial\theta_{wm} / \partial t = \partial / \partial z\left[k_{wm}(\theta_{wm})\left(\partial\psi_m / \partial z + 1\right)\right] + \Gamma_w / 1 - w_f \tag{2.12}$$

where the subscript *f* and *m* represent fracture and matrix domains, respectively; Γ_w is the mass exchange term describing the transfer of liquid between fracture and matrix domains [T^{-1}]; and w_f is the volume of fracture domain divided by the total flow domain ($0 < w_f < 1$). If $\Gamma_w > 0$ in Equations 2.11 and 2.12, liquid is transferred from the fracture to the matrix. Here, θ_{wf} is the volume of liquid in the fracture domain divided by the fracture domain volume, and θ_{wm} is the volume of liquid in the matrix domain divided by the matrix domain volume. The mass exchange term, Γ_w, is defined as (Gerke and van Genuchten, 1993):

$$\Gamma_w = b / a^2 \chi_w k_a (\psi_f - \psi_m) \tag{2.13}$$

where b is a shape factor depending on the geometry of the material, a is an effective diffusion path length and is the distance from the center of the matrix to the fracture boundary, χ_w is an empirical scaling factor, and k_α is the effective hydraulic conductivity at the interface between the two domains. The different hydraulic parameters for van Genuchten (1980)–Mualem (1976) models are assigned to each domain separately. This leads to 17 parameters being needed to solve Equations 2.11 and 2.13.

2.2.2 Review of existing modelling approaches for MSW materials

In the previous section, various conceptual models have been presented to describe fluid flow in complex soil systems including single-porosity, dual-

permeability, dual-porosity, and multiple-porosity/permeability models (*Šimůnek* et al., 2003; Šimunek and van Genuchten, 2008).

The single-porosity model conceptualizes the landfilled waste as a homogeneous porous medium (Johnson et al., 2001) and is the most common approach for describing gas or liquid flow through waste. They used Hydrus to model unsaturated flow through MSW bottom ash by Richards' equation but found that it failed to capture the dynamics that were leading to fast responses to rainfall events. Various authors have proposed flow models for MSW based on the assumption of a homogeneous porous medium with a single domain of flow. Straub and Lynch (1982) attempted to combine unsaturated flow and transport theory to simulate leachate flow and quality. Korfiatis et al. (1984) formulated a mathematical model for the simulation one-dimensional, vertical movement of moisture through waste. Richards' equation (Equation 2.7) was solved using the power law equations of Clapp and Hornberger (1976).

Demetracopoulos et al. (1986) carried out a sensitivity analysis on the model formulated by Korfiatis et al. (1984) for both saturated and unsaturated surface conditions. Noble and Arnold (1991) developed the FULFILL program solving the Philip's equation (Equation 2.14) for moisture transport within a landfill.

$$\partial\theta/\partial t + \partial k(\theta)/\partial z - \partial/\partial z(D(\theta)\partial\theta/\partial z) = 0 \qquad (2.14)$$

where z is the vertical co-ordinate, positive downwards from the surface to the datum. D is the medium-liquid diffusivity and K is the hydraulic conductivity. Both these properties are functions of volumetric moisture content θ.

McDougall et al. (1996) applied saturated/ unsaturated flow theory to simulate leachate movement in saturated and unsaturated zones in landfills. Yuen (1999) used SEEP/W to simulate moisture content changes in a full-scale landfill cell due to leachate recirculation (Equation 2.15).

$$\partial/\partial x(k_x \partial h/\partial x) + \partial/\partial z(k_z \partial h/\partial z) + Q = \partial\theta/\partial t \qquad (2.15)$$

Jang et al. (2002) used the model HELP to predict the leachate level change according to the degree of compaction and cover soil thickness variation. It was found that the increase in the degree of compaction for intermediate cover soil and

waste results in the decrease of field capacity and hydraulic conductivity, hence, the increase of leachate level.Many authors have used the HYDRUS model to solve Richards' equation (Eq.2.7) for landfill simulations. Haydar and Khire (2005) used HYDRUS-2D to simulate the hydraulics of liquid injection in landfills for horizontal trenches. Later Khire and Mukherjee (2007) carried out numerical evaluation of key design variables for leachate recirculation system consisting of vertical wells using HYDRUS-2D as well. Similarly, Kulkarni and Reddy (2010) simulated the effect of different leachate injection rates and injection modes on moisture distribution for horizontal trenches using a single porosity approach. Fluid flow was described by Darcy's law (Equation 2.6), and the unsaturated hydraulic conductivity parameters were modelled using a van Genuchten function. Recently, Breitmeyer and Benson (2011a) used HYDRUS-1D to inverse simulate the unsaturated hydraulic conductivities of MSW in a bioreactor landfill.

However, field studies have shown that the moisture content in a landfill may vary from saturated to dry conditions (Uguccioni and Zeiss, 1997; Bendz et al., 1997; McCreanor and Reinhart, 2000). Some materials in the landfill may create either barriers to flow (plane components, e.g. plastic sheets) or preferential flow routes (permeable materials like paper, textiles) that will affect the uniform distribution of flow. Different models can be used to describe the liquid flow in the two domains. Uguccioni and Zeiss (1997) used the model PREFLO to simulate the moisture movement. According to this model the rapid flow in the channel domain follows Poiseuille's Law (Equation 2.16) and the slow flow in the matrix follows Richards' equation.

$$Q = (-\pi r^4 / 8\mu)(\partial p / \partial l) \tag{2.16}$$

where r is the radius of the flow path, μ is the dynamic viscosity, *l* is the length of the flow path, p is the liquid pressure and Q is the volumetric flow rate.

Then they compared this model with model HELP to predict the leachate generation from pilot scale test cells but neither model was able to reproduce the exact shape of the observed leachate hydrographs. Due to these unsatisfactory simulation results, Uguccioni and Zeiss (1997) called for a new two domain model approach reflecting channel and matrix flow. Bendz et al. (1998) used a power function (the kinematic wave model) proposed by Beven and Germann (1982) for

describing the water flows in macroporic soils, to determine the channel flow in landfills. During wet conditions water flows from the channel to the matrix domain, whereas during dry conditions it is realised to the channel domain.

Beaven et al. (2003) measured the concentration of tracer in the leachate outflow after an injection with a steady state leachate circulation in the waste. They showed that while a high concentration of tracer was rapidly observed, a residual tracer concentration was measured even a long time after the injection. Consequently, a conceptual matrix-fracture transport model was proposed to represent this behaviour. The same observation was made earlier by the tracer tests of Zeiss and Major (1993) and Zeiss and Uguccioni (1995, 1997). They argued that the tracer test results indicated two-domain moisture flow in MSW. One flow domain was characterised by flow in larger voids in which the flow velocity was higher and the other flow domain was characterised by smaller pore systems in the matrix. Johnson et al. (2001) showed that such a description was necessary to describe the drainage of water through a municipal solid waste incinerator bottom ash landfill.

McCreanor and Reinhart (2000) carried out hydrodynamic modeling of leachate recirculation in landfills by including the effect of MSW properties (anisotropy and heterogeneity) and a recirculation system on leachate routing. Using a modified form of SUTRA (Equation 2.17) they were able to simulate the forces driving liquid movement through a landfill.

$$(S_w \rho S_{op} + \varepsilon \partial S_w / \partial p)\partial p / \partial t + (\phi S_w \partial \rho / \partial U)\partial U / \partial t - \nabla\left[(k_s k_r \rho / \mu)(\nabla p - \rho g)\right] = Q_\rho \tag{2.17}$$

The permeability values were randomly selected from either a normal or exponentially increasing or decreasing functions. Cumulative measured and simulated leachate generation were compared and the results showed that channelled flow was a major leachate movement mechanism that was not well understood.

Rosqvist and Destouni (2000) proposed a double porosity–double permeability model for contaminant transport. The model assumed uniform distribution of the solutes in each water phase. The assigned equations failed to describe some of

the specific flow features, such as the macropore water flow and the mixing of solutes between different flow domains. Han et al. (2011) determined the water retention function for paper and fitted a single porosity and a dual permeability model to their multistep drainage experiment using HYDRUS-1D. A dual-permeability model performed significantly better than a single-porosity model for water movement, suggesting that a dual domain description is required to describe water flow in landfills with significant amounts of paper and paperboard. However, a single-porosity model was adequate for describing gas transport.

Recently, Tinet et al. (2011) simulated leachate injection experiments in meso-scale pilots of MSW that were monitored to study the evolution of moisture content with different moistening procedures (Bayard et al., 2009; Staub et al., 2010; Gourc et al., 2009). Tinet et al. (2011) tested single and dual porosity models with unimodal and bimodal moisture retention curves. The use of a double porosity bimodal model seemed able to describe the phenomena occurring during infiltration. A flow model in the macroporosity based on the classic van Genuchten–Mualem hydraulic parameters description did not describe correctly the drainage process. A bimodal model for hydraulic properties (Ross and Smetten, 2000), was successfully used as a solution to this problem. The same conclusion was made by Kazimoglu (2007). His tests (Kazimoglu et al., 2005) showed that hydraulic conductivity at low moisture contents was adequately represented by predictive functions such as van Genuchten's (1980), however, at high moisture contents, the agreement between the experimental data and calculated hydraulic conductivities was lost. He suggested that a dual porosity bimodal model would describe better the moisture retention curve of MSW.

Preferential flow in soils can be caused by the presence of macropores and other structural features (Simunek et al., 2003). Models for simulating the liquid flow in landfill waste using the two domain approach have been based on models for macropore soils. However, the mechanism and degree of preferential liquid flows in landfills and macropore soils are different. In macropore soils water follows preferential flow paths during wet periods only, while in landfills significant liquid flow during dry periods could happen as well. Also, in landfills liquid may flow horizontally owing to the anisotropic characteristics. In landfills preferential flow tends to increase with depth due to funnelling while in macropore soils, heterogeneity of water flow decreases with depth (Rosqvist et al., 1997). Due to the above differences, many 'soil' models are inadequate to describe liquid flow in

landfills. In particular the funnelling of liquid flow in landfills caused by impermeable layers cannot be simulated by one-dimensional vertical flow models and even two-domain concepts may fail to reproduce this characteristic (Fellner and Brunner, 2010).

2.2.3 Impact of landfill gas on saturated hydraulic conductivity

The interaction between gas and water / leachate in soils and wastes appears to be complex. Gas in the void spaces of a porous medium results in a reduction in available flow paths and hence a reduction in hydraulic conductivity compared to fully saturated conditions. In wastes the problem of maintaining fully saturated conditions is compounded by the generation of gas from degradation of some of the waste constituents. Hudson et al. (2001, 2002) found that significant volumes of gas would accumulate in the void spaces of a nominally saturated waste sample even though the gas was free to vent to atmosphere. As a result, the hydraulic conductivity was up to 30 times lower than determined in nominally saturated condition.

Data presented by Hudson et al. (2001) and Powrie et al. (2005) from tests on a Dano-processed MSW waste sample (DN1) indicated a two orders of magnitude reduction in hydraulic conductivity as a result of the *in situ* generation and accumulation of gas. Increasing the pore water pressure then compressed the gas and reduced its effect on hydraulic conductivity. Further investigations into the effect of gas accumulation and pore water pressure on hydraulic conductivity at lower compression stresses, on sample of fresh shredded domestic waste (SW1) were reported by Powrie et al (2008). The tests were carried out at constant volume following initial compression under applied stresses of 40 kPa and 87 kPa, representing landfill depths of approximately 4 m and 9 m respectively.

Figure 2.6 shows the changes in average bulk hydraulic conductivity and the volume of accumulated gas over a 27 day period for a test conducted at constant volume (corresponding to an initial applied stress of 40 kPa) with a relatively high average pore water pressure of 60 kPa. The reduction in hydraulic conductivity in response to the increase in the volume of gas contained within the sample is clear.

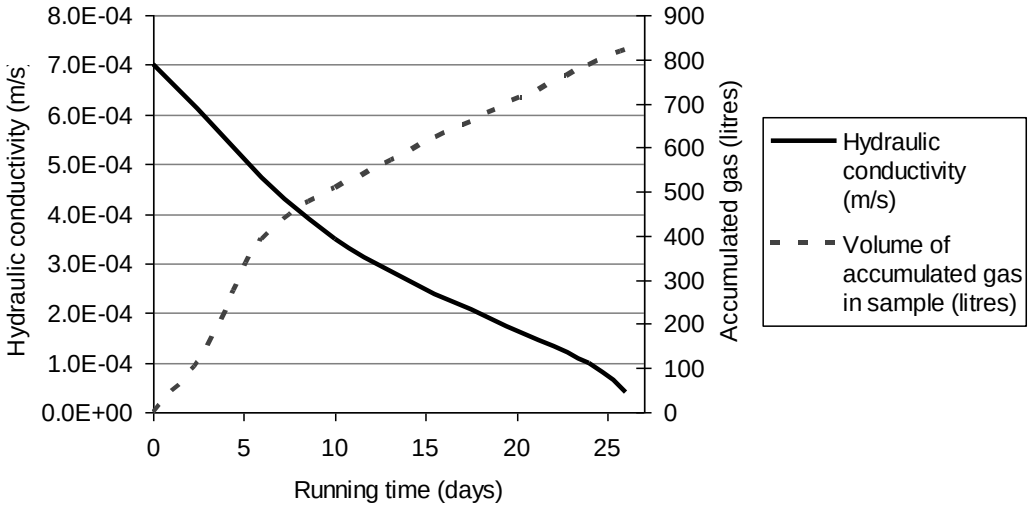

Figure 2.6 Changes in hydraulic conductivity with time for sample SW1 at a constant volume corresponding to an initial applied stress of 40 kPa, with an average pore water pressure of 60 kPa (Powrie et al., 2008)

Table 2.1 summarises the results of hydraulic conductivity tests undertaken by Powrie et al (2008) at initial stresses of 40 kPa and 87 kPa under both high (60 kPa) and low (25 kPa) average pore pressure conditions. At both stresses the hydraulic conductivity was reduced by gas accumulation, by approximately two orders of magnitude in low pore water pressure conditions and one order of magnitude in high pore water pressure conditions. These reductions are explained by Powrie et al (2008) by the large volumes of leachate displaced from the sample by gas accumulation, and the resulting high degree of unsaturation indicated in the last column of Table 2.2.

Table 2.2 Summary of the test results, sample SW1 (Powrie et al, 2008)

Applied Stress[1] (kPa)	Av. pore water pressure (kPa)	Length of test (days)	Accumulated volume of gas (litres)	Initial K (m/s)	Final K (m/s)	% of drainable pore volume occupied by gas (range)
40	25	36	1064	1.0×10^{-3}	1.5×10^{-5}	77.7 – 87.3
40	60	27	820	7.0×10^{-4}	4.0×10^{-5}	57.7 – 67.2
87	25	37	297	1.1×10^{-4}	1.1×10^{-6}	36.5 – 59.9
87	60	34	571	1.5×10^{-4}	1.2×10^{-5}	93.1 – 100

[1]Initial stress at which constant volume was established

Figure 2.7 summarises the variation in hydraulic conductivity of fresh processed MSW varies following compression to stresses between 40 and 228 kPa, in different conditions of gas accumulation and pore water pressure.

The results indicate that gas accumulation in fresh, shredded MSW can significantly reduce the hydraulic conductivity, especially at lower pore water pressures. The reduction in hydraulic conductivity could be up to two orders of magnitude, compared with generally only a one order of magnitude reduction in the drainable porosity and hence the saturated area available for liquid flow. This implies that the intrinsic permeability for liquid flow is also reduced, for example because of a reduction in the size of the pore network through which flow occurs.

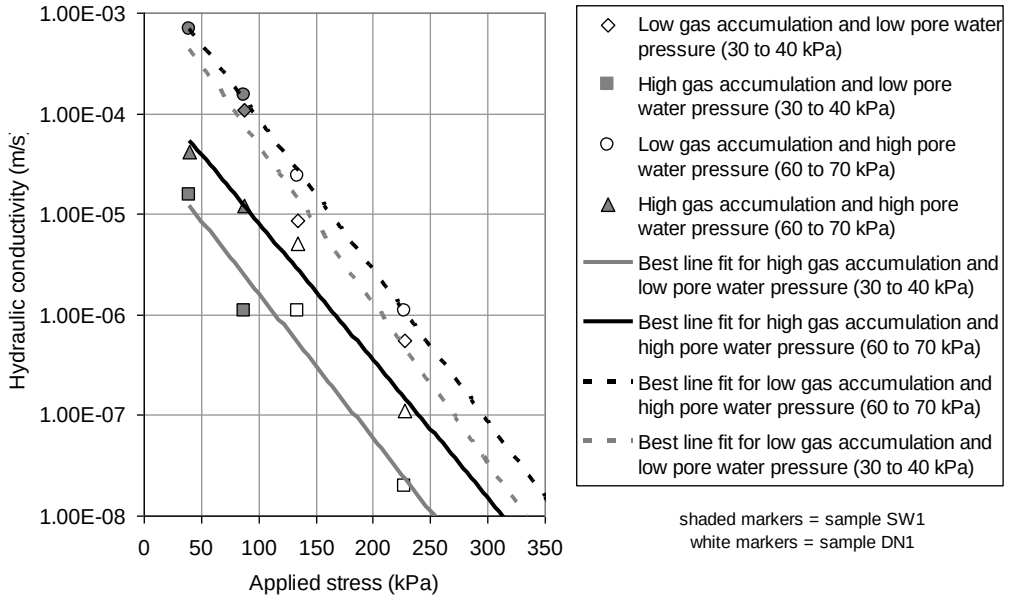

Figure 2.7 Hydraulic conductivity for fresh processed MSW in different conditions of gas accumulation and pore water pressure (Powrie et al, 2008)

Similar effects are likely in any biodegradable waste, even those that have been highly processed (MBT) prior to landfilling. Muennich (1999) found after laboratory tests and calculations that a decrease of the moisture content of MBT waste by 10%, decreased the hydraulic conductivity by more than an order of magnitude as a consequence. The hydraulic conductivity of a gassy waste must be expected to increase if the pore water pressure is increased (e.g. in the vicinity of leachate injection infrastructure), and to reduce if the pore water pressure is reduced (e.g. around a pumped leachate extraction well). Other factors influencing the saturated

hydraulic conductivity are the density (Powrie and Beaven, 1999) and the presence of plastic sheet fragments in the waste (Xie et al., 2006).

2.2.4 Effect of landfill gassing on drainable porosity

Hudson et al (2001) investigated changes in the drainable porosity of MSW in response to gas generation within initially saturated waste in the Pitsea compression cell. Figure 2.8 indicates how gassing significantly reduces the drainable porosity of a waste, and how the drainable porosity is also affected by the pore water pressure (as a result of changes in gas volume).

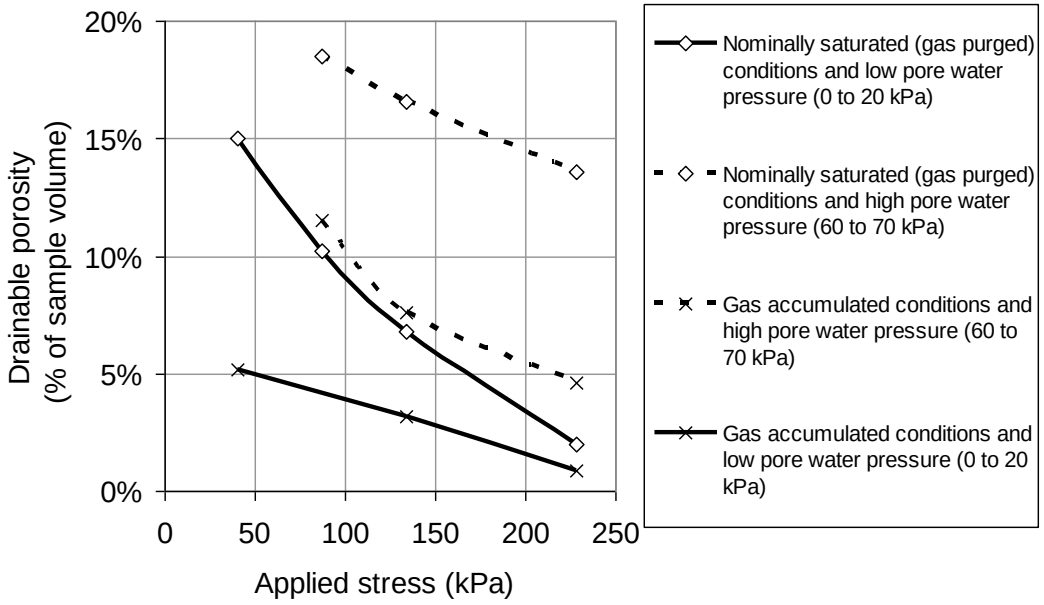

Figure 2.8 Comparison of drainable porosities for sample DN1 according to stress and gas conditions / pore water pressure (Hudson et al, 2001)

When gas was allowed to accumulate in the waste sample there was a reduction in drainable porosity with the largest changes occurring at low effective stresses. This may suggest that gas accumulates preferentially within large voids. When the pore water pressure in the specimen was increased to 60-70 kPa, an increase in drainable porosity was observed. The largest increases were seen when the waste was in low gas accumulation conditions. Smaller drainable porosity increases occurred when the pore water pressure were increased to 60-70 kPa with an initially high volume of accumulated gas in the voids. These changes in drainable porosity are again attributed to gas compression on increasing the pore water pressure and water displacement when gas is allowed to accumulate.

2.3 Relationships of unsaturated flow parameters

2.3.1 Background and definition of moisture (water) content-suction relationship

As discussed in Section 2.1.4, when the water content of an unsaturated waste is below field capacity, water in the pores is affected by surface tension (capillary tension) and the physical attraction (adhesion) between the water and the particles (adhesion). These forces are responsible for developing negative pressure heads in the liquid phase or suction heads ($\psi = p_c/\rho g$) relative to the pressure in the gas phase, equation 2.5.$\psi$is sometimes referred to as the matric suction (e.g. Hillel, 1971). Suction head gradients control liquid flow in the unsaturated zone at water contents below field capacity; hence an understanding of the factors governing suction is important.

As the moisture content falls below the saturation level the larger pores drain first. At a given moisture content the suction head primarily depends on the size of pores at the liquid gas interface. Thus the suction head (ψ) needs to increase in order to reduce the water content, as the moisture retreats into smaller and smaller pores. The relationship between the suction and the water content is conventionally expressed by the water (or moisture) retention curve (WRC; also known as the soil water characteristic curve, SWCC). It is conventional to use the volumetric water content θ for this purpose, although there is no reason why the gravimetric water content or even the degree of saturation S (= V_w/V_v) should not be used. The water retention curve is viewed as a fundamental hydraulic property of a porous medium, and is needed to solve the constitutive equations for water flow in the unsaturated zone; Richards' equation is a well-known example, Richards (1931).

At a given suction, the water content during drainage is larger than during wetting; i.e., the water retention curve exhibits hysteresis. Hysteresis can be attributed to the "ink-bottle" effect (water remaining trapped in closed-bottomed voids during drainage that are inaccessible on wetting from the bottom up), trapped air, and the difference in contact angle between a solid surface and an advancing and a receding liquid front (Hillel, 1998). The main drying curve and the main wetting curve initiate from points of θ_s (saturated moisture) and θ_r (residual moisture). Cycles that do not initiate from these two points follow paths within the region enclosed by the main curves and are referred to as scanning curves in Figure2.9).

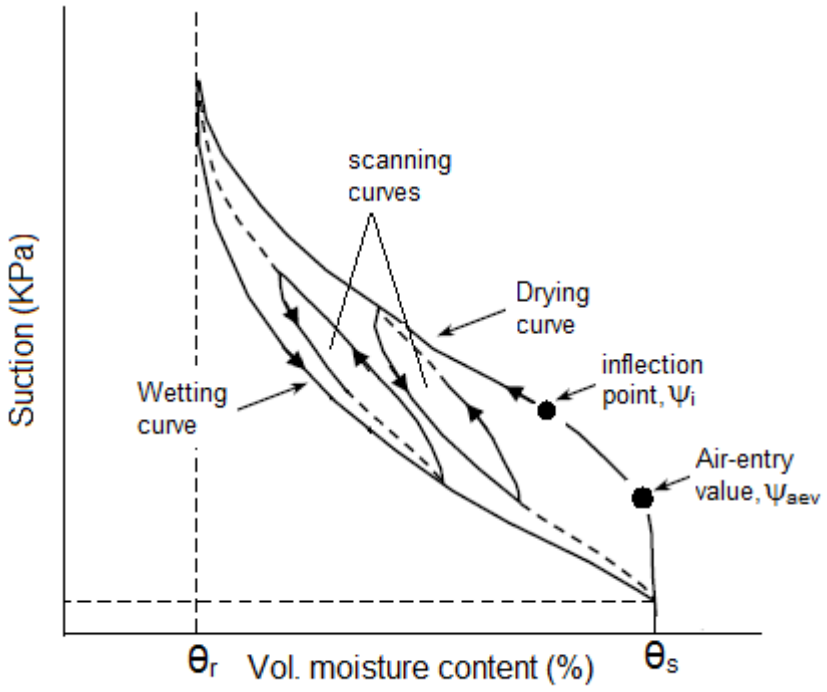

Figure 2.9 Schematic moisture retention curve and hysteresis effect (after Huang et al, 2004)

The suction at which the material starts to desaturate is defined as the air entry value, ψ_{aev}. As the suction increases above ψ_{aev}, the water content decreases following an S-shaped curve with an inflection point, ψ_i(Figure 2.9) towards the residual value, θ_r. The air-entry value depends on the maximum pore size and the pore-size distribution. Materials with large, uniformly shaped pores have relatively low air entry values of suction. The slope of the water retention curve indicates the amount of liquid taken up or released by the waste as a result of a change in pore suction.

2.3.2 Functional Forms of Moisture Retention Curve

The typical form of a moisture (water) retention curve for a particulate porous material is indicated in Figure 2.9. The key physical parameters are

- the saturated water content, θ_s
- the suction at which the material starts to desaturate on drying, generally known as the air entry value, ψ_{aev}
- the irreducible water content θ_r, to which the moisture retention curve becomes asymptotic at very high suctions.

The air entry value depends on the maximum pore size and the pore size distribution. Materials with large, uniformly shaped pores have relatively low air entry values. By observation, the θ-ψcurve is approximately hyperbolic in form, passing through the point ($\theta = \theta_s$, $\psi = \psi_{aev}$) and tending towards an asymptote at $\theta = \theta_r$. A number of empirical expressions have been proposed to describe the curve; three of the more well-known forms that have been applied to wastes are summarized below and in Table 2.2.

Brooks and Corey (1964) proposed an algebraic relationship of the form

$$\theta = \theta_r + (\theta_s - \theta_r)(\psi / \psi_{aev})^{-\lambda} \quad (2.18)$$

The parameter λ characterises the range of the pore size distribution, and is referred to as the pore size distribution index. Theoretically, its value approaches infinity for a medium with a uniform pore-size distribution, whereas it approaches a lower limit of zero for soils with a wide range of pore sizes.

This expression is only used to the point (θ_s, ψ_{aev}), and is not applicable in the region $\psi<\psi_{aev}$. Taking this into account, and defining the effective degree of saturation, S_e, (or normalized moisture content) as the volume of free water / volume of drainable pores, $S_e = (\theta - \theta_r)/(\theta_s - \theta_r)$, the form of the Brooks and Corey Equation becomes:

$$S_e = (\psi_{aev} / \psi)^{\lambda} \text{ for } \psi \geq \psi_{aev} \text{ and} \quad (2.19)$$

$$S_e = 1 \text{ for } 0 \leq \psi < \psi_{aev}$$

The expressions proposed by **Clapp and Hornberger (1978)** and by **Campbell (1974)** have the same power law function as Brooks and Corey (1964), but the dependent variable is the degree of saturation, S (= θ/θ_s) rather than the effective saturation, S_e.

$$\psi = \psi_{aev} (\theta / \theta_s)^{-b} \quad (2.20)$$

S follows the conventional definition and includes moisture in effectively inaccessible pores.

The **van Genuchten (1980)**formula covers the whole of the suction-moisture content range with a single continuous expression (Equation 2.21), which is one reason for its popularity compared with that proposed by Brooks and Corey (1963) when the relationship is required to be used in a numerical algorithm.

$$\theta = \theta_r + (\theta_s - \theta_r)/[1+(\alpha|\psi|)^n]^m \quad (2.21)$$

The parameter α is related to the inverse of the air-entry value; n (n>1) is related to the width of pore size distribution and *m* is an indication of the asymmetry of the curve. Van Genuchten proposed the formula in response to the work of Mualem (1976) which required a function that could be integrated to derive a relationship linking relative permeability with moisture content. A closed form integral can be obtained when m=1-1/n.

The impact of the van Genuchten parameters α and n on the moisture retention curves up to 10kPa is shown in Figures 2.10 and 2.11. It may be observed that as both α and n increase the suction calculated by the van Genuchten function, equation 2.21, reduce or as both α and n decrease the moisture retention curve is getting steeper and the air-entry value increases.

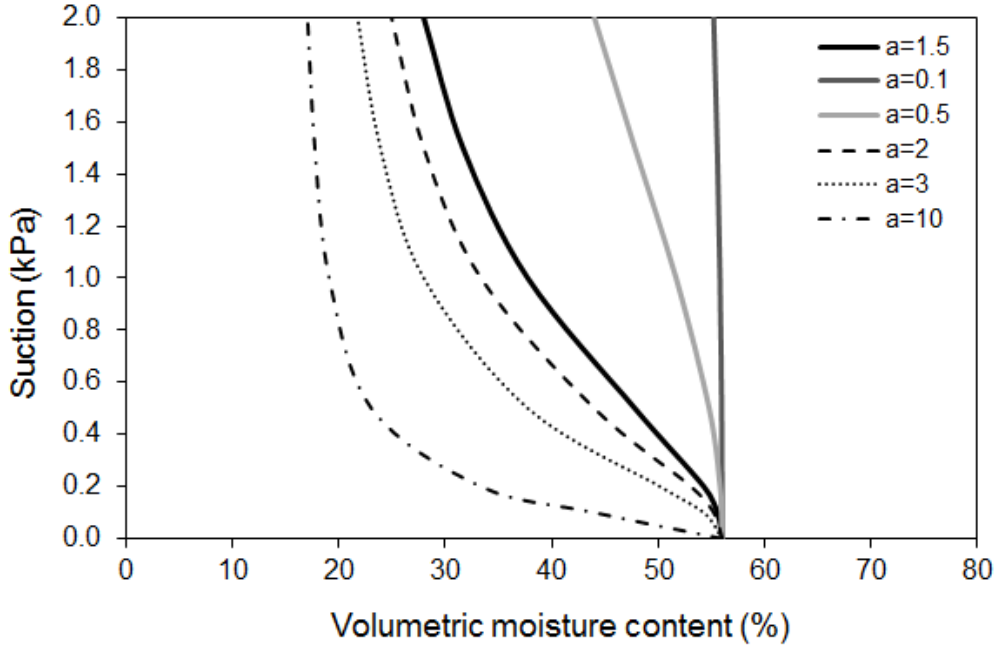

Figure 2.10 Impact of the van Genuchten parameter α on the moisture retention curve

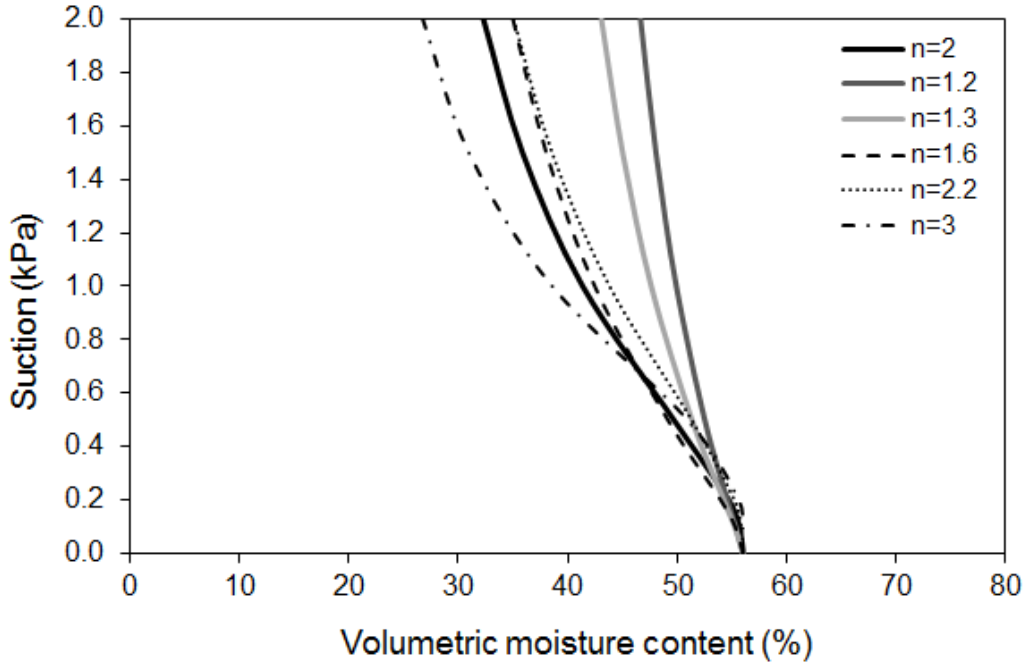

Figure 2.11 Impact of the van Genuchten parameter n on the moisture retention curve

McKee and Bumb (1984):

$$\theta = \exp\left[-\left(\frac{\psi - \alpha}{b}\right)\right] \tag{2.22}$$

here ψ: suction head and α, b: curve fitting parameters

McDougall et al (2006) modified the form given by McKee and Bumb (1984) to

$$\theta = (-0.1)\ln\left(\frac{\psi - 0.622}{-20.622}\right) \tag{2.23}$$

Functional forms of the suction-moisture content relationship such as Equations 2.18 to 2.23 permit the numerical solution of Richards' equation (Equation 2.7). They can also be used to solve other unsaturated flow equations because they provide a convenient means of calculating the capillary pressure from the water content which then allows the liquid and gas pressure fields to be de-coupled and solved separately using Equation 2.5.

2.3.3 Moisture retention curves in waste

The moisture retention curve represents a series of equilibrium states of moisture contents and corresponding suctions. Determination of a moisture content-suction relation is difficult even in relatively well understood granular media such as soils, owing to the effects of hysteresis and the dependence of the relation on state variables such as void ratio and properties such as particle and pore size distributions and shapes.

The moisture retention curve represents a series of equilibrium states in which the water content and the corresponding suction are known. The moisture (water) content is usually determined by oven drying or by non-destructive and easily repeatable indirect methods (Appendix B). Yuen et al. (2000) and Imhoff et al. (2006) reviewed several techniques for measuring the moisture content of landfilled wastes. They concluded that there are difficulties with using tensiometers (Korfiatis et al, 1984) and gypsum blocks(Reinhart, 1996 and Rosqvist et al., 1997),but that the neutron probe offers the possibility of at least measuring relative changes in moisture content (Holmes, 1984). Electrical resistivity and TDR sensors tended to give biased estimates, with instrument-determined moisture contents larger than independent estimates.

There are a number of methods for determining suction in the field and the laboratory. These methods are categorised as either ‘direct’ or ‘indirect’, depending on whether the suction is measured directly or indirectly through an intermediate medium or parameter. Direct methods include tensiometers (Tarantino and Mongiovi, 2001), suction probes (Ridley and Burland, 1993; Guan and Fredlund, 1997), the hanging water column (Haines 1930; Vanapali et al, 2008) and pressure plate apparatus (Soilmoisture Equipment Corp., 2002). The pressure plate apparatus technique may not be sensitive enough for some wastes at low suctions (< 5 kPa), and the equilibration time at higher suctions can be in the order of months (Kazimoglou, 2007).

Indirect methods include the filter paper technique (Gardner, 1937; ASTM 1997; Ridley, 1995), gypsum block (Ridley and Wray, 1995) and psychrometry (Spanner, 1951; Campbell & Gardner, 1971; Ridley and Wray, 1995). These methods involve equilibration of the pore suction in the sample with that in a second medium (e.g. a filter paper or a gypsum block), whose water content-suction relationship has been determined in a previous calibration or correlation with a

third parameter such as relative humidity (Agus and Schanz, 2005). Changing the pore water chemistry may invalidate previous calibrations of intermediate media (Fredlund and Rahardjo, 1993).

A number of researchers have determined moisture retention curves for MSW or waste-like materials, as summarized in Table 2.3, and have then usually applied one or more of the more popular curve-fits (Equations 2.18-2.23) to the data. Table 2.4 summarises the fitted parameter values and Figure 2.12 illustrates most of the experimental results (as individual data points) and the fitted continuous curves. The data have been semi-normalised as suction against degree of saturation, rather than plotted as suction against volumetric moisture content. This enables moisture retention curves for materials with different values of θ_s to be compared more easily on the same graph. Moisture retention data from the sources indicated in Table 2.4 have been fitted to the van Genuchten (Equation 2.21) and Brooks and Corey (Equation 2.18) expressions, with the former giving a better match (Appendix C).

Table 2.3 Summary of experimentally determined moisture retention curves for wastes and waste-like materials

Author(s)	Material(s)	Method
Korfiatis(1984)	MSW	Column cell instrumented with two vertical lines of tensiometers
Jang (2002)	MSWKimpo metropolitan landfill, Korea	Pressure plate (7.2 cm diam., 12cm height)
Imam (2003)	Synthetic waste	Filter paper
Kazimoglu (2005,2006)	MSW with similar composition to waste in Lyndhurst landfill site	Pressure plate (25 cm diam., 14 cm height)
Stoltz (2007)	Drilled French MSW (1 year) <100 mm	Suction oedometer(27 cm diam., 4.4 cm height)
Muennich (2009)	German MBT <25 mm	Suction ceramic plate
Staub (2010)	French fresh and degraded MSW<70mm	Pressure plate (15.4 cm diam., 6.4 cm height)
Stoltz (2011)	Drilled French MSW (fresh) <40 mm (high organic)	Suction oedometer(27 cm diam., 4.4 cm height)
Breitmeyer (2011a)	MSW <25 mm from S.Wisconsin landfill USA (4 months old)	Hanging column (15 cm diam., 2.5 cm height)
Wu (2012)	MSW borehole sampling, landfill in China <40 mm	Pressure plate (15.6 cm diam., 12 cm height)
McDougall (1996)	Mix of partially humified peat and cocoa shells	Hanging column

Table 2.4Moisture retention parameters for modeled waste

Author	Fitted curve	Dry density (kg/m^3)	ψ_{aev} (kPa)	θ_s	B	θ_r	α (kPa^{-1})	n
Korfiatis (1984) MSW	Clapp and Hornberger (1978)		0.62	0.55	1.5			
Jang (2002) MSW 80% compaction	van Genuchten (1980) - Mualem (1976)	-		0.45		0.125	0.49	1.81
Jang (2002) MSW 100% compaction		-		0.36		0.1	0.12	1.27
Jang (2002) MSW 120% compaction		-		0.26		0.19	0.092	2.14
Imam (2003) synthetic		750		0.35		0.01	0.049	1.45
Kazimoglu MSW (2005,2006)		560		0.58		0.14	1.4	1.60
Stoltz (2007) MSW		540		0.62		0.27	1.85	2.42
Stoltz (2007) MSW		770		0.45		0.33	0.5	2.29
Stoltz (2011) MSW (fresh-high organic)		460		0.64		0.35	1.75	1.37
Muennich (2009) MBT		660		0.52		0.24	0.42	1.42
Muennich (2009) MBT		810		0.38		0.21	0.18	1.4
Staub (2010) fresh MSW		380		0.77		0.15	3.5	1.37
Staub (2010) degraded MSW		580		0.68		0.15	0.9	1.34
Breitmeyer (2011a) fresh MSW		561		0.60		0.21	3.38	1.85
Breitmeyer (2011a) fresh MSW		632		0.53		0.22	2.92	1.58
Wu (2012) 1-4m deep, 3 years old MSW		712		0.69		0.2	1.18	1.59
Wu (2012) 22-25m deep, 10 years old		1460		0.53		0.27	0.71	1.49

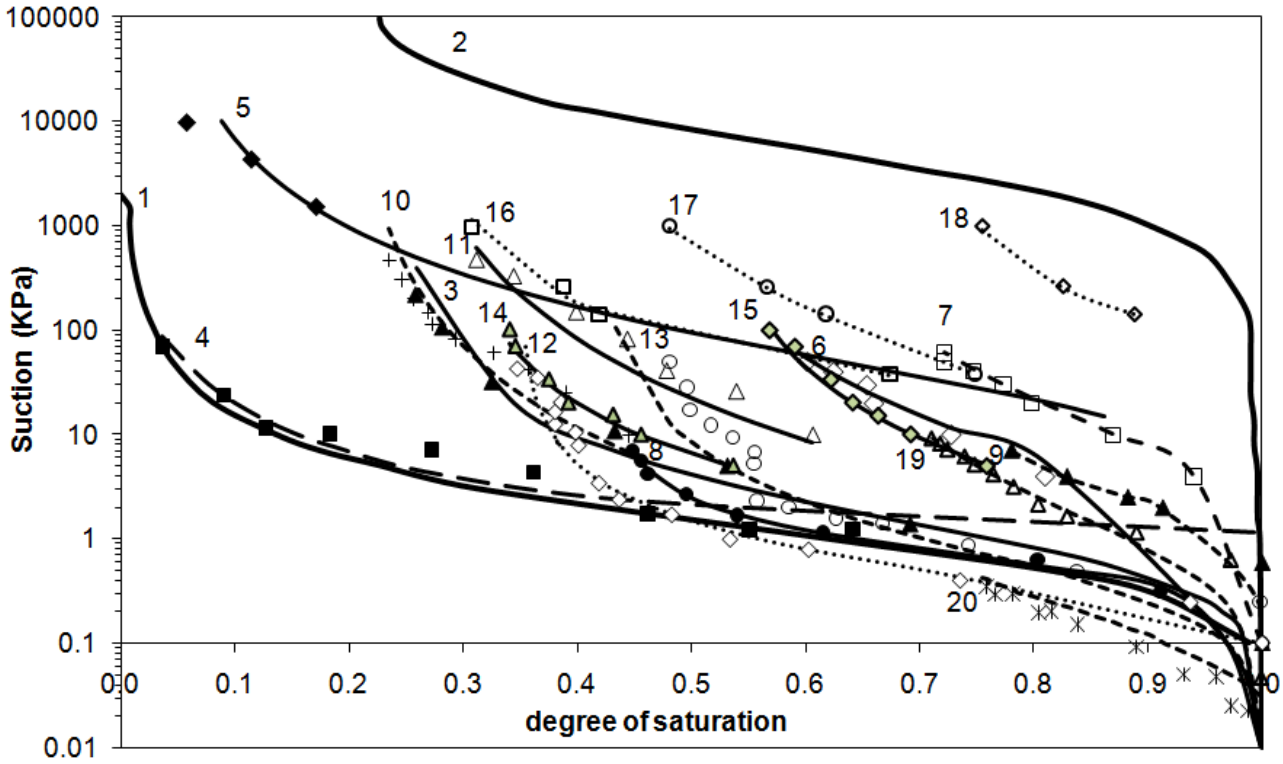

1. Coarse sand (Karvonev,2001)
2. Clay (Warrick,2002)
3. MSW Kazimoglu (2005) van Genuchten curve fit
4. MSW Korfiatis (1984) Clapp & Hornberger curve fit
5. Synthetic waste Imam (2003) vanGenuchten curve fit
6. MBT Muennich (2009) van Genuchten curve fit
7. MBT Muennich (2009) van Genuchten curve fit
8. MSW Stoltz (2007) van Genuchten curve fit
9. MSW Stoltz (2007) van Genuchten curve fit
10. MSW fresh Staub (2010) van Genuchten curve fit
11. MSW degrated,Staub (2010) van Genuchten curve fit
12. MSW Breitmeyer (2011) van Genuchten curve fit
13. MSW Breitmeyer (2011) van Genuchten curve fit
14. MSW Wu (2012) van Genuchten curve fit
15. MSW Wu (2012) van Genuchten curve fit
16. MSW Jang (2002) van Genuchten curve fit
17. MSW Jang (2002) van Genuchten curve fit
18. MSW Jang (2002) van Genuchten curve fit
19. MSW Stoltz (2011) van Genuchten curve fit
20. Cocoa shells+peat McDougall (1996) McKee & Bumb curve fit

data 560 kg/m3
data 620 kg/m3
data 350 kg/m3
data 660 kg/m3
data 810 kg/m3
data 540 kg/m3
data 770 kg/m3
data 380 kg/m3
data 580 kg/m3
data 561 kg/m3
data 632 kg/m3
data shallow (1-4 m)
data deep (22-24 m)
data 80% compaction
data 100% compaction
data 120% compaction
data 460 kg/m3
data

Figure 2.12 Comparison of moisture retention curves for waste materials

Curves 1(coarse sand) and 2 (clay) are included for comparison.

The van Genuchten parameter values for coarse sand (Karvonev, 2001) are:

θ_r=0.01, θ_s= 0.4, α=1.6 kPa^{-1} and n= 1.73

and for clay (Warrick, 2002):

θ_r=0.098, θ_s= 0.46, α= 0.15 kPa^{-1} and n= 1.25

As shown in Figure 2.12 a sharp decrease in moisture content was observed at low suction levels ranging from 0 to 10 kPa. This is mainly attributed to the wide pores in MSW (in the order of millimeters). The drainage of the wide pores occurring at even low suction resulted in low air-entry values, ψ_{aev}.

Table 2.4 shows that the van Genuchten parameters α and n tend to decrease with increasing dry density for the same waste material. This is because increasing the density tends to eliminate the largest pores, increasing the suction needed for air entry and desaturation.

According to the study of Wang et al. (2000), ψ_{aev} can be determined from the equation:

$$\psi_{\mathrm{aev}} = \frac{1}{\alpha}\left[\frac{n-1}{n(m+1)-n+1}\right]^{1/n} = \frac{m^{1/n}}{\alpha} \qquad (2.24)$$

and indicates that ψ_{aev} increases with n (note the influence of m=1-1/n in Equation 2.24)

The air-entry value (ψ_{aev}) obtained from Equation 2.24varied from 0.18 kPa to 2.46 for the waste materials listed in Table 2.4, except the case of Jang (2002) MSW with compaction 120% where the calculated ψ_{aev} was 8.1 kPa. The increase in n ψ_{aev} with density and age is attributed to the larger overburden pressure, higher decomposed organic matter, and finer and more uniform pore space presented by the high proportion of fine particles in the deeper layer (Wu et al, 2012).The evolution of overburden pressure, organic matter, and pore space is also reflected by the steepness of the MRC, which is associated with the parameter n presented in Table 2.10. In general, the MSW data had an n value ranging from 1.27 to 2.42

Breitmeyer (2011b) evaluated the hydraulic properties of municipal solid waste at various dry unit weights and levels of decomposition at laboratory and field-scales. He found that the changes in the MRC of MSW with increasing dry unit weight were consistent with expected increases in air-entry value (ψ_{aev}). Data obtained from the laboratory-scale MRC tests indicated increases in the size of the largest pores (decreases of the air-entry value) with increasing decomposition.

2.3.4 Unsaturated permeability definition

Leachate movement through the waste mass is controlled by the hydraulic conductivity or permeability of the waste. The distribution of permeability within the waste, which will vary as a result of anisotropy, heterogeneity, partial saturation and changes in waste density or effective stress, is also of vital importance. Most of the waste in many landfills will probably be above the leachate level and therefore experiencing unsaturated flow, through the vertical percolation of rainwater or other infiltrating liquid. It is generally only the bottom layers in a landfill below the leachate level and in a capillary saturated zone, or possibly perched horizons that will be fully saturated. The presence of landfill gas would also tend to reduce the degree of saturation, even at the base. While the model of uniform Darcy flow may or may not be appropriate to wastes with their large range of particle size and material type, likely anisotropy and presence of preferential flow channels, it is analytically convenient and has formed the basis of nearly all studies of waste hydraulic behaviour. Dual-porosity and dual permeability models have been suggested to describe the two domain flow (Section 2.2.2). The hydraulic conductivity is the key parameter used to characterise and quantify liquid flow. The hydraulic conductivity of a porous medium varies significantly with the degree of saturation (Fredlund and Rahardjo, 1993), and this is true in wastes as in soils.

In an unsaturated porous medium, the coefficient of permeability is affected by combined changes in the void ratio and the degree of saturation (or water content) of the medium. Thus, since the largest pores are drained first, the unsaturated hydraulic conductivity falls quickly as the volumetric water content decreases (Warrick, 2002). This is due to the fluid that is confined in smaller scale pore spaces which have different pore geometry and therefore different intrinsic permeability (K)[1]. The unsaturated hydraulic conductivity, k, may therefore be related to the volumetric water content, θ. The relative permeability, $k_{r,L,G}(\theta)$ for the liquid and gas phase may be defined as:

$$k_{rL,G}(\theta) = k_{L.G}(\theta) / k_s \qquad (2.25)$$

[1]Intrinsic permeability is a coefficient that depends only on the pore geometry characteristics, pore size, porosity, pore connectivity and tortuosity.It relates to the permeability of a porous material to a fluid by the equation : $k^F = K\rho^F g / \mu^F$

where $k_{LG}(\theta)$ is the permeability at a volumetric water content θ and k_s is the permeability in saturated conditions. The range of the saturated hydraulic conductivity values reported in previous studies on MSW and MBT is shown in Appendix D.

The typical variations in the relative permeabilities, k_{rG} and k_{rL}, for soil are presented in Figure 2.13. In this graph the residual saturations S_{RG} and S_{RL} are introduced. These saturations correspond to the quantity of fluid that cannot be removed from the porous medium by fluid flow.

If a porous medium is fully saturated, all possible liquid flow channels are available to water and the liquid permeability will be at its highest (and the relative liquid permeability equal to 1). By definition, the gas permeability must be zero in the fully saturated state. As the medium becomes unsaturated, liquid will drain initially from the largest pores to be replaced by gas. This means that the liquid permeability will immediately start to decrease quite rapidly as permeability is lost from the largest pores first. However, permeability to gas will rely on the flow of gas through liquid filled pores, until the stage is reached at which there is continuity within the gas phase. At this point, a rapid increase in the gas permeability might be expected. Similarly, the liquid permeability might reduce dramatically when the liquid phase becomes discontinuous, but there is a possibility that liquid flow will remain possible through mainly gas filled pores. In an inhomogeneous material such as a waste, the sudden development of a gas-permeable channel is perhaps more likely than in a uniform porous medium, in which water will more reliably drain from the largest pores first.

As shown in Figure 2.13, the relative permeability of the gas phase is greater than that of the liquid phase at low to moderate liquid saturations because the gas occupies larger pores. The relative permeabilities do not sum to one. This has been attributed to flow pathways traversed by two fluid phases being more tortuous than those traversed by a single phase (Scheidegger, 1974) or to pores with static menisci that do not contribute to flow (Demond and Roberts, 1987).

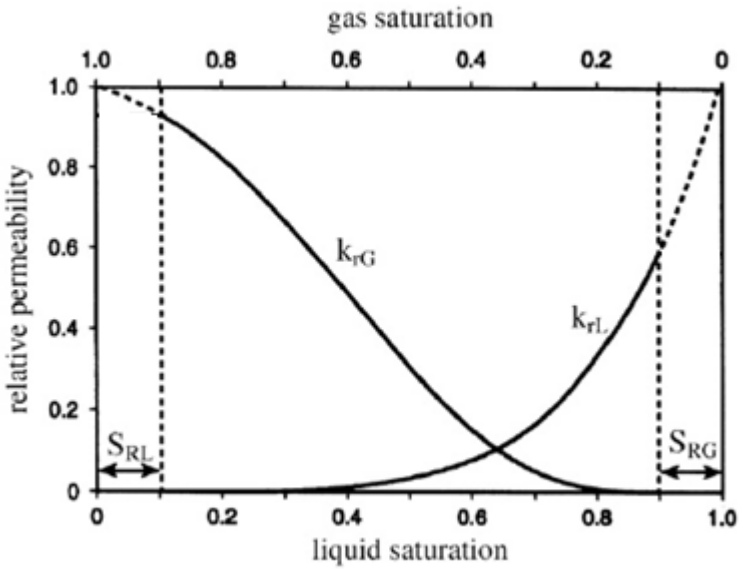

Figure 2.13 A typical example of relative permeability curves (after Warrick, 2002)

Relative permeabilities, like capillary pressure, depend on the distribution of the two fluids in the pores. Owing to capillary hysteresis, the relationship between the relative permeability and the suction is different in wetting and drying for the gas phase.

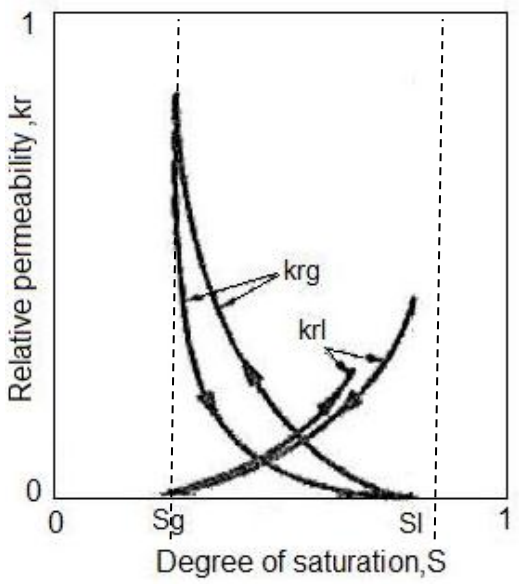

Figure 2.14 Hysteresis effect of relative permeability curves (after Marle, 1981)

The relative permeability of the liquid phase changes only slightly with the direction of the variation of saturation (Figure 2.14). The relative permeability of the gas phase, in contrast, is clearly less during wetting than during drainage. This is the result most frequently observed in porous media (Marle, 1981).

2.3.5 Functional forms of unsaturated permeability for waste materials

Direct measurement of unsaturated hydraulic conductivity is difficult in soils (Lam et al, 1987), and more so in waste because of the degradable, compressible and heterogeneous nature of the material. Thus it is tempting to try to estimate the unsaturated hydraulic conductivity on the basis of the moisture content (Campbell, 1974). Several empirical relationships between unsaturated hydraulic conductivity and moisture content or relative permeability and effective degree of saturation have been proposed for the liquid phase, including:

van Genuchten (1980) after Mualem (1976):

$$k_r\left(S_e\right) = S_e^l\left(1-\left(1-S_e^{1/m}\right)^m\right)^2 \tag{2.26}$$

The parameter$l$ accounts in Mualem's original interpretation for tortuosity and connectivity, so that in a physical sense> 0. Mualem (1976) determined an optimal value of l = 0.5 (an average value for soils).However, its physical meaning is questioned, and l is often treated as a free fitting parameter that is frequently negative. Breitmeyer and Benson (2011a) recommended $l$values for MSW between -0.65 and -3.59.The parameter m is taken equal to: m=1-1/n (Mualem, 1976) and S_e the effective degree of saturation and is estimated from the equation:

$$S_e = \frac{\theta - \theta_r}{\theta_s - \theta_r}$$

Clapp and Hornberger (1978):

$$k(\theta) = k_s\left(\frac{\theta}{\theta_s}\right)^B \tag{2.27}$$

Campbell (1974):

Campbell argued that the coefficient B should be replaced by the relationship B=2b+3.

$$k(\theta) = k_s\left(\frac{\theta}{\theta_s}\right)^{2b+3} \tag{2.28}$$

Brooks and Corey (1966):

$$k(\theta) = k_s \left(\frac{\theta - \theta_r}{\theta_s - \theta_r} \right)^{(2+2.5\lambda)/\lambda} \quad (2.29)$$

Davidson et al (1969):

$$k_r = 10^{10\varphi(S-1)} \quad (2.30)$$

where φ: porosity and S: degree of saturation.

Noble and Arnold (1991) compared the power law equations proposed by both Korfiatis et al. (1984) and Straub and Lynch (1982); to an exponential relationship:

$$k(\theta) = k_s e^{\gamma(S_e - 1)} \quad (2.31)$$

A number of researchers have estimated the unsaturated conductivity by using the above functions. Only two, Kazimoglu et al (2006) and Breitmeyer and Benson (2011a) carried out experiments to measure the unsaturated hydraulic conductivity of MSW materials. Table 2.5 summarises the fitted parameter values and Figure 2.15 illustrates both the experimental results (as individual data points) and the fitted continuous curves. The data have been semi-normalised as relative permeability against degree of saturation, rather than plotted as relative permeability against volumetric moisture content. This enables relative permeability curves for materials with different values of θ_s to be compared more easily on the same graph.

Table 2.5 Parameters of the unsaturated hydraulic conductivity for modeled waste

Author (dry density)	model	γ	k_s (m/s)	θ_s	θ_r	B	α(kPa^{-1})	n	*l*
Straub andLynch (1982)	Campbell		$6.3x10^{-9}$	0.375	-	8		-	-
Ahmed et al (1992)	Campbell	-	$2.0x10^{-4}$	0.42	-	11		-	-
Korfiatis et al (1984)	Clapp and Hornberger	-	$1.2x10^{-4}$	0.55	-	11		-	-
Noble and Arnold (1991)	Exponential equation	11	-	-	-	-		-	-
McDougall et al (1996)	Davidson et al (1969)	-	-	0.82	-	-		0.35	-
Haydar and Khire (2005)		-	10^{-5}	0.45	0.067	-		1.41	0.5
Kazimoglu et al (2006) 560 kg/m^3	van Genuchten (1980)-Mualem (1976)	-	10^{-5}	0.58	0.14	-	1.4	1.60	0.5
Breitmeyer (2011a) 561 kg/m^3		-	$7.0x10^{-5}$	0.60	0.21	-	3.38	1.85	-0.65
Breitmeyer (2011a) 632 kg/m^3		-	$2.7x10^{-5}$	0.53	0.22	-	2.92	1.58	-1.23
Breitmeyer (2011a) 795 kg/m^3		-	$4.0x10^{-7}$	0.41	0.03	-	1.18	1.33	-3.59

Kazimoglu et al. (2006) compared the unsaturated hydraulic conductivity of MSW obtained using Passioura's (1976) one-step outflow test method on waste with a dry density of 0.56 t/m^3 with calculations using van Genuchten's model (Equation 2.26: Figure 2.15). Recently, Breitmeyer and Benson (2011a) measured the unsaturated hydraulic conductivities of MSW samples with different dry densities using the transient outflow data (Gardner method, 1956) from the hanging column tests. The unsaturated data were fitted to the van Genuchten and Brooks and Corey models. In Figures 2.15 and 2.16 only van Genuchten fittings (Equation 2.26) are presented. In Figure 2.16, it is observed that the measured and calculated values of calculated hydraulic conductivities showed good agreement at

low moisture contents (high suctions). At higher moisture contents, the measured and calculated hydraulic conductivities diverged. This may be a result of the wide range of pore sizes, and may indicate dual porosity effects. At lower moisture contents, the hydraulic conductivity is controlled by the smaller pores. However at higher moisture contents, the onset of desaturation and the air entry value are governed by the larger pores: thus there is an indication that a single van Genuchten type curve might not be able to capture the whole range of behaviour and may require some refinement possibly through use of the dual porosity concept. This problem might resolve itself at higher stresses, as the larger pores close and the range of pore size is reduced, this is noticed in the case of the high density of MSW of 795 kg/m^3 in Figure 2.16. So, dual porosity might only be an issue at low stresses.

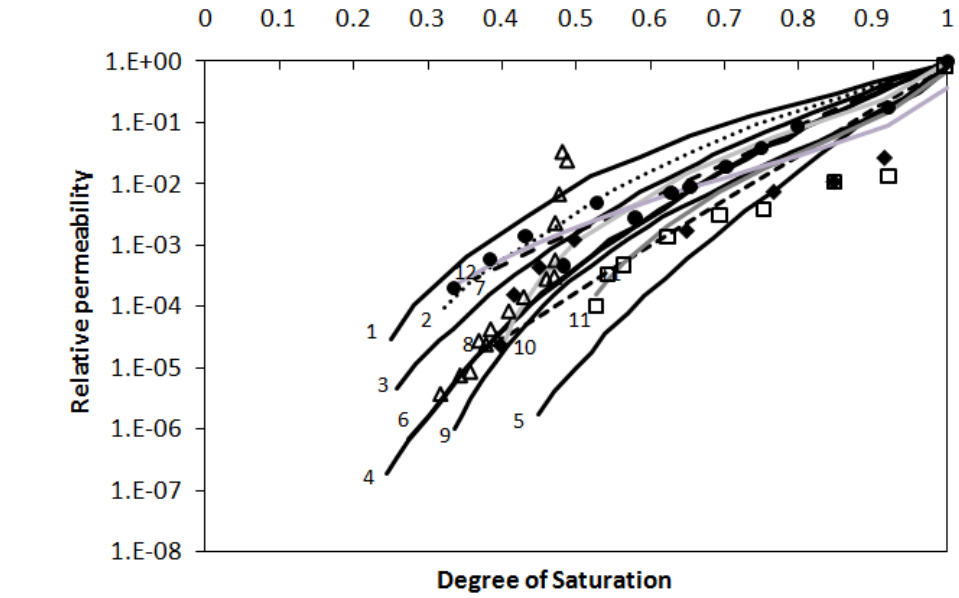

1. Miller & Wright (1988), Brooks & Corey fit
2. Straub & Lynch (1982), Clapp & Hornberger fit
3. Demetrakopoulos & Korfiatis (1986), Clapp & Hornberger fit
4. Ahmed et al. (1992), Campbell fit
5. Demetrakopoulos & Sehayek (1986), Campbell fit
6. Korfiatis & Demetrakopoulos(1984), Clapp & Hornberger fit
7. McDougal et al (1996), Davidson et al. fit
8. Noble & Arnold (1991), exponential equation fit
9. Kazimoglu et al. (2006), van Genuchten fit
10. Breitmeyer & Benson (2011) van Genuchten fit
11. Breitmeyer & Benson (2011), van Genuchten fit
12. Breitmeyer & Benson (2011), van Genuchten fit

data 560 kg/m3
data 561 kg/m3
data 632 kg/m3
data 795 kg/m3

Figure 2.15 Comparison of relative permeability functions for MSW materials

The influence of the dry density on unsaturated hydraulic conductivity is not clear from the above graph. In Figure 2.16, it is observed that the unsaturated hydraulic conductivity of MSW at a given degree of saturation decreases as the dry density increases.

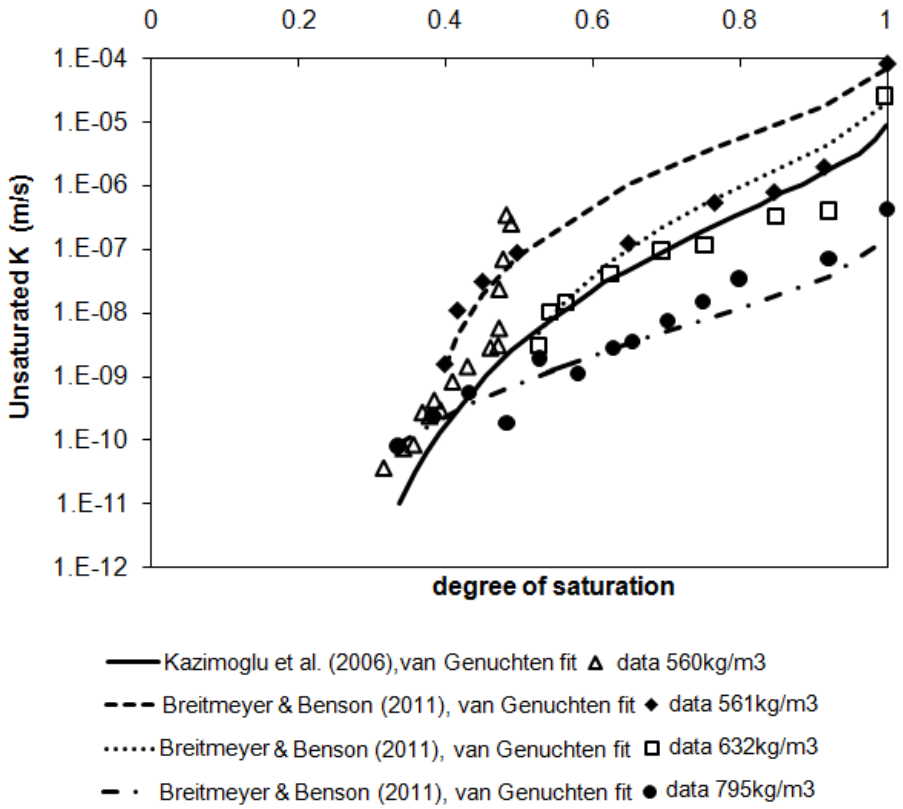

Figure 2.16 Influence of dry density to unsaturated hydraulic conductivity functions for MSW materials

Finally, Breitmeyer (2011b) found that at lab and field-scale, the unsaturated hydraulic conductivity, k(θ), decreased with decomposition and compression, suggested that unsaturated flow through degraded MSW is confined primarily to small pores after large pores that develop because of decomposition drain under very low matric suction.

2.4 Summary

In this chapter the description and basic definitions of the characteristics of unsaturated flow in porous material were presented. These characteristics attempt to take into account the complexities of a three-phase micro-system in which the solid, liquid and gas phases all interact.

Some of the constitutive equations of unsaturated fluid flow have been described together with the modelling approaches required to solve the equations. These approaches involve determining analytical relationships between capillary pressure and moisture content and relative permeability and moisture content, and where these have been found to be inadequate further refinements have been made based on the concept of dual porosity. The application of these models is difficult because many complex input parameters are required, for which there are no readily available databases of values appropriate for waste.

A comprehensive review of previous work on moisture retention characteristic curves and unsaturated permeability functions for wastes has been made, demonstrating the influence of dry density on these functions using the parameters of the van Genuchten function.

It may be observed that most of the data found in the literature are derived from pressure plate and hanging column experiments on MSW waste. The research work reported in this thesis adds new moisture retention and relative permeability data from a drainage column experiment on mechanically and biologically treated (MBT) waste specimens. The data is supported by conventional tests using the pressure plate apparatus and hanging water column which enables a comparison to be made between the difference techniques.

The data has been analysed using the framework of the van Genuchten function. This was chosen because it was derived from considerations of the geometry of the physical characteristics of the pore structure of the porous media involved following the work of Mualem (1976) which offers the prospect of extrapolating functional relationships obtained from one material type to another. This feature has made it a very popular function with other workers and as a result a number of parameter values have been obtained and are available to use as a method for comparing results.

The underlying physics of the van Genuchten function also provides a stepping stone into refinements based on the dual porosity concept. Extending the analysis of the new experimental results to a dual porosity framework is outside the scope of this thesis although some runs of the HYDRUS model described in Chapter 6 have included the HYDRUS dual permeability capability.

CHAPTER 3

EXPERIMENTAL METHODOLOGY AND MATERIALS

3.1 Introduction

The previous chapter provided a detailed literature survey on the characteristics of three-phase systems, fluid flow in the unsaturated zone and a review of previous laboratory work on moisture retention characteristic curves and unsaturated permeability functions for wastes plotted in semi-normalised way for easy comparison. This chapter describes the waste samples tested and the different experimental techniques (drainage, pressure plate and hanging water column) used for the determination of the moisture retention characteristics and unsaturated permeability for Mechanically and Biologically Treated (MBT) waste specimens.

The waste samples were from a (MBT) waste residue processed to a maximum particle size of 10mm, and are described in detail in Section 3.2. The three different experimental techniques, which are described further in Sections 3.3, 3.4 and 3.5 were:

(1) The analysis of the time-dependent data obtained during the transient drainage of a 0.56 m high column of the waste from an initially saturated state. The data consisted of the leachate outflow volume (measured using an electrical balance) and, at various elevations, volumetric moisture content (measured using Delta-T Devices model ML2x theta probes) and pore pressure (measured using Delta-T Devices model SWT5 tensiometers). .
(2) The hanging water column method, in which the water within a small waste sample is subjected to suction pressures by a “hanging” column of water below it. This is convenient for suctions 0 to 10 kPa (0 to 1 m of water). Equilibrium times vary with waste texture and volume of micropores, and may be hours or days.
(3) The pressure plate technique, where instead of applying liquid phase suctions, specimens are subjected to elevated air pressures. This technique, which

assumes that it is the relative rather than absolute values of pore air and liquid pressures that govern the water retention characteristics, is convenient for suctions from 10 to 1500 kPa (1 to 150 m of water). Equilibrium times may vary from days to weeks.

The hanging water column method and the pressure plate technique are well established in the field of soil mechanics. The purpose of developing the drainage column method was that it enabled the testing of much larger samples of what is a fairly heterogeneous material, and also provided data that could be used in conjunction with numerical models that simulated the transient behaviour of two phase flow in porous materials.

3.2 Description of the MBT waste sample

Approximately 300 kg of MBT residue (particle size < 10mm or < 9 mm) was obtained from a waste processing plant (New Earth Solutions Ltd) at White's Pit, Dorset, UK. This plant includes a shredder, conveyor belts, magnets, screens and windrows for aerobic composting. Initially, waste was sorted to extract recyclable material. The remaining waste was then broken down into smaller parts by shredding and screened followed by recovery of ferrous metals. Thereafter, the waste was aerobically composted in forced aerated windrows with regular wetting and turning in fully enclosed halls for a period of six weeks. After processing, the material was screened again to extract any remaining dry recyclables, giving a maximum particle size for the residual waste of about 10 mm. The flow diagram of the MBT process is shown in Figure 3.1.

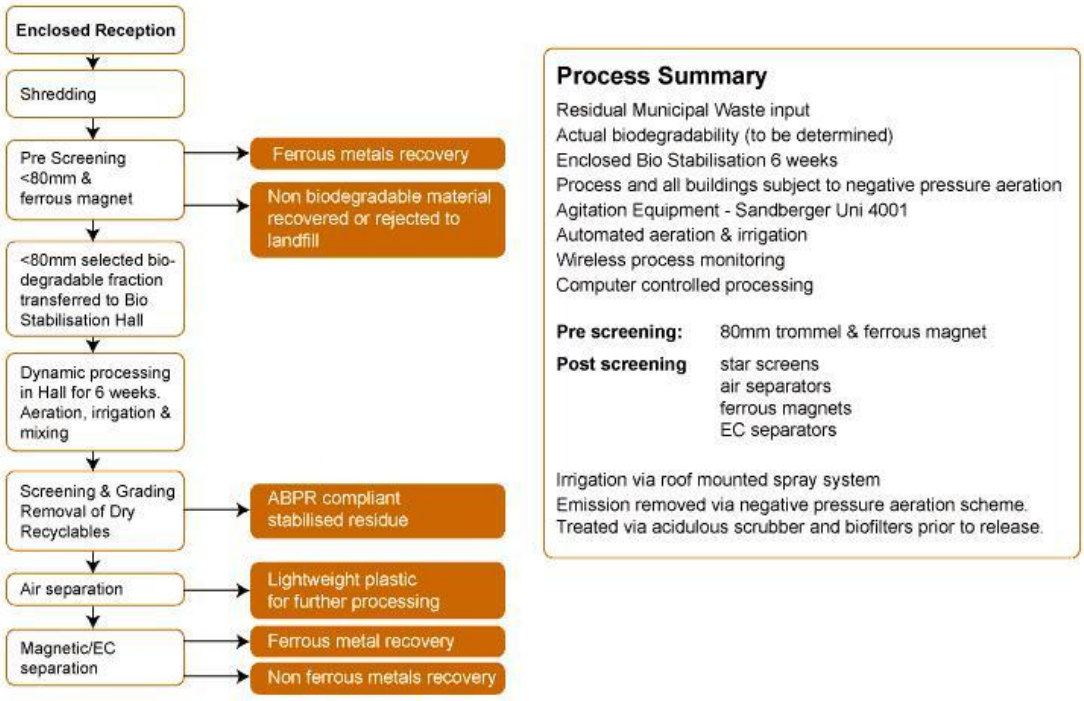

Figure 3.1 Schematic description of typical MBT process (after New Earth Solutions: http://www.newearthsolutions.co.uk/residual-waste-treatment/process-description/ access date March 2009)

A representative sample containing 100 kg of well mixed waste was dried and the components separated manually into various groups (Velkushanova et al, 2009). Table 3.1 shows the components of the waste of particle size 0-10 mm (Figure 3.2). 70.48% of the waste was classified as ‘miscellaneous’, a term covering a mixture of different but unidentifiable materials, of particle size less than 5 mm. A representative sub-sample comprising 24kg of well mixed waste obtained by riffling was used for the drainage experiment, and smaller samples of the same material for the hanging column and pressure plate tests. The as-received moisture content expressed as the ratio of the mass of water to the dry mass of solid particles was approximately 30%.

Table 3.1 Composition of the MBT waste sample (particle size<10mm)

Component	% of dry mass
Plastic	6.80
Textiles	0.88
Glass	18.12
Ceramics	0.15
Stones	0.89
Metals	0.41
Paper/Cardboard/Wood	2.20
Rubber	0.06
Miscellaneous	70.48

Figure 3.2 Photo of the MBT waste sample

The elements of the 'miscellaneous' fraction of particle size less than 5 mm was identified by X-ray fluorescence (XRF) analysis (Fitton, 1997) by GAU-Radioanalytical Laboratories at the National Oceanography Centre, Southampton. Before the trace elements analysis the MBT sample (≈1-2 gram) was ground to a fine powder (<200μm mesh). Elemental concentrations for a wide range of elements were acquired using a Philips Magix-Pro WD-XRF spectrometer and include S. The sample was ashed at 450^{o}C and then mixed with lithium tetraborate flux (sample: flux ratio was 10:1) in a platinum-gold dish and fused at 1100^{0}C for 15 minutes before casting as a glass disk in a Pt-Au dish. The samples were measured using a Philips Magix-Pro wavelength dispersive XRF spectrometer 4kW Rh end-window X-ray tube. The loss on ignition (LOI) content was measured as the weight loss from the dried sample on ignition at 450°C for 4 hours. The XRF results are shown in Table 3.2.In addition C and N were measured on a carlo erba elemental analyzer (the sample was essentially combusted at 1200 ^{o}C in pure oxygen and the CO_2 and NO_x formed measured by electrochemical detection). C was 24.6% and N 1.5%. As shown in Table 3.2 the MBT sample was high in C (as given by the C % composition and LOI), in silicate and aluminium. It was also high in Pb, Zn, Cu, so leaching from the waste of some heavy metals may be a problem during treatment.

Table 3.2 Trace elements analysis of MBT

Chemical compound	wt %	Trace element	ppm
SiO_2	23.48	As	18
TiO_2	0.366	Ba	544
Al_2O_3	4.97	Bi	<3
Fe_2O_3	2.04	Ce	47
MnO	0.062	Co	12
MgO	1.07	Cr	121
CaO	10	Cu	519
K_2O	0.8	Ga	<2
Na_2O	0.5	La	25
P_2O_5	1.42	Mo	1320
S	0.1	Nb	5
Sum	44.81	Ni	58
		Pb	661
LOI_{450}	55.79	Rb	18
		Sn	60
		Sr	185
		Th	17
		U	<3
		V	114
		Y	20
		Zn	1175
		Zr	137

Dry sieving of a 200g portion was carried out according to BS1377-2:1990 giving the particle size distribution shown in Figure 3.3. (As explained later, one test was carried out on the same material sieved to a maximum particle size of 9 mm: the PSD for this material is also shown).

Particle densities were determined using the pycnometer method (Appendix E) and the average was between 1.67 $Mg/m^3$and 1.69 $Mg/m^{3.}$ Stolz et al. (2011) determined the particle density of MSW by the gas pycnometer method equal to 1.62 Mg/m^3.The field capacity was determining by drying one small-scale MBT waste specimen, which was first saturated and then left to drain until the drainage

ceased. The field capacity was estimated to be between 0.30 $m^3/m^3$and 0.35 m^3/m^3 for a dry density of about 0.50 Mg/m^3. The typical range of field capacity for MSW landfills reported in literature is between 0.20 and 0.40, expressed on a volumetric basis (Korfiatis etal. 1984; Zeiss and Major 1993; Yuen et al. 2001).

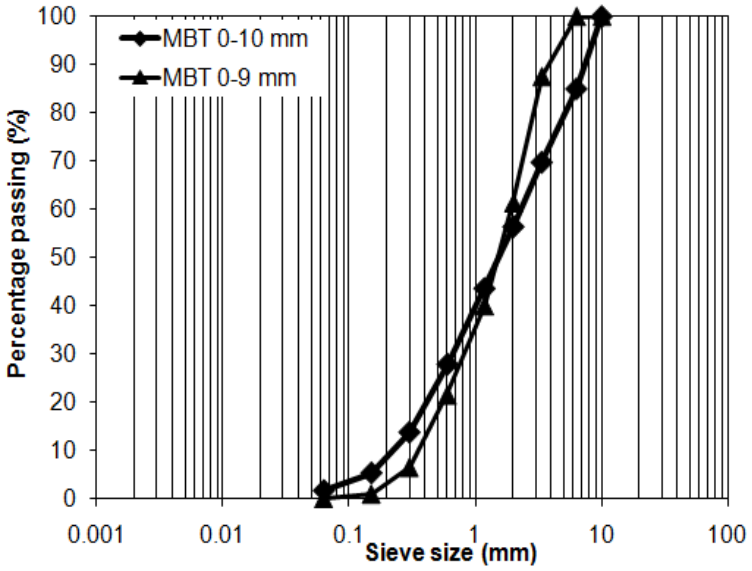

Figure 3.3 Particle size distribution of the MBT waste sample

3.3 Drainage experiments

3.3.1 Design and instrumentation

The principle of the drainage experiment was to allow an initially saturated column of 0-10mm MBT waste to drain downward under gravity. Measurement of the suction and moisture content at various elevations within the column would give direct data concerning the relationship between them. The rate of outflow of water from the column will also depend on the suction-moisture content - permeability characteristics of the waste; thus measurement of the cumulative outflow against time, combined with suitable analysis and modelling, should provide further information (Chapters 4 and 5).

The experiments were carried out on specimens of the MBT waste placed in a clear Perspex cylinder of inside diameter 26cm, 1m in height.

Measurements of the volume of the liquid drained from the column were made using an electrical balance.

Measurements of the moisture content through the waste column height were made using six capacitance probes (Delta-T Devices, model Theta probes ML2x) of 40mm diameter and 105mm length. The Theta probes were calibrated in the laboratory for the MBT waste. Section 3.3.2 and 3.3.4.

Measurements of the pore water pressures in the waste were made using six mini tensiometers (Delta-T Devices, model SWT5) of 5mm diameter and 75mm length, which are able to measure both positive and negative pore water pressures (+100 to -85kPa). The tensiometers were used with the factory calibration in this drainage experiment. Section 3.3.3 and 3.3.4.

Eight pressure transducers (Omega, model PX309-030A5V), having a range of 0-2.1 bar, with resolution 0.001 bar, were used to measure gas pressure during the drainage experiment under unsaturated conditions. The range of the gas pressure transducers was selected to accommodate their application in this project and another PhD project which involved aeration experiments using the same sample and experimental set-up as the drainage experiments. As the pressure transducers were aimed at measuring pressures in the gas phase, (although they did measure water pressure when the sample was saturated) they were connected into this phase via a plastic mesh filter with large pores. The pressure transducers were calibrated using a portable digital pressure indicator DPI 601.

Three thermistors were installed in the waste column for recording the temperature of the sample during the experiment. Finally, the air flow from the atmosphere into the cell was measured by a gas flow meter (Icenta Controls, model Red-y-mart series GSM-B5TA-EN00) installed on the centre of the top lid. All instruments were coupled to a data-logger system (Delta-T Devices, model DL2e). The entire assembly was placed onto an electrical balance for recording weight changes. A web camera connected to a computer recorded the readings of the electrical balances at regular intervals. A photograph of the experimental set-up is shown in Figure 3.4 and Figure 3.5 shows photographs of the instruments used. Figure 3.6 illustrates the instrumentation layout for the experiment. The pressure transducers were located on the back side of the column (obscured in this view), at the same levels as the manometer ports.

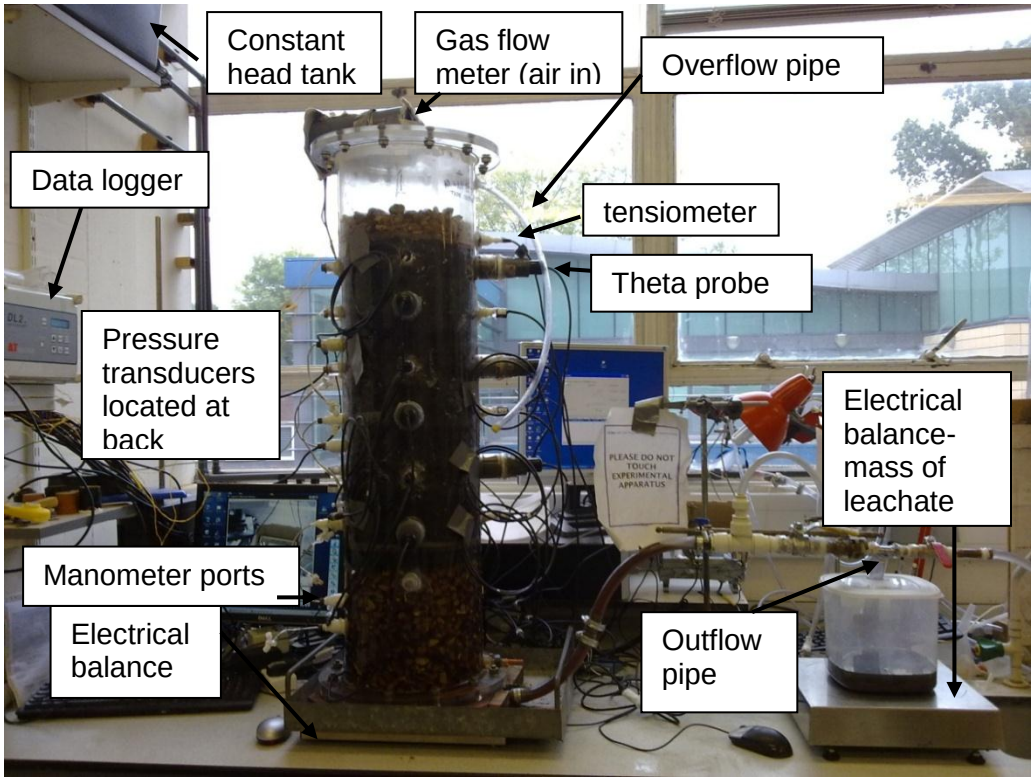

Figure 3.4 Photo of the instrumentation set up of the column for the drainage experiments

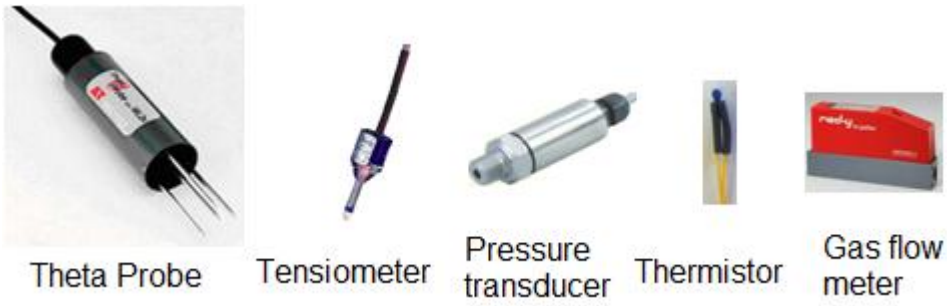

Figure 3.5 Photo of the instruments used for the drainage experiment

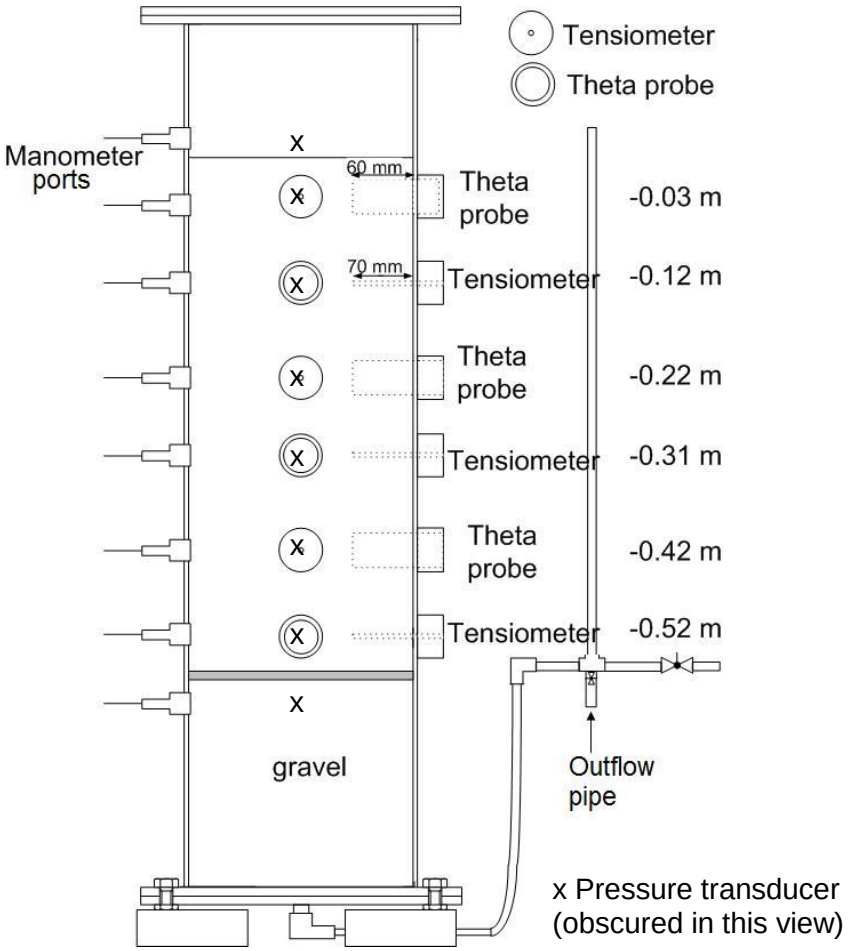

Figure 3.6 Schematic diagram of the column showing the instrumentation for the drainage experiments

3.3.2 Description and operating principles of Theta Probe ML2x

The Theta Probe ML2x (Delta-T Devices, 1999; Atherton et al., 2001; Tsegaye et al., 2004; Cosh et al, 2005; Kaleita et al., 2005a; Yang and Davidson-Arnott, 2005) is designed to measure volumetric water content (θ_v) using a novel technique that matches other methods, such as time-domain reflectometry (TDR) or capacitance measurement, for accuracy and ease of use, while reducing the complexity and expense. The Theta probe is based on the impedance technique (a description of the theory is given in Appendix F).

Each theta Probe (Figure 3.7) consists of a waterproof housing which contains the electronics, and, attached to it at one end, four sharpened 316 grade stainless steel rods that are inserted into the medium. The probe generates a 100 MHz sinusoidal signal which is applied to a specially designed internal transmission line that extends into the medium by means of the array of four rods. The impedance of

this array varies with the impedance of the medium, which has two components - the apparent dielectric constant (capacitance) and the ionic conductivity (1/resistance). The 100 MHz signal frequency has been chosen to minimise the effect of ionic conductivity, so that changes in the transmission line impedance are dependent almost solely on the medium's apparent dielectric constant. Because the dielectric constant of water (~81) is very much higher than soils (typically 3 to 5) and air (1), the dielectric constant of a medium depends primarily on its water content. The impedance of the rod array affects the reflection of the 100 MHz signal, and these reflections combine with the applied signal to form a voltage standing wave along the transmission line. The output of the Theta Probe is an analogue voltage (0-1V) proportional to the difference in amplitude of this standing wave at two points, which forms a sensitive and precise measure of the water content of the medium. The Theta Probe should be inserted without causing air pockets or localised compression. The sampling volume (approx. 75 cm^3), consists of a cylindrical four signal rod array roughly 4.0 cm in diameter and 6.0 cm long surrounding a center signal rod (Gaskin and Miller, 1996, 1999; Delta-T Devices, Ltd., 1999). The readout from the Theta Probe is θ_v (%).

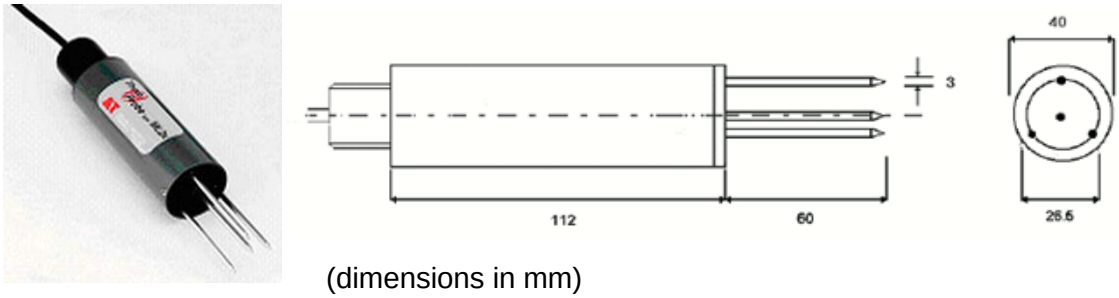

(dimensions in mm)

Figure 3.7 Photo and dimensions of the Theta probe ML2x (Delta-T devices, user manual 1999)

The main advantages of the theta probes include ease of use, simply inserting the probe into the porous medium and connecting it to the data-logger. They have excellent temperature and salinity stability, there is no need of coating like in TDR probes (Staub et al, 2009, 2010).The compact sensors can be placed at any angle and their small size makes them suitable for laboratory use. Also, they are much cheaper than TDR or neutron probe systems. The only limitation of the theta probe is that while it is sensitive to the water content of the sample held within its array of 4 stainless steel rods, this sensitivity is biased towards the central rod and falls off

towards the outside of the cylindrical sampling volume. The presence of air pockets around the rods, particularly around the central rod, will reduce the value of moisture content measured. The output of the theta probe is also affected by the ionic conductivity of salts dissolved in the moisture within the medium. This effect is not major, and is limited to salinity levels below about 250 $mS.m^{-1}$, there is no significant change for salinities between 250 and 2000 $mS.m^{-1}$ (Delta-T Devices, Ltd., 1999). The electrical conductivity (EC) of the MBT leachate was measured as approximately $1768mS.m^{-1}$. Landfill leachate typically has an EC in the range 250-3500 $mS.m^{-1}$, Christensen et al (2001).

3.3.3 Description and operating principles of Tensiometer SWT5

The SWT5 (Delta-T Devices, Cambridge, England) is a miniature pressure transducer tensiometer (Figure 3.8) with good accuracy (± 0.2 kPa) over the range +100 to -85 kPa. The sensor body incorporates the pressure transducer and all electronic parts. The pressure transducer offers the soil water tension as a linear output signal, with 1 mV corresponding to 1 kPa. Given that the tensiometers were required to measure pore liquid pressures in unsaturated conditions, they were fitted with high air-entry value porous stones to increase the likelihood that they would remain hydraulically connected with the liquid phase within the waste, as the waste desaturated during drainage and the remaining liquid retreated into the smaller pores. The tensiometer measures the medium water tension, transmitted via the porous ceramic cup into the acrylic glass shaft onto the water and pressure transducer, giving a continuous analogue signal. The atmospheric reference pressure is provided through a membrane on the cable, a distinctive patented method. If the suction in the medium exceeds 85 kPa, the tensiometer runs dry and must be refilled as soon as the medium is sufficiently moist again. The tensiometers require a stabilized 10.6V DC 1.3 mA power source. Therefore the DL2e Data Logger is fitted with a TVB1 Voltage Regulator which powers and logs up to 30 tensiometers.

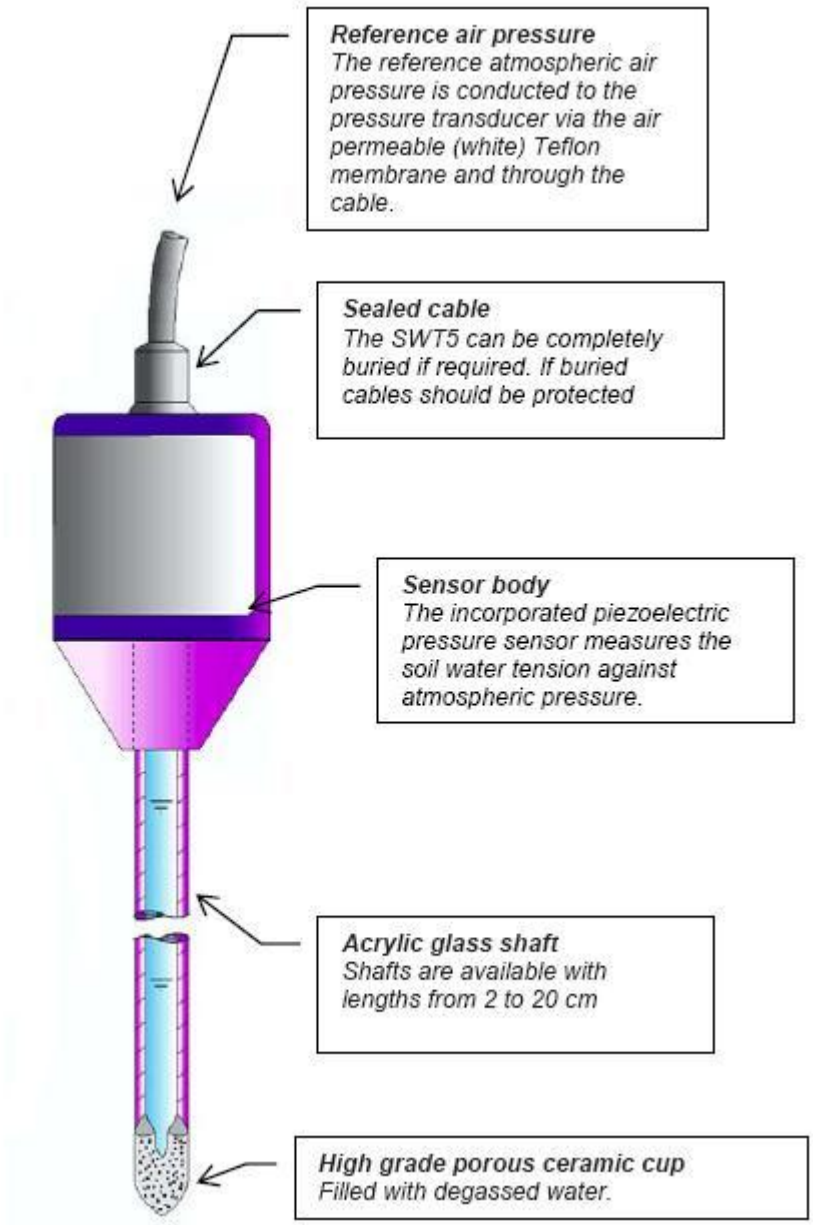

Figure 3.8 Photo of the tensiometer SWT5 (Delta-T devices, user manual 2008)

The SWT5 Tensiometer is specially designed for point measurements, e. g. in medium columns, pots or laboratory lysimeters, or when the measurement of a minimal span is desired. With an active surface of only 0.5 cm^2 and a diameter of 5 mm the ceramic tip has all advantages of small dimensions: little medium disturbance, point measurement and fast response

3.3.4 Calibration of the instruments

The Theta probes and the tensiometers were calibrated in the laboratory for the MBT waste. The manufacturer's theta probe calibration method (Delta-T Devices, Ltd. 1999) was tested and found not to be applicable on the MBT waste sample(Appendix G).Then, a calibration of the theta probes was carried out by measuring the voltage for MBT samples at known moisture contents with a dry density of about 550 kg/m^3. The data were fitted to the polynomial equation:

$$\theta = 3.8635V^4 - 4.5244V^3 + 0.7907V^2 + 0.786V - 0.0459 \quad (3.1)$$

The theta probes were calibrated before the start of the multistep drainage experiment by measuring the voltage for MBT samples at known moisture contents with dry density around 550 kg/m^3.The data were fitted to the polynomial equation:

$$\theta = 2.0093V^3 - 2.5888V^2 + 1.3392V - 0.0642 \quad (3.2)$$

The calibration data of the theta probes for two experiments were very close. The different polynomial fitting equation may be attributed to the fact that the multistep drainage experiment was carried out after 1.5 years so that the MBT waste composition may have been a little different although the PSD curves were similar.

Two different shredded MBT samples were used for the theta probes calibration and the impact of waste density was investigated. The second MBT sample with particle size 0-9 mm had a greater amount of organic material as a result of the use of a different shredder. The results demonstrated that dry density and composition do not affect the measurements in a significant way (Figure 3.9). The 0-9 mm MBT sample appeared to have a higher saturated moisture content value that the other samples; this is consistent with the higher organic amount in it. Similar conclusions were made by Staub (2009) for TDR probes.

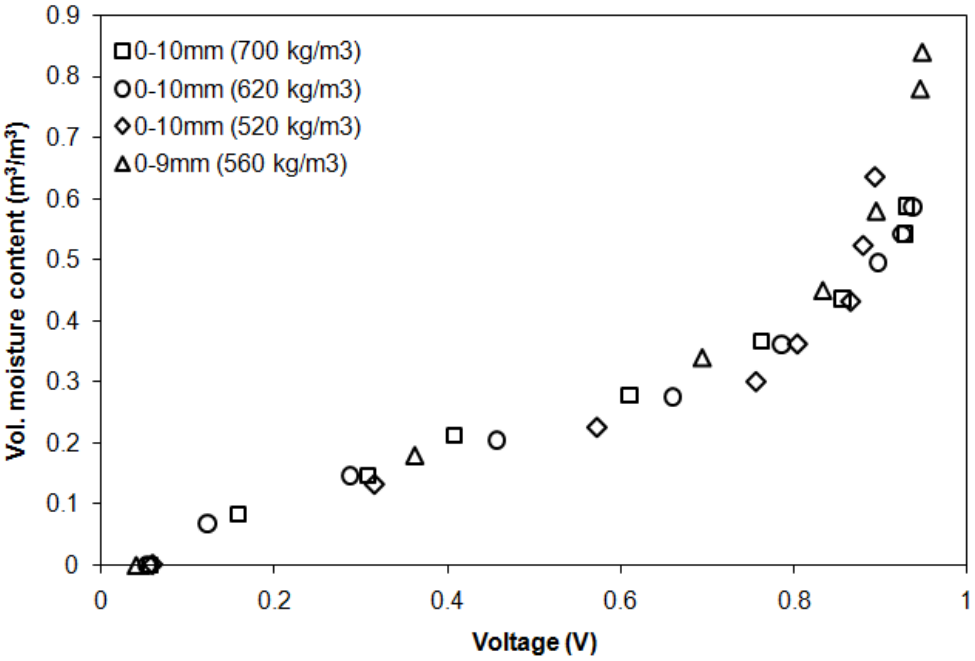

Figure 3.9 Influence of dry density on theta probe measurements in MBT waste

For calibration in negative values of pore liquid pressure (suction) a tensiometer was inserted in a MBT waste sample in a hanging column apparatus. The tensiometer was connected to a voltage meter and measurements of suction and voltage (mV) were taken for different pressure steps. This test was repeated twice and the calibration data were repeatable. For the positive values of pore liquid pressure a tensiometer connected to a voltage meter was submerged in a cylinder below a known depth of water and measurements of pore liquid pressure (ρgh) and voltage readings (mV) were taken for different water levels (h).In both cases the data were fitted to a linear equation similar to the factory calibration (1 mV corresponding to 1 kPa). The teniometers were refilled before each drainage experiment.

The pressure transducers were calibrated using a portable digital pressure indicator DPI 601 against pressures up to 50 kPa. The calibration was done for all of the pressure transducers (A-H). Three of the pressure transducers (A, D and F) were connected to a different data-logger. The calibration equations for the one-step and multistep drainage experiments are presented below. The equations are quite different because the DL2e data-logger is fitted with a TVB1 Voltage Regulator because the tensiometers connected to the DL2e data-logger require a stabilized 10.6V DC 1.3 mA power source.

One-step drainage experiment:

A: Gas pressure (kPa) = 0.0412x(mV) – 101.35

B: Gas pressure (kPa) = 0.1448x(mV) – 56.421

C: Gas pressure (kPa) = 0.1409x(mV) – 50.099

D: Gas pressure (kPa) = 0.0143x(mV) – 100.28

E: Gas pressure (kPa) 0.147x(mV) – 53.908

F: Gas pressure (kPa) = 0.0413x(mV) – 101.15

G: Gas pressure (kPa) = 0.1455x(mV) – 55.603

H: Gas pressure (kPa) = 0.1457x(mV) – 55.188

Multistep drainage experiment:

A: Gas pressure (kPa) = 0.1583x(mV) – 55.079

B: Gas pressure (kPa) = 0.1604x(mV) – 58.001

C: Gas pressure (kPa) = 0.1659x(mV) – 55.175

D: Gas pressure (kPa) = 0.1558x(mV) – 53.574

E: Gas pressure (kPa) 0.1623x(mV) – 55.482

F : Gas pressure (kPa) = 0.1697x(mV) – 59.861

G: Gas pressure (kPa) = 0.1619x(mV) – 57.558

H: Gas pressure (kPa) = 0.1715x(mV) – 59.646

All the above instrument calibrations were repeated after the end of each drainage experiment giving the same data.

3.3.5 Set-up of the one step drainage experiment

The process for setting up the column was as follows. A 25cm gravel layer (particle size 10 to 20 mm) was installed at the bottom of the column and a geotextile filter (1 cm thick) was installed above the gravel layer to prevent waste infiltration. The permeability of the filter was measured using the constant-head method in a 75 mm diameter permeameter to be between 1.42×10^{-4} m/s and 5.56×10^{-4} m/s. Below the filter a Plexiglas base with holes was installed to hold the filter horizontal. Before filling of the cell with MBT waste, the cell was filled with water and drainage tests were carried out with and without the filter and Plexiglas base on the fully saturated gravel layer to check the effect of the filter on top of the outflow rate (Appendix H). It was concluded that the filter system would have no significant effect on the results.

About 24 kg MBT waste of initial volumetric moisture content 28% was placed in 8 equal lifts (approx. 7cm, 3 kg each) above the saturated filter, with compaction following each lift (5 repetitions) by hand tamping with a 230 mm round tamper. A 5 cm gravel layer was placed to give even distribution of leachate over the top surface of the waste and separated from the waste by a geotextile membrane. The MBT column of 0.56 m height was first flushed with carbon dioxide (CO_2)to facilitate the solution of air bubbles into the water. Then, the column was saturated upwards by introducing a solution of deaired water and 0.7258 g/L sodium molymbate (Ranade et al., 1998) and 0.12 g/L 2-bromoethanesulfonate (BES) to inhibit sulphate reducing bacteria and methanogenesis (Chae et al., 2009) during the experiment. The column was left overnight to develop full saturation. The saturated permeability (k_s) of the MBT was measured as between 1×10^{-5} m/s and 5×10^{-5}m/s by the constant-head method (*BS* 1377-5:1990). The physical properties of the MBT column are shown in Table 3.3.Initially, excess water in the column was drained by setting the height of the outflow tubing level with the top of the sample. The fully saturated column was allowed to drain by opening the drainage tap located at the bottom of the cell.

Table 3.3 Physical properties of the MBT column (one step drainage)

Physical property of the MBT sample in the cell	Units	Method	Value
Height of the column	m		0.56
Dry mass	kg		15.33
Water	litres		20.47
Total Volume	litres		29.73
Dry density	kg/m^3	mass of solids/total volume	516
Particle density (ρ_s)	kg/m^3	by pycnometer method	1.69
Volume of voids	litres	total volume - (mass of solids/particle density)	20.66
Porosity (ϕ)		volume of voids/total volume	0.695
Volume of gas	litres	volume of voids-volume of water	0.19
Saturation ratio (S_r)		volume of water/volume of voids	0.99
Saturated moisture content (θ_s)		(porosity)x(S_r)	0.69
Drainable porosity		volume of leachate drained out/total volume	0.3
Leachate drained out	kg		8.82

3.3.6 Set-up of the multistep drainage experiment

Multistep drainage experiments were carried out to verify whether the capillary pressure and moisture content measured in the MBT column apparatus provided a consistent dataset at each depth when lowering the head at the lower boundary in steps. The set-up of the multistep drainage experiment was exactly the same as above, except for the outflow system (Figure 3.10). Initially, excess water in the column was drained by setting the height of the outflow tube level with the top of the sample. Then, six pressure steps were applied sequentially by lowering the height of outflow tubing six steps (0.475 m, 0.39 m, 0.31 m, 0.22 m, 0.12 m, 0 m above the bottom of the MBT column) until the outflow tubing was level with the bottom of the sample. The saturated permeability (k_s) of the MBT was measured as between 1×10^{-5} m/s and 5×10^{-5} m/s by the constant-head method (*BS* 1377-5:1990). The physical properties of the MBT column are shown in Table 3.4.

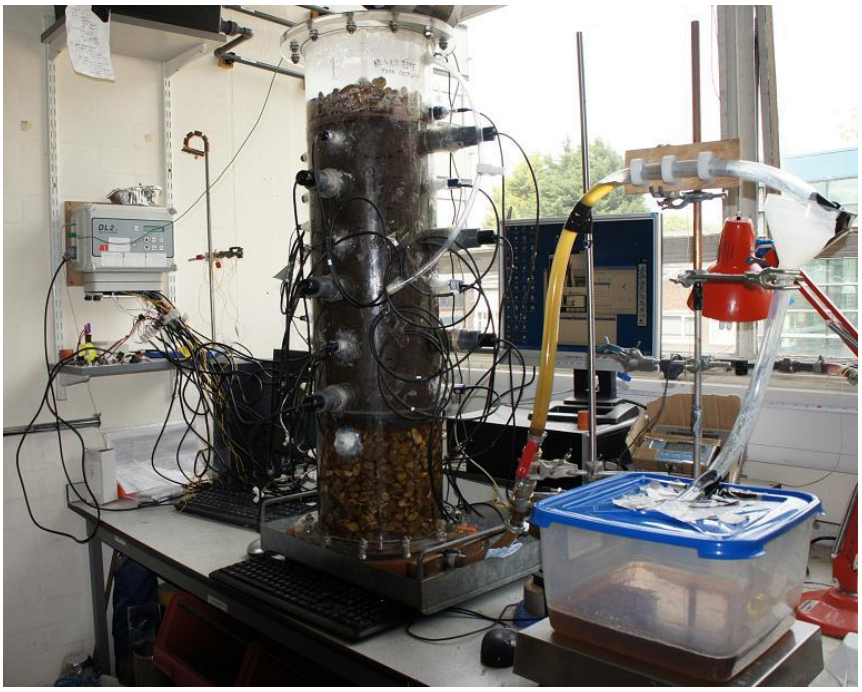

Figure 3.10 Photo of the instrumentation set up of the column for the multistep drainage experiment

Table 3.4 Physical properties of the MBT column (multistep drainage)

Physical property of the MBT sample in the cell	Units	Method	Value
Height of the column	m		0.56
Dry mass	kg		15.41
Water	litres		20.54
Total Volume	litres		29.73
Dry density	kg/m^3	mass of solids/total volume	518
Particle density (ρ_s)	kg/m^3	by pycnometer method	1.69
Volume of voids	litres	total volume - (mass of solids/particle density)	20.61
Porosity (ϕ)		volume of voids/total volume	0.693
Volume of gas	litres	volume of voids-volume of water	0.07
Saturation ratio (S_r)		volume of water/volume of voids	0.997
Saturated moisture content (θ_s)		(porosity)x(S_r)	0.69
Drainable porosity		volume of leachate drained out/total volume	0.27
Leachate drained out	kg		8

3.3.7 Saturated hydraulic conductivity of the MBT waste column

Hydraulic gradients and flow velocities in landfills generally correspond to laminar flow conditions, and Darcy's law can be assumed to apply to wastes. This was first demonstrated by Powrie and Beaven, 1999; and has subsequently been supported by Durmrsoglu et al, 2006; Capelo and de Castro, 2007; McDougall, 2007. The constant head approach was used to determine the saturated hydraulic conductivity of the waste column before and after the drainage experiment, as follows. The MBT column was first saturated with CO_2 and then deaired water from the constant head tank was allowed to flow into the cell from the bottom upwards. Measurements of the volume of the leachate drained out of the overflow pipe (Figure 3.4) were taken at different times using a measuring cylinder and a stopwatch. The difference in the tensiometer readings corresponded to differences in hydraulic head Δh at two points at a distance L apart along the direction of flow. The hydraulic gradient (Δh/L) was found for different flow rates q. The saturated hydraulic conductivity (k_s) was then calculated from the slope of a graph of q vs. Δh/L according to Darcy's equation:

$$q = Ak_s(\Delta h/L) \rightarrow k_s = qL/A\Delta h \quad (3.3)$$

where A is the cross-sectional area of the MBT column: 0.0531 m^2.

3.3.8 Problems faced during the drainage experiment set-up

The first type of experiment was the one step drainage experiment. The fully saturated MBT column was allowed to drain by opening the drainage tap located at the bottom of the cell (U-tube outflow system). Three one-step drainage experiments were carried out for development purposes and to overcome some problems, such as deciding the best method for full saturation and deposition of the waste in the cell to achieve a constant dry density along the column. Saturation from the bottom under vacuum damaged the structure of the MBT column as bubbles of gas coalesced and migrated out of the column through suction enlarged pores, which subsequently acted as preferential pathways. Saturation of the column from the bottom after CO_2 injection was finally used as a successful method of full saturation. The infiltration rate was faster during wetting after CO_2 saturation.

Another problem that appeared was evidence of slight pitting corrosion on some of the theta probes (Figure 3.11). After tests in the column to check if the whole system generates two different "ground" (0V) voltages, it was concluded that a second ‘small’ current existed in the system that caused electrolytic corrosion. This problem was solved by inserting an ‘earth’ rod in the MBT column and connected to the DL2e data-logger. Evidence of corrosion was also observed on the wire mesh used to connect the pressure transducers with the gas phase in the column and on the cup of one pressure transducer (Figure 3.12). Plastic mesh was used thereafter. Another major problem was the generation of gas in the gravel layer after about four days of drainage. The presence of gas in the gravel, the ‘rotten egg’ odour and the covering of the bottom of the cell and the gravels with soft black deposits (Figure 3.13) indicated the presence of hydrogen sulphide (H_2S) in the gas. The production of H_2S often indicates the activity and presence of sulphate-reducing bacteria (SRB), which generated in anaerobic conditions and tend to cover flat surfaces in this case the surface of the gravels. The same observation was made by Nikolova (2003). Sodium molymbate (Ranade et al., 1999) and 2-bromoethanesulfonate (BES) were used to inhibit sulphate reducing bacteria and methanogenesis (Chae et al., 2009) during subsequent experiments. Last but not least, the wiring connection of all the instruments to the data-logger was a real challenge. There were some noise and unexplained readings initially; it was concluded that too many instruments were connected onto the same card of the data-logger. This problem was solved by using a second small portable data-logger for connecting three of the eight pressure transducers. After overcoming all

these problems with the set up and instrumentation of the column, a fully saturated MBT column was prepared and drained in one-step. The results from and analysis of that experiment are presented in Chapter 4.

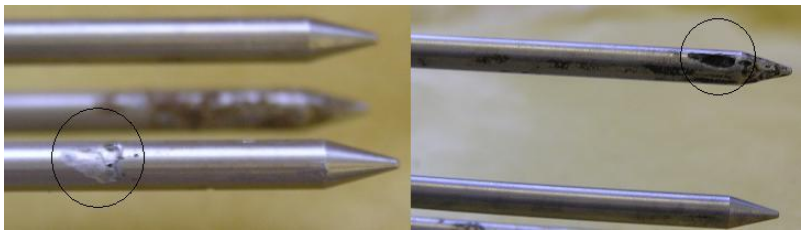

Figure 3.11 Corrosion of the theta probe rods

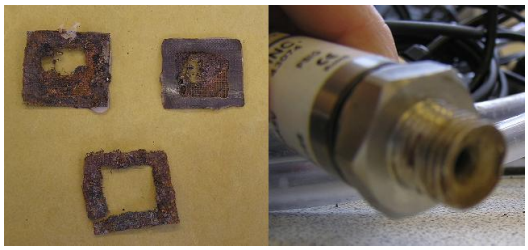

Figure 3.12 Corrosion of the wire mesh and pressure transducer cap

Figure 3.13 Black deposits covering the bottom of the cell and gravels after dismantling

Analysis of the one-step drainage experiment (Chapter 4) indicated that the moisture retention curve varied significantly along the depth of the column during the drainage process even though there was initially a uniform density. The sudden lowering of the bottom boundary pressure from hydrostatic to atmospheric may have caused fine particles to migrate as the leachate drained out. Hence multistep drainage experiments were carried out to verify whether the capillary

pressure and moisture content measured in the column apparatus provide a consistent dataset at each depth when lowering the head at the lower boundary in steps.

3.4 Hanging water column technique

The hanging water column apparatus (Vomocil, 1965), also known as the Haines apparatus, is illustrated in Figure 3.14. It consists of a Buchner funnel, which contains a fritted-glass, porous plate. In this case, the funnel (supplied by Fisher Scientific) was of capacity 1000 ml and diameter 130 mm. The plate has pore size 10-16 μm, which implies an air entry value of 0.3 bar (30 kPa).During the test, the underside of the plate was in continuous contact with a column of water contained within a flexible plastic tube terminating in a 100 ml burette, graduated in intervals of 0.2 ml and open to the atmosphere.

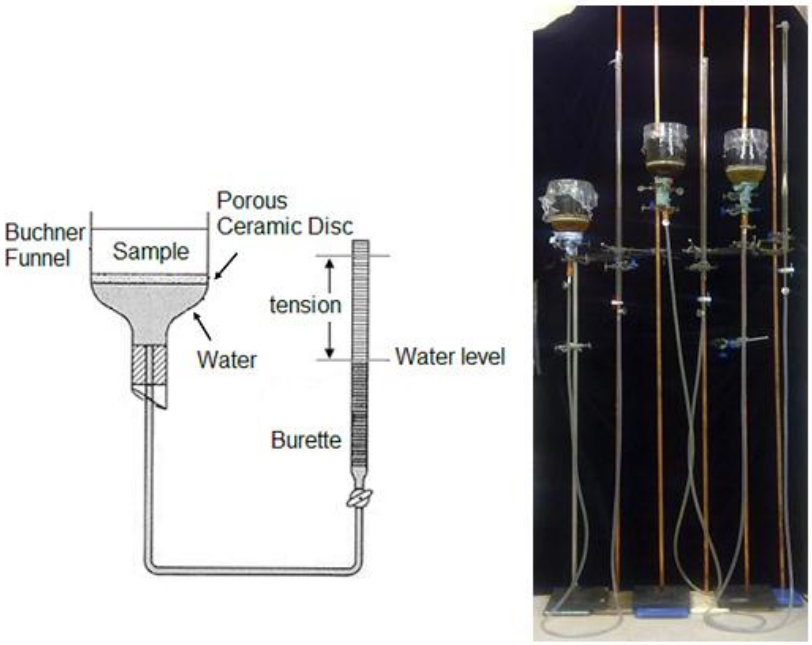

Figure 3.14 Schematic diagram and photograph of the hanging water column apparatus

The general test procedure was as follows. The porous plate was saturated and the plastic tube below it filled with de-aired water. The MBT waste was saturated by inundation in a saturation tray for 24 hours (ASTM D6836-02) and then placed in the Buchner funnel. The saturated waste specimen was placed in the funnel in contact with the plate (130 mm diameter and 65-75 mm in height). Excess water

was removed from the top of the waste. During the test, the top of the funnel was covered with cling film to minimize evaporation and the temperature of the room was kept constant at 20°C ±½°C. Initially, the tubing and burette were positioned so that the water surface in the burette was level with the top of the porous plate. The burette stop tap was closed and the burette lowered so that the top of the water column was some distance below the top of the plate. The stop tap was then opened. At that stage, the specimen was subjected to a mean negative pressure head (suction) equal to the distance between the centre of the specimen and the water level in the burette. The difference between the atmospheric pressure above the specimen and the suction below it created an hydraulic gradient across the specimen, in response to which water flowed from the waste through the porous plate into the burette until an equilibrium condition was reached and the water level in the burette stopped rising. At this point, the average suction in the waste was $-\rho_w gH$, where H was the distance between the centre of the specimen and the water level in the burette.

The total amount of water leaving the specimen was determined from the burette volume readings. The burette was then lowered again and a new set of measurements made. On completion of the experiment, the final water content of the specimen was determined by oven drying. The moisture contents associated with the suctions applied at each stage in the test were calculated by adding to the final water content the incremental volumes of water drained at each step. In this way, a set of equilibrium values of moisture content and suction was obtained.

Hanging water column tests were carried out to define the moisture retention curve at lower suctions (0-10 kPa) of MBT waste specimens of dry density 560, 500 and 350 kg/m^3. In the first two cases, 0-10mm MBT was used while for the specimen with a dry density of 350 kg/m^3, 0-9 mm MBT was used. The latter contained a greater amount of organic material as a result of the use of a different shredder; for example, the original shredder tended to crumple paper into a ball rather than shred it, resulting in its rejection as being over-sized.

Three tests were carried out at each density. The time needed for stabilisation was approximately 2 days at each step. The water retention data were found to be repeatable to within ±3% and a representative test at each dry density was selected for further interpretation. The physical parameters of the individual MBT

waste specimens are summarized in Table 3.5 and the moisture retention data are shown in Figure 4.16.

Table 3.5 Physical parameters of MBT waste samples used in hanging water column tests

Physical parameter	Test 1 (0-10 mm)	Test 2 (0-10 mm)	Test 3* (0-9 mm)
Dry density (kg/m^3)	560	500	350
Initial dry mass (g)	555	468	306
Initial mass of water (g)	653	641	613
Total (wet) mass (g)	1208	1109	919
Total volume (wet) (ml)	995	929	873
Porosity (Φ)	0.67	0.70	0.7
Saturated moisture content (m^3/m^3)	0.655	0.69	0.7
Volume of leachate out (ml)	137	296	215
Drainable porosity	0.14	0.31	0.24
Degree of saturation (S_r)	0.98	0.99	1

* Test 3: Higher amount of organic material

The drainable porosity of the MBT sample with dry density 500 kg/m^3 (test 2) is similar to the drainable porosity of the MBT columns in the drainage experiments. 'The increase in drainable porosity with decreasing dry density seen between tests 1 and 2 is as expected. Direct correlation with test 3 is not possible. However, the results tentatively suggest that increasing the proportion of organic material lowers the drainable porosity

3.5 Pressure plate technique

Pressure plate extractors (Figure 3.15) apply a relative matric suction in the range 10-1500 kPa. The pressure plate extractor (Soilmoisture Equipment Corp., 2002) consists of an airtight chamber enclosing a porous ceramic plate of air entry value 1500 kPa. The plate is connected on its underside to a tube that passes through the chamber to the atmosphere.

The MBT waste specimen was saturated by inundation in a saturation tray for 24 hours (ASTM D6836-02). The ceramic plate was saturated by allowing an excess of de-aired water to stand on it for 1-2 days to wet the plate thoroughly. After removing the excess water the saturated plate was placed in the extractor and the

outflow connection was made. Owing to the wide range of pore and particle sizes in wastes, the sample was as large as possible (200 mm diameter and 45 mm in height) to minimise the potential for errors due to inhomogeneity orlack of representativeness.

The waste was packed into a mould at a dry density of 520 kg/m^3 and placed on the saturated ceramic plate; excess water was removed from the top. To prevent the uncontrolled flow of water from an initially very wet specimen during setting up the experiment, the apparatus was modified as shown in Figure 3.16. A rubber O-ring was attached at the bottom of the mould using silicon grease, and a plate of mass 1 kg placed on the top of the mould to keep the bottom of the waste and the rubber O-ring in close contact with the ceramic plate. This meets the requirements of ASTM D6836. The lid was placed on the chamber and secured with screws. The air in the chamber was then pressurized to u_a. The pore water pressure u_w remained at atmospheric, with the pressure difference ($u_a - u_w$) sustained by the surface-water interface in the saturated high-air entry value ceramic plate.

The drying moisture retention curve was measured by increasing u_a in a series of increments to achieve different relative suctions ($u_a - u_w$). Each increment in u_a causes water to be expelled from the sample until the water content in the sample is in equilibrium with the relative suction that has been established. The volume of water expelled during each increment was measured daily to determine when equilibrium conditions had been reached and the equilibrium water content for each value of suction applied. Equilibrium was assumed to have been established when the weight of the leachate in the beaker was the same for at least 2 days in row or was changing by less than 0.2 ml per day. The pressure was then increased to the next stage. After the last pressure increment, the waste specimen was removed and dried in the oven at 70^{0}C for 4 days. After determining the gravimetric and volumetric moisture contents, the moisture retention curve for the specimen was produced.

Two tests were carried out, from initial conditions summarised in Table 3.6. Each test lasted for 7-8 months. Pressure increments of 20, 50, 75, 100, 150 and 200 kPa were applied in the first test and of 6, 10, 20, 50, 75 and 100 kPa in the second. Biodegradation was negligible over the period of the test because low moisture contents were reached quickly.

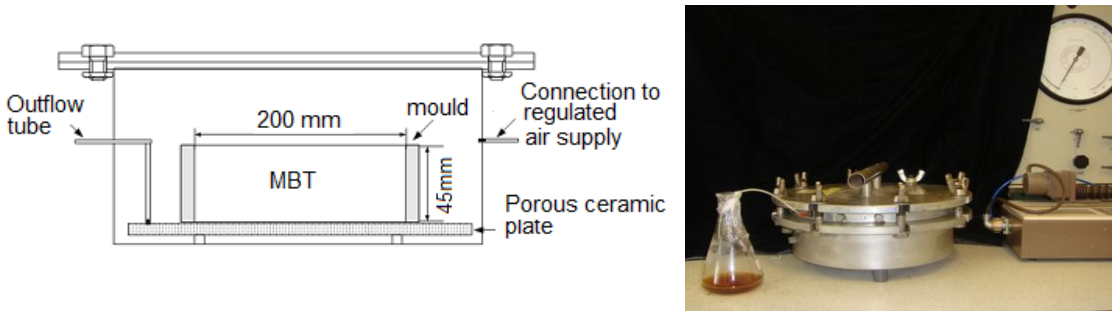

Figure 3.15 Cross section view and photo of the pressure plate extractor and sample (Soilmoisture Equipment Corp., 2002)

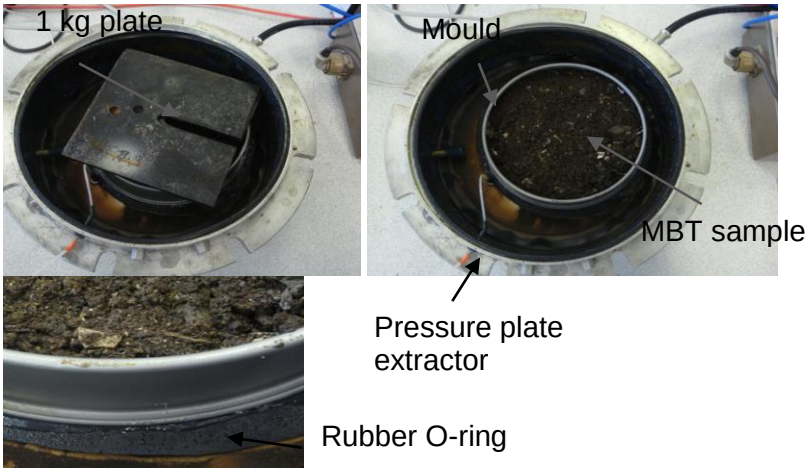

Figure 3.16 Preparation of the MBT waste sample and placement in the pressure plate apparatus

Table 3.6 Initial physical parameters of the MBT waste specimens (pressure plate)

	Test 1	Test 2
Dry MBT (kg)	0.606	0.734
Deaired water (kg)	0.809	0.98
Saturated MBT (kg)	1.415	1.714
Volume (m^3)	1.351	1.414
Dry density (kg/m^3)	450	520
Porosity (φ)	0.73	0.69
Saturated moisture content (m^3/m^3)	0.60	0.69
Degree of saturation (S_r)	0.82	1

3.6 Summary

This chapter has described the waste sample tested and presented the three different techniques used for the determination of the moisture retention characteristics of MBT waste (drainage, pressure plate and hanging water column) at different dry densities and the estimation of unsaturated permeability. The problems faced during the set-up of these experiments were described and the solutions for each indicated. The moisture retention curves and relative permeability functions K (θ) obtained from the experiments are presented in the next two Chapters.

CHAPTER 4

DETERMINATION OF THE MOISTURE RETENTION CURVES OF MBT WASTE FROM THE EXPERIMENTAL TECHNIQUES

4.1 Introduction

The previous chapter described the waste sample tested and different techniques (drainage, pressure plate and hanging water column) used for the determination of the moisture retention characteristics and unsaturated permeability for MBT waste specimens. In this chapter new data from a drainage column experiment, pressure plate apparatus and hanging water column tests on specimens of MSW that had been subjected to mechanical-biological treatment (MBT) as required by the EU Landfill Directive prior to landfilling are presented and compared. Then, for the reasons discussed in Section2.4, their fit to the empirical relationship proposed by van Genuchten (1980) is explored. Finally, recommendations for the reliable determination of moisture retention curves for waste materials are made.

4.2 Drainage experiment results

4.2.1 One-step drainage

The fully saturated column was allowed to drain by opening the drainage tap located at the bottom of the cell. Equilibrium was achieved after 4 days and8.82 litres of leachate drained out, most of it within the first day. The same amount of air entered the cell from outside. Figure 4.1 shows the cumulative mass flow of leachate from the MBT during drainage, as measured by the electrical balance (dot points) and the air flow (litres) into the column as measured by the gas flow meter.

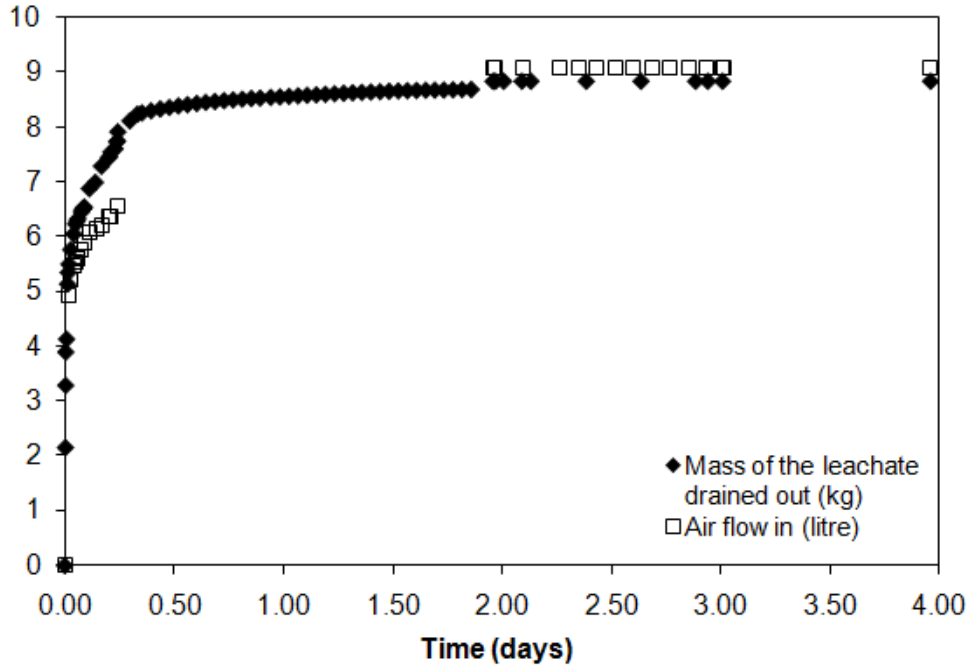

Figure 4.1 Mass of leachate drained out (kg) and air flow in (litre) during the time period (days) of the one-step drainage experiment

Figure 4.3 shows the transient values of the moisture content as measured by the six theta probes and Figure 4.4 shows the transient values of the suction as measured by the six tensiometers. It is clear that the moisture content of the MBT waste column generally declined during the drainage experiment. The largest change in the moisture content and pore liquid pressure of the MBT waste column occurred during the first day. This is consistent with the large pores draining first and liquid remaining in the smaller pores as a residual moisture content retained by capillary effects. The greater amount of drying did not occur at the top of the MBT waste column (theta probe at depth -0.03 m) as expected but at levels -0.12m (theta probe 9) and -0.31m (theta probe 8) as showed in Figure 4.3. The moisture contents at levels -0.12 m and -0.31 m fell more quickly because the horizontal layers at those points were observed to be less dense. A horizontal 'crack' was observed at those points, which may have been caused by the layering effect or internal movement of fine particles which disturbed the structure of the column (Figure 4.2).

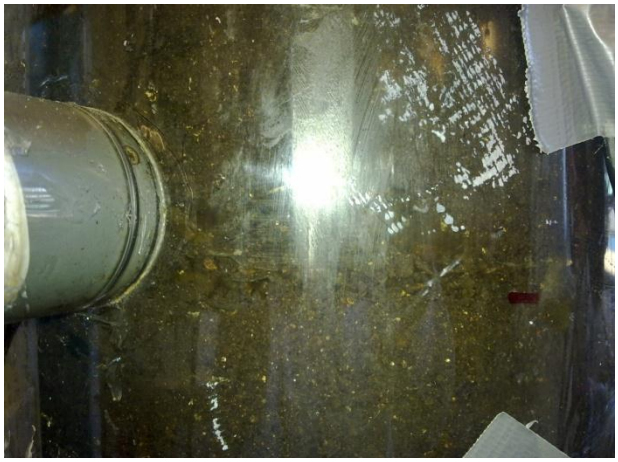

Figure 4.2 Photo of the horizontal 'crack' at level -0.34 m

The pore liquid pressures measured by the tensiometers at the six measuring points were initially positive, indicative of saturation of the column. After drainage, the pore liquid pressure becomes negative (i.e. in suction), indicative of unsaturated conditions in the column (Figure 4.4).

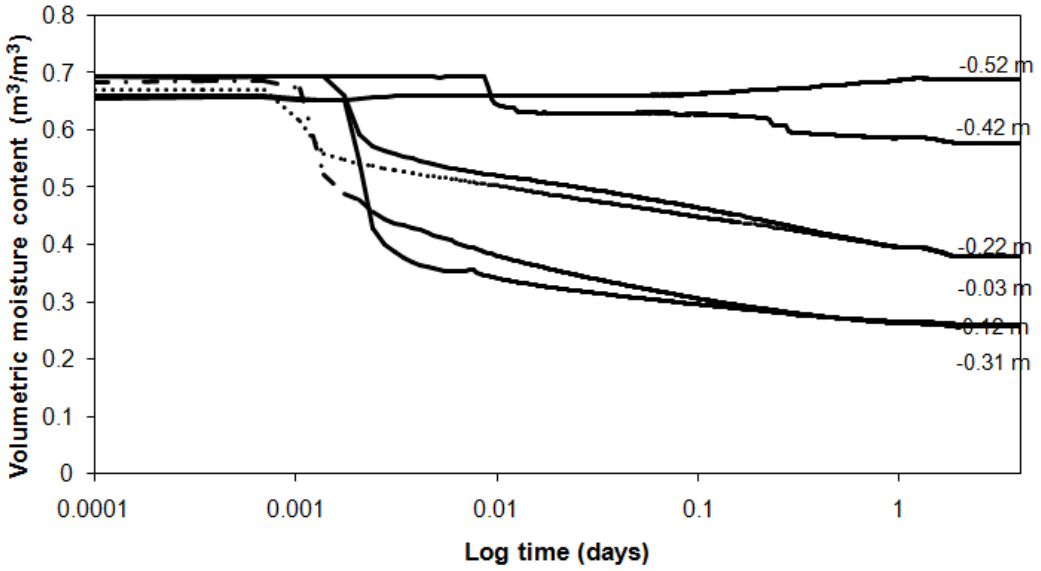

Figure 4.3 Measurements of the volumetric moisture content (m^3/m^3) of the MBT waste column by the six Theta probes during the one-step drainage experiment

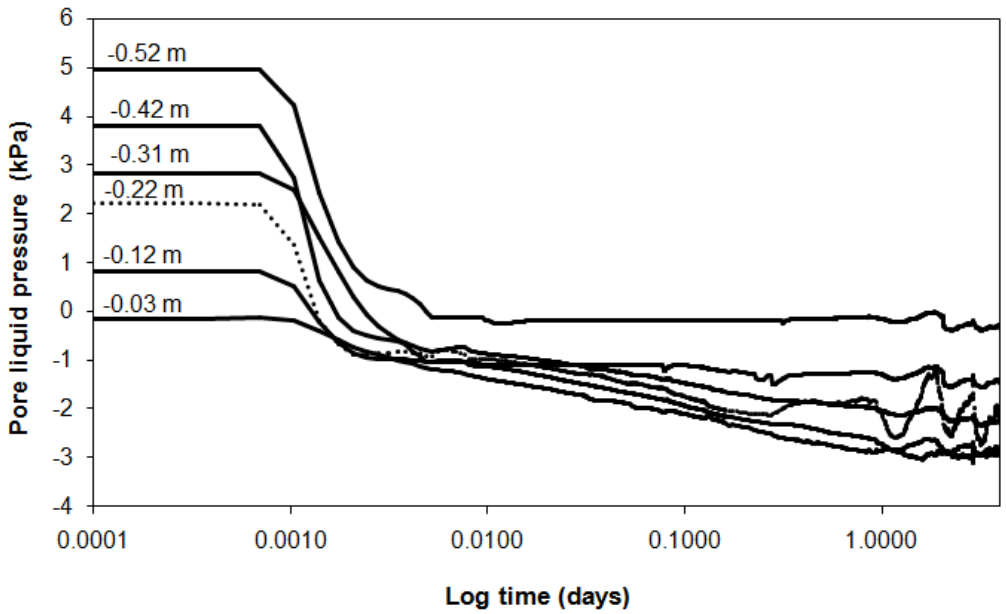

Figure 4.4 Measurements of the pore liquid pressure (kPa) of the MBT waste column by the six tensiometers during the one-step drainage experiment

The unstable behaviour (Figure 4.4) of the tensiometer readings in the last days of the drainage is probably due to the presence of air in the tensiometer bodies.

Figures 4.5 and 4.6 show the pore liquid pressure and moisture content distributions (profiles) over the height of the column at times 0, 10 mins, 12 hrs, 1 day and 4 days (end of drainage). The results show that the moisture content decreased mainly in the upper layers of the column where higher suctions were observed in the top layer of the MBT column. Assuming that the profile is linear, for a sample height of 0.56 m the theoretical maximum suction is 5.69 kPa while the maximum recorded in the test is 3 kPa. This means that under the partly saturated conditions the full theoretical downward force provided by a liquid density of 1000 kg/m^3 is not being applied. Thus the impact of the drained and unsaturated condition is to introduce a degree of discontinuity into the liquid phase to the extent that the liquid density is reduced to an effective density of about 600 kg/m^3. This is a significant reduction and consideration should be given to making an allowance for this effect in the constitutive equations used to model unsaturated flow. Such an allowance is made in the University of Southampton Landfill Degradation and Transport model LDAT. The volumetric moisture profiles (Figure 4.6) are not homogeneous, some scatter is observed and there is an increase in moisture content with depth due to gravity. These results express the heterogeneity of the

MBT waste as well the difficulty of measuring accurately the local volumetric moisture content when there is some variation in the structure (layering effect, loosening of the sample) and hence in the microporosity of each layer.

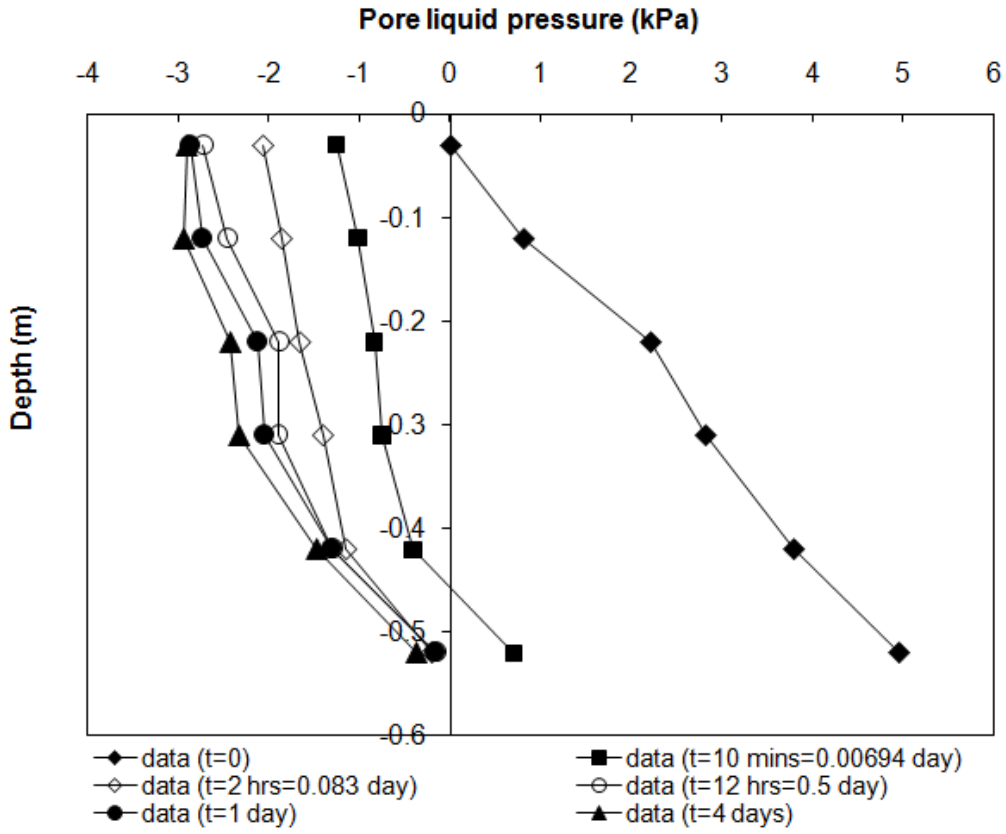

Figure 4.5 Distribution of the pore liquid pressure (kPa) along the MBT column, measured by tensiometers, at selected times of the one-step drainage experiment

On the basis of the limited data shown in Figure 4.5, the rate of decrease of the pore liquid pressure reading at the upper part of the column does appear to reduce significantly after the first day. One possible explanation for this is that the horizontal 'crack' observed at a depth of around -0.34 m (Figure 4.2) caused a discontinuity in the liquid phase suctions along the MBT column.

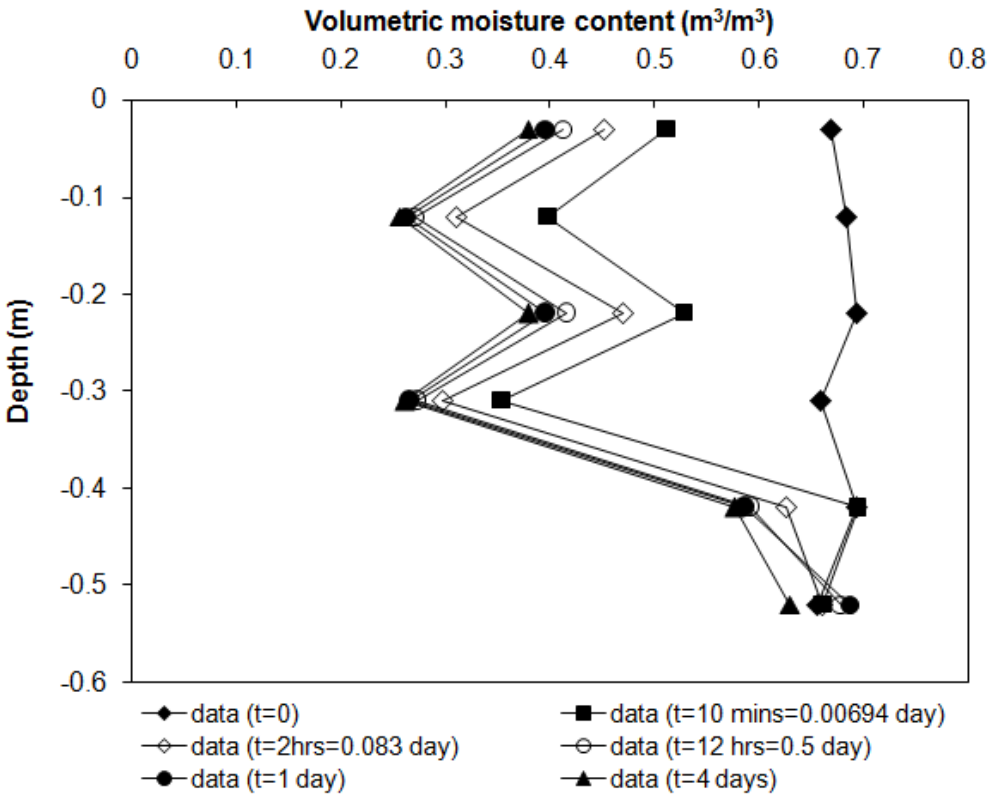

Figure 4.6 Distribution of the volumetric moisture content (m^3/m^3) along the MBT column, measured by Theta probes, at selected times of the one-step drainage experiment

The accuracy of the theta probe measurements were verified by estimating the area under the graph theta probe readings between t=0 and t=4 days (Figure 4.6). The total volume of leachate drained out estimated by this method was 8.73 litres, which close to the reading of the electrical balance (8.82).

Figures 4.7 shows the gas pore pressure measurements at different horizons with time for the first 8 minutes and then it had been almost stabilized. The gas phase was initially at hydrostatic pressure. Leachate draining from pore space, caused gas expansion resulting in a negative pressure which drove atmospheric air ingress into the top of column. This phenomenon repeats itself successively at the depths z=-0.31m and z=-0.52m allowing atmospheric air to fully penetrate the column.

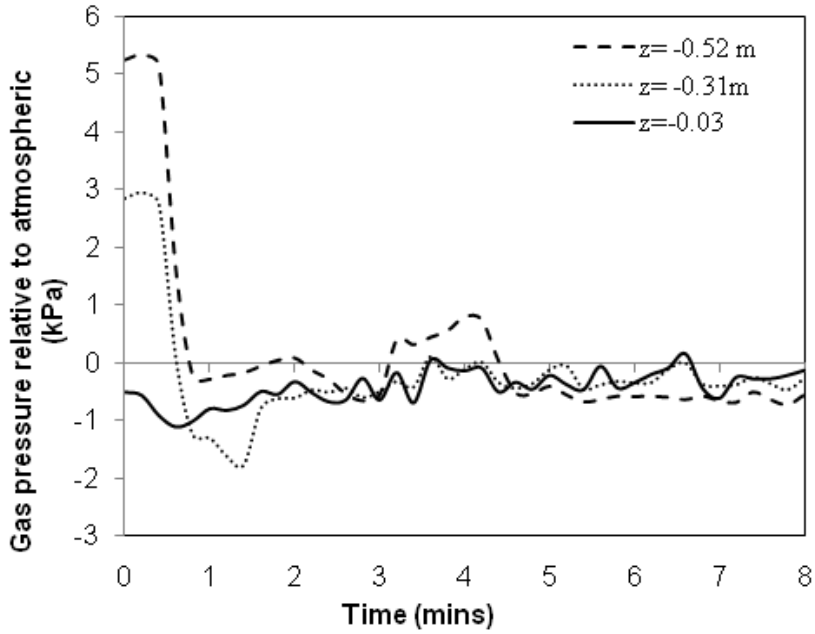

Figure 4.7 Measurements of the gas pressure (kPa) at top, bottom and middle of the MBT waste column for the first minutes of the one-step drainage experiment

The temperature of the MBT column was measured by three thermistors during the drainage experiment (Appendix I).

The moisture retention data derived from the instrument readings after the end of the one-step drainage experiment (at equilibrium) fitted to the van Genuchten equation (Equation 2.20) are plotted in Figure 4.8. The best-fitting curve was obtained by the method of least squares (in solver).The least square method defines the estimate of the van Genuchten parameters as the values which minimize the sum of the squares between the measurements and the predicted values. The value of θ_r was taken from the pressure plate tests at suction 100 kPa, the θ_s value was taken from the initial theta probe readings and mass balance calculations, and the k_s value was taken close to that estimated by the constant head method. The tortuosity parameter,l, was assumed to be 0.5, which is an average value used for many soils (Mualem, 1976). Hence, only the van Genuchten parameters α and n were fitted to the drainage data.The van Genuchten parameters fitted to represent the capillary pressure functions were: θ_r=0.15 m^3/m^3, θ_s= 0.69 m^3/m^3, α= 0.8 kPa^{-1}, n=2.5.In addition to the equilibrium measurements, we can get a suction-moisture content curve from the transient measurements (dynamic profiles) at each depth. These are shown in Figure 4.8 as well. It is observed that the dynamic capillary pressure is lower than the equilibrium measured capillary pressure at horizons z=-0.12m and z=-0.31m. Hassanizadeh,

Celia et al. 2001 theorise that the measured dynamic capillary pressure measured at certain horizons should be greater than the one measured under quasi-static conditions, i.e. under stepwise lowering of the bottom boundary condition to atmospheric pressure. In our experiments, due to the sudden gravitational pull caused by lowering the bottom boundary pressure from hydrostatic to atmospheric pressure, movement of fine materials through the pores between the larger ones may have occurred as the leachate is drained out. This could explain the anomalous water content distributions shown in Figure 4.6.

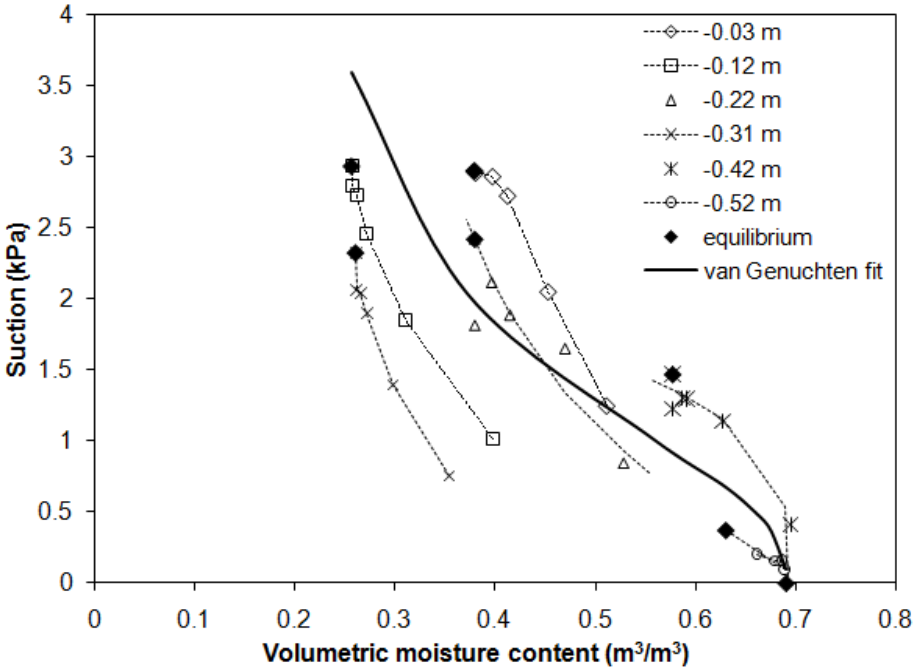

Figure 4.8 Measured dynamic and static (at equilibrium) moisture retention curves from the one-step drainage experiment

Further experiments were carried out to verify whether or not the capillary pressure and moisture content measured in the column apparatus provide a consistent dataset at each depth when lowering the head at the lower boundary in steps.

4.2.2 Multistep drainage

Six pressure steps were applied by sequentially lowering the height of the outflow tubing to 0.475 m, 0.39 m, 0.31 m, 0.22 m, 0.12 m, 0.03 m and 0 m above the bottom of the MBT column. Figure 4.9 shows the cumulative mass flow of leachate from the MBT during the multistep drainage, as measured by the electrical balance. About 8 litres of leachate had drained out after 9 days.

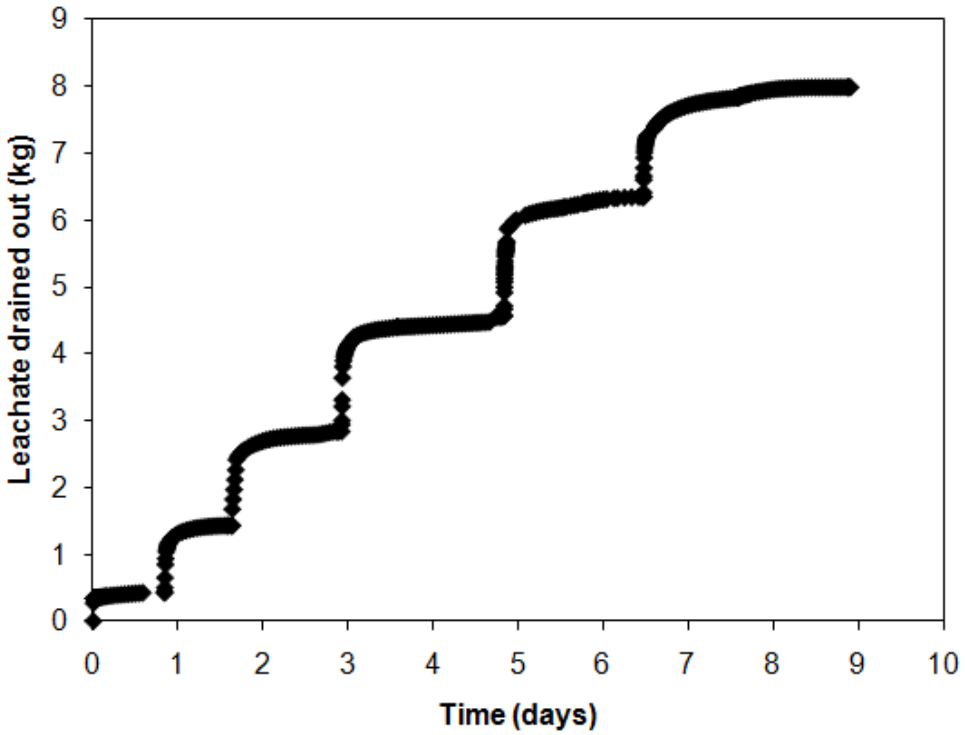

Figure 4.9 Mass of leachate drained out (kg) during the time period (days) of the multistep drainage experiment

Figure 4.10 shows the transient moisture contents as measured by the six theta probes. Figures 4.11 and 4.12show the moisture content distributions and pore liquid pressure (profiles) over the height of the column at equilibrium for each step. It may be observed in Figure 4.11 that the initial volumetric moisture content, as measured by the Theta probes, decreases with depth down the column. Given that these were saturated conditions this indicates that the porosity decreases with depth despites attempts to produce a sample with uniform density. This might have been the result of the lower layers becoming slightly more compacted after their placement by the action of installing new layers of material above them. The constant head method, to determine the saturated hydraulic conductivity of the waste column, was carried out before the drainage experiment and it is possible that the upward flow of the de-aired water caused disturbances in the vertical density of the MBT column. However there is some indication that the permeability falls with depth, which would be consistent with the porosity falling with depth.

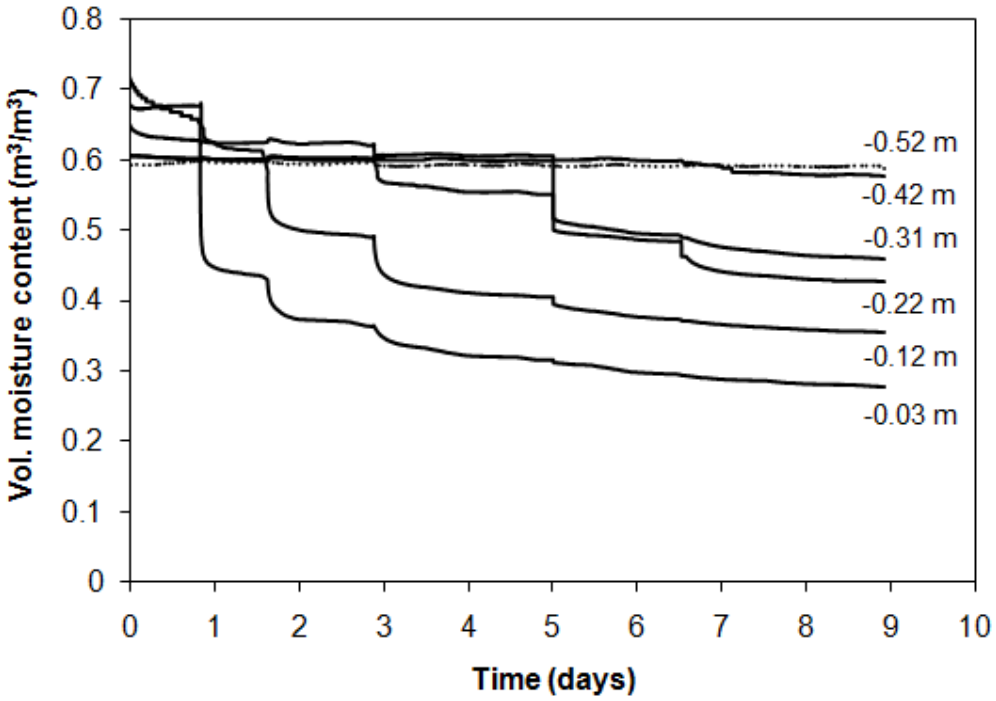

Figure 4.10 Measurements of the volumetric moisture content (m^3/m^3) of the MBT waste column by the six Theta probes during the multistep drainage experiment

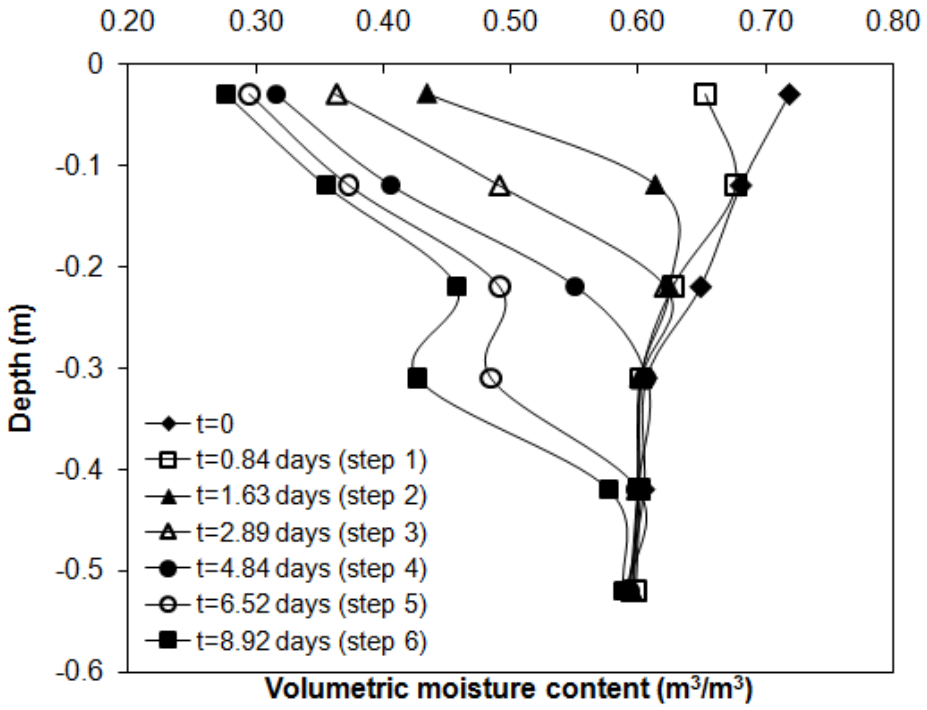

Figure 4.11 Distribution of the volumetric moisture content (m^3/m^3) along the MBT column, measured by Theta probes, at equilibrium for each step of the multistep drainage experiment

The accuracy of the theta probes measurements was verified by estimating the area of the theta probe readings between t=0 and t=8.92 days and adding the amount of leachate in the outflow tube during the multistep drainage experiment (Figure 4.11). The total volume of leachate drained out estimating by this method was 8.31 litres close to the reading of the electrical balance (8).

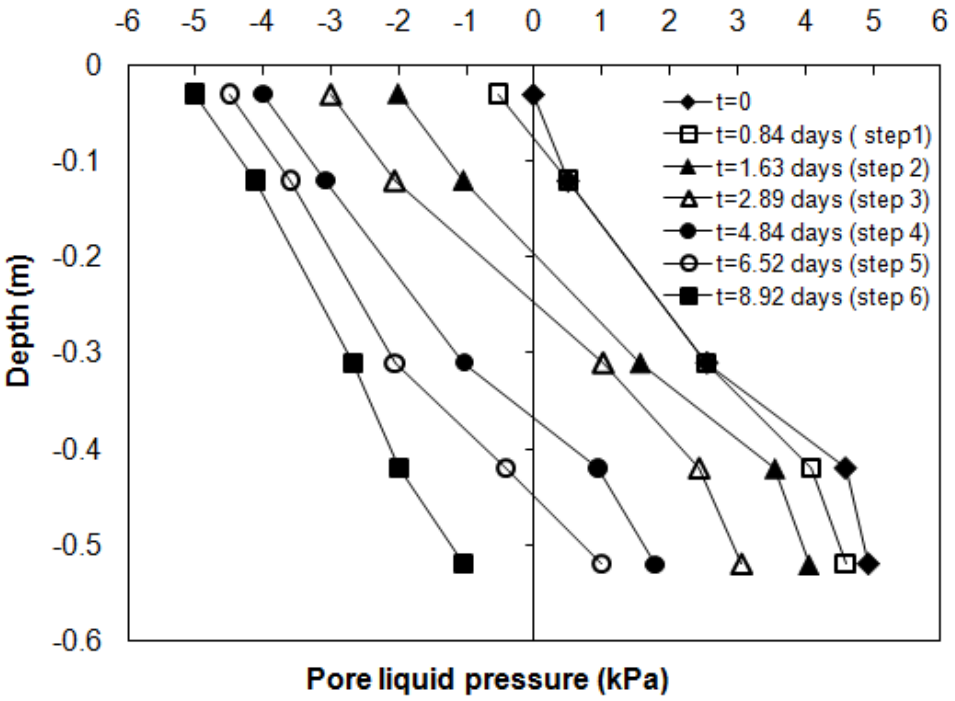

Figure 4.12 Distribution of the pore liquid pressure (kPa) along the MBT column, measured by tensiometers, at equilibrium for each step of the multistep drainage experiment

The moisture retention data derived from the instrument readings after the end of the multistep drainage experiment fitted to the van Genuchten equation (Equation 2.20) are plotted in Figure 4.13. The best-fitting curve was obtained by the method of least squares. The van Genuchten parameters fitted to represent the capillary pressure functions were: θ_r=0.15 m^3/m^3, θ_s= 0.70 m^3/m^3, α= 0.47 kPa^{-1}, n=2.6. It was observed that the waste drains significantly more freely in the one-step drainage experiment than in the multistep one. Figure 4.14 shows that the capillary pressure curves deduced from the transient readings at different horizons are close to each other. This shows that each layer drains in a similar way, in terms of the $p_c(\theta)$ path curve.

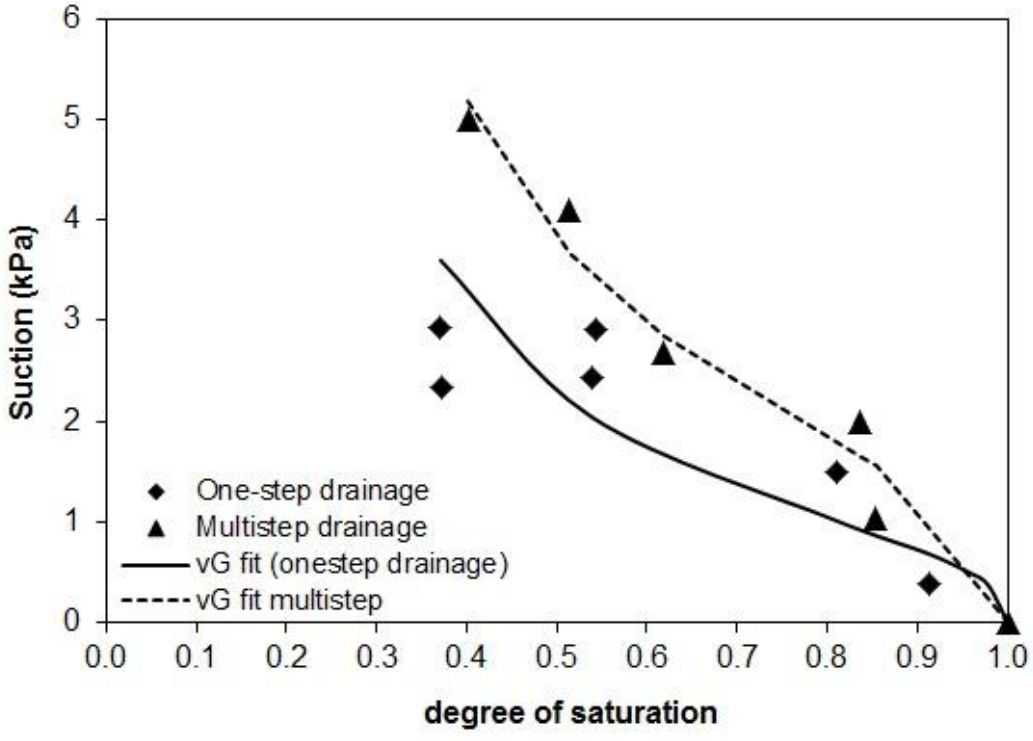

Figure 4.13 Moisture retention data from the one-step and multistep drainage experiments fitted to van Genuchten curves

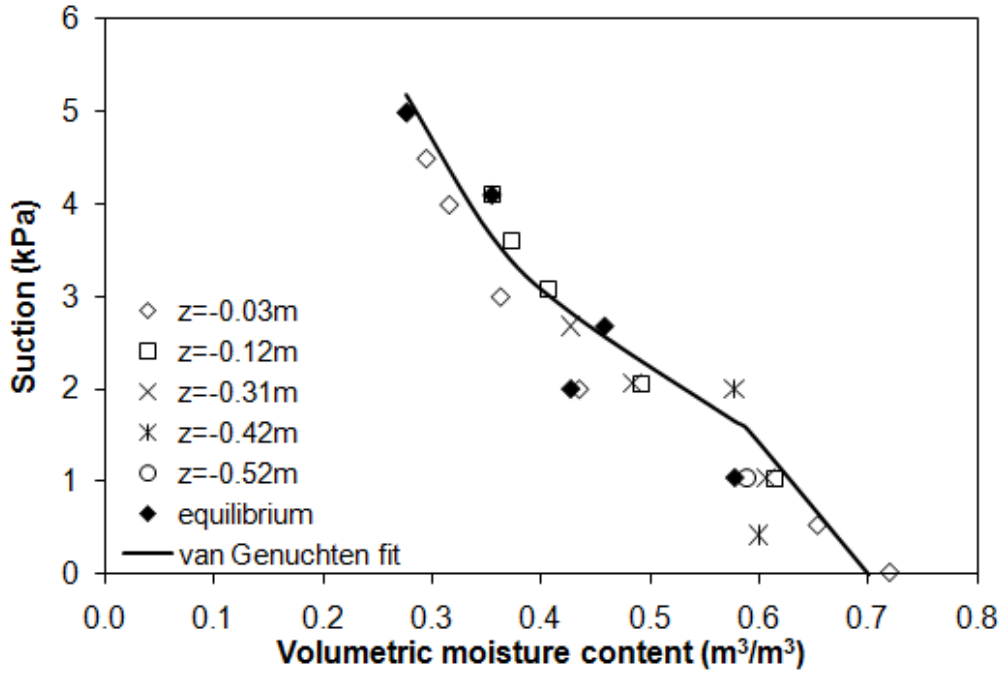

Figure 4.14 Measured dynamic and static moisture retention curves from the multistep drainage experiment

4.2.3 Saturated hydraulic conductivity

The saturated hydraulic conductivity of the MBT column was determined by the constant head method before and after the one-step drainage experiment and before the multistep drainage experiment.

As may be seen in Figure 4.15 the initial saturated hydraulic conductivity (k_s) of the MBT waste before the one-step drainage experiment was almost homogeneous along the column, at about 4 x 10^{-5} m/s. Some slight changes of k_s profile were observed after the drainage experiment. The fact that the k_s value after the drainage at the top layer was doubled is explained by surface disturbance expected due to drainage under gravity. Possible internal movement of fine materials started happening at the point of the sudden gravitational pull. The initial saturated hydraulic conductivity (k_s) of the MBT waste of the multistep drainage experiment was between 2 x 10^{-5} m/s and 4 x 10^{-5} m/s. The saturated hydraulic conductivity (k_s) of the MBT waste after the multistep drainage experiment was not measured. A constant head permeability test (BS 1377 Part 5, 1990) on a sample of MBT carried out in a 75 mm diameter permeameter gave a saturated hydraulic conductivity of between 2.26 x 10^{-5} m/s and 4.52 x 10^{-5} m/s.

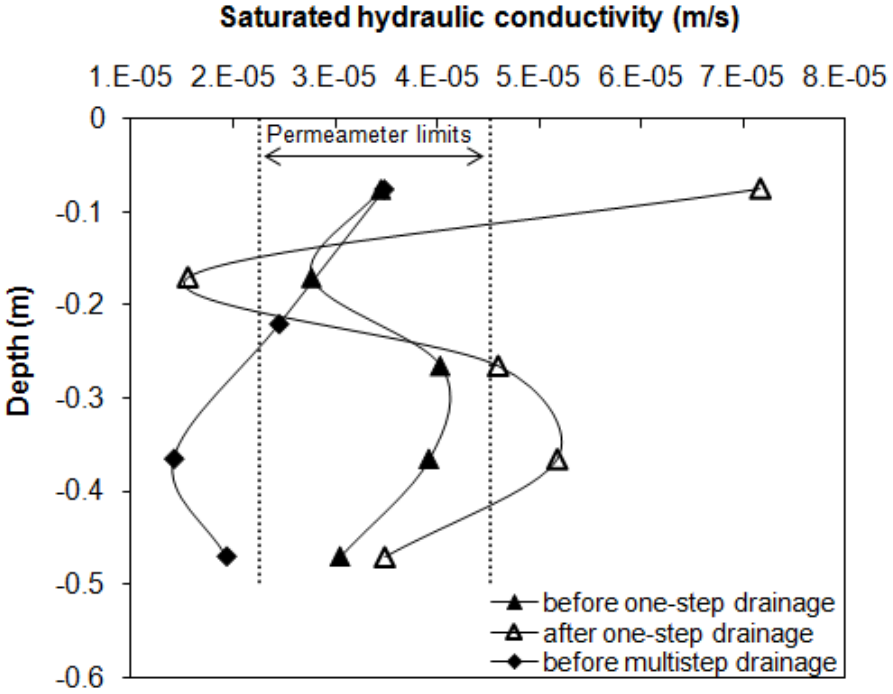

Figure 4.15 Profiles of the saturated hydraulic conductivity before and after the drainage experiments

4.3 Hanging column tests results

Semi-normalised moisture retention curves at equilibrium for the three representative MBT hanging column tests described in Table 4, and for MBT waste at a dry density of 520 kg/m^3 derived from the one-steo and multistep drainage experiments, are plotted in Figure 4.16. The best-fitting curves were obtained by the method of least squares (in solver).The van Genuchten fitting parameters are shown in Table 4.1 along with the correlation coefficient, R^2.The experimental data were also fitted to Brooks and Corey model (Appendix J) but the van Genuchten model gave a better fit to the data.

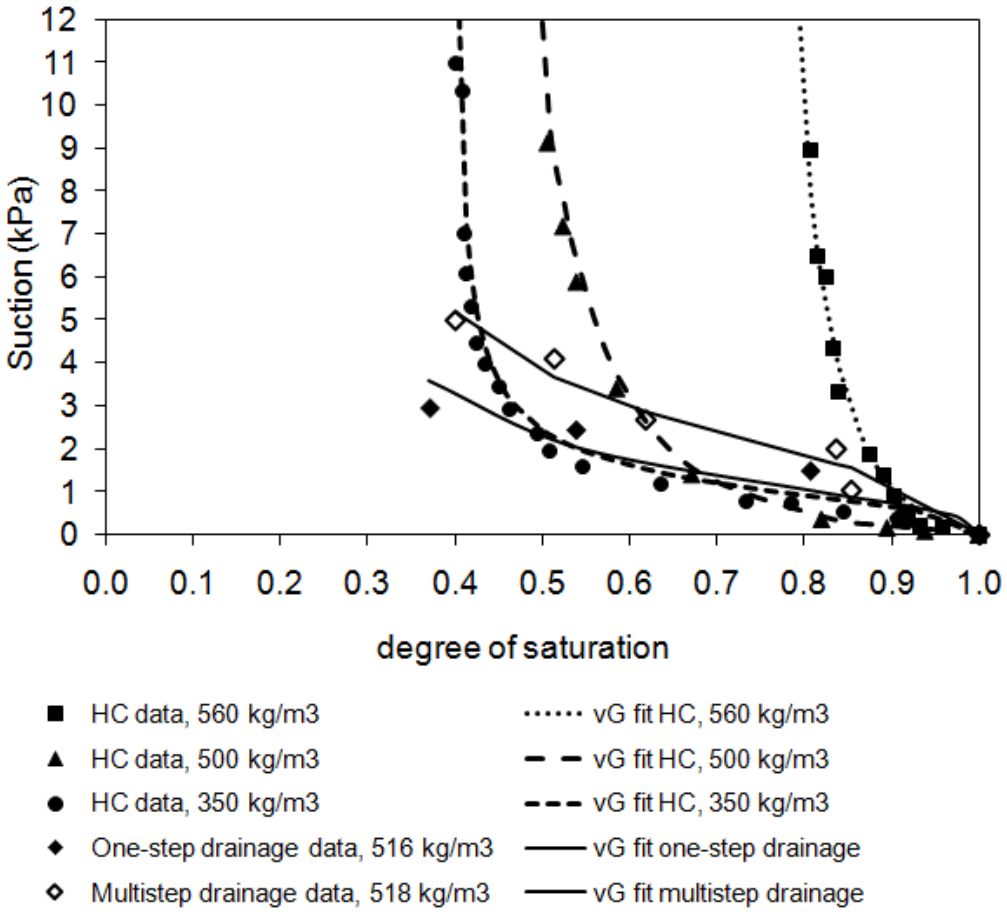

Figure 4.16 Moisture retention data for different MBT waste specimens derived from the drainage experiments and the hanging water column tests fitted to van Genuchten curves

Table 4.1 van Genuchten parameters fitted to the hanging column (HC), pressure plate and data from the drainage experiments (by least squares method)

vG parameter	HC, p_d=560 kg/m^3	HC, p_d=500 kg/m^3	HC, p_d=350 kg/m^3	Pressure plate test, p_d=520 kg/m^3	One-step drainage, p_d=516 kg/m^3	Multistep drainage, p_d=518 kg/m^3
θ_r (m^3/m^3)	0.20	0.15	0.27	0.15	0.15	0.15
θ_s (m^3/m^3)	0.65	0.69	0.7	0.70	0.69	0.70
α (kPa^{-1})	3	3.55	1.57	1.65	0.8	0.47
n	1.10	1.26	2.32	1.64	2.5	2.6
R^2	0.985	0.996	0.962	0.988	0.830	0.974

In Figure 4.16, the moisture retention curves for specimens of higher density are located to the right, indicating that at a given suction the moisture content is higher and that denser samples have a greater air entry value. This is consistent with a generally smaller void size. The van Genuchten parameters α and n decrease with increasing dry density in the two hanging column tests using 0-10 mm MBT waste, while in the third test using 0-9 mm MBT waste the parameter α is smaller than for the higher density specimens. This is because the 0-9 mm waste contains more paper; hence it retains more water and has a higher air entry value. Also, the saturated moisture content (θ_s) increases with decreasing density and increasing proportion of organic matter in the waste, while the residual moisture content (θ_r) increases with increasing density and proportion of organic matter in the waste. The same observation was done by Stoltz et al. (2011) for MSW with high organic component.

4.4 Pressure plate test results

On removing the specimen from the pressure plate apparatus at the end of test 1, it was noted that the top half of the sample was drier than the bottom. This is indicative of a partial or full interruption of the liquid phase within the specimen, inhibiting the drainage of liquid and resulting in an increase in the retained moisture content at a given relative suction. This was not observed in test 2. Also the sample in test 1 was not fully saturated initially (S_r=0.82), so there was some air in the sample reducing the initial continuity of the liquid phase. A further difference between the two tests was in the pressure increments applied, which were smaller and started from a lower value (6 kPa rather than 20 kPa) in test 2

than in test 1. It is possible that the larger starting pressure and greater increments in test 1 also contributed to the loss of continuity of the liquid phase within the specimen, as described above.

Figure 4.17 shows the cumulative mass of leachate drained out of the specimen (g) against time (days) during pressure plate test 2. The moisture retention data for the six applied pressures are shown in Figure 4.18 together with a van Genuchten curve (Equation 3) fitted using the parameter values given in Table 6.

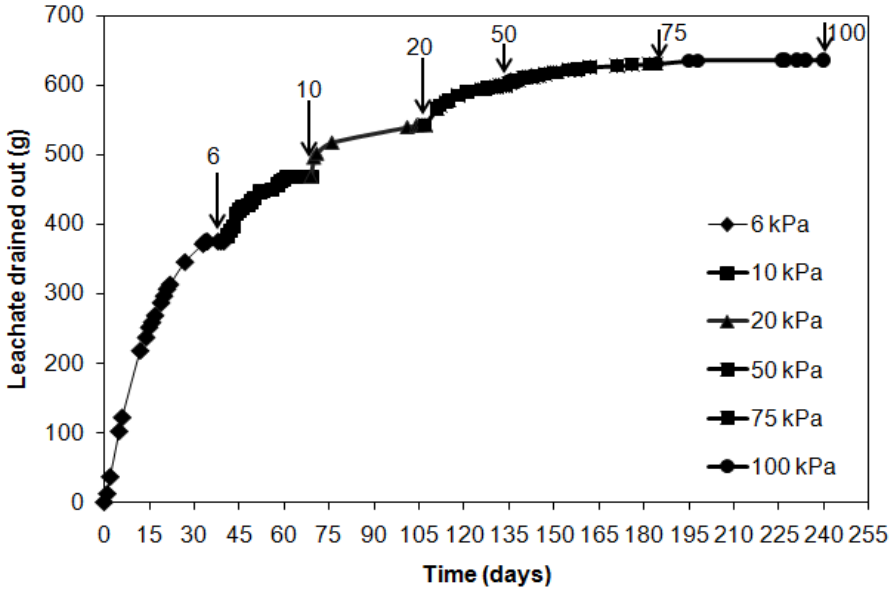

Figure 4.17 Leachate drained out (g) against time (days) during the pressure plate test 2

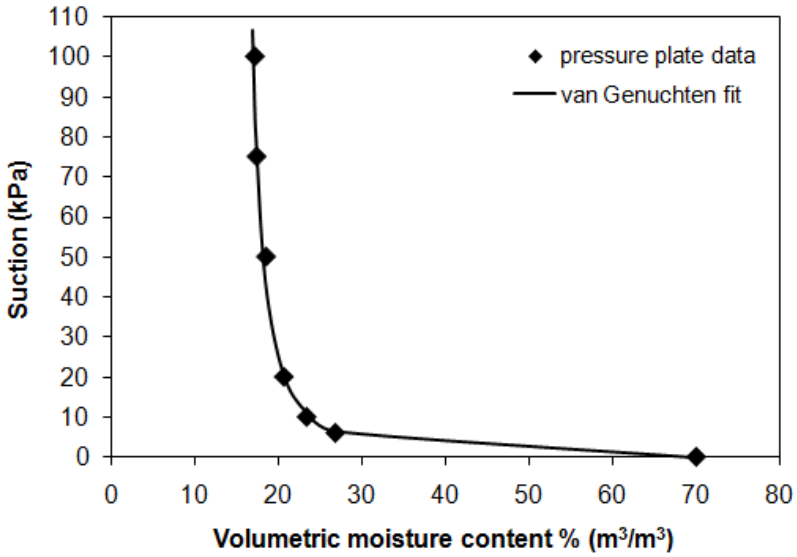

Figure 4.18 Moisture retention data for MBT waste sample derived from the pressure plate test fitted to van Genuchten curve for the six applied pressures

4.5 Effect of dry density on the van Genuchten parameters

The van Genuchten parameters α, n and θ_r are plotted in Figures 4.19, 4.20 and 4.21against dry density in an attempt to see to what extent it might be possible to correlate the van Genuchten parameters with dry density. Breitmeyer (2011) and Stoltz et al. (2011) have suggested on the basis of limited data that there might be a linear relationship between α, n and dry density. The data shown in Figures 4.19 – 4.21 come from the current laboratory experiments and the literature (Breitmeyer, 2011; Staub, 2010; Stoltz, 2007; Kazimoglu, 2005 and Muennich, 2003).The parameters α and n do appear to have a tendency to decrease with increasing dry density (decreasing porosity).This is as might be expected from the sensitivity analysis carried out in Sections 7.1 and 7.2 where the expected ranges of the values of the parameters α and n are discussed further. There it is shown that as α and n decrease (and from Figures 4.19 and 4.20, as dry densities increase) suctions increase. This indicates that compression of waste materials results in an increase in the number of smaller pores, which therefore become more evenly distributed within the specimen. The value of the parameter θ_r would also be expected to increase with increasing dry density and organic matter but this is not clear from Figure 4.21.

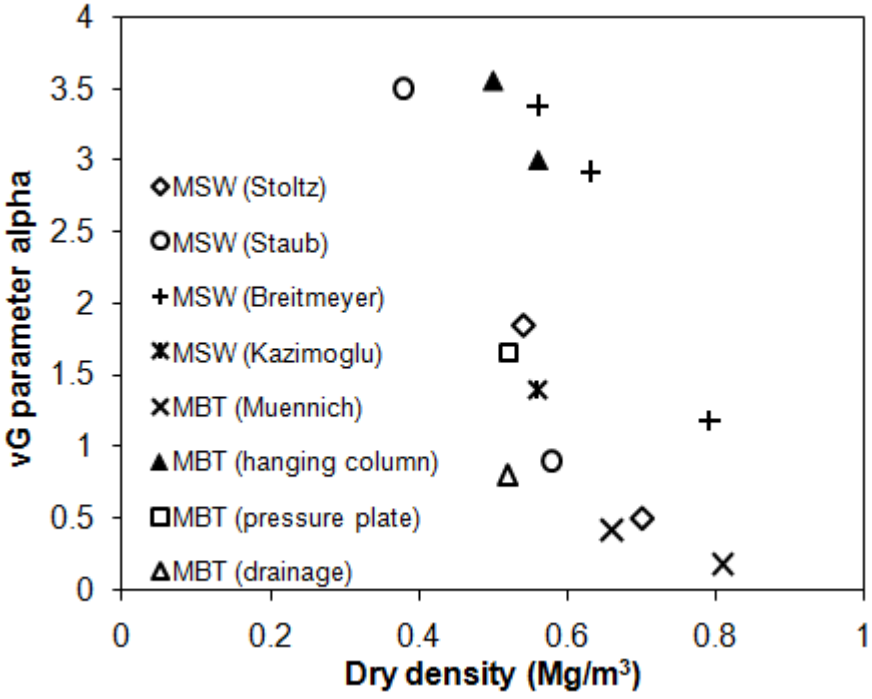

Figure 4.19 van Genuchten parameter α versus dry density for laboratory tests and reported in literature

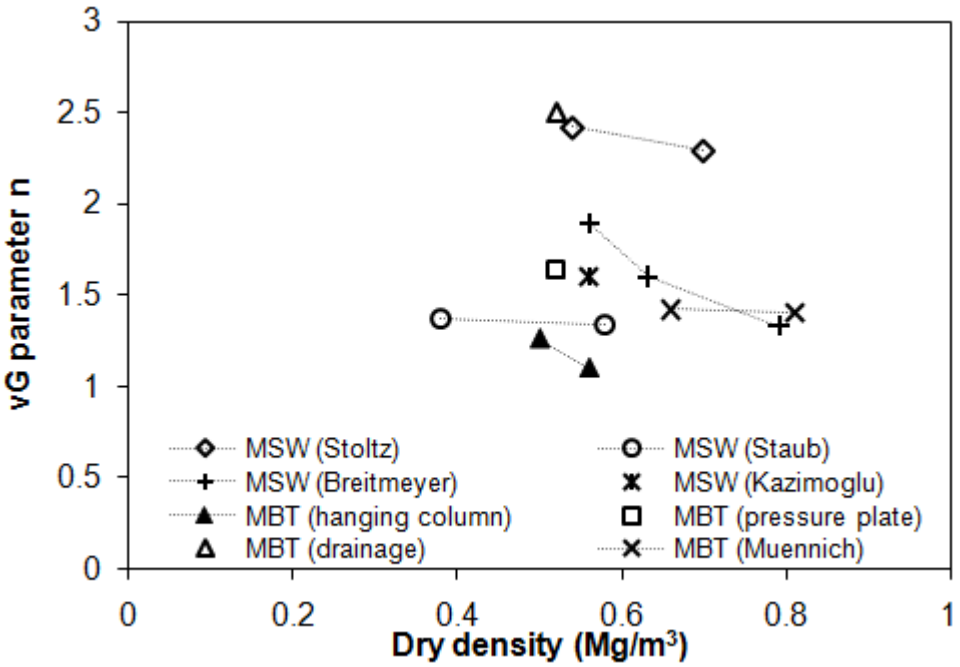

Figure 4.20 van Genuchten parameter n versus dry density for laboratory tests and reported in literature

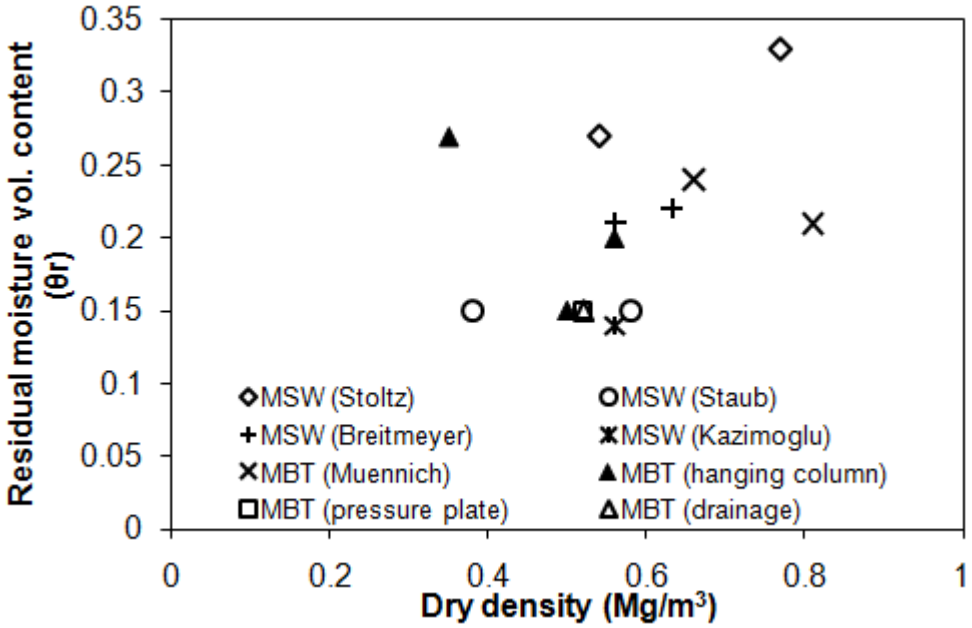

Figure 4.21 van Genuchten parameter θ_r versus dry density for laboratory tests and reported in literature

4.6 Comparison of the different techniques for the determination of the MRC for MBT waste

Figure 4.22 shows the moisture retention data for MBT waste specimens with similar dry densities (p_d=500 kg/m^3) obtained using the three different techniques, and the respective van Genuchten fitted curves. The general appearance is of a single drying curve (labelled A in the Figure 4.22) and a series of apparent curves branching from it when the continuity of suction within the specimen or between the specimen and the porous plate is lost.

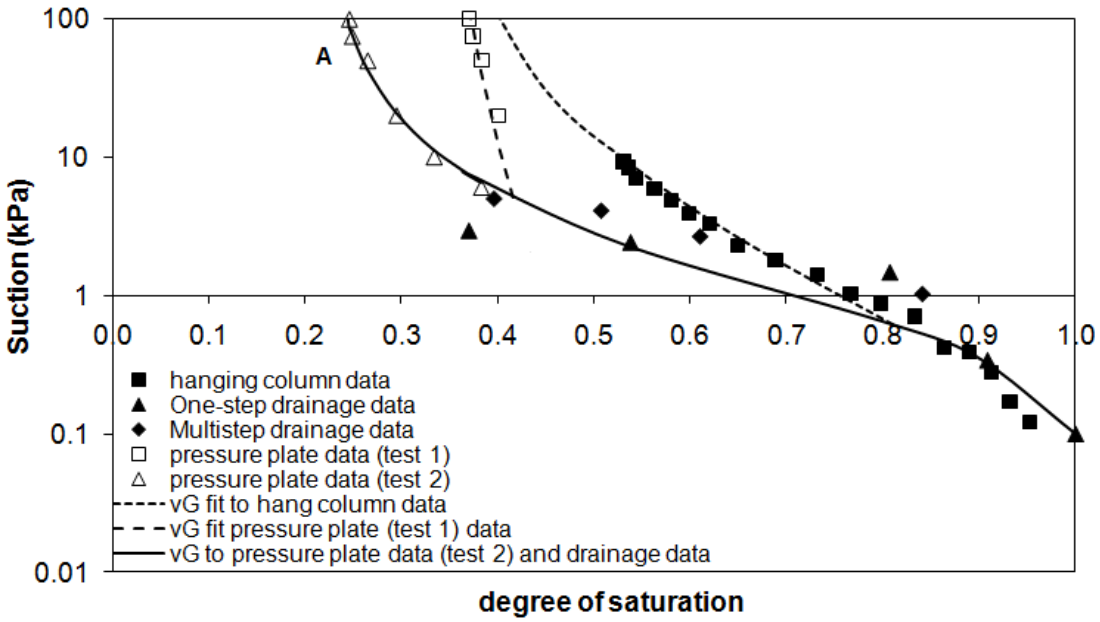

Figure 4.22 Comparison of the moisture retention curves determined for a fine MBT waste of particle size 0-10 mm by a column drainage experiment, hanging water column technique and pressure plate apparatus

The hanging column and pressure plate techniques require a perfect hydraulic contact between the specimen and the porous plate. A partial or full interruption of the liquid phase within the specimen, or between the specimen and the plate will inhibit the drainage of liquid from the specimen, resulting in an increase in the retained moisture content at a given applied external suction.

White (2010) identified reasons why variations might occur in the results obtained from hanging column apparatus tests on samples of waste material. The hanging column apparatus applies a suction pressure from a water column to a material

sample through a porous plate. The pores in the plate connect into the pores in the sample and the suction pressures partially drain the sample. The greater the applied suction pressure the more the sample drains. The pore space geometry of a porous material is perceived to be a collection of variable sized pores connected into a network by narrow throat like channels in which the throat diameters are small in relation to the pore sizes. The concept is extended further by assuming that, when a suction pressure p_C is applied to a sample, the pores that are drained are those connected by pore throats that have a throat diameter d_T for which p_C can overcome the surface tension forces. Further to Equation 2.3, the relationship between p_C and d_T may be assumed to be,

$$p_C = \frac{4T}{d_T}\cos\beta \tag{4.1}$$

where T is the coefficient of surface tension, which for a water/air interface is about 0.07 N/m and β is the contact angle of liquid with the solid particles.

Assuming that the range of values of p_C that might be applied to a sample in a laboratory or field context are between 1 kPa and 100 kPa the corresponding throat diameters would be for a contact angle β of zero: d_T =0.28 mm for p_c= 1 kPa, d_T =0.028 mm for p_c= 10 kPa and d_T =0.0028 mm for p_c= 100 kPa. Thus the application of a small suction pressure of 1 kPa would drain all of those pores connected to a network in which the pore throats were greater than 0.28 mm (a fraction of a millimeter).

As the suction increases more drainage paths with smaller pore throat diameters are mobilised and a greater fraction of the pore space is drained. As the saturated network reduces, some zones may become disconnected from a drainage path so that the water within them becomes trapped. Plastic elements in the sample may also reduce the pore connectivity.

It is also important to realise that in the context of a hanging column apparatus the suction pressure will only be applied to a drainage path (continuous or not) if that drainage path is successfully connected to the hanging column of water through the porous plate. Thus the hanging column apparatus technique relies on the sample being set up so that all of the range of drainage path scales is connected.

This may be more difficult to achieve in the case of a 10mm sample of MBT than it would be with clayey silty sand.

In the hanging column and pressure plate apparatus, suction can only develop in a drainage path if that drainage path is connected to the suction applied at the porous plate. In the drainage experiment, moisture content and suction are point measurements. Thus the hanging column and pressure plate apparatus techniques rely on the specimen being set up so that the whole range of drainage path scales is connected, and remains connected, to the applied suction at the boundary.

This issue will be returned in Chapter 5 when the results of estimating the unsaturated hydraulic conductivity functions are discussed.

4.7 Mercury porosimetry test

Mercury intrusion porosimetryis a technique used to measure pore size and pore volume distribution of pores from 0.0036 micron to over 950 micron diameters. The operation of all mercury porosimeters is based upon the physical principle that a non-reactive, non-wetting liquid will not penetrate fine pores until sufficient pressure is applied to force its entry. It measures the volume of mercury intruded into a sample in relation to the pressure of mercury that is applied. The assumption is that the same volume of water would be intruded by water but at a lower pressure because the surface tension coefficient for water is lower. Thus the equivalent water curve is obtained by multiplying the mercury pressures by the ratios of the surface tensions and wetting angle cosines using equation 4.1:

$$p_c(\text{water}) = (\gamma_w \cos\beta_w / \gamma_m \cos\beta_m) * p_c(\text{mercury}) \qquad (4.2)$$

where the surface tension (γ_w) of water is 0.07 N/m and the surface tension (γ_m) of mercury is 0.47 N/m.β_w is the contact angle of water with the solid particles and β_m is the contact angle of mercury with the solid particles.

A mercury porosimetry test was carried out by MCA Services for a very small sample of dry MBT of mass 1.23 g and dry density 823 kg/m^3. The moisture retention curve obtained from the experimental data was compared to the one obtained from the porosimetry (Figure 4.23). The curves seem close at very low

and very high values of suction but the curve estimated by the porosimetry method rises more rapidly as the suction is increased instantly. This is to be expected, as the dry density of the sample used was higher. However a firm conclusion cannot be reached because only one porosimetry test was carried out using a very small sample. It is certainly difficult to infer anything about the role of macropores in MBT waste from such a small sample.

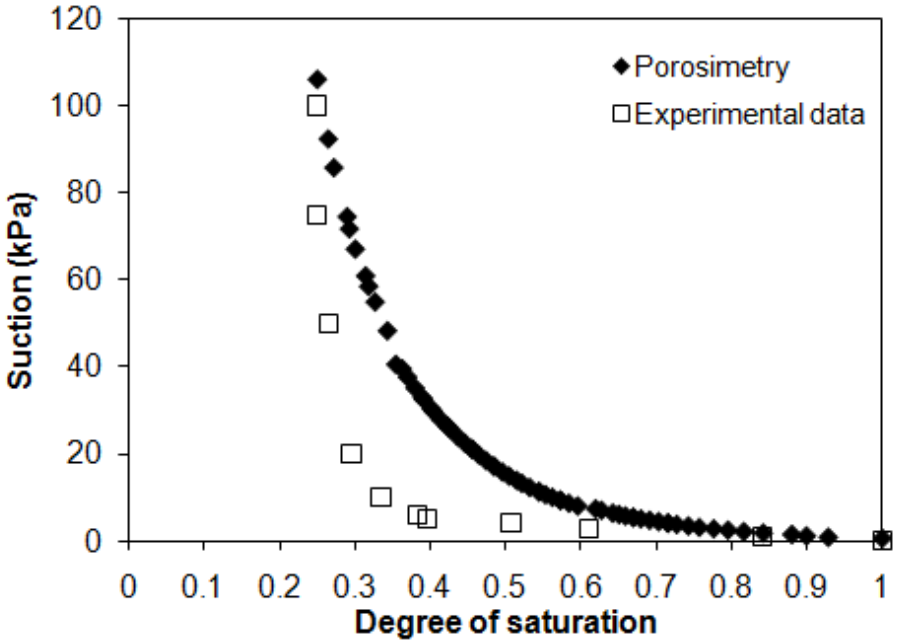

Figure 4.23 Moisture retention curves of the MBT waste derived from the multistep drainage/hanging column/pressure plate techniques and from mercury porosimetry

The pore distribution of the MBT sample was also estimated by mercury porosimetry method. It is obviously a unimodal pore size distribution (Figure 4.24). For comparison Figure 4.25 shows a multimodal pore size distribution of a spray dried catalyst sample derived from the same method (Giesche, 2006). The unimodal soils are characterized by a single pore-size distribution function (Nimmo, J.R., 2004).Again, since it is just one result, any extensive claim cannot be done but it may be of interest.

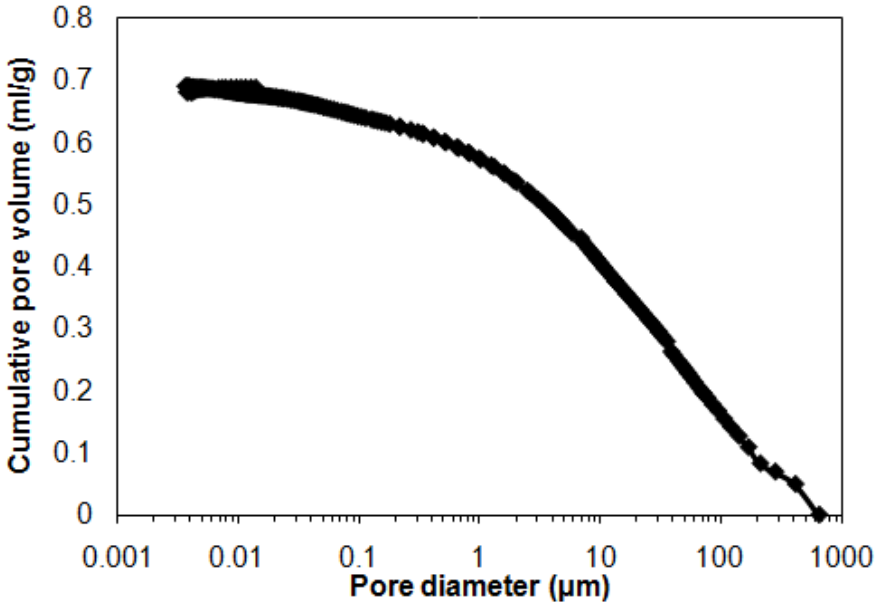

Figure 4.24 Unimodal pore size distribution of MBT sample (MCA Services)

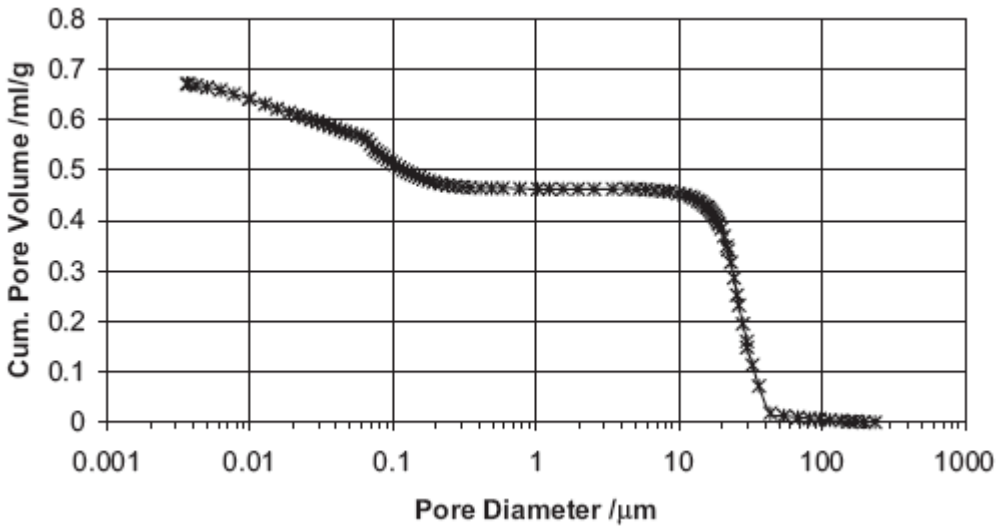

Figure 4.25 Multimodal pore size distribution of a spray dried catalyst sample (after Giesche, 2006)

However, undisturbed soils may occasionally exhibit retention curves with more than one inflection point. This multimodality of pore-size distribution may be the result of specific particle-size distributions or be due to the formation of secondary pore systems (macroporosity) by various processes such as soil aggregation or biological soil forming (Durner, 1994). For these types of soils, the moisture

retention curve is separated into two regions joined at a common suction value, referred to as the matching point. The data in each region are fit separately using a unimodal moisture retention curve functions (Smetten and Kirkby, 1990).

Finally, the zone covered by the van Genuchten fit to the experimental data (hanging column, pressure plate and drainage column data) and the mercury porosimetry data is shown in Figure 4.26.The lower bound is the van Genuchten fit to the experimental data and the upper bound is the curve of the porosimetry data.

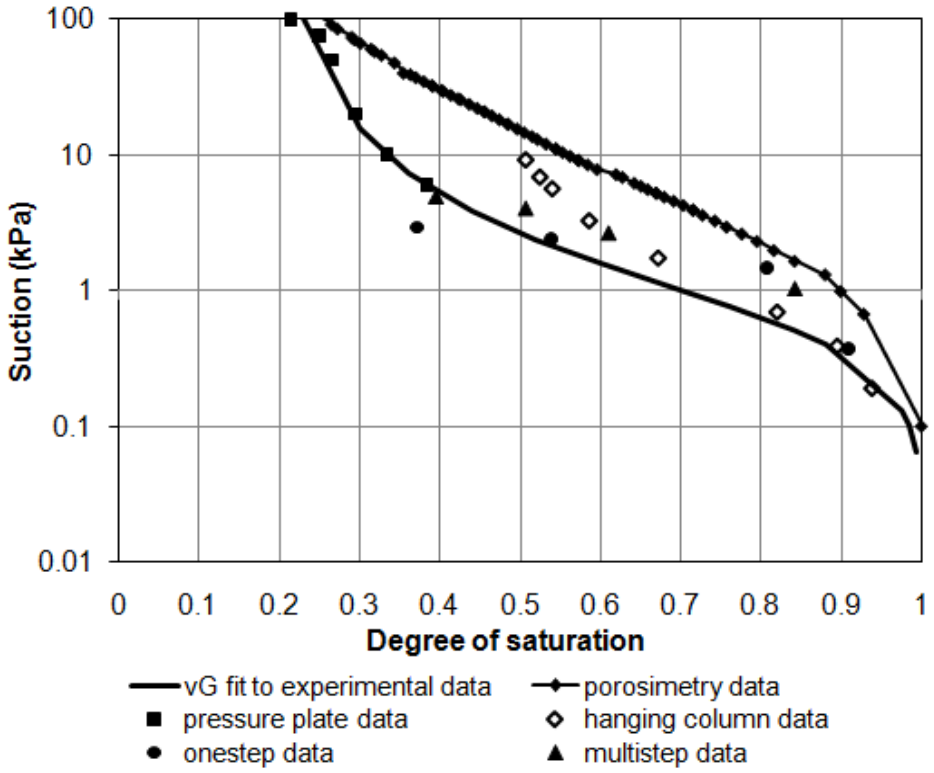

Figure 4.26 Lower and upper bounds of the moisture retention curves

4.8 Summary

Moisture retention curves were determined for a fine MBT waste of particle size 0-10mm using three different methods: a column drainage experiment (one-step and multistep), the hanging water column technique and a pressure plate apparatus. A satisfactory fit to each data set could be obtained using the van Genuchten (1980) curve, but there were significant discrepancies between the three sets of results. In particular,

- hanging column tests showed an apparently plausible variation of moisture retention curve with density and were self-consistent, but different from those obtained using the other apparatuses

- two tests in the pressure plate apparatus gave two different curves, one of which was close to the drainage column test data and the other to the hanging column test data. On inspection of the specimen used to generate the latter, a clear horizontal discontinuity was found which could have been caused by the too rapid application of large pressures.

- the waste drains significantly more freely in the one-step drainage experiment than in the multistep one where each layer drains in a similar way.

It is considered that the curves obtained using the hanging column apparatus and in the first pressure plate test were affected by a lack of adequate hydraulic continuity within the specimen, or between the porous plate to which the boundary suction is applied and the specimen, resulting in the retention of too much water at a given suction. The moisture retention characteristic curve for a waste was better determined from direct measurements of suction and moisture content, as in the drainage column apparatus for low suction range and from pressure plate apparatus for high suction range. This has significant implications for the study of liquid movement in unsaturated wastes.

CHAPTER 5

DETERMINATION OF THE UNSATURATED PERMEABILITY OF MBT WASTE FROM THE EXPERIMENTAL TECHNIQUES

5.1 Introduction

A review of some of the previous work done on the estimation of the relationship between hydraulic conductivity and moisture content in unsaturated waste materials was presented in Chapter 2. This Chapter presents the results of the analysis that has been carried out of the transient data obtained from the drainage experiments of the MBT column described in Chapter 4.The analysis used to determine the unsaturated hydraulic conductivity is based on the instantaneous profile method (Richards and Weeks, 1953). In addition the outflow data from the pressure plate experiments described in Chapter 4were used to calculate the unsaturated hydraulic conductivity of the MBT specimens using the methods of Gardner (1956) and Passioura (1976). The unsaturated hydraulic conductivities of MBT thus obtained are also compared with calculations using the algebraic function proposed by van Genuchten (1980) after Mualem (1976) equation (2.26) (Chapter 2).

5.2 Determination of the unsaturated permeability from the drainage experiment results using the instantaneous profile method

Unsaturated hydraulic conductivities have been determined in the laboratory and the field using the instantaneous profile method. Richards and Weeks (1953) first described the instantaneous profile method and since then it has been refined by several investigators (Bruce and Klute 1956; Watson 1966; Rogers and Klute 1971; Klute 1972, Hamilton et aI. 1981; Daniel 1983; Malicki et aI. 1992).

The instantaneous profile method analyses transient data from a single imbibing/drainage test to obtain the wetting and/or drying curve relating unsaturated hydraulic conductivity to moisture content. The method was applied to the data from the drainage experiments described in Chapter 4 to estimate of the unsaturated hydraulic conductivity of the MBT waste as follows.

The unsaturated hydraulic conductivity was calculated using Equation 5.1:

$$k_{unsat} = -\frac{\Delta V}{A\Delta t}\left(\frac{1}{dh/dz}\right)_{z=zi} \quad (5.1)$$

where ΔV is the volume of leachate estimated to move past a point Z_i (the i^{th} point) in the MBT column of cross-sectional area *A* during an increment of time Δ*t.* The variable *z* is the vertical coordinate (the origin being at the top of column) and *dh/dz* is the gradient in hydraulic head *(h).* Flow was assumed to occur one-dimensionally in the vertical direction. The following steps were used to calculate the unsaturated hydraulic conductivity from Equation (5.1)*:*

1. Graphs of suction and volumetric moisture content vs. depth were prepared from data collected at various times during a test (Figure 4.4).

2. Hydraulic gradients at point Z_i at times t and t' were determined from the profiles of suction against depth (Figure 4.4) using the equation:

$$-\left(\frac{dh}{dz}\right) = 1 + \left(\frac{d\psi}{dz}\right)_{i,tj} \quad (5.2)$$

where t_j= t or t' (t>t'). Calculations were made using Equation 5.2 for each of the six instrumented points in the MBT column. The hydraulic gradient for the time period between t and t' was taken as the arithmetic mean of the hydraulic gradients computed with Equation 5.2 at times t and t', for each point z_i.

3. The volume of leachate that passed point Z_i in the time period between t and t' (ΔV_i) was calculated by integrating the difference in the moisture content profiles (Figures 4.6 and 4.11).

$$\Delta V_i = A\int_{Z_i}^{L} \left|\theta' - \theta\right| dz \quad (5.3)$$

where θ' is the moisture content at time t' and θ is the moisture content at time t.

4. Unsaturated hydraulic conductivity was calculated for each depth Zi and each increment of time by substituting the results obtained from Equations 5.2 and 5.3 into Equation 5.1. The suction assigned to the unsaturated hydraulic conductivity was the arithmetic mean of the suctions measured at the i^{th} instrumentation point at times t and t'.

The unsaturated hydraulic conductivity of the MBT column, for the one-step and multistep drainage experiments, derived using the above method is plotted against volumetric moisture content in Figure 5.1.In Chapter 6 the results of the drainage experiments are assessed using the Hydrus numerical model. Simulations using the single porosity model gave a best-fit to the van Genuchten-Mualem function (Equation 2.23)with parameters θ_r=0.15 m^3/m^3, θ_s= 0.69 m^3/m^3, α= 0.8 kPa^{-1}, n=2.5, m=0.6, k_s=4.5x10^{-5} m/s for the one-step drainage experiment and and θ_r=0.15 m^3/m^3, θ_s= 0.7 m^3/m^3, α= 0.47 kPa^{-1}, n=2.6, m=0.61, k_s=4.5x10^{-5} m/s for the multistep drainage experiment. Using these results, the van Genuchten-Mualem functions for unsaturated hydraulic conductivity are also plotted in Figure 5.1 for comparison.

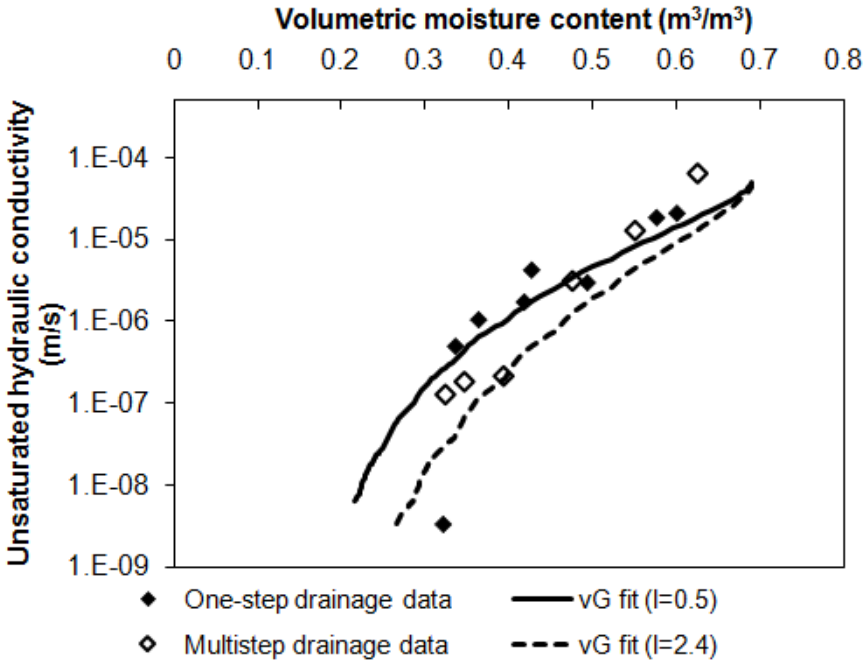

Figure 5.1 Unsaturated hydraulic conductivity against volumetric moisture content derived using the instantaneous profile method from the drainage experiments together with the corresponding van Genuchten curves using parameters obtained from the Hydrus simulations in Chapter 6.

In Figure 5.2 the graph of relative permeability against effective degree of saturation derived from the one-step drainage experiment is fitted to van Genuchten-Mualem function (R^2=0.68), the Brooks and Corey function (for λ=1, R^2=0.69).

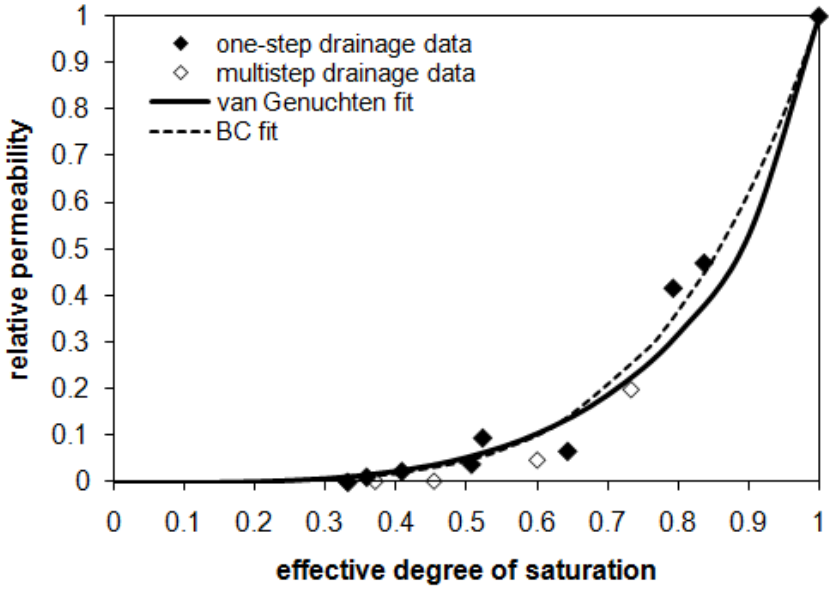

Figure 5.2 Relative permeability against effective degree of saturation derived from the drainage experiments fitted to different algebraic functions

In Figure 5.3 the relative permeability against degree of saturation derived from the one-step drainage experiment is compared to literature data of MSW materials with similar dry density and all fitted to van Genuchten-Mualem curves. Kazimoglu (2006) used the Passioura (1976) method on the pressure plate outflow data and Breitmeyer (2011) used the Gardner (1956) method on the outflow data from hanging column tests. It is observed that the van Genuchten-Mualem calculated relative permeability and the experimental data match well at low moisture content while at higher moisture contents, the agreement between them diverges. This may be attributed to the presence of very large pores in MSW. Though, this observation is not made for the MBT waste where the pore size distribution is more homogeneous. As discussed in Chapter 4, the MBT waste seems to have a unimodal pore size distribution and a single van Genuchten equation may describe well the relative permeability of the MBT waste. While for the MSW material a bimodal model (Ross and Smetment, 2000) would be more suitable to describe the relative permeability of the MSW. In this case the retention curve and relative permeability are described by the sum of two van Genuchten-Mualem models or a van Genuchten-Mualem model and an exponential model (Tinet et al., 2011). A comparison between a unimodal van Genuchten-Mualem and the bimodal

permeability functions is shown in Figure 5.4.The increase in permeabilities for low moisture content is clearly demonstrated.

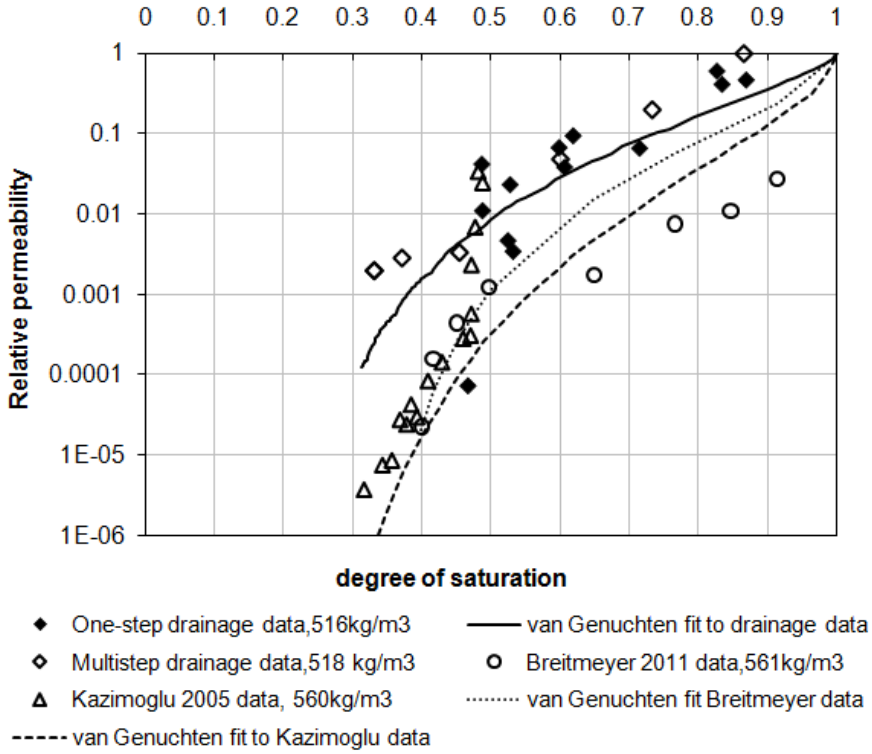

Figure 5.3 Relative permeability against degree of saturation derived from the drainage experiment compared to literature dataand van Genuchten-Mualem curves

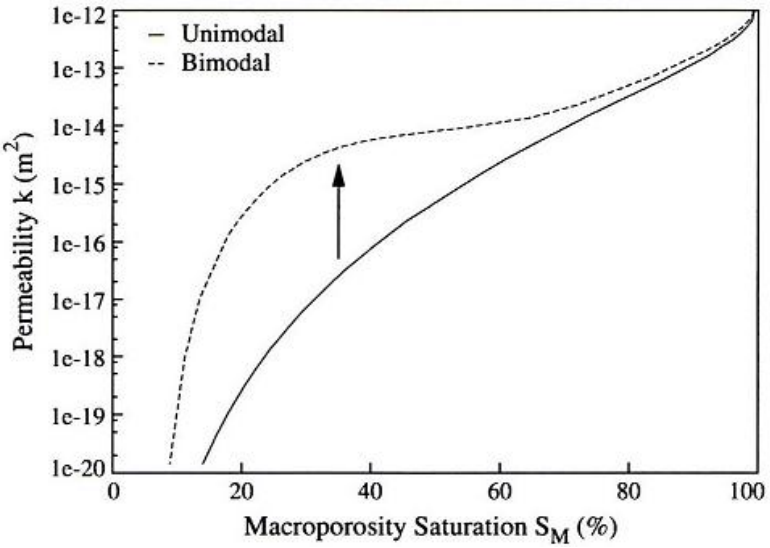

Figure 5.4 Intrinsicpermeability bimodal and unimodal model comparison (Tinet et.al, 2011)

The Breitmeyer (2011) and Kazimoglu (2005) data in Figure 5.3 and Figure 2.13 (literature) indicates that the liquid permeability of waste could fall by several

orders of magnitude in the unsaturated state. If this were to happen then drainage would effectively cease at only moderately low reductions in saturation. This is not what the column drainage experimental data reported here suggest, nor was it observed in afield scale trial at Beddington landfill (White et al. 2011).

5.3 Determination of the unsaturated permeability from the pressure plate test using Passioura's method

The outflow data from the pressure plate tests described in Chapter 4 were also used to determine the unsaturated hydraulic conductivity using the Gardner (1956) method (Appendix K). The results give higher relative permeabilities than those calculated using the instantaneous profile method for the drainage experiment data (Figure 5.5). It was concluded that this method was not suitable for application to the pressure plate test results because it requires very small suction increments. It also assumes that the hydraulic conductivity is constant over these increments. In the pressure plate test the suction increments were not small (Δψ) and probably this made the results unreliable. This method could not be applied to the hanging column test data, as Breitmeyer (2011) did successfully, because the data of the cumulative outflow volume with elapsed time for a given suction were not sufficiently detailed enough for the calculation method. The outflow data from the pressure plate tests described were also used to determine the unsaturated hydraulic conductivity using the Passioura (1976) method. The theory and calculation methods are shown in Appendix L. Kazimoglu et al (2005) used this method for MSW.

In Figure 5.5 unsaturated hydraulic conductivity against degree of saturation derived from the pressure plate data using Passioura and Gardner methods is plotted along with the data from the drainage experiments. The data are fitted to van Genuchten-Mualem function (Equation 2.23).

As show in Figure 5.5 the unsaturated hydraulic conductivity data derived from the pressure plate technique by Passioura method follow a van Genuchten curve (m=0.39) different from the one (m=0.6) that the data derived from the drainage experiments follow. There is a point jump (at degree of saturation 0.5) where the moisture content is falling and the liquid phase from that point is not continuous anymore. Hence the unsaturated hydraulic conductivity (or relative permeability)

from that point falls more orders suddenly and follows a different van Genuchten curve. This matter of 'discontinuity' is probably due to different experimental techniques giving different relative permeability results.

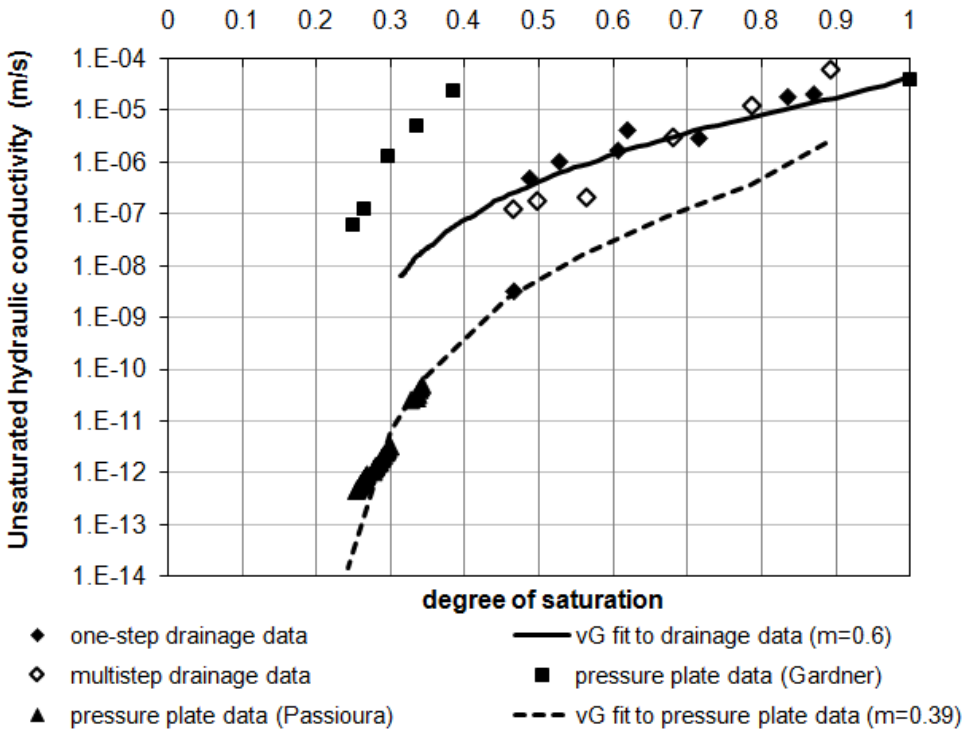

Figure 5.5 Unsaturated hydraulic conductivity of MBT against degree of saturation derived from the pressure plate experiment (using the Passioura and Gardner methods of analysis) and drainage experiments (using the instantaneous profile method)

Mualem (1976) noticed that there should possibly be a link between K(θ) and MRC since they both depend on pore space geometry. The results on Figure 5.5 could be linked with the MRCs in Figure 5.6. This figure shows that the van Genuchten curve A (referred in Figure 4.22, mainly supported by the pressure plate test 2 data) got a good fit in the region of degree of saturation 0.25 - 0.5 and the van Genuchten curves (blue and green) fitted to the drainage data have a good fit in the region of degree of saturation 0.5 - 1. So, it has been showed that by carefully choosing the MRC data we can obtain the van Genuchten curve for this data and then map it onto the K(θ) curve using the same m (0.6 and 0.39 in this case). It would be advisable to conduct further experimental studies with other complex materials to validate it as a general proposition.

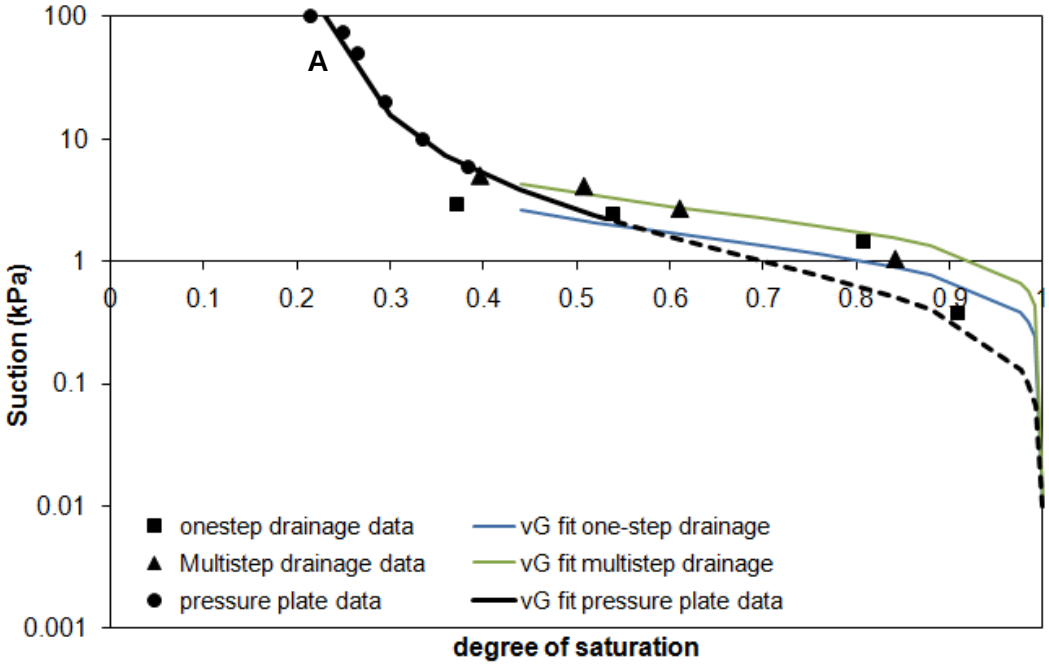

Figure 5.6 Moisture retention curves determined for a fine MBT waste of particle size 0-10 mm by column one-step and multistep drainage experiments and pressure plate apparatus

5.4 Consistency between the relative hydraulic conductivity results from the drainage experiment and relative gas permeability data

The relationship between the relative permeability of liquid in unsaturated porous media and effective degree of saturation, $k_r^L(S_e)$, is given by van Genuchten (1980) after Mualem (1976) (Equation 2.26):

$$k_r^L(S_e) = S_e^l\left(1-\left(1-S_e^{1/m}\right)^m\right)^2 \quad (2.26)$$

Mualem proposed that the correlation function should be $(S_e)^l = (S_e)^{0.5}$ with l =0.5.

The derivation of a gas relative permeability function that corresponds to Equation 2.26 for the liquid phase can in theory be obtained as follows. First remove the squared function in Equation 2.26 and the correlation function $(S_e)^l$ to get back to the basic Mualem integral result,

$$k_r^L = 1 - \left(1 - S_e^{\frac{1}{m}}\right)^m \qquad (5.4)$$

Assume that in an ideal porous material $k_r^G = 1 - k_r^L = \left(1 - S_e^{\frac{1}{m}}\right)^m$. Thus replacing the square and introducing a gas correlation function $(S_e)^g = (1 - S_e)^l$ we obtain,

$$k_r^G = (1 - S_e)^l \left(1 - S_e^{\frac{1}{m}}\right)^{2m} \qquad (5.5)$$

Whilst the source of this function is not known, it is quoted in the ModFlow model (Hydrogeologic, Inc., 1996) documentation with l =0.5. It also appears in the paper by (Stoltz, Gourc et al. 2010) which is referred to later.

Taking a van Genuchten m parameter value of 0.37,which is typical of the values used for waste materials (the average of m (=1-1/n) values in Table 2.4), and plotting Equation 2.26, gives the 'Liquid krel' curve in Figure 5.7 which is a van Genuchten fit curve with m=0.37. The symmetrical gas curve $k_{REL}^G = 1 - k_{REL}^L$ is also shown in which the van Genuchten correlation function (l =0.5 and m=0.37) (Equation 5.5) is applied together with a curve proposed by (Stoltz, Gourc et al. 2010) for which the correlation function is $(S_e)^g = (1 - S_e)^{5.2}$, l =5.2 and m = 0.3.

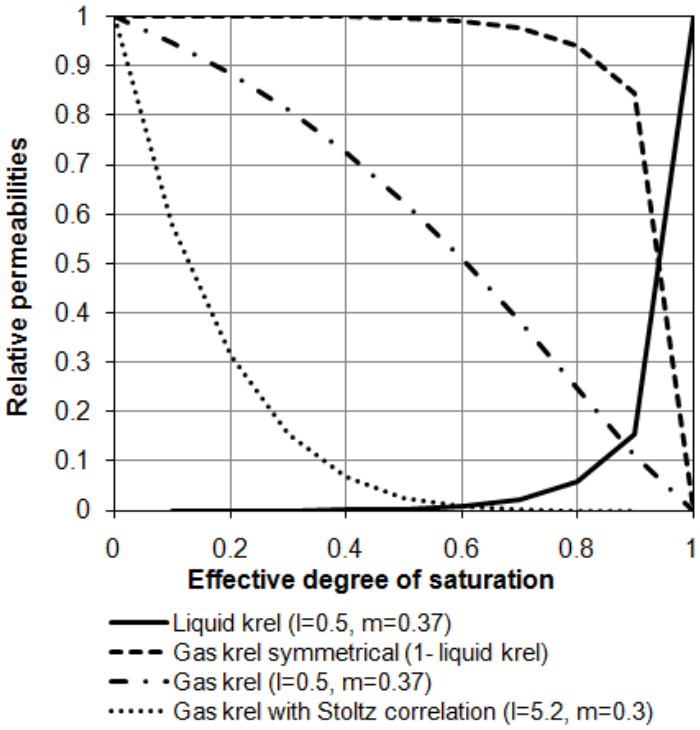

Figure 5.7 Derivation of relative gas permeability from liquid relative permeability

Holmes (2012) gives gas relative permeability data measured in small permeameters and these together with the drainage column liquid relative permeability data have been added in Figure 5.8. The Holmes gas data agrees well with the Stoltz data, and the drainage data indicates that the liquid relative permeability does not reduce as severely as a Mualem/van Genuchten approach might predict.

The liquid relative permeability curve data is supported by the fact that if it is transformed into the gas relative permeability curve using a Stoltz correlation it coincides with the Stoltz/Holmes curve (Figure 5.8).

The final Mualem/van Genuchten relationships are compared in Figure 5.9.

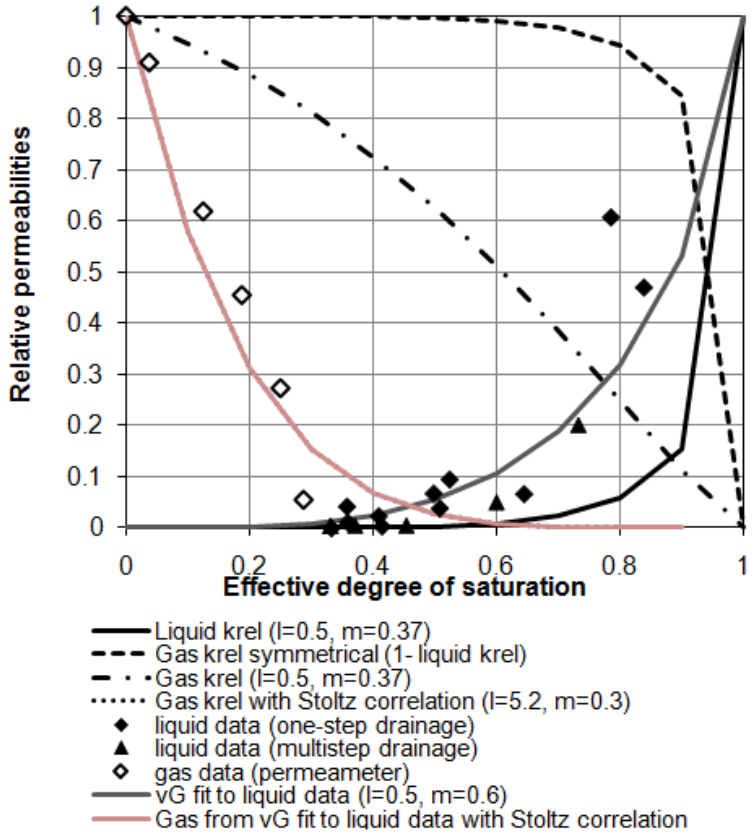

Figure 5.8 Addition of gas (small permeameter, Holmes 2012) and liquid(drainage column) relative permeability data

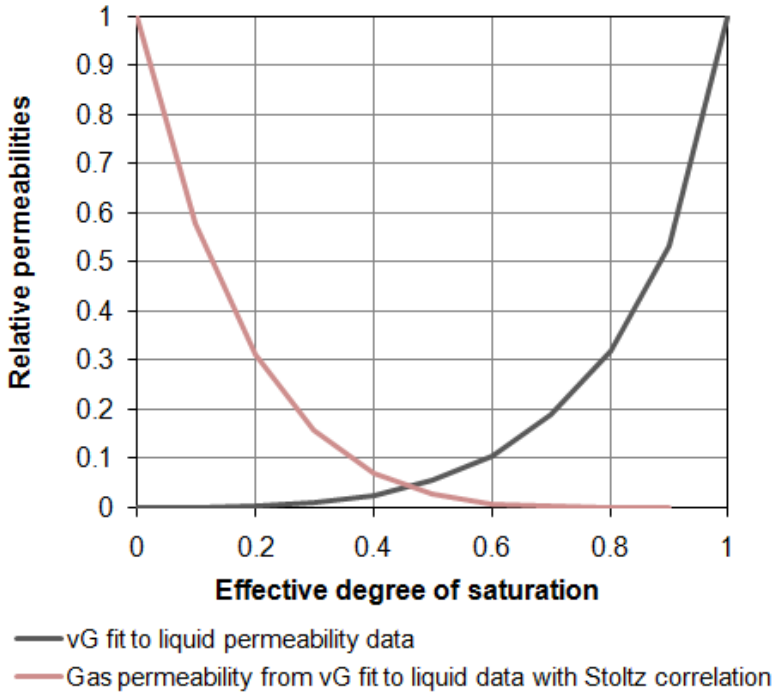

Figure 5.9 Comparison of relative liquid and gas permeabilities derived from fittings to the measured data and van Genuchten-Mualem functions

The liquid and gas relative permeabilities derived from the drainage experiments (Figure 5.9) have similar shapes with the typical permeability graphs obtained for soil showed in Figure 2.11 (after Warrick, 2002).

5.5 Summary

The relationship between unsaturated hydraulic conductivity and moisture content for MBT has been obtained from the drainage experiments using the instantaneous profile method and, for higher suction values, from the pressure plate apparatus data using the Passioura method. The relationship could be represented by a Genuchten-Mualem function that was consistent with the gas data of Holmes (2012) with the Stoltz correlation function (Stoltz, Gourc et al. 2010). The liquid and gas relative permeabilities are also consistent with thetypical permeability graphs obtained for soils (Warrick, 2002). However to fit the data the van Genuchten-Mualem m parameter value needed to be 0.6 whereas the m parameter value that would typically be found for the capillary pressure function is 0.37. The implication of this is that the unsaturated liquid permeability will not fall as rapidly with moisture content as might be expected from the capillary pressure function. The shape of the curve supports the use of a unimodal single porosity model as discussed in the next Chapter where the results from the drainage experiments were interpreted with Hydrus-1D and LDAT models.

CHAPTER 6

ANALYSIS OF THE DRAINAGE EXPERIMENT DATA WITH HYDRUS-1D AND LDAT MODELS

6.1 Introduction

This Chapter describes the interpretation of the results from the one-step and multistep MBT column drainage experiments using the unsaturated flow model Hydrus-1D (Šimůnek et al., 2005). One purpose of this chapter was to explore the applicability of other model fits to the drainage data. The one-step drainage data were modelled using the HYDRUS-1D single porosity model. A dual permeability model was also run for comparison and a dual porosity model approach was checked as well. The drainage results were also used to develop parameters for the gas and leachate transport algorithms of the LDAT model (White et al., 2004). The parametric curve-fit suggested by Mualem (1976) and van Genuchten (1980) was used to describe the moisture retention characteristics of the sample in the MBT column. As described in Chapter 3 two types of drainage experiment were carried out; one-step and multistep. In the first, it was suspected that the initial sudden change in boundary condition caused movement of fine materials and a consequential scatter of the moisture content data. The multistep drainage experiments, in which the head at the lower boundary was lowered in small incremental steps, were carried out in an attempt to eliminate the scatter and provide a consistent dataset throughout the depth of the column. Table 6.1 summarises all the model types run.

Table 6.1 Summary of the model types run for the drainage experiments

	HYDRUS-1D	LDAT
One-step drainage	Single layer–single porosity (direct) Six layers-single porosity (inverse) Six layers-dual permeability (inverse) Six layers-dual porosity (inverse)	Single layer–single porosity (direct)
Multistep drainage	Single layer–single porosity (direct)	Single layer–single porosity (direct)

6.2 Description of the HYDRUS-1D model

The experimental data were analyzed using the Hydrus-1D program (Šimůnek et al., 2005), which solves Richards' equation (Equation 2.7) numerically for saturated-unsaturated water flow.

The Hydrus-1D code uses the relationships between moisture content, capillary pressure head and hydraulic conductivity that are represented by one of the three sets of parametric equations: van Genuchten (1980), Brooks and Corey (1964) and modified van Genuchten type equations (Vogel and Cislerova, 1988) for the single porosity approach. It also includes dual porosity and dual permeability models. In this study, the van Genuchten (1980) empirical equations (vG equations) were selected (see Equations 2.20 and 2.23) for single porosity modelling, for dual permeability modelling the relationships (Equations 2.11-2.13) suggested by Gerke and van Genuchten (1993) were used and for dual porosity modelling the relationships (Equations 2.8-2.10) sugested by Šimůnek et al.(2003) were used. The Hydrus-1D code also allows the user to estimate the best fit of the van Genuchten equations to a dataset using an inverse method based on parameter optimisation.

Parameter optimization is an indirect approach for the estimation of the van Genuchten equation parameters of a material from transient flow data. Inverse methods are typically based on the minimization of a suitable objective function that compares the simulated versus observed space-time (auxiliary) variables (see Šimůnek et al. (1998). In Hydrus-1D the objective function Φ to be minimized during the parameter estimation process maybe defined as (Šimůnek et al., 1998):

$$\Phi(b,q,p) = \sum_{j=1}^{m_q} v_j \sum_{i=1}^{n_{qj}} w_{i,j}\left[q_j^*(x,t_i) - q_j(x,t_i,b)\right]^2 \quad (6.1)$$

where the term on the right-hand side represents deviations between measured and simulated space-time variables (e.g. pressure heads, moisture contents, and/or concentrations at different locations and/or times in the flow domain, or cumulative fluxes versus time (t). In this term, $m_q$is the number of different sets of measurements and $n_{qj}$is the number of measurements in a particular measurement set. Specific measurements at time t_i for the j_{th} measurement set at location x(r,z) are represented by $q_j^*(x,t_i), q_j(x,t_i,b)$ are the corresponding model predictions for the vector of optimized parameters b (such as θ_r, θ_s, α, n, k_s in Equation 2.20) and v_j and $w_{i,j}$ are weights associated with a particular measurement set or point, respectively. Weighting coefficients were calculated as the inverse product of the measurement variance and the number of observations for each auxiliary variable (Clausnitzer and Hoplmans, 1995), which causes the objective function to become the average weighted squared deviation normalized by the measurement variances. Minimization of the objective function Φ is accomplished by using the Levenberg-Marquardt nonlinear minimization method (a weighted least-squares approach based on Marquardt's maximum neighbourhood method) (Marquardt, 1963).

6.3 Description of the LDAT model

Over the past ten years the Waste Management Research Group at the University of Southampton has developed a Landfill Degradation and Transport model known as LDAT, White et al. (2004). The work on LDAT has been aimed at understanding how wastes degrade in landfills, and how we can intervene to accelerate the bio-chemical stabilisation of wastes. LDAT models the transport and bio-chemical behaviour of the solid, liquid and gas phases of waste contained in a landfill (White & Beaven, 2008).

One of the objectives of the experimental work described in this thesis was to use the results to support the incorporation of capillary pressure/moisture content and relative permeability/moisture content functions into LDAT. Initially LDAT did not cater for the two distinct pore-pressure fields, one for liquid and one for gas, that are present in partially saturated flows. However, as part of the project, this was remedied by incorporating the van Genuchten (1980) equations into the code. . It

has also been found necessary to incorporate into the LDAT flow algorithm the concept of effective density for both the gas and liquid phases. The reason for this is that at low and high leachate saturation conditions the gas/liquid fluid does not appear to behave as a fully mixed entity and this impacts on the calculations of the gravity induced pressure gradients in the vertical direction. This is particularly relevant when modelling the predominantly vertical flows found in the landfill remediation techniques of leachate recirculation, flushing and aerobic treatment (Rees-White et al (2008), Nayagum et al (2009)).

In LDAT the waste in a landfill is represented as a porous medium. It is assumed that in the waste there are a number of chemical compounds and species, components (i), each of which can exist in one or more of the solid, liquid and gas phases (S, L, G [F]) as the degradation process takes place, and which contribute to the source terms G^{Li} and G^{Gi} in Equation 6.2. This equation is the constitutive multicomponent-multiphase equation of flow in the *x* direction used in LDAT. (The derivation is given in Appendix M)

$$z^L S^L \frac{\partial p^L}{\partial t} + z^G S^G \frac{\partial p^G}{\partial t} + \frac{\partial \phi}{\partial t} = z^L \frac{k^L}{\rho^L g} \frac{\partial^2 p^L}{\partial x^2} + z^G \frac{k^G}{\rho^G g} \frac{\partial^2 p^G}{\partial x^2} + \sum \left(G_i^L + G_i^G \right) \tag{6.2}$$

The flow equation can be solved if the relationship between the gas pressure (p^G) and the liquid pressure (p^L) is known. This can be achieved by invoking a van Genuchten capillary pressure type of relationship. The compound concentrations (z_i^F) can then be obtained by a back calculation using the constitutive equations (19, 20 and 21, Appendix M) for each phase.

The main difference between Hydrus-1D and LDAT is that although Hydrus-1D takes into account the gas phase it does not model the gas flow or the impact of bio-degradation and settlement. LDAT has been developed to include these so that it can be applied to landfill management technologies such as gas collection, leachate recirculation and aeration.

6.4 Application of HYDRUS-1D model to the drainage data

6.4.1 One-step drainage experiment

To evaluate whether the van Genuchten equation and parameters were suitable for the case of MBT waste, they were used in the Hydrus 1D direct model to calculate the cumulative leachate flux and the liquid pressure and moisture content profiles measured in the column experiment (Chapter 4). The column of MBT was represented as a uniform material descretised into 100 one dimensional elements and 101 nodes. The initial and boundary conditions used for the Hydrus-1D analyses were: the upper boundary flux was set to zero because no water came in/out at the top of the column. The lower boundary condition was set as variable pressure head because the pressure head from the hydrostatic condition initially (0.56 m) went to pressure head equal zero after the start of the drainage.

The van Genuchten parameters fitted to represent the moisture retention function at equilibrium, obtained by the method of least squares, were: θ_r=0.15 m^3/m^3, θ_s= 0.69 m^3/m^3, α= 0.8 kPa^{-1}, n=2.5. The value of k_s was taken as 4.5 x 10^{-5} m/s and the tortuosity parameter,l, was assumed to be 0.5, which is a typical value used for many soils (Mualem, 1976) (Equation 2.23). The Hydrus 1D direct model was used with these parameters and initial and boundary conditions to calculate the cumulative leachate flux in the one-step drainage experiment. The results were then compared with the measured data (Figure 6.1). Figures 6.2 and 6.3 compare the simulated pore liquid pressure and moisture profiles with the experimental observations at selected times (t=0, 10 mins, 2 hours, 1 day and 4 days).

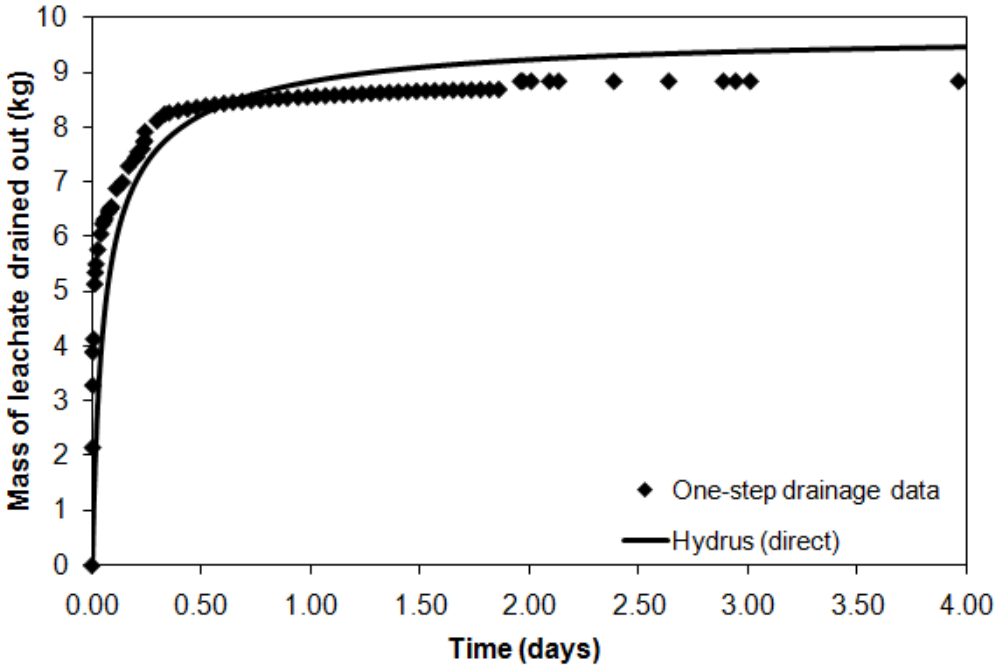

Figure 6.1 Measured and Hydrus-1D simulated mass of leachate drained out (kg) against elapsed time (one-step drainage)

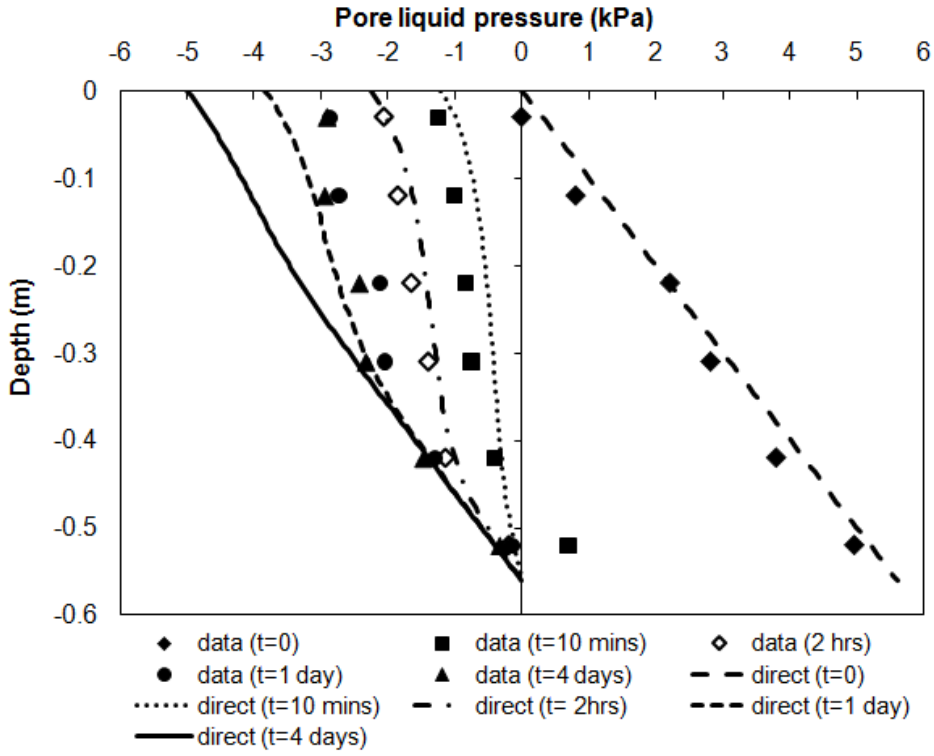

Figure 6.2 Measured and Hydrus-1D simulated pore liquid pressure profiles (one-step drainage)

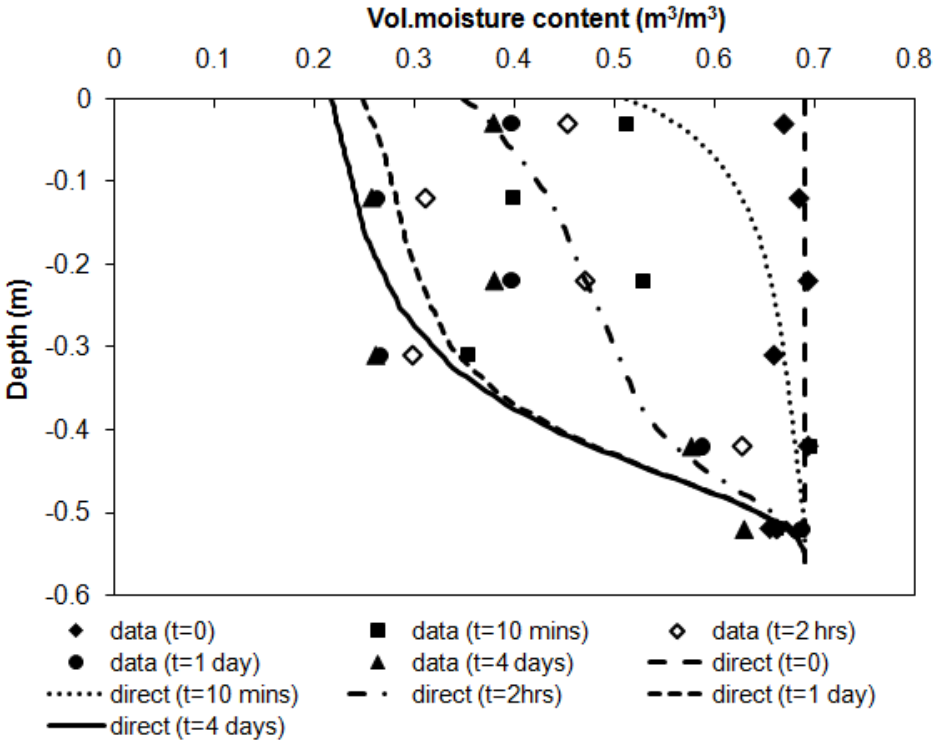

Figure 6.3 Measured and Hydrus-1D simulated volumetric moisture profiles (one-step drainage)

The Hydrus-1D direct model reproduced the cumulative leachate flux in the column experiment successfully, but the suction and moisture content profiles were not simulated as satisfactorily. As shown in Figure 4.7 the moisture retention curve varies significantly along the depth of the column during the drainage process even though great care was taken to ensure that the initial density of the sample was uniform throughout. The scatter of the moisture content data in the one-step drainage experiment may have been caused by movement of fine materials through the larger pores during drainage as a result of the change in applied particle forces caused by suddenly lowering the bottom pressure from hydrostatic to atmospheric pressure. The moisture contents below levels -0.12 m and -0.31 m fell more quickly. This could be also explained by horizontal cracks observed at these levels (see a photo of the horizontal 'crack' at level -0.34 m in Figure 4.2).

To investigate the change of the saturated hydraulic conductivity along the MBT column, the column was divided in 6 layers and an inverse solution was carried out. The data for the inverse solution (auxiliary variables) were the pressure head at six locations (obtained from tensiometer readings) and cumulative flux (balance readings) at specific times during the drainage experiment. The same van

Genuchten parameters (θ_r=0.15 m^3/m^3, θ_s= 0.69 m^3/m^3, α= 0.8 kPa^{-1}, n= 2.5, l = 0.5) were applied for each layer. The saturated hydraulic conductivity, which was the optimised (fitted) parameter was allowed to vary between 10^{-6} and 10^{-4} m/s. This case was named 'inverse 1'.

Whereas the value of the parameter l was initially taken as 0.5 following Mualem (1976), there is no general agreement on this. Breitmeyer et. al (2011) concluded after his modelling work in MSW that *l* ranged from -0.002 to 6.99. A second inverse modelling exercise was carried out by keeping constant the parameter l *(*≠ 0.5) along the column and fitting the saturated hydraulic conductivity for each of the six layers. After many trials using values of $l$between -5 and 5, a value of 2.4 was found to give the best fit to the outflow data. This case was named 'inverse 2'.

Table 6.2 shows the inverse solution for each layer and Figures 6.4, 6.5 and 6.6 compare the measured data with the inverse simulations. As shown in these figures, the case 'inverse 2' with l =2.4 simulated the data better than l =0.5 (inverse 1). The significant conclusion that may be drawn from Table 6.2 is that in both inverse cases the saturated hydraulic conductivity value was of the order of 10^{-5} m/s along the column except at layers 2 and 5, where it was greater. This is consistent with the saturated hydraulic conductivity calculated from the tensiometer readings above and below the horizontal crack. As it is observed in Figure 6.7 the saturated hydraulic conductivity of the layer that includes the crack is two orders higher than the value of the saturated hydraulic conductivity of the layers above and below. The inverse simulated moisture content profile at t=10 mins (Figure 6.6) also supports this observation with two 'peaks' at these depths. As observed in Figure 6.7, the high permeability of layer 5 in the inverse model includes the effect of the crack. The effect of this can be demonstrated using a simple equation for a three layer system which evaluates the effective overall vertical permeability k_v of a layered system with a thin layer of permeability k_2 and thickness d_2, which represents the crack, sandwiched between two layers of thickness d_1, d_3 and permeability k_1, k_3. The permeability of the thin layer (k_2) can be calculated using the equation (Powrie, 2004):

$$k_v=(d_1+d_2+d_3)/(d_1/k_1+d_2/k_2+d_3/k_3) \quad (6.3)$$

The vertical permeability and the permeabilities of the layers above and below the crack were calculated using the tensiometer readings. The vertical permeability of

the system was calculated to be 9.66×10^{-4} m/s, with $k_1 = 1.45 \times 10^{-5}$ m/s and $k_3 = 3 \times 10^{-5}$ m/s. The thickness of the crack (layer 2) was taken to be equal to 1.4 cm. From Equation 6.3, the permeability of the thin layer was calculated as 0.38 m/s, which is very high as expected because water is effectively of infinite permeability.

Table 6.2 Saturated hydraulic conductivity optimised with Hydrus-1D single porosity inverse model

Layers	Depth (m)	inverse 1 k_s (m/s) for l =0.5	inverse 2 k_s (m/s) for l =2.4
1	0-0.078	5.6×10^{-6}	3.73×10^{-5}
2	0.078-0.162	4.97×10^{-5}	9.17×10^{-4}
3	0.162-0.246	1×10^{-5}	3.76×10^{-5}
4	0.246-0.338	2×10^{-5}	6.5×10^{-5}
5	0.336-0.437	2.8×10^{-3}	5×10^{-3}
6	0.437-0.56	1.69×10^{-5}	3.46×10^{-5}

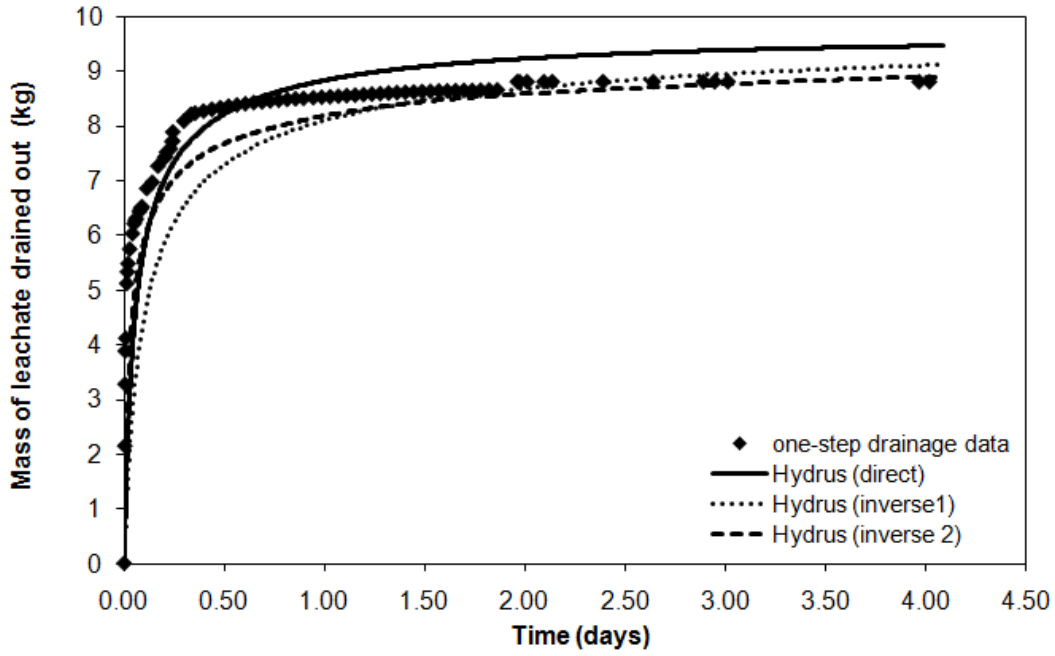

Figure 6.4 Measured and Hydrus-1D (direct and inverse) simulated mass of leachate drained out (kg) against elapsed time (one-step drainage)

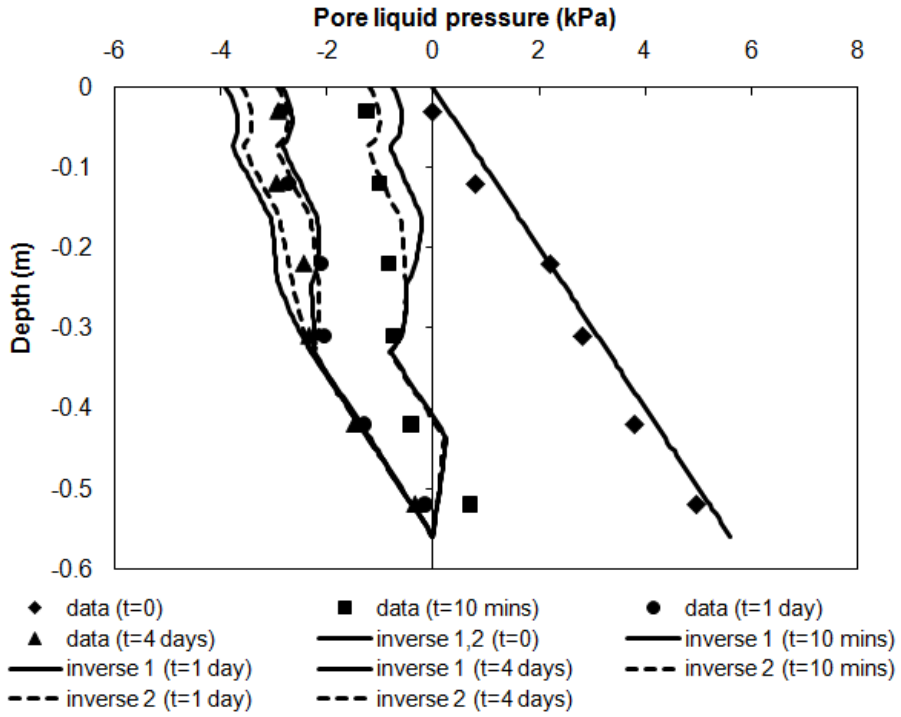

Figure 6.5 Measured and Hydrus-1D inverse simulated pore liquid pressure profiles (one-step drainage)

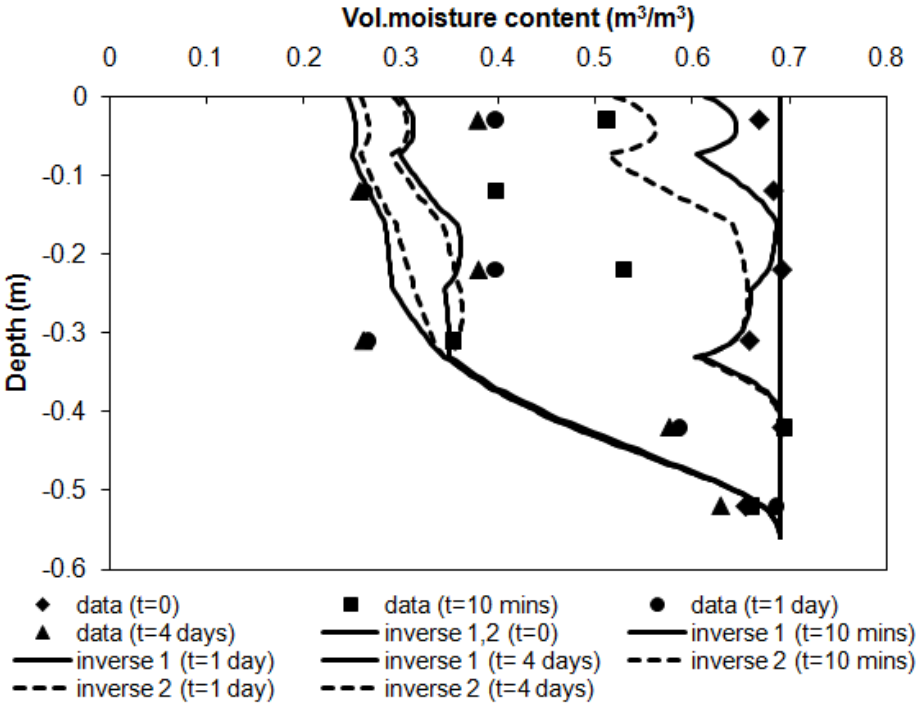

Figure 6.6 Measured and Hydrus-1D inverse simulated volumetric moisture profiles (one-step drainage)

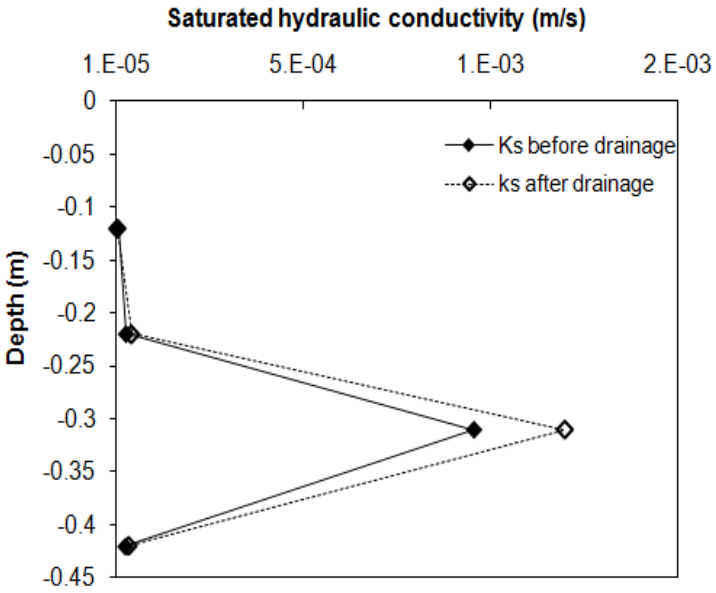

Figure 6.7 Profiles of the saturated hydraulic conductivity before and after the drainage of the layer that includes the crack and the layers above and below the crack

The inverse dual permeability model in Hydrus-1D was also applied to check if the fits to the data could be improved. The dual permeability model requires 17 parameters, compared with the six parameters needed in the single porosity model. The MBT column was divided into 6 layers and the van Genuchten parameters for the matrix, α_m or l and k_s were fitted for each layer using the pore liquid pressure and cumulative outflow as the data for the inverse solution (auxiliary variables). An inverse model run was also made in which the column was represented as one layer in order to optimise more parameters, but the simulations were not close to the measured data and the simulated outflow flux was significantly underestimated.

To reduce the number of the unknown parameters the values suggested by Kodešova et al. (2008) and Han et al. (2011) were used for specific parameters. The van Genuchten parameters for the matrix were taken to be the same as those used in the single porosity model (θ_s=0.69, θ_r=0.15, n=2.5). The parameters for the fracture, a_f and n_f , were close to the values of α and n used in the single porosity model (α= 8 m^{-1} and n =2) since by definition water drained mainly from fractures. The saturated hydraulic conductivity of the fracture domain (k_{sf}) was assumed equal to 5x10^{-3} m/s. The tortuosity parameters for the fracture and matrix, l_f and l_m, were set to 0.5 (a typical value for soils, Mualem (1976)). The volume of the fracture domain divided by the total flow domain was assumed equal to w_f=0.1.

The residual water content of the fracture domain, θ_{rf} , was set to zero, since water should easily drain through the fractures at modest capillary pressures (Han et al., 2011). The parameter b describing the geometry of aggregates, was set to 8, the midpoint value for the range b=3 for rectangular slabs and b=15 for spheres (Kodešovα et al., 2008); $\chi_{w,}$ an empirical coefficient, was set to 0.4 and is more or less independent of the geometry (Gerke and van Genuchten, 1993); and a, the distance from the center of a matrix block to the fracture, was assumed to be 10 cm. The effective hydraulic conductivity describing exchange between fracture and matrix domains, K_a, was taken $5x10^{-8}$ m/s. (Gerke and van Genuchten, 1993).

Here, it must be mentioned that the inverse modelling gave the best simulations only when the MBT column was divided in 6 layers, fitting the α_m or l and k_s parameters for each layer and using the parameter values described above. Additional Hydrus-1D runs were carried out fitting the other parameters but the simulations of the outflow flux were not close to the measured data (Appendix N).

Table 6.3 shows the inverse solution for each layer when fitting the α_m and k_s parameters and Figures 6.8, 6.9 and 6.10 compare the measured data with the inverse single porosity and dual permeability models' simulations. The same results were taken when fitting the l and k_s parameters for each layer (Table 6.3). The dual permeability simulation fittings were not significantly different from the single porosity ones. Also, the dual permeability results appear to confirm the conclusion from the earlier inverse single porosity modelling that there are variations in permeability down the column. Dual porosity model approach was also run but the simulations of the outflow flux were not close to the measured data (Appendix O).

Table 6.3 Hydrus-1D dual permeability inverse model, case1: optimised αand $k_{smatrix}$, case 2: optimised l and $k_{smatrix}$

Layer	Depth (m)	α_{matrix} (m^{-1})	$k_{smatrix}$ (m/s)	l	$k_{smatrix}$ (m/s)
1	0-0.078	5.18	$5.74x10^{-5}$	4.4	2.65×10^{-4}
2	0.078-0.162	14.1	$1.35x10^{-4}$	2	2.7×10^{-4}
3	0.162-0.246	13.7	$2.22x10^{-4}$	5.2	3×10^{-4}
4	0.246-0.338	16.4	$1.64x10^{-4}$	5.08	1.13×10^{-4}
5	0.336-0.437	12.3	$4.5x10^{-4}$	3.94	8.15×10^{-4}
6	0.437-0.56	20.9	$6x10^{-5}$	6.74	8.15×10^{-5}

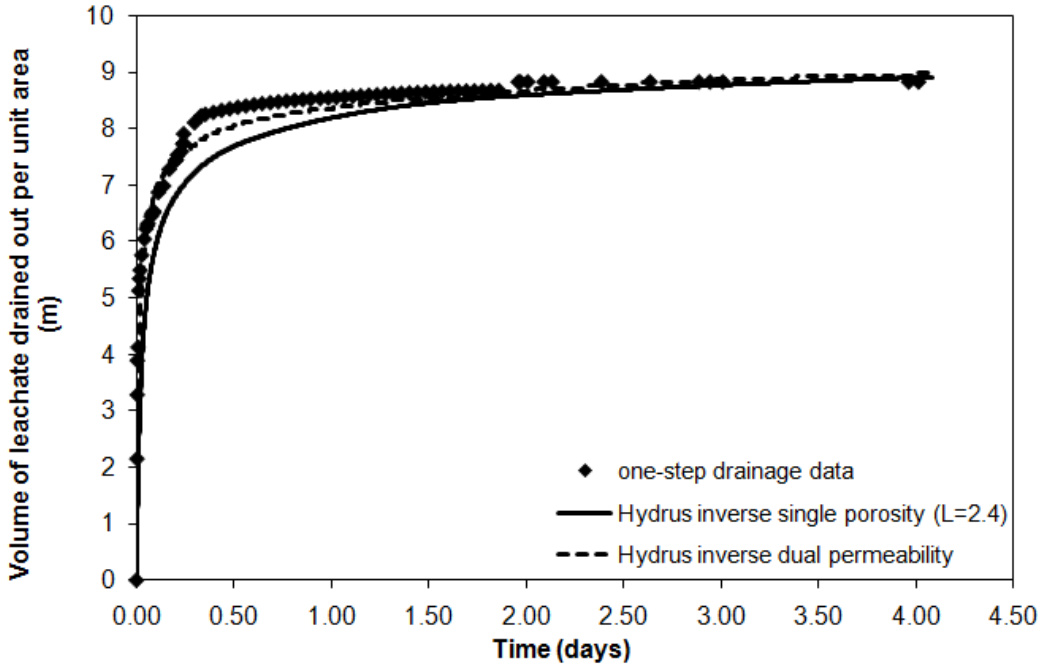

Figure 6.8 Measured and Hydrus-1D inverse (single porosity and dual permeability) simulated mass of leachate drained out (kg) against elapsed time (one-step drainage)

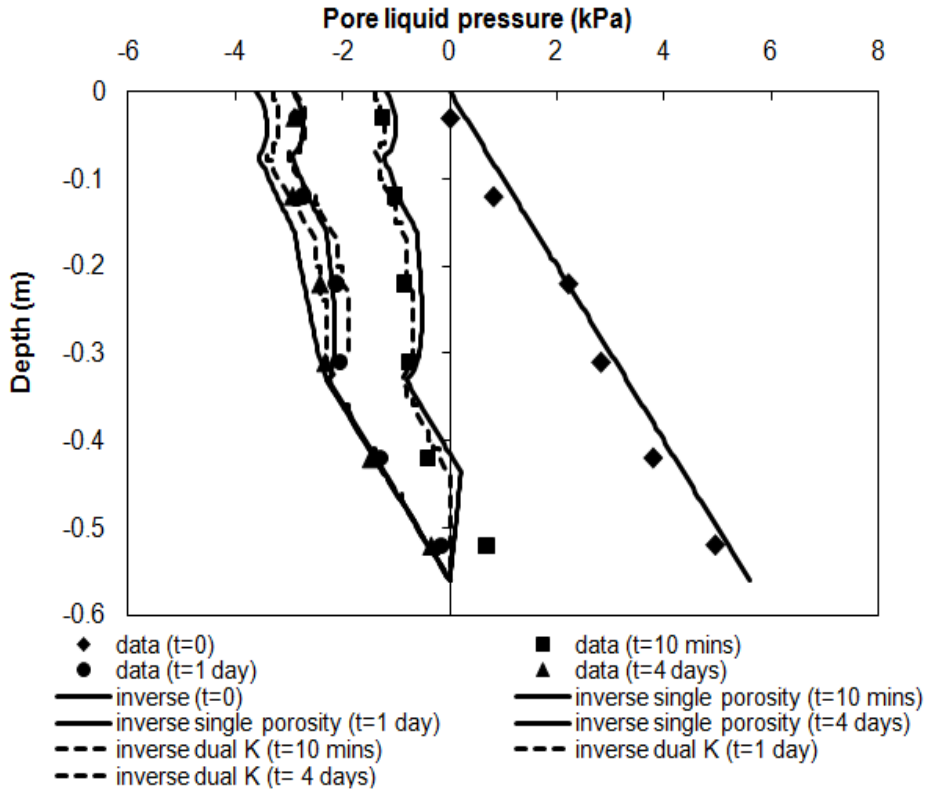

Figure 6.9 Measured and Hydrus-1D inverse (single porosity with L=2.4 and dual permeability) simulated pore liquid pressure profiles (one-step drainage)

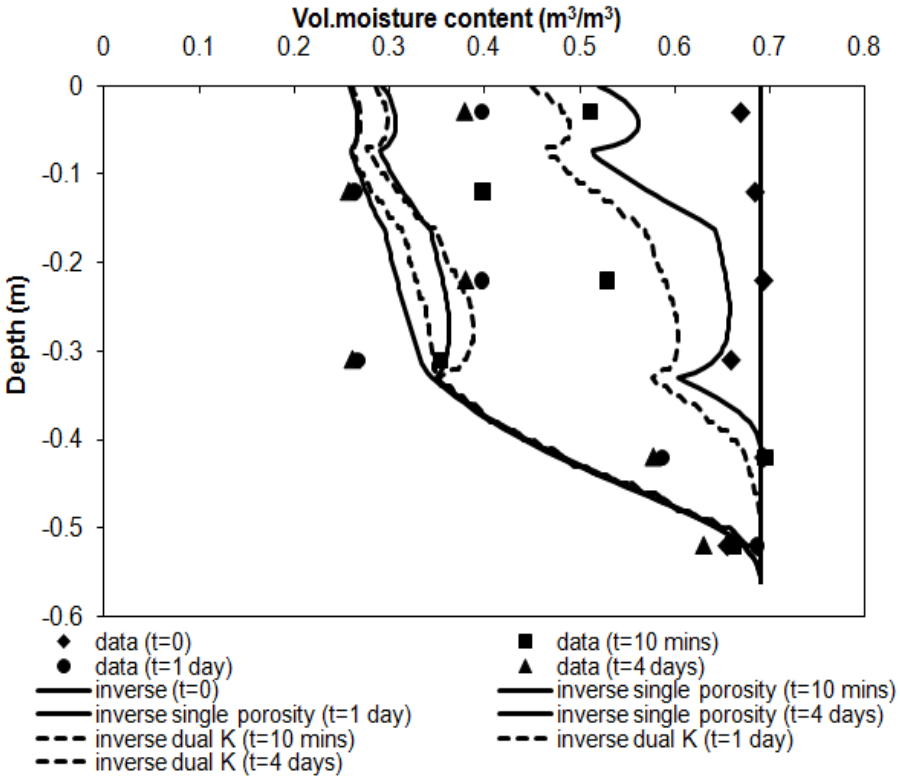

Figure 6.10 Measured and Hydrus-1D inverse (single porosity with L=2.4 and dual permeability) simulated volumetric moisture profiles (one-step drainage)

6.4.2 Multistep drainage experiment

To apply Hydrus-1D to the multistep drainage data (Chapter 4) the profile of the MBT column was again represented as a uniform material with 101 nodes. The initial and boundary conditions used for the Hydrus-1D runs were: the upper boundary condition flux was set zero because no water came in/out at the top of the column. The lower boundary condition was set as a variable pressure head because six pressure steps were applied sequentially by lowering the height of the outflow tubing in six steps from the top until the outflow level was level with the bottom of the sample. The time-varied prescribed head boundary conditions are shown in Table 6.4.

Table 6.4 Time-varied prescribed head boundary conditions (GWL)

Step number	time (days)		GWL (m)
	Beginning of step	End of step	
		0.00	0.56
1	0.00	0.84	0.475
2	0.84	1.63	0.39
3	1.63	2.89	0.310
4	2.89	4.84	0.220
5	4.84	6.52	0.120
6	6.52	8.92	0.000

In this Hydrus-1D direct simulation, the van Genuchten parameters fitted to represent the moisture retention function at equilibrium, obtained by the method of least squares, were: θ_r=0.15 m^3/m^3, θ_s= 0.70 m^3/m^3, α= 0.47 kPa^{-1}, n=2.6, *l*=0.5.These values are similar to the van Genuchten fitting to the one-step drainage retention curve except the value of the parameter alpha is reduced by almost half (Chapter 4). The value of k_s was taken as 4.5 x 10^{-5} m/s. Figure 6.11 compares the multistep drainage leachate outflow data with the Hydrus-1D simulated curve. Only the last step does not represent the outflow well.

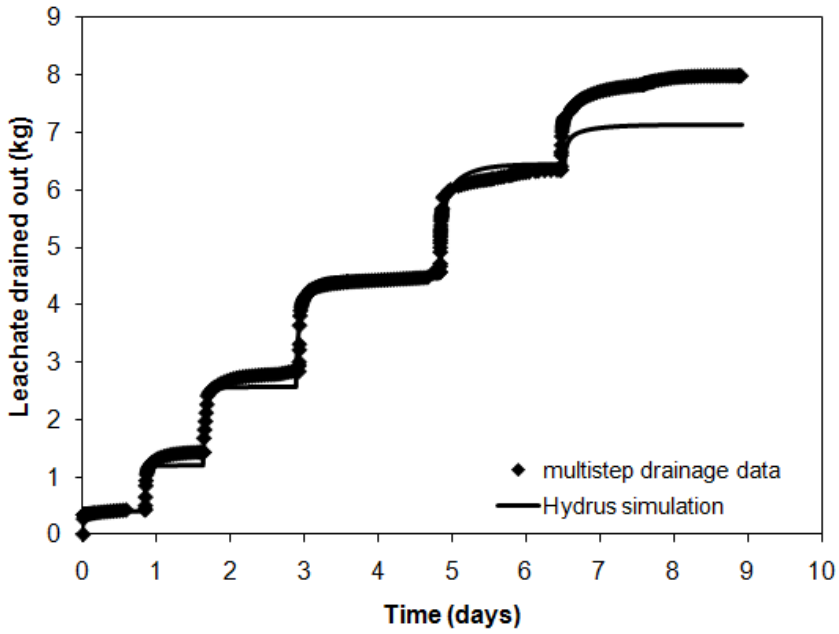

Figure 6.11 Measured and Hydrus-1D simulated mass of leachate drained out (kg) against elapsed time (multistep drainage)

In Figures 6.12 and 6.13 the simulated pore liquid pressure and moisture profiles are compared with the experimental observations at equilibrium after each step. The readings are more consistent now, the moisture content data less scattered and Hydrus-1D model simulates both profiles satisfactory.

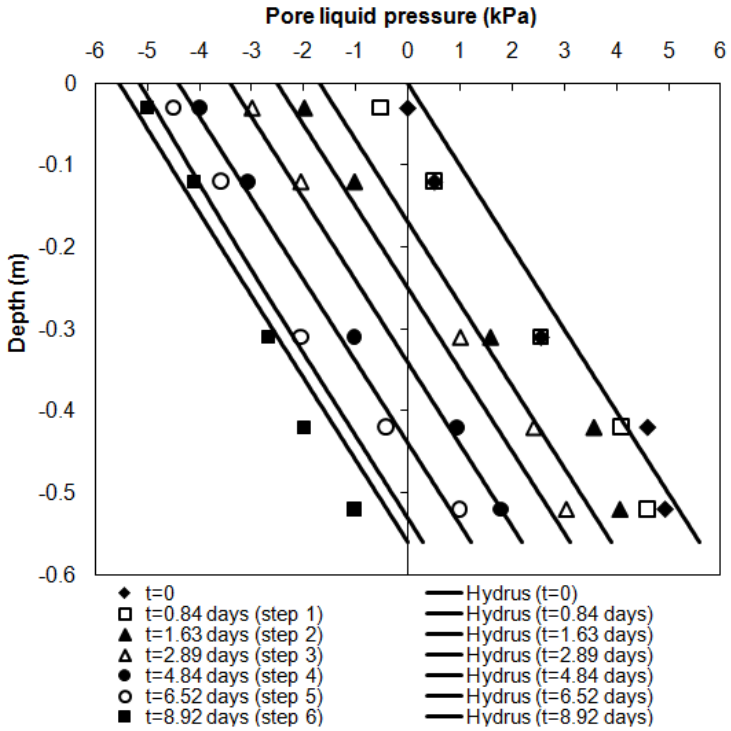

Figure 6.12 Measured and Hydrus-1D simulated pore liquid pressure profiles (multistep drainage)

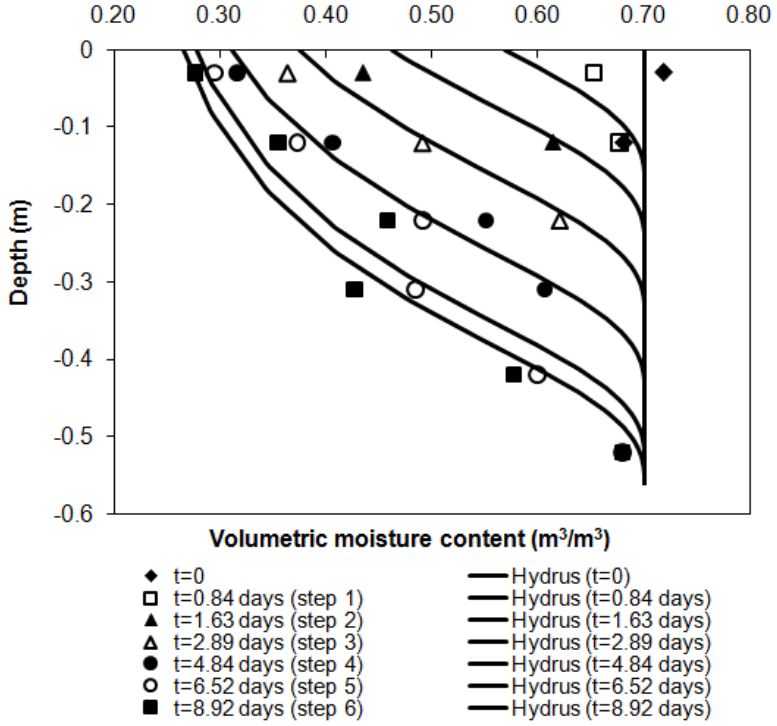

Figure 6.13 Measured and Hydrus-1D simulated volumetric moisture profiles (multistep drainage)

6.5 Application of LDAT model to the drainage data

The LDAT model used the same van Genuchten relationships as the Hydrus model and the model results were compared with the drainage experimental data. The input data for the LDAT run were taken from the drainage experiment characteristics. The model column height of 0.56 m was divided into 17 elements. Elements 0 and 17 were boundary elements. Elements 1 to 13 represented the MBT specimen with levels chosen to coincide with the instrumentation levels. Elements 14, 15 and 16 represented the gravel layer. Only nitrogen (representing air) was contained in the upper boundary, while reserves of both nitrogen and water were available in the lower boundary. The lower boundary liquid and gas pressures were set at the equivalent of 250 mm of water, corresponding to the saturated depth of the gravel layer. In the initial conditions for each element the solids were set to be 100% inert, the liquid 100% water, and the gas 100% nitrogen. The time-varied prescribed head boundary conditions applied were the same as those in the Hydrus-1D model described earlier.

6.5.1 One-step drainage experiment

The LDAT model was run for the same van Genuchten parameters used in the Hydrus-1D model (θ_r=0.15 m^3/m^3, θ_s= 0.69 m^3/m^3, α= 0.8 kPa^{-1}, n=2.5, *l*=0.5 and k_s= 4.5 x 10^{-5} m/s). The results of the LDAT runs simulating the vertical drainage experiment are shown in the figures below. Figure 6.14 compares the measured and LDAT simulated masses of leachate drained out (kg) during the time period (days) of the drainage experiment for element 17, which represents the lower boundary. It is a reasonably good fit taking into account the approximations/idealisations made in the modelling and the uncertainties attached to the experimental results. The model idealises the waste as a uniform homogeneous material and takes no account of heterogeneity such as spatial variation in pore-size distributions and spatial variability of drainage path geometry.

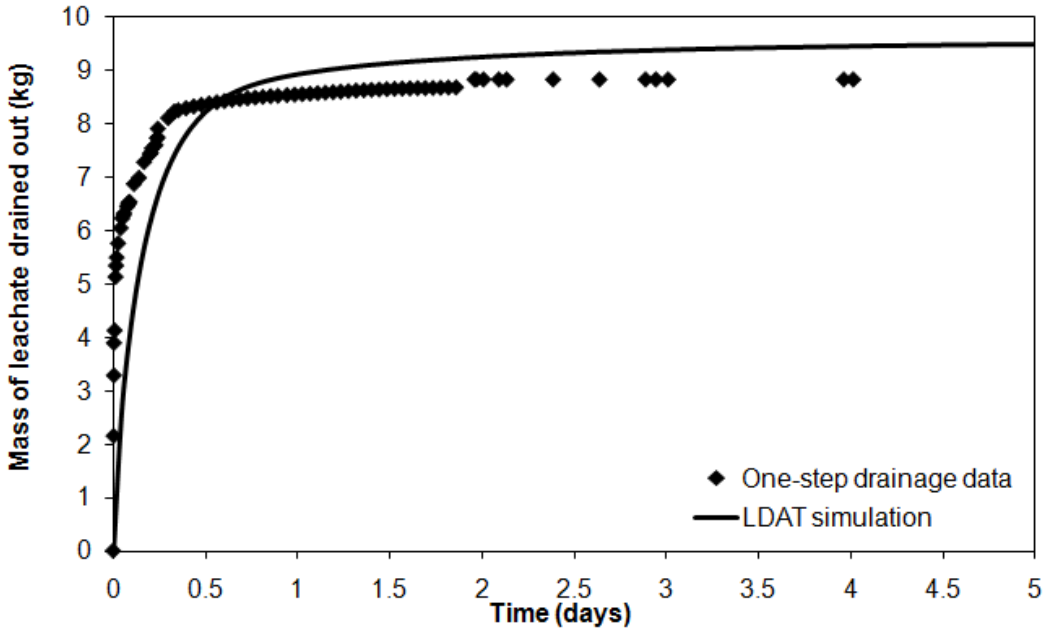

Figure 6.14 Measured and LDAT simulated mass of leachate drained out (kg) against elapsed time (one-step drainage)

Figures 6.15 and 6.16 compare the measured and LDAT simulated volumetric moisture content (m^3/m^3) and pore liquid pressure (kPa) profiles at times t=0, t=2 hours and t=4 days (equilibrium) for the case of the one-step drainage experiment. Simulated moisture profiles are on average close to the measured data as shown in Figure 6.15. However, the model was not able to reproduce the moisture content measured at the top of the column. The simulated suctions were greater than those measured (Figure 6.16). The measured suctions are less than hydrostatic; possibly due to the pore sizes being too large or the presence of disconnected pockets of water that do not maintain capillary contact with the tensiometer.

As discussed above a horizontal ‘crack’ was observed at a depth of around -0.34 m and this may have caused a discontinuity in the liquid phase along the MBT column. Also, as discussed above, the internal movement of fine particles due to the sudden change in applied particle forces could have changed the dry density of each layer. Hence the saturated hydraulic conductivity, which was assumed in the LDAT model to be the same in each layer, may in fact have been different, as indicated by the Hydrus-1D inverse modelling.

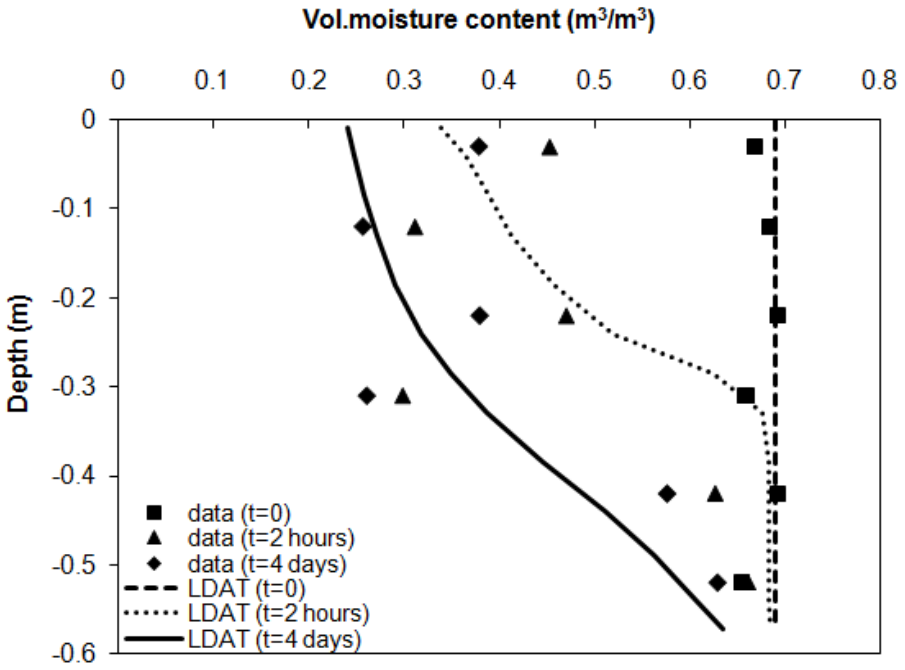

Figure 6.15 Measured and LDAT simulated volumetric moisture profiles at t=0, t=2 hours and t= 4 days (equilibrium) (one-step drainage)

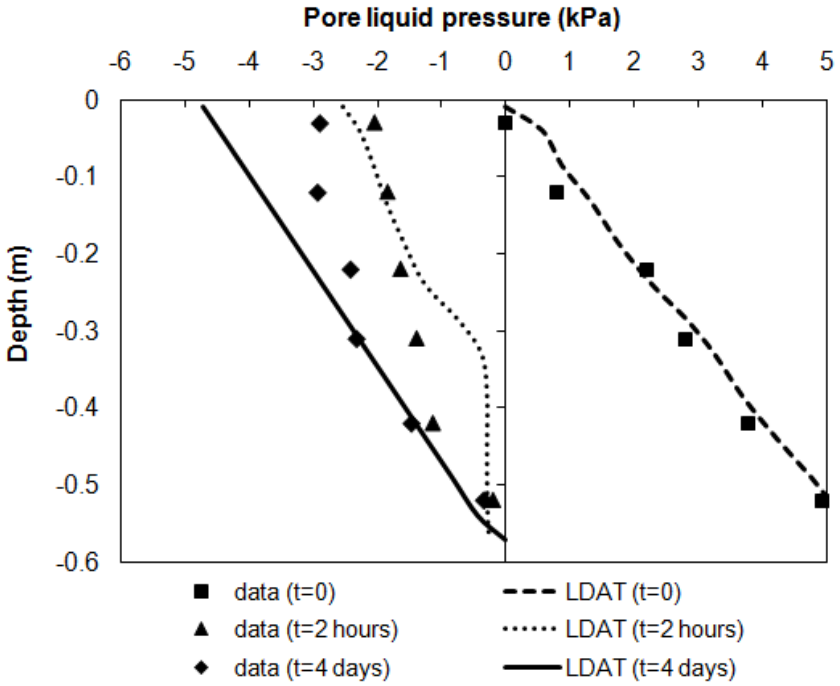

Figure 6.16 Measured and LDAT simulated pore liquid pressure profiles at t=0, t=2 hours and t= 4 days (equilibrium) (one-step drainage)

6.5.2 Multistep drainage experiment

For the multistep drainage experiment the LDAT model was run for three different cases of the van Genuchten parameter alpha (Table 6.5). Figure 6.17 shows the LDAT simulations of the measured mass of leachate drained out (kg) during the time period (days) of the drainage experiment for element 17, which represents the lower boundary. Case 1, which presents the van Genuchten parameters used in Hydrus-1D modelling, nearly produced a total drained mass of 8 kg as measured in the drainage experiment, however the intermediate steps were not well represented. Increasing alpha was a simple way of lowering the levels of saturation for a given suction, and hence increasing the amount drained. Interestingly the improved fit in case 3 has a van Genuchten alpha value that is similar to that used in the application to the one- step drainage test above. Overall the simulated outflow for case 2 seems to fit the data better than the other cases. It is a good fit for the first five steps but for the final step overestimates the amount of leachate drained out.

Table 6.5 van Genuchten parameter sets for LDAT cases 1, 2 and 3

Case	θ_r (m^3/m^3)	θ_s (m^3/m^3)	α(kPa^{-1})	n	l	ks (m/s)
1	0.15	0.7	0.47	2.6	0.5	$4.5x10^{-5}$
2	0.15	0.7	0.6	2.6	0.5	$4.5x10^{-5}$
3	0.15	0.7	0.77	2.6	0.5	$4.5x10^{-5}$

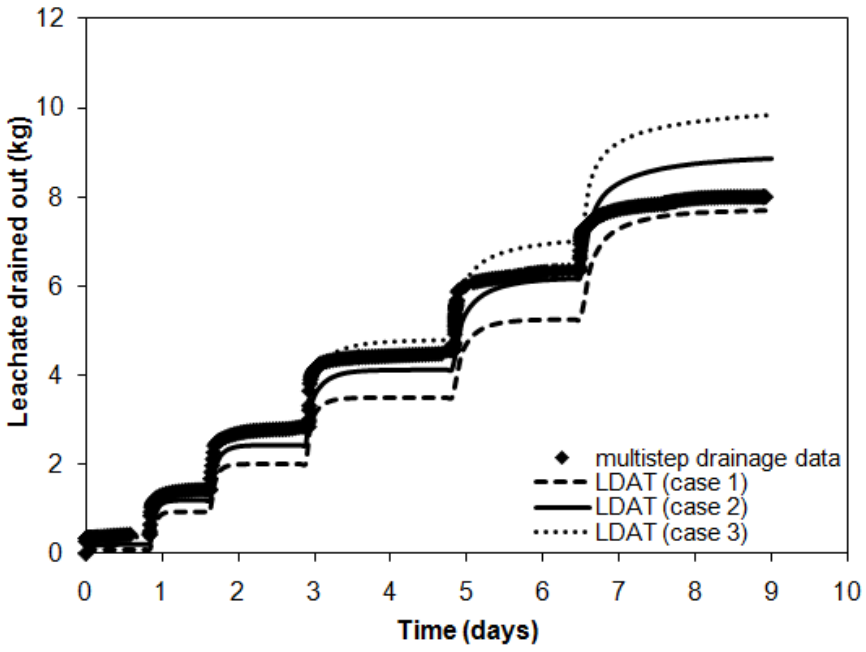

Figure 6.17 Measured and LDAT simulated mass of leachate drained out (kg) during the time period (days) of the multistep drainage experiment

Figures 6.18 and 6.19 compare the measured and LDAT simulated volumetric moisture content (m^3/m^3) and pore liquid pressure (kPa) profiles at the end (equilibrium) of the multistep drainage experiment using the van Genuchten parameters for case 2.

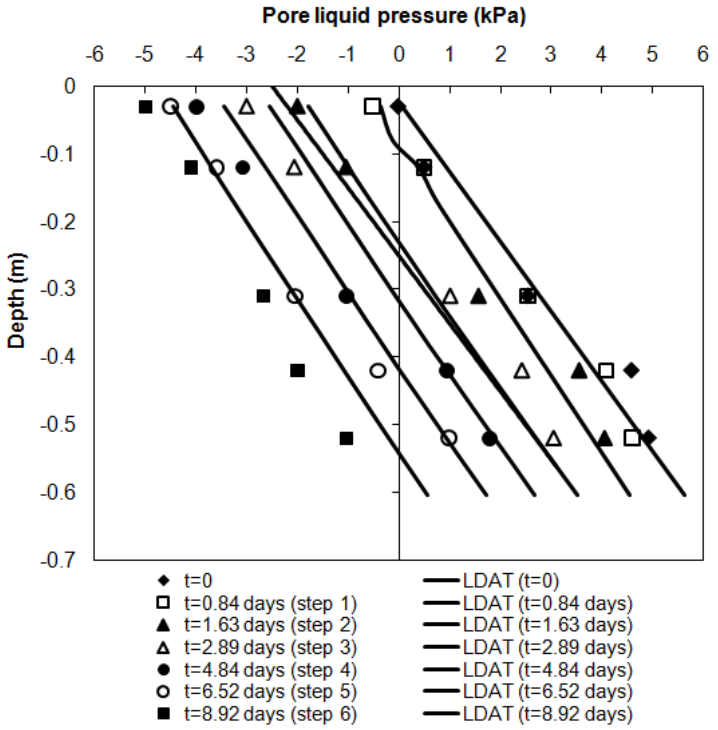

Figure 6.18 Measured and LDAT simulated pore liquid pressure profiles at equilibrium (multistep drainage, case 2)

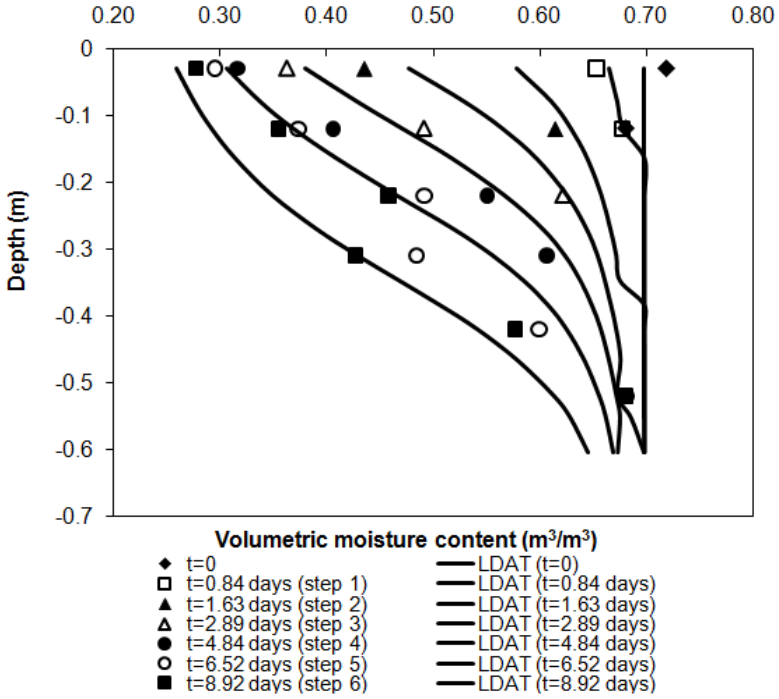

Figure 6.19 Measured and LDAT simulated volumetric moisture profiles at equilibrium (multistep drainage, case 2)

6.6 Summary

Table 6.6 summarises all models run for the one-step and multistep drainage experiments and the associated parameters.

Table 6.6 List of the models runs run for the one-step and multistep drainage experiments and the associated parameters

Hydrus-1D	θ_r (m^3/m^3)	θ_s (m^3/m^3)	α (m^{-1})	n	k_s (m/s)	l
One-step drainage Single layer-Single porosity (direct)	0.15	0.69	8	2.5	$4.5x10^{-5}$	0.5
One-step drainage Six layers-single porosity (inverse 1)	0.15	0.69	8	2.5	Optimised 10^{-6} to 10^{-4}	0.5
One-step drainage Six layers-single porosity (inverse 2)	0.15	0.69	8	2.5	Optimised 10^{-6} to 10^{-4}	2.4
Multistep drainage Single layer-single porosity (direct)	0.15	0.7	4.7	2.6	$4.5x10^{-5}$	0.5
LDAT	θ_r (m^3/m^3)	θ_s (m^3/m^3)	α (m^{-1})	n	k_s (m/s)	l
One-step drainage Single layer-Single porosity (direct)	0.15	0.69	8	2.5	$4.5x10^{-5}$	0.5
Multistep drainage Single layer-single porosity (direct 1)	0.15	0.7	4.7	2.6	$4.5x10^{-5}$	0.5
Multistep drainage Single layer-single porosity (direct 2)	0.15	0.7	6	2.6	$4.5x10^{-5}$	0.5
Multistep drainage Single layer-single porosity (direct 3)	0.15	0.7	7.7	2.6	$4.5x10^{-5}$	0.5
Hydrus-1D	θ_{rm} (m^3/m^3)	θ_{sm} (m^3/m^3)	α_m (m^{-1})	n_m	k_{sm} (m/s)	l_m
One-step drainage Six layers-dual permeability (inverse) Matrix parameters	0.69	0.15	Optimised 5-25	2.5	Optimised 10^{-6} to 10^{-4}	0.5
One-step drainage Six layers-dual permeability (inverse) Fracture parameters	θ_{rf} (m^3/m^3)	θ_{sf} (m^3/m^3)	α_f (m^{-1})	n_f	k_{sf} (m/s)	l_f
	0		8	2	$5x10^{-3}$	0.5
	w_f	b	χ_w	a (cm)	k_a (m/s)	
	0.1	8	0.4	10	$5x10^{-8}$	

The outflow behaviour from the column can be reproduced using both Hydrus-1D and LDAT models based on a van Genuchten curve fit using parameters determined from the instrumentation within the column after steady state conditions had been established at the end of the drainage experiment. In view of the fact that the experimentally obtained van Genuchten parameters were used it is not suprising that a good general agreement was obtained between the simulations and the measured data. However the agreement did serve to support the underlying assumptions and computational integrity of both models. Of particular interest was the inverse Hydrus-1D modelling carried out for the case of the one-step drainage and which indicated the need to apply different saturated hydraulic conductivity values to each layer of the column. This is not surprising because a) the material is heterogeneous b) additional local disturbance to the particle structure could have been caused by the changes made at the boundary and c) there was a visible crack.

The multistep drainage experiment significantly reduced the scatter of the experimental data and enabled both models Hydrus-1D and LDAT to reproduce more satisfactory representations of the drainage experiment results. The slight differences between the Hydrus-1D and LDAT simulations may be attributed to the different level of discretisation (number of elements/nodes) of the column used by the two models, and the different values of the van Genuchten parameter alpha used in the case of multistep drainage.

Finally the strengths and weaknesses of the models Hydrus-1D and LDAT are listed below:

Hydrus-1D:
(+) A robust industry standard model, easy to learn, fast, it has been used in many publications in soils and waste materials. It has inverse modelling and dual porosity/permeability functions. A good model for benchmarking the liquid phase component in other models
(-) It does not explicitly include the gas or solid phases although the impact of the presence of gas is represented by van Genuchten type functions

LDAT:
(+) Integrated model including waste degradation settlement and liquid and gas transport by seepage and diffusion. Each phase can contain a number of different

bio-chemical components for which chemical equilibrium and bio-chemical reactions are calculated. Heat generation and transfer, temperature dependent parameter values.

(-) A research tool – not commercially robust. Takes time to run, single porosity approach only and many input parameters (tries to include everything that is going on in a landfill). No inverse modelling capability.

CHAPTER 7 SENSITIVITY ANALYSIS

7.1 Introduction

The output from unsaturated flow models such as Hydrus and LDAT depend on the specification of the functions that describe the moisture retention and relative permeability hydraulic properties of the material being modelled. These functions may be represented, as in the case of the van Genuchten equation, equation 2.21, by parametric algebraic equations the parameters for which may be derived from experimental measurements as we have seen in earlier chapters. A crucial part of the parameter estimation procedure is the choice of rational boundaries for the range of values that the parameters should take. In the first part of this Chapter these parameter constraints are identified for the van Genuchten parameters. The range of parameter values that may be used to obtain physically sound moisture retention and relative permeability functions with the highest possible flexibility on the one hand, and some guarantee of physical consistency on the other, are identified and then compared with the values obtained from experiment and already presented in Figures 4.19 and 4.20. In the second part of the Chapter, some results are presented and evaluated for the sensitivity of Hydrus modelling to the changing of van Genuchten parameters within these ranges of values.

7.2 Constraints on the van Genuchten parameters

In the van Genuchten (1980) function (Equation 2.21), the parameter α is related to the inverse of the air-entry value; n (>1) is related to the width of pore size distribution and *m* is an indication of the asymmetry of the curve. In Equation 2.21, θ_r and θ_s are the residual and saturated moisture contents and can be measured independently. Figure 4.21 shows the results found experimentally for values of θ_r in waste material. These values lie in the range 0.15 – 0.34. The relative unsaturated hydraulic conductivity function (Equation 2.26) suggested by van Genuchten (1980)-Mualem (1976) has two unknown parameters, the parameter m (m=1-1/n) and the parameter l that accounts for pore tortuosity and connectivity. The saturated hydraulic conductivity (k_s) is not taken as a sensitivity variable since it can be measured independently. In Chapters 5 and 6 it was shown that it does not help much to vary the parameter $l$and that reasonable modelling results may

be obtained when it is set equal to 0.5 as originally proposed by Mualem for applications in soils. Hence, since it will be assumed that (m=1-1/n), the sensitivity analysis will be carried out only for the van Genuchten parameters: αand n.

The range of α values may be constrained on the basis that it gives a reasonable range of air entry pressure values. The range of alpha α values found by the van Genuchten (by least-squared method) fits to the experimental data (Chapter 4) is 0.47 - 3.55 kPa^{-1}. This appears to be a sensible range of values since from Equation 2.21the range gives air entry pressures of 10.74 - 1.38 cm of water when the effective degree of saturation, $(\theta - \theta_r)/ (\theta_s - \theta_r)$ is 90%.

The van Genuchten parameters m and n are linked and the reasonable ranges of values for these two may be identified by taking into account the constraints on the α parameter discussed above. A possible form of constraint for m and n is that, for a given α value, these values should make the suction pressures reasonable as the residual degree of saturation is approached. If it is assumed that 100 kPa is a suction limit when the effective degree of saturation has reached 0.01, the range of m corresponding to α values 0.47 - 3.55 kPa^{-1} is 0.54 - 0.44, and the range of n is 2.2 - 1.78. It is interesting to note that this range of values corresponds quite well with the range found experimentally, Figure 4.2, and this gives some support to the assumptions that have been made here to obtain these estimated values.

For the sensitivity analysis the possible combinations of α and n were taken at the extremes of their ranges. The combination (α, n) = (0.8, 2.0), was used to create benchmark values against which the accuracy of fit was evaluated for values generated by the other combinations of (α, n). Table 7.1 lists the combinations of the parameters used for the sensitivity analysis.

Table 7.1 Combinations of α and n parameters for the sensitivity analysis

	α (kPa^{-1})	n	m (=1-1/n)
benchmark case	0.8	2	0.5
case 1	0.47	1.78	0.44
case 2	0.47	2.2	0.54
case 3	3.55	1.78	0.44
case 4	3.55	2.2	0.54

7.3 Evaluation of the sensitivity of Hydrus results on the van Genuchten parameters

Figures 7.1, 7.2 and 7.3 plot the moisture retention and relative permeability van Genuchten functions for the combinations of the parameters α and n listed in Table 7.1 with θ_r=0.15 m^3/m^3 and θ_s=0.69 m^3/m^3. Figure 7.1 shows the moisture retention curves up to 10kPa while in Figure 7.2, the moisture retention curves are plotted logarithmically up to 100kPa. It may be observed that as both α and n increase the suction pressures calculated by the van Genuchten function, equation 2.21, reduce.

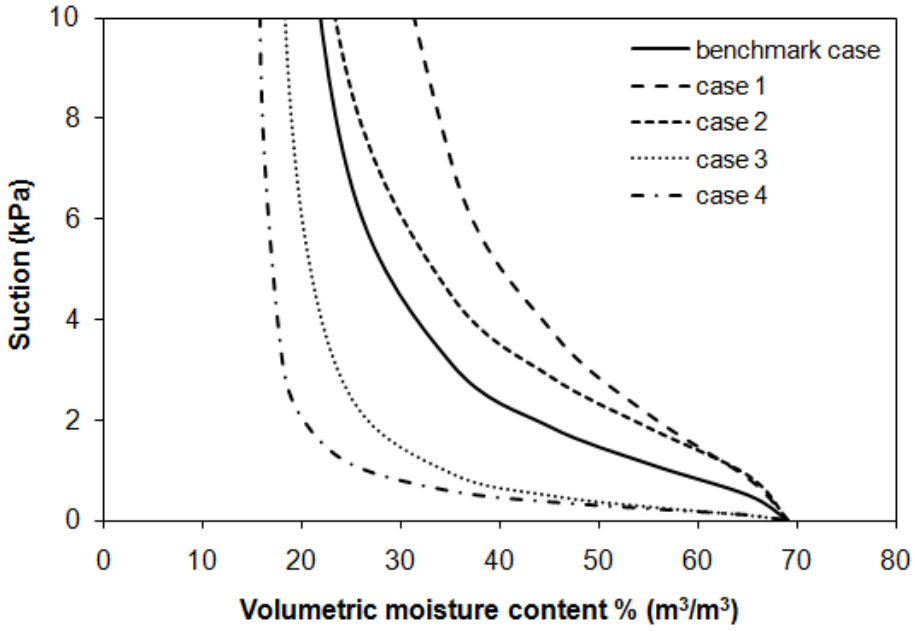

Figure 7.1 Sensitivity analysis of the moisture retention curve to van Genuchten parameters α (kPa^{-1}) and nfor suction range 0-10 kPa

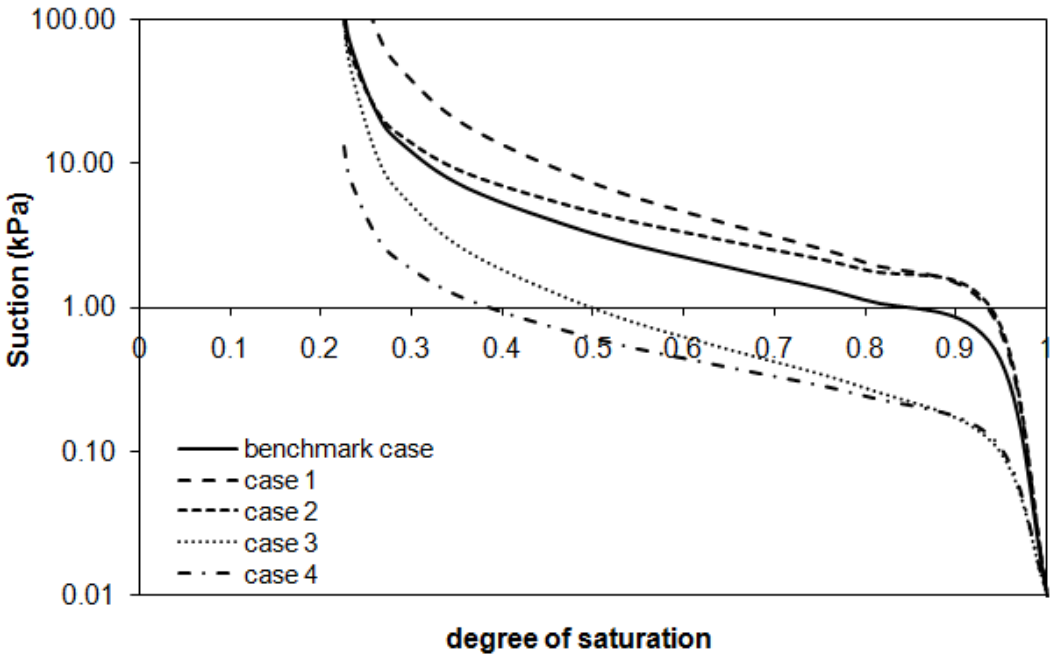

Figure 7.2 Sensitivity analysis of the moisture retention curve to van Genuchten parameters α (kPa^{-1}) and n for suction range 0-100 kPa

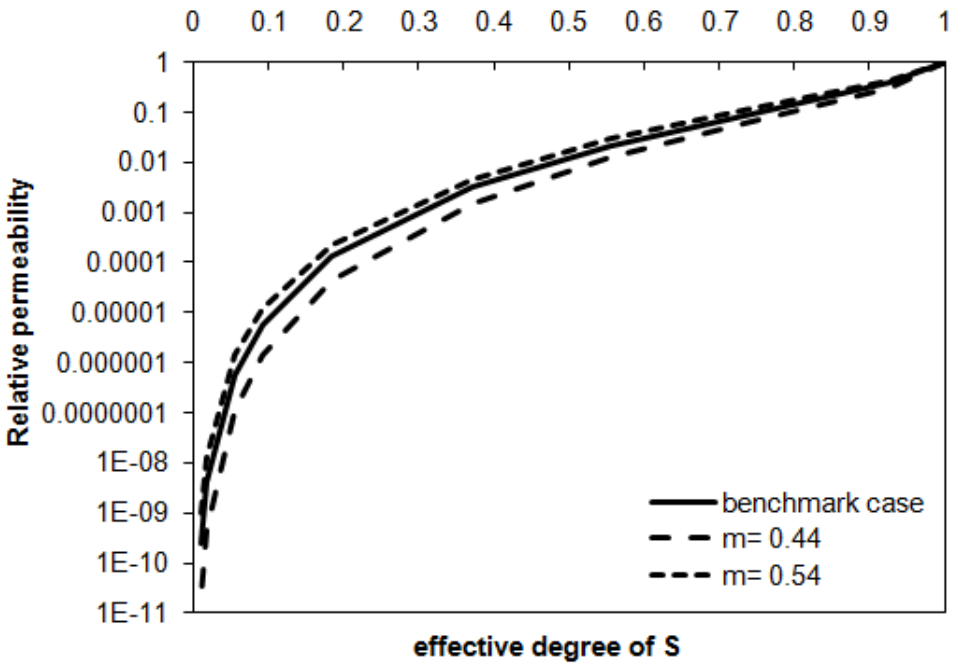

Figure 7.3 Sensitivity analysis of the relative permeability functionto van Genuchten parametersα (kPa^{-1}) and n

A measure of the change in the model results as the result of changes to the parameter benchmark values was evaluated as the square root of the mean of the

squares of the changes at 10 data points along the curves depicting the model results using Eq.7.1

$$\text{Mean square error} = \sqrt{\frac{\sum\left(\frac{yi-Yi}{Yi}\right)^2}{N}} \quad (7.1)$$

where yi are the model simulated values of suction, volumetric moisture content, mass of leachate drained out and relative permeability for cases 1-4 and Yi are the respective values for the benchmark case. N is the number of data points.

The Hydrus model results, at the beginning of the drainage (t=0) and at the end of it (t=4 days), for the sensitivity analysis using the combination of the parameters listed in Table 7.1 are show in Figures 7.4 – 7.6.

The errors measured for the moisture retention and relative permeability functions over the whole range of suction (0-100 kPa) are listed in Table 7.2. The modelling range is limited to up to 10kPa. Table 7.3 includes the errors in the moisture retention, relative permeability curves and in Hydrus results for suctions up to 10kPa.

Table 7.2 Mean Square Error (MSE) values for moisture retention and relative permeabilitycurves for the combinations of van Genuchten parameters in Table 7.1 for suction range 0-100 kPa

	MSE (Moisture retention curve)	MSE (Relative permeability)
case 1	2.56	0.62
case 2	0.40	1.3
case 3	0.57	0.62
case 4	0.79	1.3

Table 7.3 Mean Square Error (MSE) values for moisture retention curve, relative permeability and Hydrus results for the combinations of van Genuchten parameters in Table 7.1for suction range 0-10 kPa

	MSE (Moisture retention curve)	MSE (Relative permeability)	MSE (Hydrus mass of leachate drained)	MSE (Hydrus-pore liquid pressure)	MSE (Hydrus-vol. moisture content)
case 1	1.43	0.48	0.38	0.018	0.32
case 2	0.51	0.59	0.23	0.018	0.176
case 3	0.69	0.48	0.27	0.514	0.192
case 4	0.80	0.59	0.47	0.568	0.312

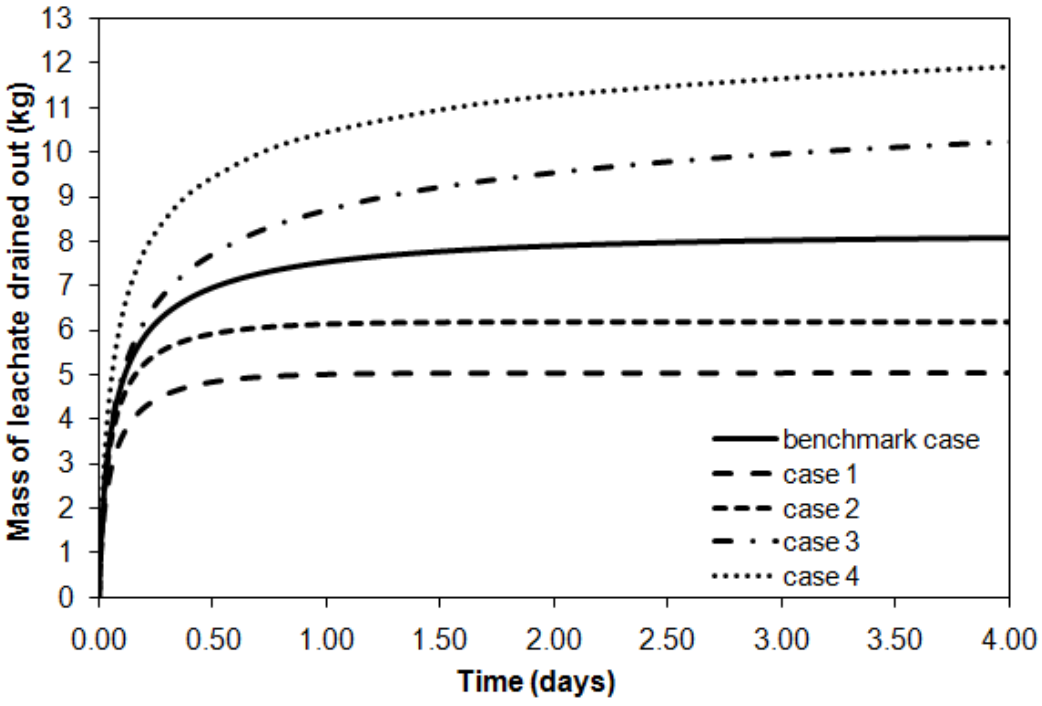

Figure 7.4 Sensitivity analysis of the mass of leachate drained out (kg) against time (days)to van Genuchten parametersα (kPa^{-1}) and n

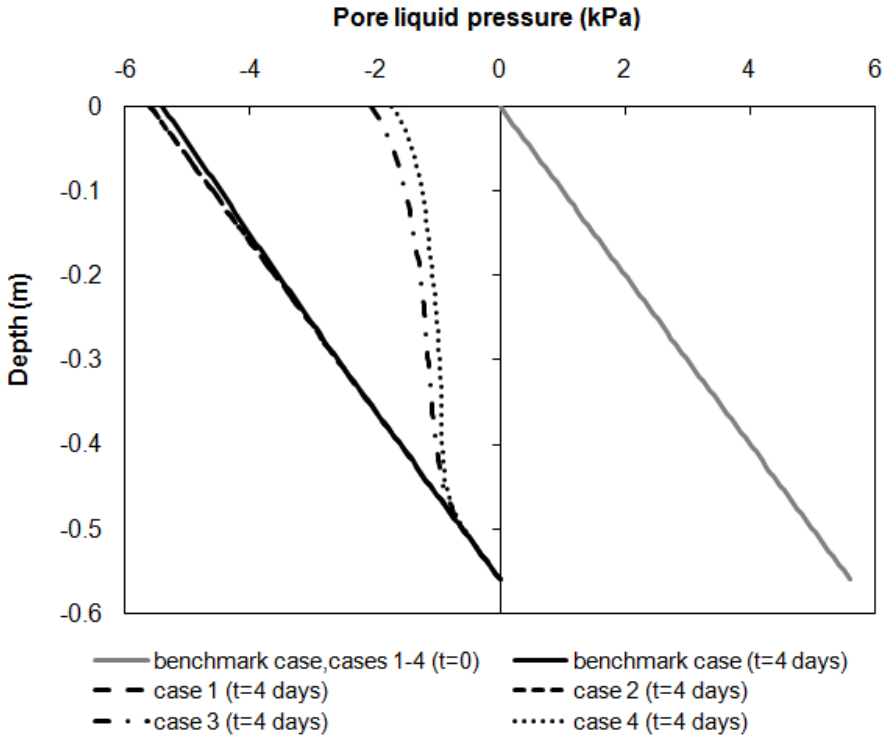

Figure 7.5 Sensitivity analysis of the pore liquid pressure profiles to van Genuchten parametersα (kPa^{-1}) and n

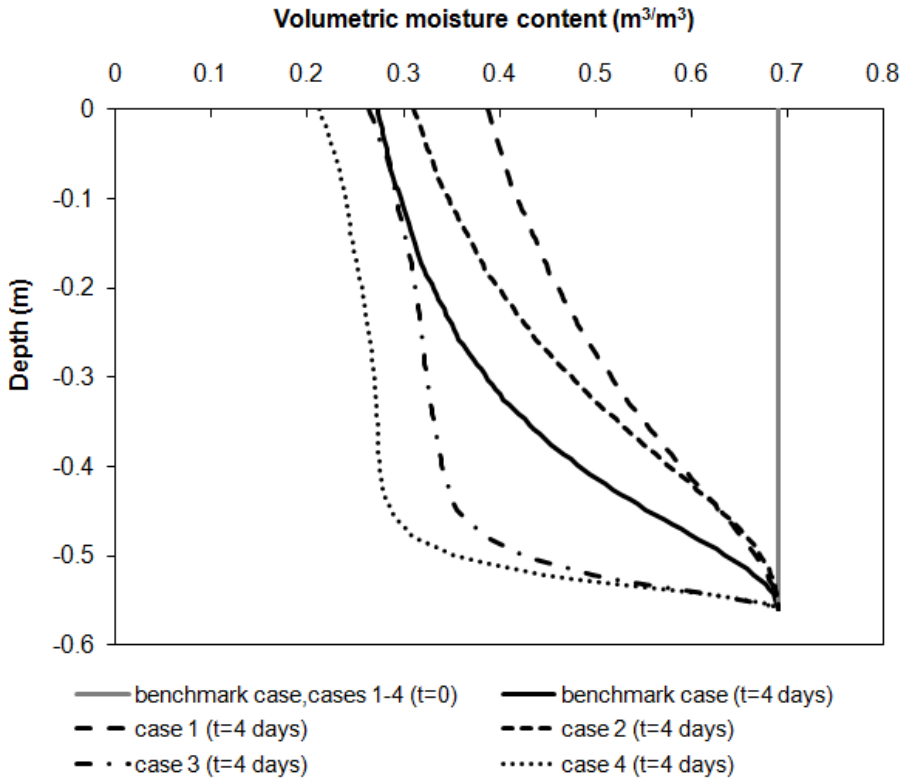

Figure 7.6 Sensitivity analysis of the volumetric moisture content profiles to van Genuchten parametersα (kPa^{-1}) and n

7.4 Summary

This chapter has given the results of an investigation into the changes in the shape of the van Genuchten moisture retention and relative permeability curves as the result of changes in the parameters α and n over a realistic range of values. It has also demonstrated the sensitivity of the results from the Hydrus drainage model to these changes in shape.

The sensitivity analysis results showed that, as might be expected, for the 'low' suction pressure cases, 3 and 4,(α high) more leachate drained out and less capillary pressure was applied to the MBT column. Whereas, when the parameter α is lower, cases 1 and 2, less leachate drained out and the capillary pressure applied to the MBT column is much higher. The changes are also reflected consistently in the steady state residual moisture content curves in Figure 7.6.

It has been shown that, for the particular models investigated, relatively small changes in the van Genuchten parameters give rise to large changes in the characteristic moisture retention and relative permeability curves and to the consequential changes in the Hydrus drainage model output. This sensitivity means that it should be possible to fit the van Genuchten parameters to experimental data with some degree of precision, and to use numerical models to extrapolate the experimental data in a reasonably robust way.

CHAPTER 8
CONCLUSIONS

Modelling of unsaturated landfill flow processes is a potentially valuable tool for the prediction of leachate and gas discharge rates, the design of leachate and gas control systems and the estimation of biodegradation and settlement in engineered landfills. However, successful modelling of moisture movement within a landfill is constrained by a lack of understanding of the unsaturated hydraulic properties of the landfilled waste. Unsaturated flow has been researched extensively in the fields of soil physics, hydrology, and geotechnical/petroleum engineering. However, there is very limited evaluation of the unsaturated hydraulic properties of landfilled waste (Korfiatis et al., 1984; McDougall et al, 1996; Imam, 2003; Kazimoglu et al, 2005, 2006; Stoltz, 2007; Münich, 2009; Staub 2010; Breitmeyer, 2011, Tinet et al, 2011). The findings reported here have important implications for the sustainable management of landfills.

This thesis has reported the findings of an investigation into the parameters of moisture retention functions of MBT waste materials and of unsaturated hydraulic conductivity or relative permeability from drainage experiments of waste columns, pressure plate and hanging water column techniques. The results from the drainage experiments have been interpreted using the unsaturated flow model HYDRUS-1D (Šimůnek et al., 2005). Also these results have given support to the modelling concepts and the integrity of the model LDAT (White *et. al* 2004) code, which was a key objective of this work.

The first section of this chapter summarises the findings of this study, the second one presents the implications of this work for practice and the third one recommends a number of topics for future investigation.

8.1 Summary of findings

8.1.1 Overview of moisture retention and relative permeability curves for waste materials

A database has been established for experimentally measured moisture retention curves and unsaturated hydraulic conductivity of MSW/MBT waste specimens with different composition, particle size and dry densities. The data have been semi-normalised as suction against degree of saturation, rather than plotted as suction against volumetric moisture content. This enables moisture retention curves for materials with different values of θ_s to be compared more easily on the same graph. Most of the moisture retention data on this database have been fitted to the van Genuchten (1980) and van Genuchten (1980)-Mualem (1976) functions.

The moisture retention characteristics database of MSW materials has shown that the van Genuchten parameters α and n tend to decrease with increasing dry density. The parameter α, which is related to the inverse of the air-entry value, decreases because increasing the density tends to eliminate the largest pores, increasing the suction needed for air entry and desaturation.

The unsaturated hydraulic conductivity database of MSW materials has shown that at higher moisture contents, the measured and calculated hydraulic conductivities diverged. This may be a result of the wide range of pore sizes, and may indicate dual porosity effects. However, this problem might resolve itself at higher stresses, as the larger pores close and the range of pore size is reduced. So, dual porosity might only be an issue at low stresses.

8.1.2 Experimental set-up: problems and solutions

During the set-up of the drainage experiment some problems had appeared. They are presented below along with their solutions:

- Saturation of the column from the bottom after CO_2 injection was a successful method of full saturation.

- Evidence of slight pitting corrosion on some of the theta probes due to a second ‘small’ current existed in the system that caused electrolytic corrosion. This problem was solved by inserting an ‘earth’ rod in the MBT column and connected to the DL2e data-logger. The accuracy of the theta probe

measurements were verified by mass balance check, so the use of theta probes for measuring moisture content in waste materials is recommended.

- Generation of gas (H_2S) in the gravel layer after about four days of drainage. Sodium molymbate (Ranade et al., 1998) and 2-bromoethanesulfonate (BES) were used to inhibit sulphate reducing bacteria and methanogenesis (Chae et al., 2009) during subsequent experiments.

- Multistep outflow is preferable to a one-step outflow drainage experiment. The capillary pressure and moisture content measured in the column apparatus provided a consistent dataset at each depth when lowering the head at the lower boundary in steps.

As far as the pressure plate technique is concerned, a major task was to prevent the uncontrolled flow of water from an initially very wet specimen during setting up the experiment. A rubber O-ring was attached at the bottom of the mould using silicon grease, and a plate of mass 1 kg placed on the top of the mould to keep the bottom of the waste and the rubber O-ring in close contact with the ceramic plate.

8.1.3 Experimental results on moisture retention curve characteristics of MBT waste

Moisture retention curves were determined for a fine MBT waste of particle size 0-10 mm using three different methods: a column drainage experiment (one-step and multistep), the hanging water column technique and a pressure plate apparatus. A satisfactory fit to each data set could be obtained using the van Genuchten (1980) curve, but there were significant discrepancies between the three sets of results.

Hanging column tests showed an apparently plausible variation of moisture retention curve with density and were self-consistent, but different from those obtained using the other apparatuses. The effect of dry density on the van Genuchten parameters α, n and θ_r from the laboratory experiments and reported in the literature was that α and n tended to decrease with increasing dry density. However it was not possible to propose a formal analytical relationship to represent this. In addition, there was no discernible correlation between θ_r and dry density. This indicates that compression of waste materials results in an increase in the number of smaller pores, which therefore become more evenly distributed

within the specimen. One of the hanging column tests was MBT of quite different composition. It contained a greater amount of organic material (paper) as a result of the use of a different shredder. It was concluded that the van Genuchten parameter α was smaller than for the higher density specimens because more water was retained in the paper and thus the specimen had a higher air entry value. Also, the saturated moisture content (θ_s) increased with decreasing density and increasing proportion of organic matter in the waste, while the residual moisture content (θ_r) increased with increasing density and proportion of organic matter in the waste.

Two tests in the pressure plate apparatus gave two different curves, one of which was close to the drainage column test data and the other to the hanging column test data. On inspection of the specimen used to generate the latter, a clear horizontal discontinuity was found which could have been caused by the too rapid application of large pressure changes. The rapid changes in pressure induce large changes in flow causing large drag and inertial forces to be applied to solid particles. Any loose particles are likely to be moved to create high permeability fissures like the one observed.

The general appearance of the moisture retention curve fitted to the data for MBT waste specimens with similar dry densities obtained using the three different techniques is of a single drying curve and a series of apparent curves branching from it when the continuity of suction within the specimen or between the specimen and the porous plate is lost. A partial or full interruption of the liquid phase within the specimen, or between the specimen and the plate will inhibit the drainage of liquid from the specimen, resulting in an increase in the retained moisture content at a given applied external suction. This has significant implications for the study of liquid movement in unsaturated wastes. It is important to realise that in the context of a hanging column apparatus the suction pressure will only be applied to a drainage path (continuous or not) if that drainage path is successfully connected to the hanging column of water through the porous plate. Thus the hanging column apparatus technique relies on the sample being set up so that all of the range of drainage path scales is connected. In the drainage experiment, moisture content and suction are point measurements. Thus the hanging column and pressure plate apparatus techniques rely on the specimen being set up so that the whole range of drainage path scales is connected, and remains connected, to the applied suction at the boundary. A key recommendation from the work is that the moisture

retention characteristic curve for a waste is perhaps better determined from direct measurements of suction and moisture content, as in the drainage column apparatus for the suction range 0-10 kPa. For higher suctions carefully set up pressure plate tests are advisable.

In the one-step drainage experiment, due to the sudden gravitational pull caused by lowering the bottom boundary pressure from hydrostatic to atmospheric pressure, movement of fine materials through the pores between the larger ones may have occurred as the leachate is drained out. This could explain the fact that the dynamic capillary pressure measured from the transient measurements at certain horizons was not greater than the one measured under quasi-static conditions. The multistep drainage experiments, in which the head at the lower boundary was lowered in small incremental steps, were carried out in an attempt to eliminate the scatter and provide a consistent dataset throughout the depth of the column. The waste drains significantly more freely in the one-step drainage experiment than in the multistep one where each layer drains in a similar way.

Finally the moisture retention characteristic curve obtained from the experiments was compared to the one derived from a mercury porosimetry test. A mercury porosimetry test was carried out by MCA Services for a very small sample of dry MBT. A unimodal pore size distribution of the MBT sample was estimated by mercury porosimetry method. But since it is just one result, any extensive conclusions cannot be drawn but it may be of interest.

8.1.4 Experimental results on unsaturated hydraulic conductivity of MBT waste

The relationship between unsaturated hydraulic conductivity and moisture content for MBT has been obtained from the drainage experiments using the instantaneous profile method and, for higher suction values, from the pressure plate apparatus data using the Passioura method.The Passioura method results showed a relative permeability that follows a ‘lower’ van Genuchten curve than the relative permeability data obtained from the drainage tests. This could be attributed to the fact that the results were obtained using different experimental techniques.

The relationship could be represented by a Genuchten-Mualem function that was consistent with the gas data of Holmes (2012) with the Stoltz correlation function

(Stoltz, Gourc et al. 2010). However to fit the data the Genuchten-Mualem m parameter value needed to be 0.6 whereas the m parameter value that would typically be found for the capillary pressure function was 0.37. The implication of this is that the unsaturated liquid permeability will not fall as rapidly with moisture content as might be expected from the capillary pressure function. The shape of the relative permeability curve supports the use of a unimodal single porosity model.

Kazimoglu (2006) observed that the van Genuchten-Mualem calculated relative permeability and the experimental data match well at low moisture content while at higher moisture contents, the agreement between them diverges. This may be attributed to the presence of very large pores in MSW. Though, this observation was not made for the MBT waste where the pore size distribution was more homogeneous. The Breitmeyer (2011) and Kazimoglu (2005) data indicated that the liquid permeability of waste could fall by several orders of magnitude in the unsaturated state. If this were to happen then drainage would effectively cease at only moderately low reductions in saturation. This is not what the column drainage experimental data reported here suggests, nor was it observed in a field scale trial at Beddington landfill (White et al. 2011).

The results of this research indicated that pressure plate and drainage tests are more reliable than hanging column tests for obtaining moisture retention data. Algebraic functions like van Genuchten (1980) used in soil science could successfully represent the moisture retention characteristics in MBT waste material. And then it is feasible to estimate relative permeability data from moisture retention data using van Genuchten (1980)-Mualem (1976) function.

8.1.5 Modelling results

The unsaturated flow model HYDRUS-1D (Šimůnek et al., 2005) and LDAT were used to simulate the experimental results. The relationships between suction, relative permeability and moisture content were introduced into LDAT for the first time and has enabled the model to couple solid phase compressibility and changes in fluid flow properties within landfill waste in order to support the engineering design of landfill management procedures (gas extraction and monitoring of settlement) and of landfill remediation systems (flushing and aeration).

The outflow behaviour from the column was reproduced using both Hydrus-1D and LDAT models based on a van Genuchten curve fit using parameters determined from the instrumentation within the column after steady state conditions had been established at the end of the drainage experiment. In view of the fact that the experimentally obtained van Genuchten parameters were used it is not suprising that a good general agreement was obtained between the simulations and the measured data. However the agreement did serve to support the underlying assumptions and computational integrity of both models. Of particular interest was the inverse Hydrus-1D modelling carried out for the case of the one-step drainage and which indicated the need to apply different saturated hydraulic conductivity values to each layer of the column. This is not surprising because a) the material is heterogeneous b) additional local disturbance to the particle structure could have been caused by the changes made at the boundary and c) there was a visible crack.

The multistep drainage experiment significantly reduced the scatter of the experimental data and enabled both models Hydrus-1D and LDAT to reproduce more satisfactory representations of the drainage experiment results.

8.2 Implications for practice

The work presented here could enhance the fundamental knowledge of the moisture retention characteristics of MBT waste. The findings make a significant contribution to the existing knowledge in experimental techniques for the determination of the moisture retention characteristics and relative permeability of

waste materials and modelling of unsaturated fluid flow in landfills and the flushing of wastes. Also, this knowledge could have a significant effect on the effectiveness of landfill remediation by flushing as simulations of the variations of hydraulic conductivity with moisture content along the depth in a landfill are necessary. Furthermore the findings of this research are applicable to the management of leachate in both conventional landfills and future sustainable designs and particularly helpful to the modelling of leachate and contaminant movement in partially saturated conditions.

The experimental datasets and constitutive relationships for fluid flow in waste materials could provide the material needed to develop a more rigorous modelling framework for the design of landfill engineering and remediation systems. A major challenge is to upscale the laboratory obtained hydraulic functions onto the in-situ mechanical and hydrological parameter values of landfill waste required by models. Nayagum et al (2010) proposed a framework to employ the effective stress and material particle size distribution to scale lab-derived hydraulic and unsaturated flow parameters to field-scale parameters.

The results of this work support the use of the van Genuchten equations for modelling unsaturated flow in MBT materials and the range of the van Genuchten parameters recommended is for α between 0.47 and 3.55 and for n between 1.1 and 2.6.

8.3 Recommendations for future work

A number of recommendations are derived from the work:

- Further experimental studies with other complex materials (MSW, synthetic waste) could be carried out to validate the proposition of different moisture retention results obtained from different experimental techniques.

- There is a need to understand better the effect of the different material components and granular distribution of the waste on the moisture retention properties. The drainage experiment could for example be run with a single component of waste material (paper, plastic, textile) and different particle sizes.

- The column only allowed suctions of up to 10 kPa to be applied. So the next stage could be to develop a means of applying greater suctions. A larger scale cell or use the same sample size but set up the pipe-work so that greater suctions could be applied to the downstream boundary. But this could have the connectivity problems encountered with the hanging column apparatus.

- Also in landfills due to the settlement phenomena and biodegradation, the properties of waste vary with time and are strongly dependent on the depth of burial and the degree of decomposition (Wu et al., 2012). The drainage experiments could be repeated using fresh and degraded MSW from different landfill depth.

- The results of this study should be compared with measurements in the field to enable their full-scale application.

- The modelling of the one-step drainage experiment showed zones in which it is possible to vary the permeability or other parameter values independently to get a better fit to the data and see if anything meaningful emerges. Hydrus has the facility to do this automatically using the inverse modelling capability. LDAT does not have this capability and does not contain a dual porosity/ dual permeability sub-model. A future development of the model LDAT including these capabilities would be useful for the complete representation of flow processes in landfills.

- A major part of the work was the design of the experimental facility. The shaft of the mini tensiometer SWT-5 was from acrylic glass and it appeared to be fragile. Two of the shafts were broken during the set-up of the experiment and they had to be replaced. A mini tensiometer with a more rigid shaft could be recommended.

REFERENCES

Agus, S.S. and Schanz, T. (2005). Comparison of Four Methods for Measuring Total Suction.Vadose Zone J., 4.

Ahmed, S., Khanbilvardi, R. M., Fillos, J., and Gleason, P. J. (1992).Two dimensional leachate estimation through landfills. Journal of Hydraulic Engineering, 118 (2), 306-322.

Anderson, W.G. (1986) Wettability Literature Survey-Part 1: Rock/Oil/Brine Interactions, and the Effects of Core Handling on Wettability. Journal of Petroleum Technology, 38, 1125-1144.

ASTM (1997).Standard test method for the measurement of soil potential (suction) using filter paper.Annual Book of Standards.Volumes 04.08 and 04.09.Soil and Rock.ASTM International, West Conshohocken, PA.

ASTM D 6836-02 (2008). Standard Test Methods for Determination of the Soil Water Characteristic Curve for Desorption Using a Hanging Column, Pressure Extractor, Chilled Mirror Hygrometer, and/or Centrifuge.

Bayard R., Benbelkacem H., Zhang Y.Y. & Gourdon R. (2009).Impact of Leachate Injection modes on Landfill Gas Production.11th International Waste Management andLandfill Symposium, Cagliari, Italy, October 2009.

Bear, J. and Verruijt, A. (1992). Modelling Groundwater Flow and Pollution, D. Reidel Publishing Company, ISBN 1-55608-015.

Beaven, R.P., Barker, J. and Hudson, A.P. (2003) Description of a tracer test through waste and application of a double porosity model. In, Ninth International Waste Management Symposium (Sardinia 2003), Sardinia, Italy, 06 - 10 Oct 2003.

Beaven R. P., Knox K., Croft B., (2001). Operation of a leachate recirculation trial in a landfill test cell."Proc. Sardina 2001, Eighth Int. Waste Management and Landfill Symp., S. Margherita di Pula, Cagliera, Italy. III 595-604.

Bendz D., Singh V.P. and Berndtsson R. (1997). The flow regime in landfills – implications for modelling in Proceedings of the 6th International Sardinia Landfill Conference, S.Margherita Dipula, Cagliari, Italy. Vol II pp97-108

Beven, K. & Germann, P. (1982). Macropores and water flow in soils. Water Resour. Res., Washington, 18: 1311-25.

Breitmeyer, R.J. and Benson, C.H. (2011a). Measurement of Unsaturated Hydraulic Properties of Municipal Solid Waste. In: Han, J., Alazamora, D. (Eds.), Geo Frontiers 2011: Advances in Geotechnical Engineering (GSP No. 211). Dallas, Texas, 1433–1442.

Breitmeyer, R.J. (2011b) Hydraulic characterization of municipal solid waste.PhD thesis, College of Engineering. University of Wisconsin -Madison, USA (abstract)

Brooks, R. H. and Corey, A. T. (1964).Hydraulic Properties of Porous Media.Hydrol.Pap. 3. Colorado State Univ. Fort Collins, CO.

Brooks, R. H. et al (1999). Fundamental changes in in-situ airsparging flow patterns. Groundwater Monitoring Rem., 19 (2),105-113.

Bruce, R. R., and A. Klute (1956).The measurement of soil moisture diffusivity, Soil Sci. Soc. Am. Proc., 20, 458–462.

BS1377-2:1990 Methods of test for soils for civil engineering purposes. Classification tests.

Campbell, G. S. (1974). A Simple Method for Determining Unsaturated conductivity from Moisture Retention Data. Soil Science, 117(6), 311-314.

Capelo, J. and M. A. H. de Castro, 2007.Measuring transient water flow in unsaturated municipal solid waste - A new experimental approach. Waste Management 27(6), 811-819.

Chae KJ, Choi MJ, Kim KY, Ajayi FF, Chang IS, Kim IS (2009) Selective inhibition of methanogens for the improvement of biohydrogen production in microbial electrolysis cells. Int J Hydrogen Energy 35:13379–13386.

Cheremisnoff, N.P. (2003) Handbook of Solid Waste Management and Waste Minimization Technologies. Butterworth-Heinemann Editions.

Christensen, T.H., Kjeldsen, P., Bjerg, P.L., Jensen, D.L., Christensen, J.B., Baun, A., Albrechtsen, H.J. and Heron, G. (2001) Review of Biochemistry of landfill leachate plumes. Applied Geochemistry 16:659-718.

CIWM, (1999).The Role & Operation of the Flushing Bioreactor.

Clapp, R. B., and Hornberger, G. M. (1978). Empirical equations for some soil hydraulic properties. Water resources research. 14(4), 601-604.

Clausnitzer, V., and J. W. Hopmans. (1995) Non-linear parameter estimation: LM_OPT. General purpose optimization code based on the Levenberg-Marquardt algorithm, Land, Air and Water Resources Paper No. 100032, University of California, Davis, CA.

Cossu, R., G. Andreottola, et al. (1996). Modelling Landfill Gas Production.Landfilling of waste: Biogas.Ed. Christensen, Cossu and Stegmann.Spon, 1996.

Crawford J.F. and P.G. Smith (1985). Landfill Technology, Butterworths, London

Daniel. D.E. (1983).Permeability test for unsaturated soil.Geotechnical Testing Journal. 2, 81-86.

Davidson,J.M. et al (1969). Fieldmeasurement and use of soil-water properties.Water resources research. 5, 1312-1321.

Delta-T Devices., (1999). Theta Probe Soil Moisture Sensor Type ML2x User Manual. Cambridge, United Kingdom: Delta-T Devices, Ltd.

Demetracopoulos, A. C., Korfiatis, G. P., Bourodimos, E. L., & Nawy, E. G. (1986). Unsaturated Flow through Solid Waste Landfills: Model and Sensitivity Analysis. Water Resources Bulletin, v.22(4).

Demond, A.H. and Roberts, P.V. (1987) An examination of relative permeability relations for two-phase flow in porous media: Water Resources Bulletin, 23, 617-628.

Durmusoglu, E., Sanchez, I., Corapcioglu, M.Y. (2006) Permeability and Compression Characteristics of Municipal Solid Waste Samples. Environmental Geology, 50, 773-786.

Ehrig, H-J.(1983). Quality and quantity of sanitary landfill leachate. Waste Management Research, 1, 53-68.

Fellner, J., Brunner, P.H., (2010). Modeling of leachate generation from MSW landfills by a 2-dimensional 2-domain approach.Waste Management 30 (11), 2084– 2095.

Fitton, G. (1997). X-Ray fluorescence spectrometry, in Gill, R. (ed.), Modern Analytical Geochemistry: An Introduction to Quantitative Chemical Analysis for Earth, Environmental and Material Scientists: Addison Wesley Longman, UK.

Fredlund, D. G. and Rahardjo, H. (1993).Soil Mechanics for Unsaturated Soils.John Wiley and Sons.70-76.

Gardner, R. (1937). A method of measuring the capillary tension of soil moisture over a wide moisture range. Soil Sci. 43:227–283.

Gardner, W. (1956).“Calculation of capilary conductivity from pressure plate data’’ Soil Science Society of America Journal, 20, 317-320.

Gaskin, G.J., and Miller, J.D. (1996). Measurement of soil water content using a simplified impedance measuring technique. Journal of Agricultural Engineering Research, 63: 153-160.

Gaskin G.J., Miller J.D. (1999) Theta Probes ML2x Principles of operation and applications. MLURI Technical Note 2nd ed. Delta-T Devices.

Gerke, H.H., van Genuchten, M.Th. (1993). A dual-porosity model for simulating the preferential movement of water and solutes in structured porous media. Water Resour. Res. 29, 305–319.

Giesche, H. (2006). Mercury porosimetry: a general (practical) overview. Part. Part. Syst. Charact. 23, 1-11.

Gourc J.P., Staub M., Conte M., Benbelkacem H., Bayard R. and Redon E. (2009).A biomechanical model to predict long term secondary settlements of MSW – Validation on large scale trials.Proc. Sardinia 2009, 11th International Waste Management and Landfill Symposium, Cagliari, Italy.

Guan, Y. and Fredlund, D. G. (1997) Use of the tensile strength of water for the direct measurement of high soil suction. Canadian Geotechnical Journal, vol. 34, (4), 604-614

Haines WB (1930) Studies in the physical properties of soil: The hysteresis effect in capillary properties and the modes of moisture distribution associated therewith. J Agric Sci 20:97-116

Hall, D., Gronow, J., Smith, R. and Blakey, N. (2004) Achieving equilibrium status and sustainable landfill - the holy grail? Waste 2004.568-578

Hamilton J.M., Daniel D.E. and Olson R.E. (1981) Measurement of hydraulic conductivity of partially saturated soils. In Permeability and groundwater contaminant transport, Zimmie T.F. and Riggs C.O. (Eds.), ASTM Special Technical Publication No. 746, American Society for Testing and Materials, 182-196.

Han, B., Scicchitano V., & Imhoff, P.T. (2011) Measuring fluid flow properties of waste and assessing alternative conceptual models of pore structure.Waste Management 31(3).

Haydar, M., and Khire, M. (2005).Recirculation using horizontal trenches in bioreactor landfills. J. Geotech. Geoenviron. Eng., 131 (7), 837–847.

Hillel, D. (1971). Soil and Water: Physical Principles and Processes.Academic Press, New York.

Hillel, D. (1998). Environmental Soil Physics. Academic Press, New York.

Huang, H. et al (2004). A novel hysteresis model in unsaturated soil.Journal of Hydrological Processes. John Wiley & Sons, Ltd

Hudson A.P., Beaven R.P. and Powrie W. (2001). Interaction of water and gas in saturated household waste in a large scale compression cell. Proceedings of the 8th International Sardinia Landfill Conference, S.Margherita Dipula, Cagliari, Italy. Vol 3, 585-594.

Hudson A.P., Beaven R.P. and Powrie W. (2002). Interaction of water and gas in saturated household waste in a large scale compression cell. In Proceedings of the Waste 2002 Conference, Stratford-upon-Avon, UK, 702-712.

Hydrogeologic, Inc (1996) “MODFLOW Surfact software manual (Version 2.2)” Hydrogeologic, Inc Herndon, VA 20170, USA 1996

Imam, M. (2003) Applications of soil mechanics principles to landfill waste. PhD thesis, School of Civil Engineering and the Environment Southampton University,UK.

Imhoff et al. (2006) Review of state of the art methods for measuring water in landfills Waste Management, Volume 27, Issue 6, 2007, 729-745.
Jang, Y. S., Kim, Y. W., and Lee, S. I. (2002). Hydraulic properties and leachate level analysis of Kimpo metropolitan landfill, Korea. Waste Manage., 22, 261-267.

Johnson, C.A., Schaap, M.G., Abbaspour, K.C. (2001).Model comparison of flow through a municipal solid waste incinerator ash landfill. Journal of Hydrology 243, 55–72.

Karvonen, T. (2001) Soil and groundwater hydrology: Basic theory and application of computational methods.

Kazimoglu, Y. K., McDougall, J. R., and Pyrah, I. C., (2005).Moisture Retention and Movement in Landfilled Waste, Proceedings of the International Conference on Problematic Soils, Famagusta, Cyprus.

Kazimoglu et al. (2006) Unsaturated Hydraulic Conductivity of Landfilled Waste. Unsaturated Soils 2006, Proc. 4th Intl. Conf. Unsaturated Soils, Arizona, 2006, eds. Miller, Zapata, Houston & Fredlund, ASCE Geotechnical Special Publication No 147, 1525-1534.

Kazimoglu et al. (2007) Moisture retention and conductivity properties of wasye refuse: a laboratory study. PhD dissertation, Napier University, School of the Built Environment.

Khire, M.V., Mukherjee, M. (2007).Leachate injection using vertical wells in bioreactor landfills. Waste Management 27, 1233–1247.

Klute, A. 1972.The determination of the hydraulic conductivity and diffusivity of unsaturated soils. Soil Science, 113: 264–276.

Knox K., (1990) ‘Assessment of landfill gas potential using leachate and gas analyses.’ Contract report for the Department of the Environment, Report no: CWM 019/90.

Kodešovα, R., Kocαrek, M., Kodeš, V., Šimunek, J., Kozαk, J. (2008) Impact of soil micromorphological features on water flow and herbicide transport in soils.Vadose Zone Journal 7, 798–809.

Korfiatis, G. P., Demetracopoulos, A., C., Bourodimos, E. L., and Nawy, E. G. (1984). Moisture transport in a solid waste column.Journal of Environmental Engineering, ASCE, 110(4), 789-796.

Kulkarni, H.S. and Reddy, K.R. (2010) 6th International Congress on Environmental Geotechnics. New Delhi, India.

Lam, L., Fredlund, D. G., and Barbour, S. L. (1987). Transient seepage model for saturated-unsaturated soil system: A Geotechnical engineering approach. Canadian Geotechnical Engineering, 24, 565-580.

Malicki, M.A., Plagge, R., Renger, M. & Walczak, R.T. (1992).Application of time domain reflectometry (TDR) soil moisture miniprobe for the determination of unsaturated soil water characteristics from undisturbed soil cores. Irrigation Science, 13, 65-72.

Marle, Charles (1981) Multiphase Flow in Porous Media, Gulf Pub Co.

Marquardt, D. W. (1963) An algorithm for least-squares estimation of nonlinear parameters, SIAM J.Appl. Math., 11, 431-441.

McCreanor P.T. and Reinhart D.R. (2000).Mathematical Modeling of Leachate Routing in a Leachate Recirculating Landfill. Water Research, Vol. 34, No.4, 1285-1295.

McDougall, J. R., Sarsby, R. W. and Hill, N. J. (1996).A numerical investigation of landfill hydraulics using variably saturated flow theory. Geotechnique, 46, 329-341.

McDougall, J. R., Pyrah, I. C., and Yuen, S.T.S. (2004). Extended phase relations and load effects in MSW. Waste Management 24., 252-257.

McDougall (2007). A hydro-bio-mechanical model for settlement and other behaviour in landfilled waste. Computers and Geotechnics 34, 229–246.

McKee,C.R. & Bumb, A.C. (1984). The importance of flow parameters in designing a monitoring system for hazardus waste and environmental emergencies.Proceedings of Hazardus Materials Control Research Institute national conference, Houston, 50-58.

Mualem, Y. (1976). A new model for predicting the hydraulic conductivity of unsaturated media. Water Resources Research, Volume 22(3), 513-522..

Münnich K., Bauer J. & Fricke K. (2009).Laboratory Tests to Determine Water Balance Parameters of MBT Material. Conference proceedings Third International Workshop: Hydro- Physico-Mechanics of Landfills, 10-13 March 2009, Braunschweig, Germany.

Müller, W & Bulson, H (2005).Stabilisation and acceptance criteria of residual waste– technologies and their achievements in Europe.Conference 'The Future of Residual Waste Management in Europe'.

Münnich, K. et al (2003) Hydraulic behaviour of mechanical biological pre-treated waste.Proceedings of the 9th International Sardinia Landfill Conference, S.Margherita Dipula, Cagliari, Italy.

Münnich, K. (1999). Hydraulische Kenngrossen von mechanisch-biologisch behandeltem Abfall. In Deponierung von Vorbehandelten Siedlungsabfallen. Heft 14, Leichtweiss-Institut fur Wasserbau, Universitat Braunschweig, Braunschweig, Germany, 11-22.

Nayagum, D., J. White, et al. (2009). Modelling study of field-scale aerobic treatment of waste using forced-air injection.Twelfth International Waste Management and Landfill Symposium.Cagliari, Sardinia, Italy.

Nikolova, R (2003). Performance of Granular Drainage Layers Permeated with Low Organic Strength Leachate. PhD thesis, School of Civil Engineering and the Environment Southampton University,UK.

Nimmo, J.R. (2004). Porosity and Pore Size Distribution, in Hillel, D., ed. Encyclopedia of Soils in the Environment: London, Elsevier, v. 3, p. 295-303.

Noble, J. J., and Arnold, A. E. (1991).Experimental and mathematical modelling of moisture transport in landfills. Chemical Engineering Comm., 100, 95-111.

Passioura, J. B. (1976). Determining soil water diffusivities from one-step outflow experiments. Australian Journal of Soil Research 15, 1-8.

Phillip, J.R. (1968). The theory of absorption in aggregated media. Aust. J. Soil Res. 6, 1–19.

Powrie, W., Beaven, R. and Hudson,A. (2008) The Influence of Landfill Gas on the Hydraulic Conductivity of Waste. Proceedings of Selected Sessions of GeoCongress 2009, New Orleans, Louisiana March 9-12, 2008. 2008; Sponsored by The Geo-Institute of ASCE.

Powrie, W. and Dacombe, P. (2006) Sustainable waste management – what and how? Proceedings of the Institution of Civil Engineers: Waste and Resource Management, 159, (3), 101-116.

Powrie, W., Beaven R.P. and Hudson A.P. (2005) “Factors affecting the hydraulic conductivity of waste” In: International Workshop "Hydro-physico-mechanics of landfills", Ed. Gourc J.P., Grenoble (2005).

Powrie, W., and Beaven, R. P. (1999).Hydraulic properties of household waste and implications for landfills. Proc. of the Institution of Civil Engineers, Geotechnical Engineering, 235 - 247.

Powrie, W. (2004) Soil Mechanics: Concepts and Applications, Second Edition, CRC Press.

Ranade et al. (1999) Evaluation of the use of sodium molybdate to inhibit sulphate reduction during anaerobic digestion of distillery waste. Bioresource Technology, volume 68, Issue 3, June 1999, pages 287-291

Rees-White T., Beaven R.P, Braithwaite P. & Purcell B. (2008).Monitoring air flow at a forced-air aerobic waste treatment plant. Proceedings of the Global Waste Management Symposium 2008, Copper Mountain conference centre, Colorado, USA.

Reinhart, D. R. (1996).‘‘The hydrodynamics of leachate in recirculation landfills.’’Proc., SWANA Landfill Symp. Wilmington, Del.

Richards, L. A. (1931). Capillary conduction of liquids through porous Mediums. Physics, 1, 318 – 333.

Richards, S.J., and Weeks, L.V. (1953).Capillary Conductivity Values from Moisture Yield and Tension Measurements in Soil Columns. Soil 17, No. 3, pp. 206-209.

Ridley, A.M., and J.B. Burland.(1993). A new instrument for the measurement of soil moisture suction. Geotechnique 43:321–324.

Ridley, A.M. and Wray, W.K. (1995). Suction measurement: A review of current theory and practices. In E.E. Alonso & P. Delage (eds), Unsaturated Soils, Proc. 1st Int. Conf. Unsaturated Soils, Paris

Ridley, A. M., Dineen, K., Burland, J. B., and Vaughan, P. R. (2003) Soil matrix suction: Some examples of its measurement and application in geotechnical engineering. Géotechnique, Vol. 53, No. 2, 241-253.

Rogers, J.S. and Klute, (1971) A. The Hydraulic Conductivity-Water Content Relationship During Nonsteady Flow Through a Sand Column, Soil Science Society America Proceedings, vol. 35, 695–700.

Rosqvist H., and Destouni G. (2000). Solute transport through preferential pathways in municipal solid waste, Journal of Contaminant Hydrology, 46, 39-60

Rosqvist, H., Bendz, D., Oman, C., and Meijer, J. E. (1997).Water flow in a pilot scale landfill.Proceedings Sardinia, Sixth Int. Landfill Symposium, Cagliari, Italy, 85-96.

Ross, P., Smetten, R. (2000). A simple treatment of physical nonequilibrium water flow in soils. Soil Science Society American Journal 64, 1926–1930.

Sears, F.W., Zemanski, M.W. (1995) University Physics 2nd ed. Addison Wesley.

Scheidegger, A.E. (1974).The physics of flow through porous media. 3rd ed., University of Toronto Press.

Siddiqui, A. et al, (2009). Experimental study on anaerobic degradation of mechanically biologically treated waste.Proceedings Sardinia 2009, 12th International Waste Management and Landfill Symposium, S.Margherita Dipula, Cagliari, Italy. 5-10 October 2009.

Siddiqui, A. (2011) Biodegradation and Settlement Behaviour of Mechanically Biologically Treated (MBT) Waste. PhD thesis, School of Civil Engineering and the Environment Southampton University,UK.

Sills, G.C., Wheeler, S.J., Thomas, S.D. and Gardner, T.N. (1991) Behaviour of offshore soils containing bubbles. Geotechnique 41 (2): 227-241.

Šimůnek, J. and M. Th. van Genuchten (2008). Modeling nonequilibrium flow and transport with HYDRUS, Vadose Zone J., Special Issue “Vadose Zone Modeling”.

Šimůnek, J., M.Th .van Genuchten, and M. Šejna. (2005). The HYDRUS-1D software package for simulating the one-dimensional movement of water, heat, and multiple solutes in variably-saturated media.Version 3.0.HYDRUS Software Ser. 1.Dep. of Environmental Sciences, Univ. of California, Riverside.

Šimůnek, J., N. J. Jarvis, M. Th. van Genuchten, and A. Gärdenäs.(2003). Review and comparison of models for describing non-equilibrium and preferential flow and transport in the vadose zone, Journal of Hydrology, 272, 14-35.

Šimůnek, J., Wendroth, O., Wypler, N., van Genuchten, M.Th., (2001). Nonequilibrium water flow characterized from an upward infiltration experiment. Eur. J. Soil Sci. 52 (1), 13–24.

Šimůnek, J., M. Th. van Genuchten, M. M. Gribb, and J. W. Hopmans, (1998) Parameter estimation of unsaturated soil hydraulic properties from transient flow processes, Soil & Tillage Research, 47/1-2, Special issue "State of the art in soil physics and in soil technology of antrophic soils", 27-36.

Soilmoisture Equipment Corp. (2002). Commercial Publications.Soilmoisture Equipment, Santa Barbara, CA.

Spanner, D.C. (1951) The Peltier effect and its use in the measurement of suction pressure.Journal of Experimental Botany,2,142-168.

Staub, M. J., (2010). Approche multi-échelle du comportement bio-mécanique d’un déchet non dangereux. PhD Thesis, LTHE, Grenoble University, France.

Staub M., Gourc J-P., Laurent J.-P., Kintzuger C., Oxarango L., Benbelkacem H., Bayard R. & Morra C. (2010). Long-term moisture measurements in large-scale bioreactor cells using TDR and Neutron probes. Journal of Hazardous Materials, 180, 165–172

Staub, M. et al (2009) TDR calibration in MSW affected by material effects and moisture distribution.3rd International workshop Hydro-Physico-Mechanics of Wastes, Braunschweig, Germany.

Stolz, G. (2007) Influence of compressibility of domestic waste on fluid conductivity. 2nd International workshop Hydro-Physico-Mechanics of Wastes, Southampton, UK.

Stoltz, G., Gourc, J.-P., Oxarango, L. (2010a).“Liquid and gas permeabilities of unsaturated municipal solid waste under compression.” J. Cont. Hydrol., 118, 27-42.

Stoltz, G., Gourc, J.-P., Oxarango, L. (2010b).“Characterisation of the physico-mechanical parameters of MSW.” Waste Management, 30, 1439-1449

Stoltz G., Tinet, A-J.Staub, M., Oxarando, L. and Gourc, J-P.(2012) Moisture retention properties of municipal waste in relation to compression. Journal of Geotechnical and Environmental Engineering, 138, 535-543

Stonestrom D.A. and Rubin J. (1989a) Air permeability and trapped-air content in two soils. Water Resources Research, 25, 1959–1969.

Straub, W. A., and Lynch, D. R. (1982). Models of landfill leaching: moisture flow and inorganic strength. Journal of Environmental Engineering, ASCE, 108(2), 231-250.

Tarantino A, Mongiovi L (2001) Experimental procedures and cavitation mechanisms in tensiometer measurements. Geotech Geol Eng 19(3–4): 189–210

Tchobanoglous et al. (1993) Integrated Solid Waste Management, McGraw-Hill, New York

Tinet, A-J, Oxarango, L., Bayard, R., Benbelkacem, H., Stoltz, G., Staub, M.J. and Gourc, J-P.(2011) “Experimental and theoretical assessment of the double porosity behaviour in a waste body during leachate infiltration.” Waste Management, Volume 31, Issue 8, August 2011, Pages 1797-1806

Uguccioni, M. and Zeiss,C. (1997). Comparison of two approaches to modeling moisture movement through municipal solid waste. Journal of Environmental Systems 25, pp. 41-63.

Vanapali et al (2008) Axis Translation and Negative Water Column Techniques for Suction Control. Geotech Geol Eng 26:645–660

van Genuchten, M. T. (1980). A Closed Form Equation for Predicting the Hydraulic Conductivity of Unsaturated Soils. Soil Sci. Soc. Of Am. J. 44, pp.892-898.

Velkushanova K, Caicedo D, Richards D. J., Powrie W., (2009). A detailed characterisation of an MBT waste. Proc XII Int Waste Man and Landfill Symposium.Sardinia, Italy, 5-9 October 2009 Paper E10, 5 - 9 October 2009 S. Margherita di Pula (Cagliari), Sardinia, Italy

Vogel, T., and Císlerová, M. (1988) On the reliability of unsaturated hydraulic conductivity calculated from the moisture retention curve, Transport in Porous Media, 3, 1-15.

Vomocil et al, (1965). An improved procedure for measuring water retention curves at low suction by the hanging-water-column method. Canadian Journal of Soil Science, 1980, 60:591-594

Walker, A.N., Beaven, R.P., Powrie, W. (1997). Overcoming problems in the development of a high rate flushing bioreactor landfill. In: Proceedings Sardinia 97, Sixth International Landfill Symposium, Vol. I, CISA, Cagliari, pp. 397–408.

Wang, Z., Wu, L., Wu, Q.J. (2000). Water-entry value as an alternative indicator of soil water-repellency and wettability. Journal of Hydrology 231, 76–83.

Warrick, A.W. (Ed.). (2002) Soil Physics Companion. CRC Press, Boca Raton.

Watson, K. (1966) An instantaneous profile method for determining the hydraulic conductivity of unsaturated porous materials. Water resources research, vol. 2, No. 4, 709–715

White, J. K., J. P. Robinson, et al. (2004). "Modelling the biochemical degradation of solid waste in landfills." Waste Management, Vol 23,3 March 2004

White, J. K. and R. P. Beaven (2008).Modelling the liquid phase in the University of Southampton model LDAT.Proceedings 1st Middle European Conference on Landfill Technology. Budapest, Hungary.

White, J.K. (2010) Technical note on hanging column data. School of Civil Engineering and the Environment Southampton University,UK.

Wu, H., Wang, H., Zhao, Y., Chen, T. and Lu, W. (2012) Evolution of unsaturated hydraulic properties of municipal solid waste with landfill depth and age.Waste Management 32, 463-470

Xie, M., Aldenkortt, D., Wagner, J., and Rettenberger, G. (2006). Effect of Plastic Fragments on Hydraulic Characteristics of Pretreated Municipal Solid Waste, Canadian Geotechnical Journal, 43, 1333-1343.

Yuen et al. (2001) Water Balance Comparison Between a Dry and a Wet Landfill - A full-Scale Experiment. Journal of Hydrology

Yuen, S. T. S.; McMahon, T. A. and Styles, J. R., 2000, 'Monitoring in-situ moisture content of municipal solid waste landfills', Journal of Environmental Engineering, vol. 126, no. 12, 1008-109

Yuen, S. T. S. (1999). Bioreactor Landfills Promoted By Leachate Recirculation - A Full-Scale Study. Unpublished Thesis Submitted for the Degree of Doctor of Philosophy, Department of Civil and Environmental Engineering, University of Melbourne.

Zeiss, C. and Major, W. (1993).Moisture flow through municipal solid waste. Journal of Environmental Systems, 22(3), 211-231.

Zeiss, C. and Uguccioni.(1995). Mechanisms and patterns of leachate flow in municipal solid waste landfills. Journal of Environmental Systems, 23, 247-270.

Zeiss, C. and Uguccioni. (1997). Modified flow parameters for leachate generation. Water Environmental Research, 69, 276-284.

APPENDICES

Appendix A - Derivation of Richard's equation for one phase flow-1D

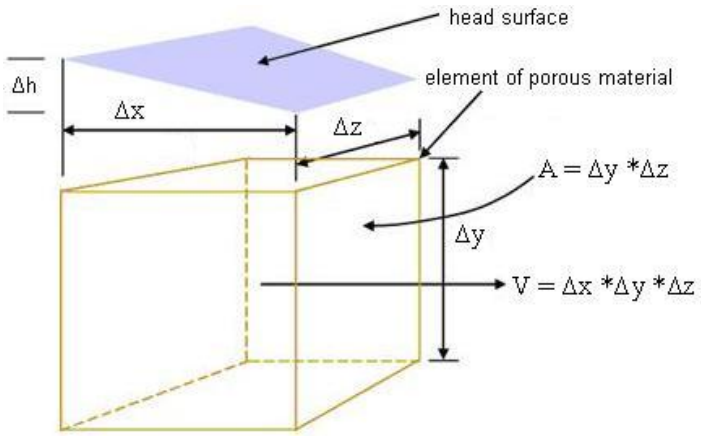

Figure A.1 Control volume

Consider the control volume in Figure 1 with sides Δx, Δy and Δz along the axes x, y and z respectively and volume $V=\Delta x*\Delta y*\Delta z$, the conservation of mass can be described as below:

Flow in: $q_x \Delta y \Delta z$ (1)

Flow out: $\left(q_x + \frac{\partial q_x}{\partial x} \Delta x \right) \Delta y \Delta z$ (2)

According to the conservation of mass or continuity principle:

Storage change = flow in – flow out

$$q_x \Delta y \Delta z - \left(q_x + \frac{\partial q_x}{\partial x} \Delta x \right) \Delta y \Delta z = - \frac{\partial q_x}{\partial x} \Delta x \Delta y \Delta z \quad (3)$$

The volume change of water is: $\frac{\partial \theta}{\partial t} \Delta x \Delta y \Delta z$

Hence, $\frac{\partial \theta}{\partial t} \Delta x \Delta y \Delta z = - \left(\frac{\partial q_x}{\partial x} + \frac{\partial q_y}{\partial y} + \frac{\partial q_Z}{\partial z} \right) \Delta x \Delta y \Delta z$ (4)

The continuity equation takes the form: $\frac{\partial \theta}{\partial t} = - \left(\frac{\partial q_x}{\partial x} + \frac{\partial q_y}{\partial y} + \frac{\partial q_Z}{\partial z} \right)$ (5)

In one dimensional flow (vertical): $\frac{\partial \theta}{\partial t} = -\frac{\partial q_z}{\partial z}$ (6)

According to Darcy's law: $q_z = -k\frac{\partial h}{\partial z}$ where $h = \psi + z$

$$\frac{\partial q_z}{\partial z} = -\frac{\partial}{\partial z}\left(-k_z \frac{\partial h}{\partial z}\right) \quad (7)$$

Thus, $\frac{\partial \theta}{\partial t} = \frac{\partial}{\partial z}\left(k_z \frac{\partial h}{\partial z}\right)$ (8)

In unsaturated flow the coefficient of permeability is a function of the water content (θ) or the matric suction (ψ). Hence, the above equation takes the form:

$$\frac{\partial \theta}{\partial t} = \frac{\partial}{\partial z}\left(k_z(\theta)\frac{\partial h}{\partial z}\right) \quad (9)$$

Since $h = \psi + z$, then

$$\frac{\partial \theta}{\partial t} = \frac{\partial}{\partial z}\left[k_z(\theta)\left(\frac{\partial \psi}{\partial z} + \frac{\partial z}{\partial z}\right)\right] = \frac{\partial}{\partial z}\left[k_z(\theta)\left(\frac{\partial \psi}{\partial z} + 1\right)\right] \text{ or} \quad (10)$$

$$\frac{\partial \theta}{\partial t} = \frac{\partial}{\partial z}\left[k_z(\theta)\left(\frac{\partial \psi}{\partial z} + 1\right)\right] \text{ or} \quad (11)$$

$$\frac{\partial \theta}{\partial t} = \frac{\partial}{\partial z}\left(k_z(\theta)\frac{\partial \psi}{\partial z}\right) + \frac{\partial}{\partial z}k_z(\theta) \quad (12)$$

The last three equations are all expressions of one-dimensional Richard's equation for the description of water flow under unsaturated conditions.

To describe Darcian flow under unsaturated conditions the term D (diffusivity) should be entered, where $D = k_z(\theta)\frac{\partial \psi}{\partial \theta}$ (13)

By using the chain rule: $\frac{\partial \psi}{\partial z} = \frac{\partial \psi}{\partial \theta}\frac{\partial \theta}{\partial z}$ and the diffusivity equation above, equation (13) becomes:

$$\frac{\partial \theta}{\partial t} = \frac{\partial}{\partial z}\left(D(\theta)\frac{\partial \theta}{\partial z}\right) + \frac{\partial}{\partial z}k_z(\theta) \quad (14)$$

Appendix B - Measurement Techniques for Moisture Content

(Yuen et al., 2000; Imhoff et al., 2006)

Device	Description	Advantages	Disadvantages
Neutron probe	The neutron probe emits neutrons that are subatomic particles from a radioactive source. As these particles travel in the medium their velocity is reduced (thermalized) by their collision with the nuclei of other atoms. Hydrogen, being the smallest atom, is extremely effective at thermalizing neutrons. The concentration of the thermalized neutrons is therefore taken as being proportional to the hydrogen atom content. Provided that there is no other significant source of hydrogen atoms other than water molecules in the media, the concentration of hydrogen atoms can be related to the moisture within the media. With a suitable calibration curve, the volumetric water content of the media can be determined from the measurements of thermalized neutrons.	• Moisture content can be measured regardless of its physical state in soils or waste • Offers large radius of influence, between 150 mm in wet soil and 700 mm in dry soil	• Measurement of absolute moisture content is difficult • Presence of non-water bound hydrogen interferes with the measurement • Some elements other than hydrogen have a propensity to absorb high-energy neutrons • Changes in density affect the results • The radioactive source of neutron probe is a highly regulated material • Automation is not possible
Electrical Resistance sensors	Electrical resistivity sensors relate electrical resistance to a current passing through the sensor to the matric potential of surrounding media. Sensors contain a well-characterized porous medium, and water moves between this porous medium and the refuse until the medium and the refuse are at equilibrium with identical matric potentials. Thus, the electrical resistance measured in the sensor varies with matric potential of the refuse, as well as liquid ion concentration and temperature. The	• Sensors are relatively inexpensive • Sensor installation is easy • Automated measurement is possible • Density does not affect readings • Fast response to	• The heterogeneity of MSW prevent a uniform flow of electric current or heat pulse • Uncertain electric contacts between the electrodes and waste may create major problems. Porous blocks (e.g., gypsum blocks) based on electrical conductivity have been used to avoid these difficulties • Other sources of error include sensor hysteresis (sensor readings will be affected by wetting and drying cycles), dependence on waste porosity and density, poor contact

	resistance measured by the sensor must be correlated to Mc by laboratory calibration.	leachate front arrival	with the media, and deterioration of the sensor over time • Electrical sensors read matric potential, they cannot reliably read potentials above the air entry pressure or below the field capacity of the refuse • Results affected by changes in electrical conductivity and temperature • Once wet the sensors do not drain quickly • Overestimate the moisture content • Sensor must be calibrated using extracted waste
Electromagnetic techniques (TDR,TDT)	These techniques are based on the propagation of electromagnetic waves in porous media. Time domain reflectometry (TDR) and time domain transmissivity (TDT) relate the time of travel of electromagnetic waves to the dielectric constant of the waste. This value can in turn be correlated to hw because of the significant differences between the properties of water and other materials	• Unaffected by organic carbon content changes • Sensors are relatively inexpensive • Results are reproducible • Automated measurement is possible • Fast response to leachate front arrival	• Results affected by changes in electrical conductivity, which affects the dielectric constant. This effect can be minimized by coating the probes. • Local heterogeneity of material properties affects the results • The TDR sensor is subject to hysteresis and requires good contact with the surrounding media • Temperature may also influence measurements • The presence of metals in landfills and high salinity influence the dielectric constant measurement • Overestimate the moisture content • Sensor must be calibrated using extracted waste

Appendix C - Experimental moisture retention data fitted to van Genuchten and Brooks & Corey models

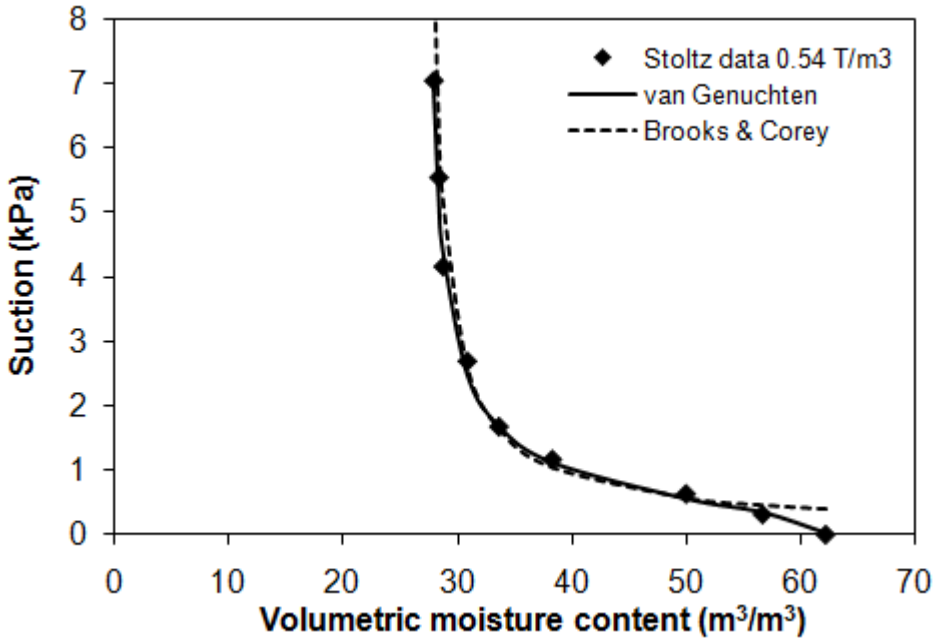

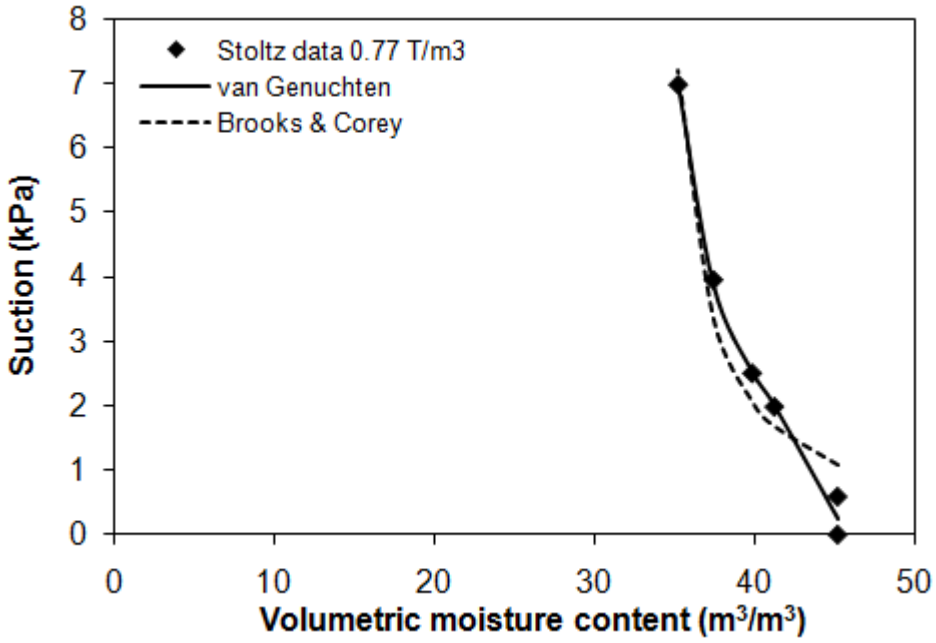

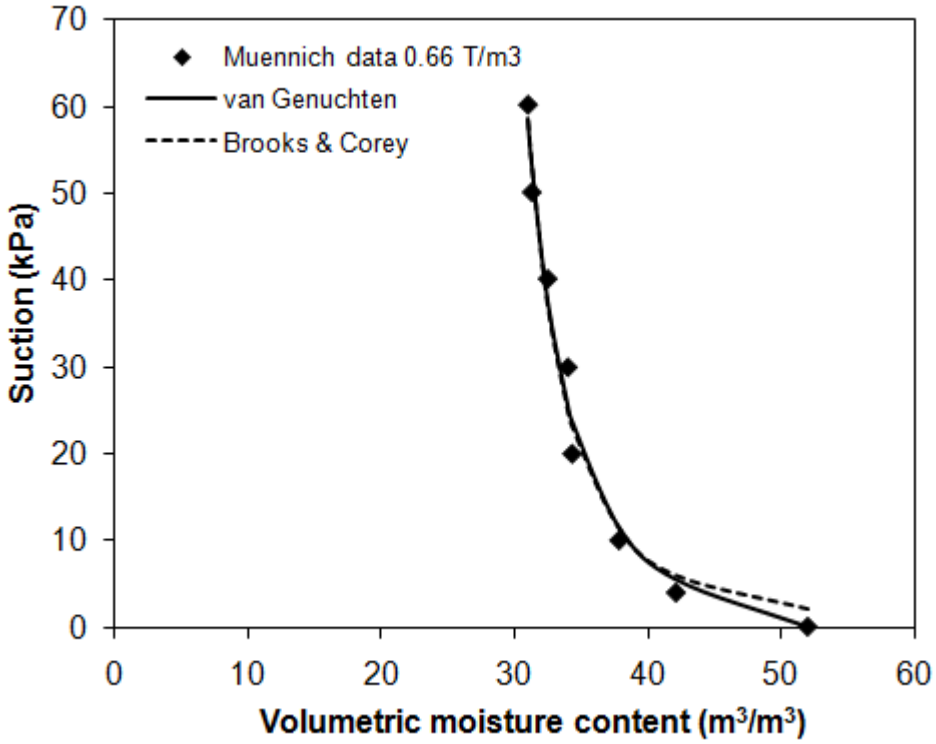
Muennich data 0.66 T/m3
van Genuchten
Brooks & Corey
Suction (kPa)
Volumetric moisture content (m3/m3)
0
10
20
30
40
50
60
70

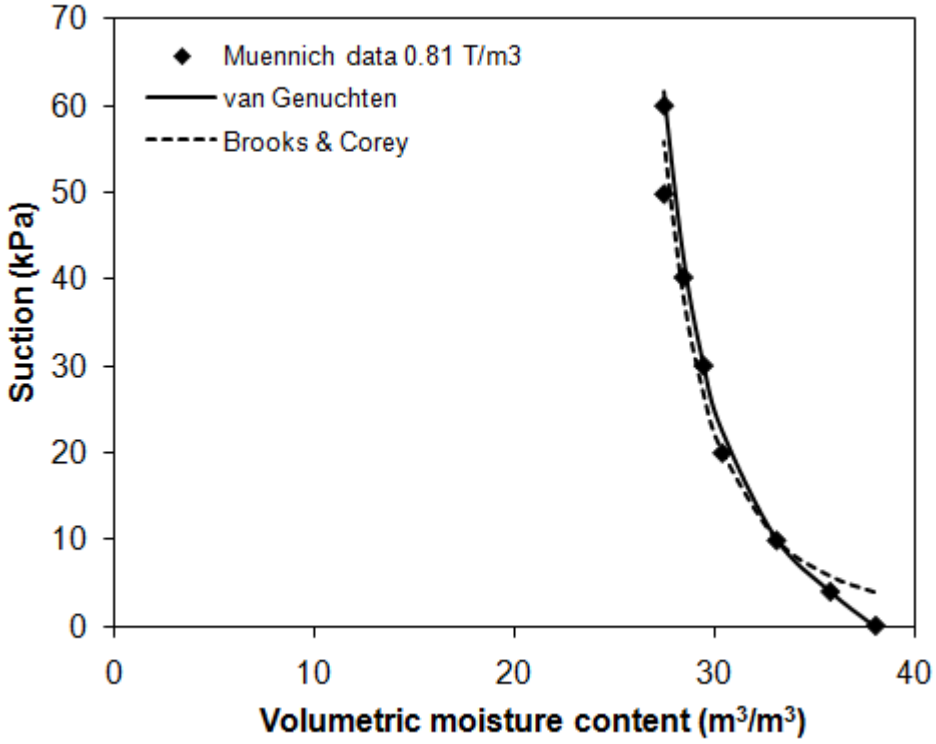
Muennich data 0.81 T/m3
van Genuchten
Brooks & Corey
Suction (kPa)
Volumetric moisture content (m3/m3)
0
10
20
30
40
50
60
70

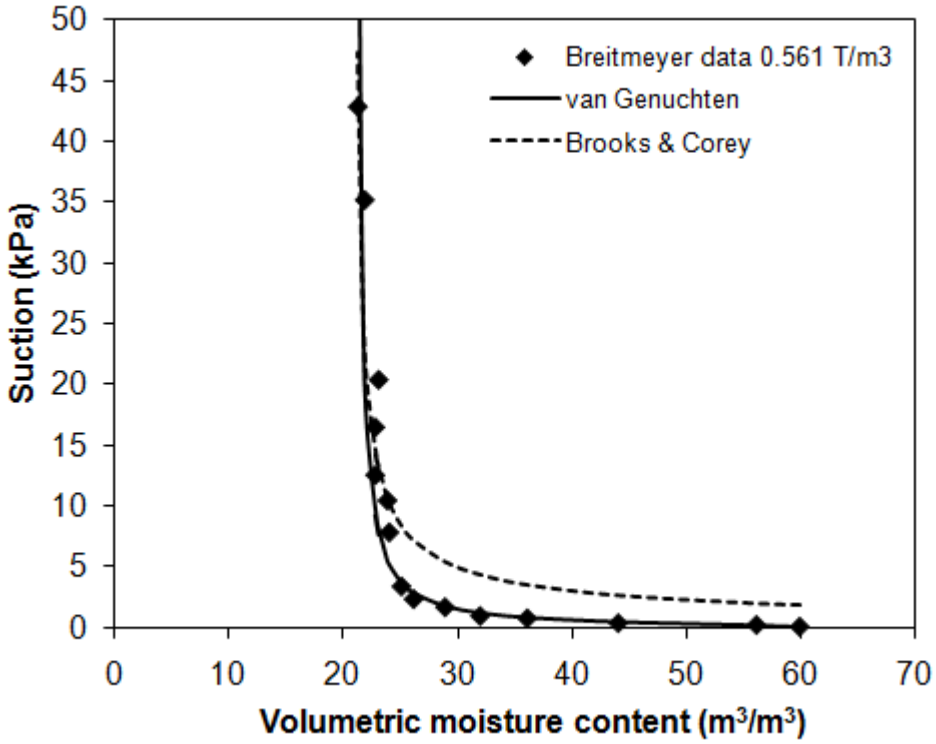
Breitmeyer data 0.561 T/m3
van Genuchten
Brooks & Corey
Suction (kPa)
Volumetric moisture content (m3/m3)
0
5
10
15
20
25
30
35
40
45
50
0
10
20
30
40
50
60
70

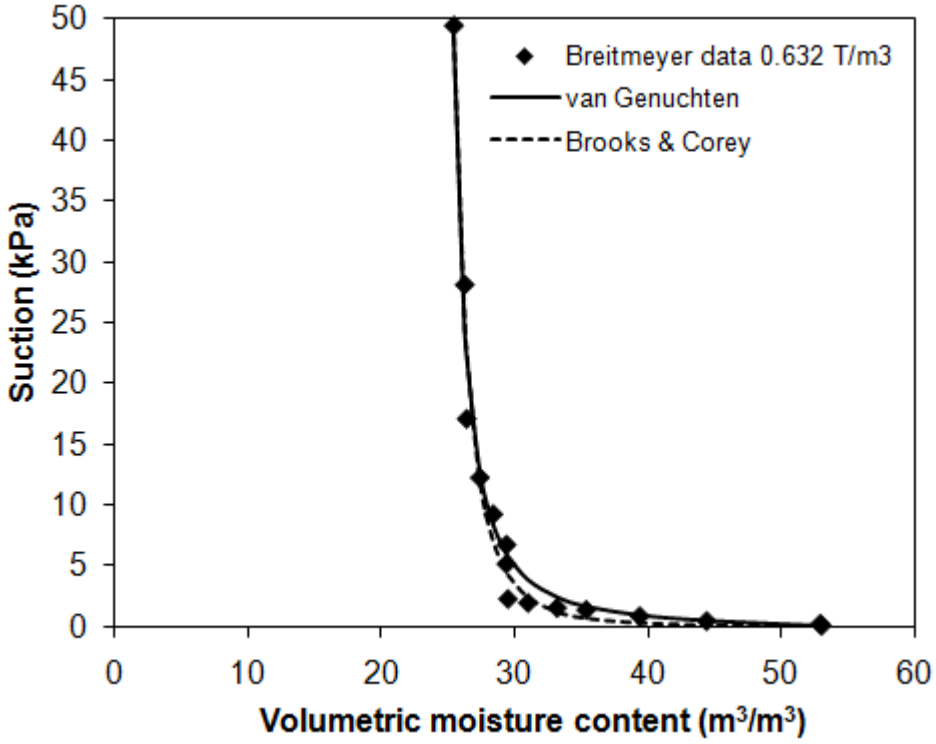
Breitmeyer data 0.632 T/m3
van Genuchten
Brooks & Corey
Suction (kPa)
Volumetric moisture content (m3/m3)
0
5
10
15
20
25
30
35
40
45
50
0
10
20
30
40
50
60

Table C.1 Fitted van Genuchten parameters to the data

Waste	θr	θs	α (kPa^{-1})	n	RSQ
MBT Munnich (2009) 0.66 T/m^3	0.24	0.52	0.42	1.42	0.984
MBT Munnich (2009) 0.81 T/m^3	0.21	0.38	0.18	1.4	0.982
Stoltz MSW (2007) 0.54 T/m^3	0.27	0.62	1.85	2.42	0.996
Stoltz MSW (2007) 0.77 T/m^3	0.33	0.45	0.5	2.29	0.999
Breitmeyer MSW (2011) 0.561 T/m^3	0.21	0.60	3.38	1.85	0.943
Breitmeyer MSW (2011) 0.632 T/m^3	0.238	0.53	2.92	1.58	0.979

Table C.2 Fitted Brooks & Corey parameters to the data

Waste	θr	θs	ψ_{aev}	λ	RSQ
MBT Munnich (2009) 0.66 T/m^3	0.24	0.52	2.82	0.415	0.981
MBT Munnich (2009) 0.81 T/m^3	0.21	0.38	4.019	0.369	0.976
Stoltz MSW (2007) 0.54 T/m^3	0.27	0.62	3.96	1.175	0.972
Stoltz MSW (2007) 0.77 T/m^3	0.33	0.45	6.04	0.448	0.967
Breitmeyer MSW (2011) 0.561 T/m^3	0.21	0.60	1.927	1.52	0.872
Breitmeyer MSW (2011) 0.632 T/m^3	0.238	0.53	0.049	0.316	0.979

Appendix D - Summary of the reported values of saturated hydraulic conductivity for MSW and MBT materials

Table D.1 Summary of the reported values of saturated hydraulic conductivity for MSW (after Siddiqui, 2011)

Reference	Hydraulic conductivity (m/s)	Dry density (kg/m3)	Test
Laboratory tests			
Bleiker et al. (1995)	$1x10^{-6}$ - $5x10^{-9}$	500 – 1200	Falling head
Chen & Chynoweth (1995)	$9.6x10^{-4}$ - $4.7x10^{-7}$	160 – 480	Constant head
Powrie & Beaven (1999)	$1.5x10^{-4}$ - $3.7x10^{-8}$	390 – 720	Constant head
Durmusoglu et al. (2006)	$1.2x10^{-4}$ - $4.7x10^{-6}$	N/A	Falling head
Olivier & Gourc (2007)	$1x10^{-4}$ - $1x10^{-6}$	490 – 710	Falling head
Reddy et al. (2009)	$2x10^{-3}$ - $7.8x10^{-7}$	320 – 960	Constant head
Staub et al. (2009)	$7.4x10^{-5}$ - $4.6x10^{-6}$	370 – 530	Falling head
Stoltz et al. (2010)	$1x10^{-4}$ - $1.1x10^{-5}$	600 – 900	Constant & falling head
Field tests			
Oweis et al. (1990)	$2.4x10^{-5}$ - $9.4x10^{-6}$	680	Pumping test
Landva & Clark (1990)	$4x10^{-4}$ - $1x10^{-5}$	1000 – 1400	Flow nets
Jain et al. (2006)	$6.1x10^{-7}$ - $5.4x10^{-8}$	N/A	Borehole permeameter
Machado et al. (2010)	$1x10^{-5}$ - $1x10^{-8}$	N/A	Borehole infiltration

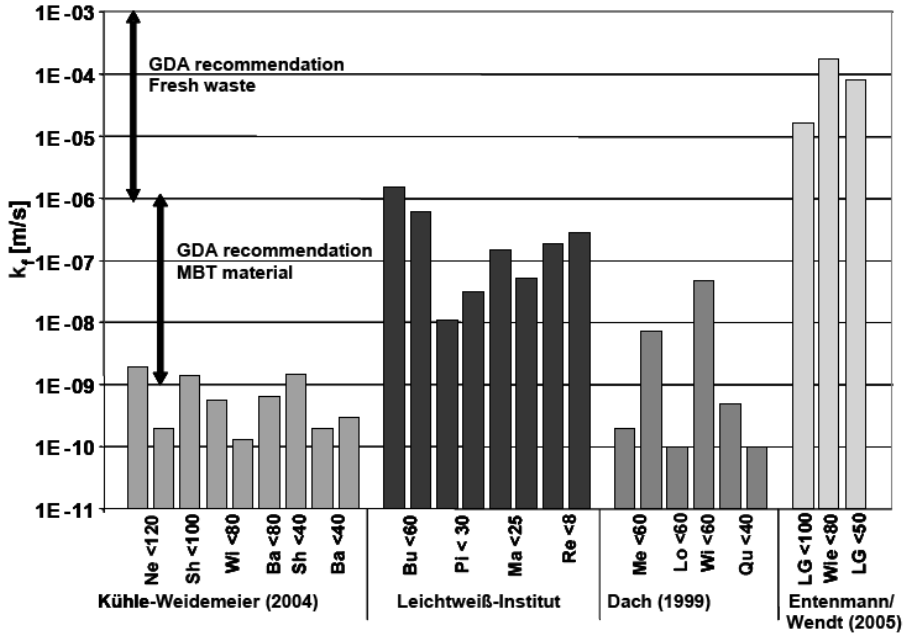

Figure D.1 Overview of saturated hydraulic conductivities for German MBT waste (Muennich et al., 2007)

Appendix E - Determination of particle density or specific gravity: Pycnometer method

For the estimation of the particle density or specific gravity of the MBT waste

The specific gravity, G_s, of a porous solid is the mass of the solid particles, M_s, divided by the mass of water occupying the same volume as the given mass of solid particles, V_s: $G_s = \frac{M_s}{V_s * \rho_w}$ (1)

At 4^0C, the density of water, p_w, is taken to be 1 Mg/m^3 (or 1g/cm^3).

Using the apparatus shown in Figure 1, the air is removed from the solid sample and the water by applying a vacuum. The test is performed at constant temperature. For all weightings of the full flask it is important to keep to a standard 'full flask'. This is obtained by slightly overfilling the flask with de-aired water until the meniscus projects above the flask's upper lip; a small Perspex disc is then slid across this upper lip and the outside of the flask dried before weighing.

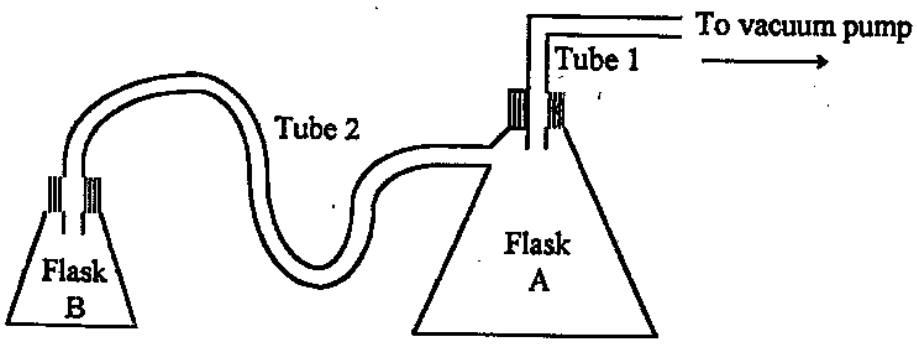

Figure E.1 Pycnometer method apparatus

Experimental Procedure:

First the flask A was half filled with de-aired water. Then 100g of dried MBT was placed in flask B. The two flasks were connected using tube 2 and the flask A connected to the vacuum pump using tube 1. The vacuum was applied for 3 mins and after the flask B was agitated to ensure the sample is fully de-aired. Then the MBT sample was flood by very slowly pouring the de-aired water from flask A to flask B through tube 2. Small increments of water were added each time to ensure full saturation of the sample. After agitating again the flask B and checking that is filled, the vacuum pump was disconnected and the flask B was removed from the arrangement after toping it up with de-aired water until the meniscus projects above the lip. Finally the flask B was weighted after drying it outside and the procedure was repeated for further samples.

Calculations:

The specific gravity of the MBT sample is the ratio of weight in air of a given volume of the MBT particles to the weight in air of an equal volume of de-aired water of 4^0C.

Thus $G_s = \frac{(W_2 - W_1) * G_T}{(W_4 - W_1) - (W_3 - W_2)}$ (2)

where G_T is the specific gravity of de-aired water at the temperature of the test. At 20^0C, G_T =0.998.

W1: weight of flask and disc = 130.70g

W2: weight of flask, disc and dry MBT = 232.33g

W3: weight of flask, disc, dry MBT and water = 450.77g

W4: Weight of flask, disc and water only = 409.79g

Substituting to eq. 2: $Gs = \frac{(232.33 - 130.70) * 0.998}{(409.79 - 130.70) - (450.77 - 232.33)}$ = 1.67 Mg/m^3

Second and third test: G_s=1.69 Mg/m^3

Appendix F - Impedance sensor theory (Theta probe ML2x)

The impedance (Z) of a coaxial transmission line is dependent on its physical dimensions and on the dielectric constant of the insulating material:

$$Z = \left(60/\sqrt{\varepsilon}\right) ln(r_2/r_1) \quad (1)$$

wherer_1 and r_2 are the radii of the signal and shield conductors respectively.

The Theta Probe consists of an input/output cable, probe body and a sensing head. The cable provides connection for a suitable power supply and for an analogue signal output. The probe body contains an oscillator, a specially designed internal transmission line and measuring circuitry within a waterproof housing. The sensing head has an array of four rods, the outer three of which, connected to instrument ground, form an electrical shield around the central, signal rod. This behaves as an additional section of transmission line having impedance that depends on the dielectric constant of the matrix into which it is inserted. If this impedance differs from that of the internal transmission line, then a proportion of the signal is reflected back from the junction (J) between the probe array and the transmission line.

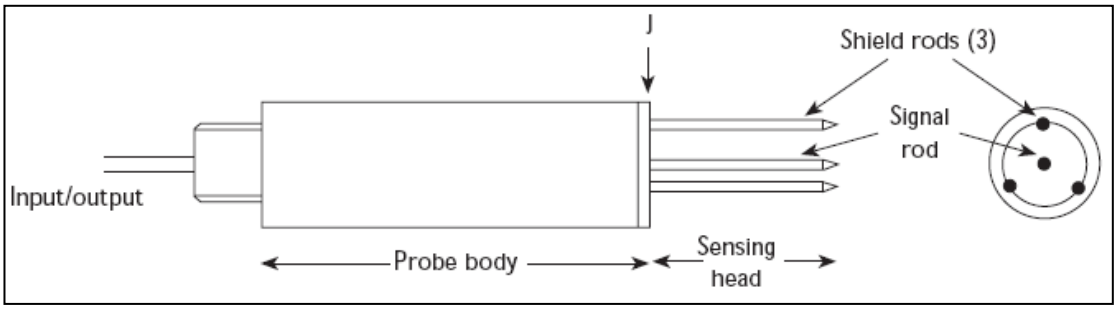

Figure F.1 Schematic diagram of the Theta Probe ML2x (Delta-T devices)

The Theta Probe consists of an input/output cable, probe body and a sensing head. The cable provides connection for a suitable power supply and for an analogue signal output. The probe body contains an oscillator, a specially designed internal transmission line and measuring circuitry within a waterproof housing. The sensing head has an array of four rods, the outer three of which, connected to instrument ground, form an electrical shield around the central, signal rod. This behaves as an additional section of transmission line having an impedance that depends on the dielectric constant of the matrix into which it is inserted. If this impedance differs from

that of the internal transmission line, then a proportion of the signal is reflected back from the junction (J) between the probe array and the transmission line.

This reflected component interferes with the incident signal causing a voltage standing wave to be set up on the transmission line, i.e. a variation of voltage amplitude along the length of the line.

If Z_L is the impedance of the transmission line and Z_M is the impedance of the probe inserted into a matrix, thenρ, the reflection coefficient is:

$$r = (Z_M - Z_L)/(Z_M + Z_L) \quad (2)$$

The transmission line is designed so that the peak voltage at its start (V_0) is:

$$V_0 = a(1 - \rho) \quad (3)$$

where a is the voltage amplitude of the oscillator output.

The peak voltage at the junction (V_J) is:

$$V_J = a(1 + \rho) \quad (4)$$

Therefore the difference in amplitude is:

$$V_J - V_0 = 2a\rho \quad (5)$$

Measuring this amplitude will give the relative impedance of the probe, hence the dielectric constant and thus a measure of volumetric water content.

The linear relationship between the square root of the dielectric constant ($\sqrt{\varepsilon}$) and volumetric water content (θ_v) has been established by many authors, including Whalley (1993), White et al (1994) and Topp et al (1980).

APPENDIX G - Theta Probe Calibration

Every Theta Probe uses the same characteristic to convert from its mV output to the square root of the apparent dielectric constant, √ε, of the soil. However, the conversion from √ε to per cent moisture content depends on the soil type encountered.

The relationship between Theta Probe output and soil moisture content is a non-linear curve of this form:

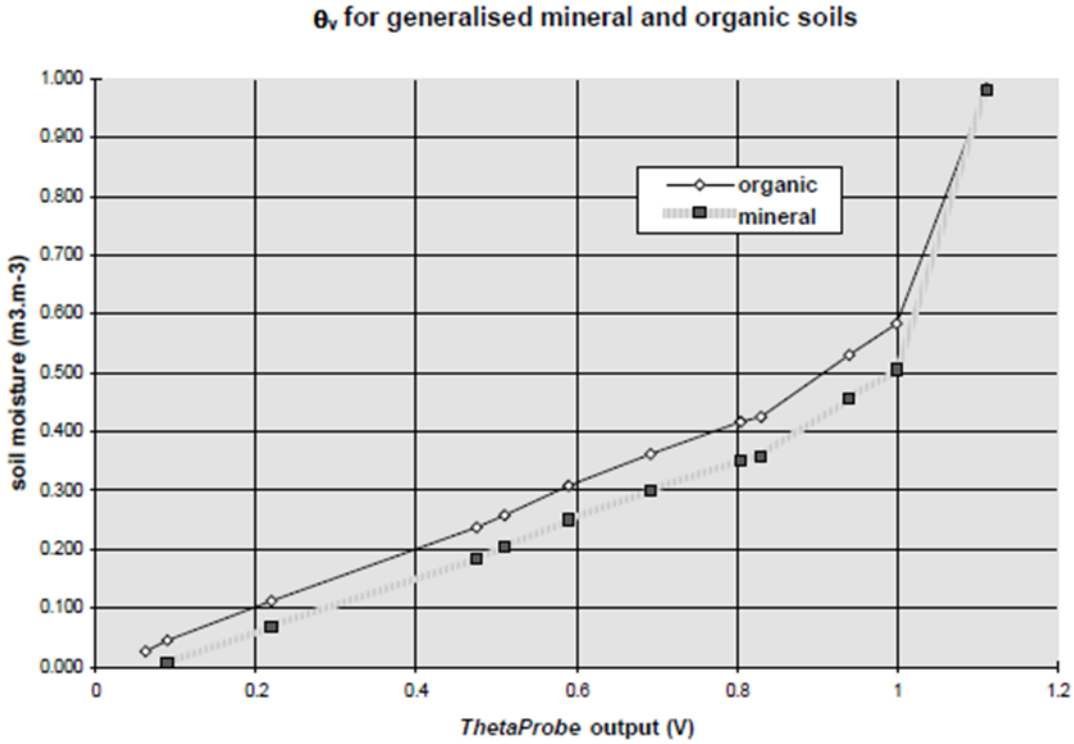

Figure G.1 Soil moisture Theta probe (m^3/m^{-3}) output (V) relationship for generalised mineral and organic soils (Delta-T Devices, Ltd. 1999)

These two curves are generalised examples for mineral and organic soils. The calibration curve for any specific medium would be slightly different from either of these because the Theta Probe is actually sensing the dielectric constant, (ε) of the medium and the relationship between the measured dielectric constant of a medium and its moisture content (θ) depends on the particular composition of the medium. Performing a soil-specific calibration is relatively straightforward, because all ML2x Theta Probes respond to dielectric constant in the same stable, uniform way, so it is only necessary to do this once for one probe. The relationship between Theta Probe output, (V), and square root of dielectric constant, (√ε), is

like this:

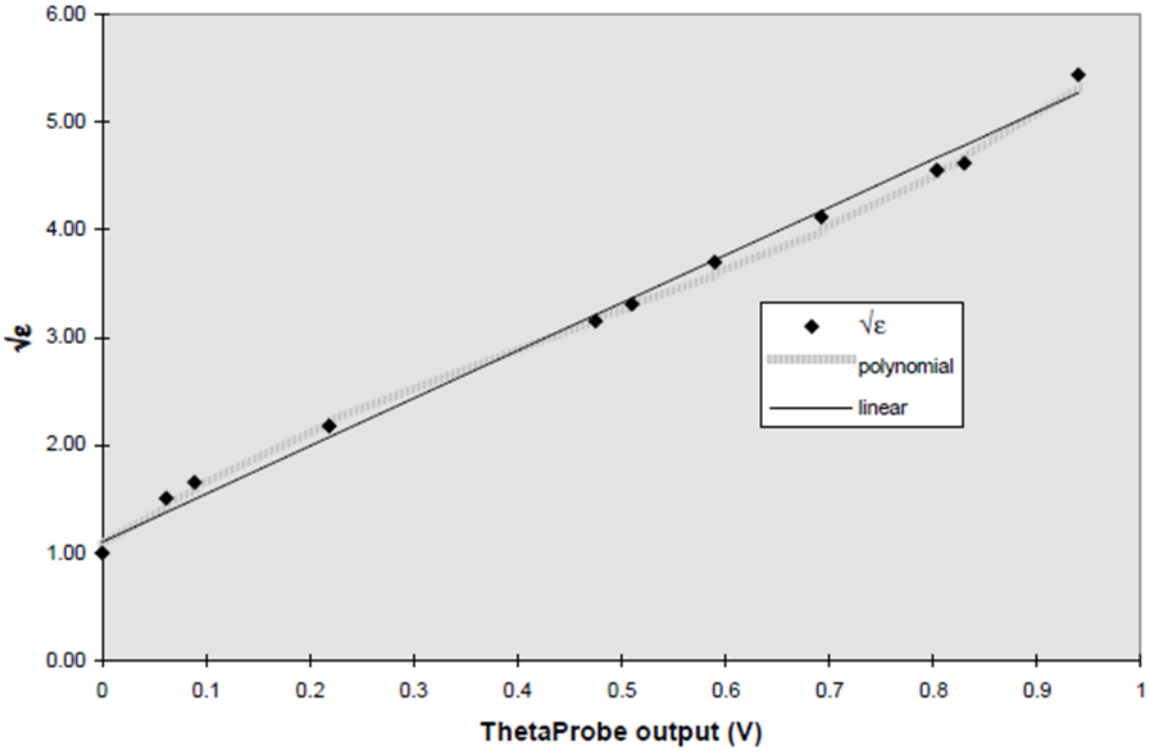

Figure G.2 Dielectric constant and Theta probe output (V) relationship for generalised mineral and organic soils (Delta-T Devices, Ltd. 1999)

In the range 0 to 1 Volt (corresponding to a soil moisture range 0 to ~ 0.55 by volume), this relationship can be fitted very precisely by a 3rd order polynomial:

$$\sqrt{\varepsilon} = 1.07 + 6.4V - 6.4V\,2 + 4.7V\,3 \quad (R^2 = 0.998) \qquad (1)$$

or by the linear relationship:

$$\sqrt{\varepsilon} = 1.1 + 4.44V \quad (R^2 = 0.99) \qquad (2)$$

For low moisture content ($\theta < 0.5$ $m^3.m^{-3}$) the linear equation should be used. For very high moisture contents ($\theta > 0.5$ $m^3.m^{-3}$), the polynomial equation should be used. This is usually only necessary for organic soils.

Soil-specific Calibration

To perform a soil-specific calibration, the manufacturer recommends a two-point technique that requires a voltage output reading for the initial moist sample, which is oven-dried and then a second voltage output reading is taken for the dry sample. Calibration coefficients α0 and α1 are then calculated from the wet and dry voltage output readings (Delta-T Devices, Ltd. 1999).

Whalley, and White, Knight, Zeggelin and Topp (1994) have shown that there is a simple linear relationship between the complex refractive index (which is equivalent to $\sqrt{\varepsilon}$), and volumetric water content, θ, of the form:

$$\sqrt{\varepsilon} = \alpha_0 + \alpha_1\theta \qquad (3)$$

Since the relationship between Theta Probe output and $\sqrt{\varepsilon}$ is already known, it is only necessary to determine the two coefficients, α_0 and α_1. The following protocol is used:

Step 1: Collect a sample of damp soil, disturbing it as little as possible so that it is at the same density as in situ. Insert the Theta Probe into the sample and measure the probe output, V_w. Use equation (1) or (2) to calculate $\sqrt{e_w}$. Weigh the damp sample, (W_w), and measure its volume (L).

Step 2: Oven-dry the sample, insert the Theta Probe into the dry soil ($\theta \approx 0$), and measure the probe output, V_0. Weigh the dry sample, (W_0). Use equation (1) or (2) to calculate $\sqrt{e_0}$. This equals α_0. It will usually have a value between 1.0 and 2.0.

Step 3: Calculate the volumetric water content θw of the original sample:
$\theta_w=(W_w-W_0)/L$

Step 4: Then $\alpha_1 = (\sqrt{\varepsilon_w} - \sqrt{\varepsilon_0})/\theta_w$ (4)

It will usually have a value between 7.6 and 8.6.

Step 5: By inverting equation (3), and substituting from equation (2), the moisture content determined from a calibrated Theta Probe will then be:

$$\theta=((1.1+ 4.44\ V) - \alpha_0) / \alpha_1 \quad (5)$$

The corresponding equation using the polynomial relationship is:

$$\theta=((1.07+6.4\ V - 6.4\ V^2 + 4.7\ V^3) - \alpha_0) / \alpha_1 \quad (6)$$

Using this relationship (rather than the linear form) will enable the Theta Probe to achieve full accuracy over the full specified range, particularly for wetter soils with $0.5 < \theta < 0.6$.

Application of Soil-Specific Calibration to MBT waste

In a sample of moist MBT waste, the Theta Probe gives an output of 0.608 V. This sample weighs 0.289 kg, and has a volume of 0.43 litres.

From equation (1), $\sqrt{\varepsilon_w} = 3.65$

After drying the sample of MBT waste, the Theta Probe gives an output of 0.041 V. From equation (1) again, we can calculate $\alpha_0 = \sqrt{\varepsilon_0} = 1.32$

The dry sample now weighs 0.189 kg, so the volume of water in the moist sample was 0.1 litres.

$\theta_w = (0.289 - 0.189)/0.43 = 0.232$ and by substituting in equation (4) $\alpha_1 = 10.04$

Finally, by inserting into equation (6),

$\theta_V = 0.468\ V^3 - 0.637\ V^2 + 0.637\ V - 0.025\ m^3.m^{-3}$

The corresponding parameters using the equations (2), (3) and (4) are:

$\sqrt{\varepsilon_w} = 3.8$, $\sqrt{\varepsilon_0} = \alpha_0 = 1.18$, $\alpha_1 = 6.09$

And by inserting into equation (5), $\theta_V = 0.73\ V - 0.013\ m^3.m^{-3}$

The manufacturer's theta probe calibration method (Delta-T Devices, Ltd. 1999) was tested and found not to be applicable on the MBT waste sample (Figure G.3).

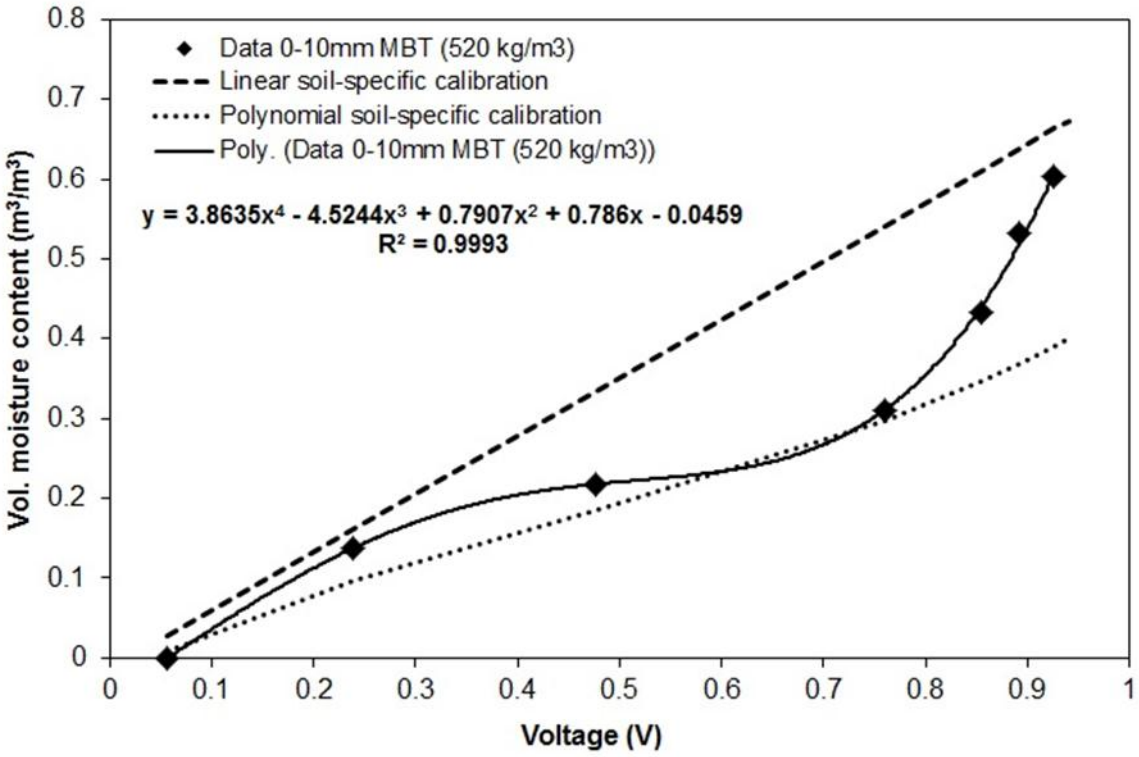

Figure G.3 Soil-Specific Calibration (Delta-T Devices, Ltd. 1999) vs. Fitting of data to polynomial equation

APPENDIX H – Filter/Plexiglas base effect on the outflow rate

Figure H.1 Photo of the geotextile filter and plexiglass base

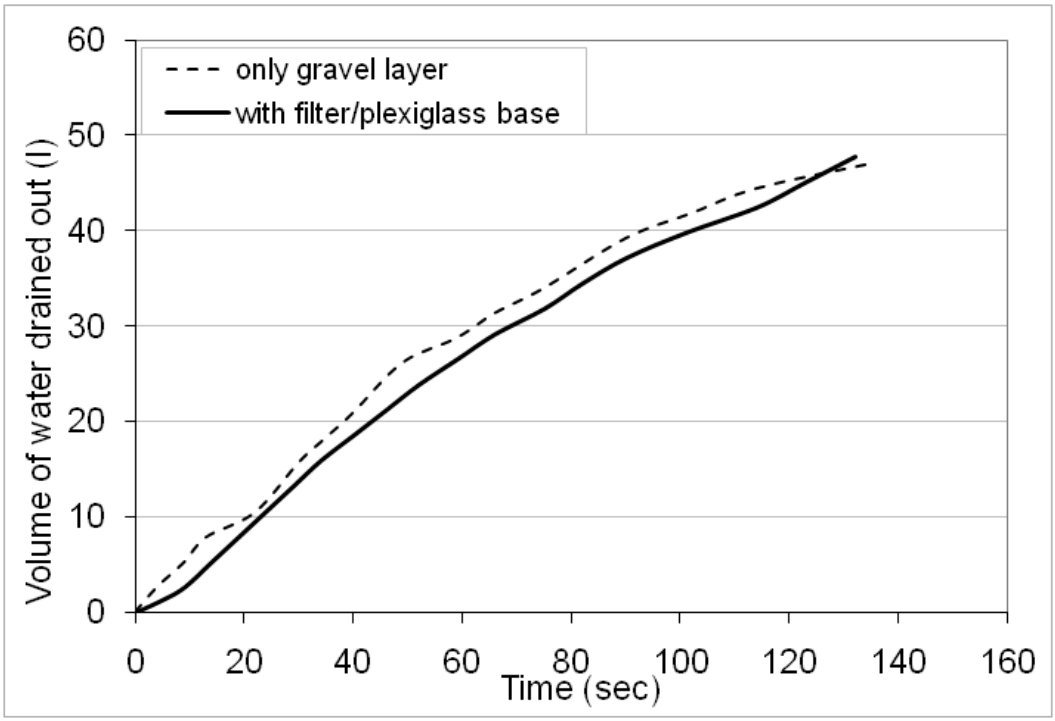

Figure H.2 Volume of water drained out (l) against time (sec) for the saturated gravel layer with and without the filter/Plexiglas base

APPENDIX I - Temperature along the MBT column

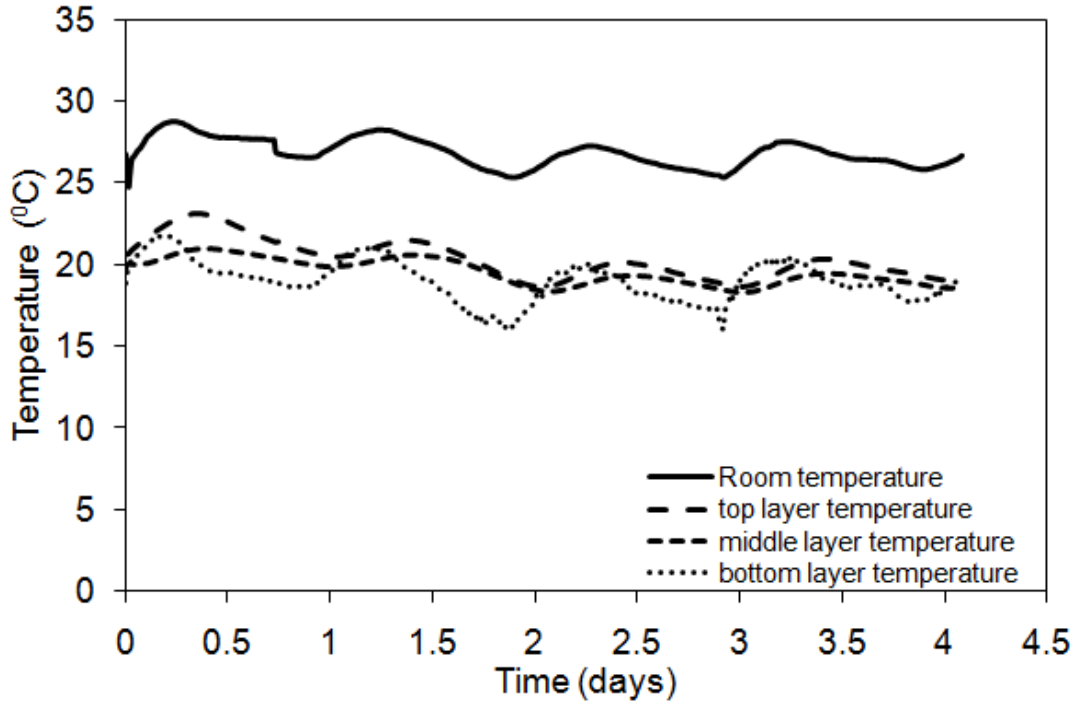

Figure I.1 Temperature readings at three thermistors along the MBT column during the one-step drainage experiment

Appendix J - Experimental moisture retention data fitted to van Genuchten and Brooks & Corey models

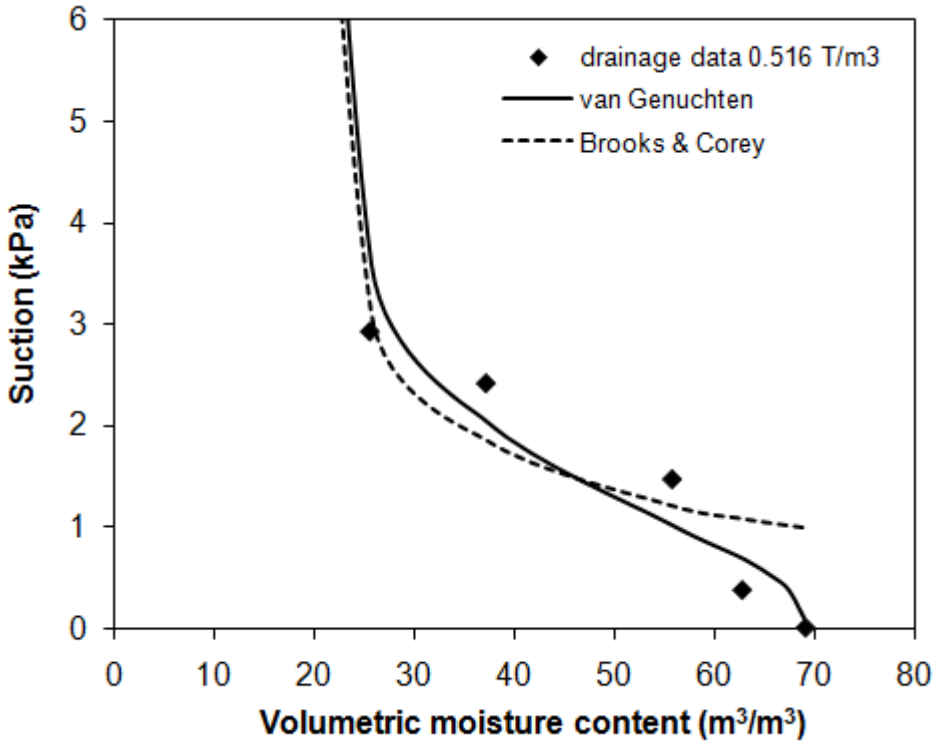

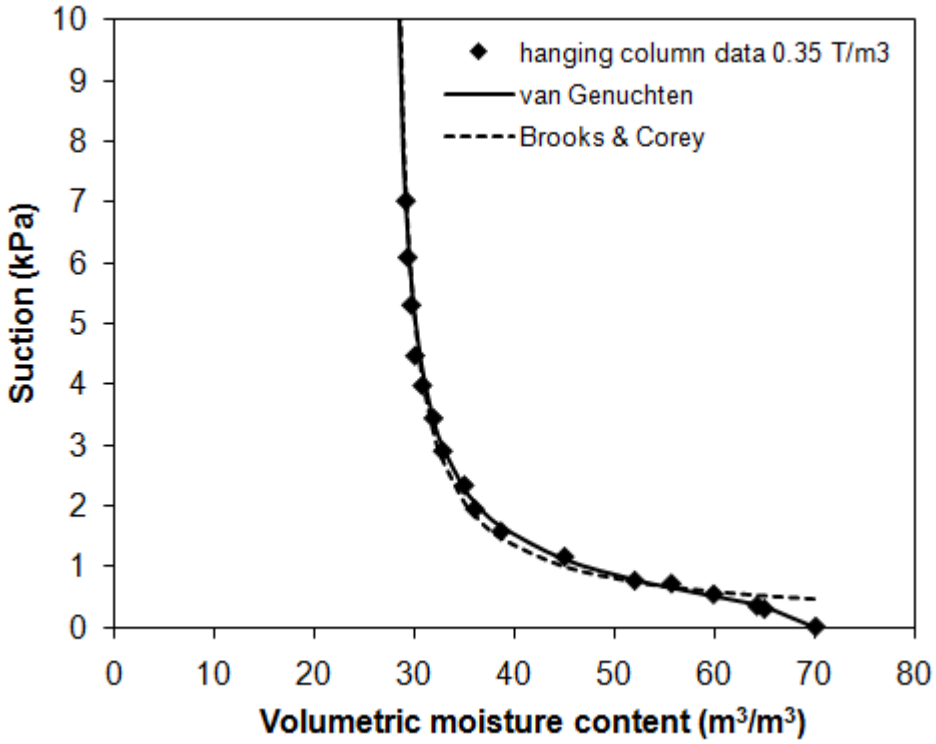
hanging column data 0.35 T/m3
van Genuchten
Brooks & Corey
Suction (kPa)
Volumetric moisture content (m3/m3)
0
1
2
3
4
5
6
7
8
9
10
0
10
20
30
40
50
60
70
80

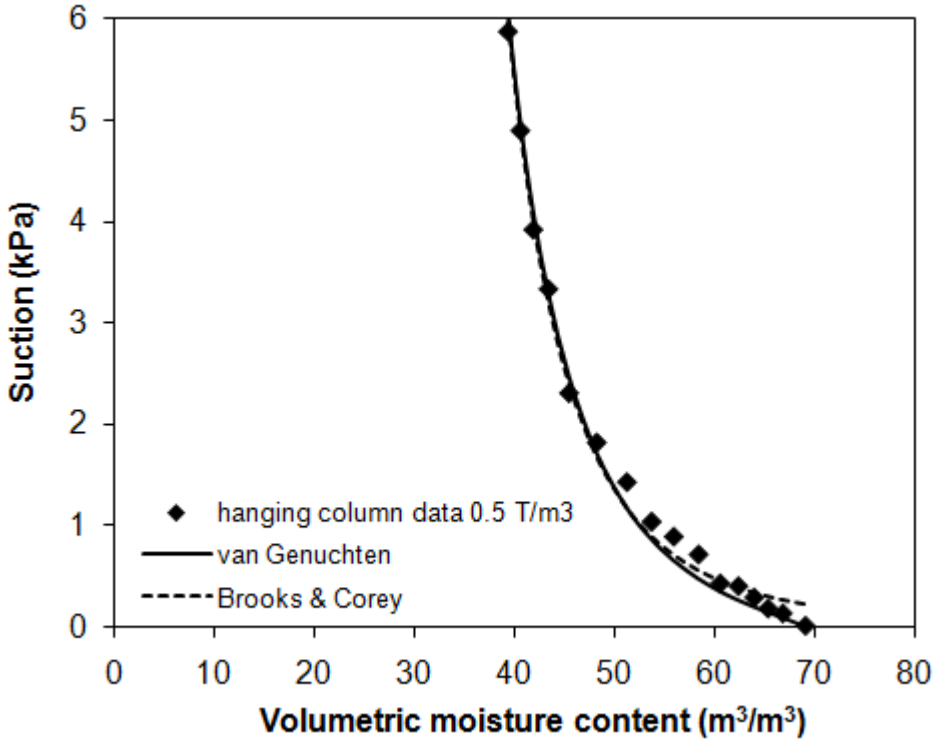
hanging column data 0.5 T/m3
van Genuchten
Brooks & Corey
Suction (kPa)
Volumetric moisture content (m3/m3)
0
1
2
3
4
5
6
0
10
20
30
40
50
60
70
80

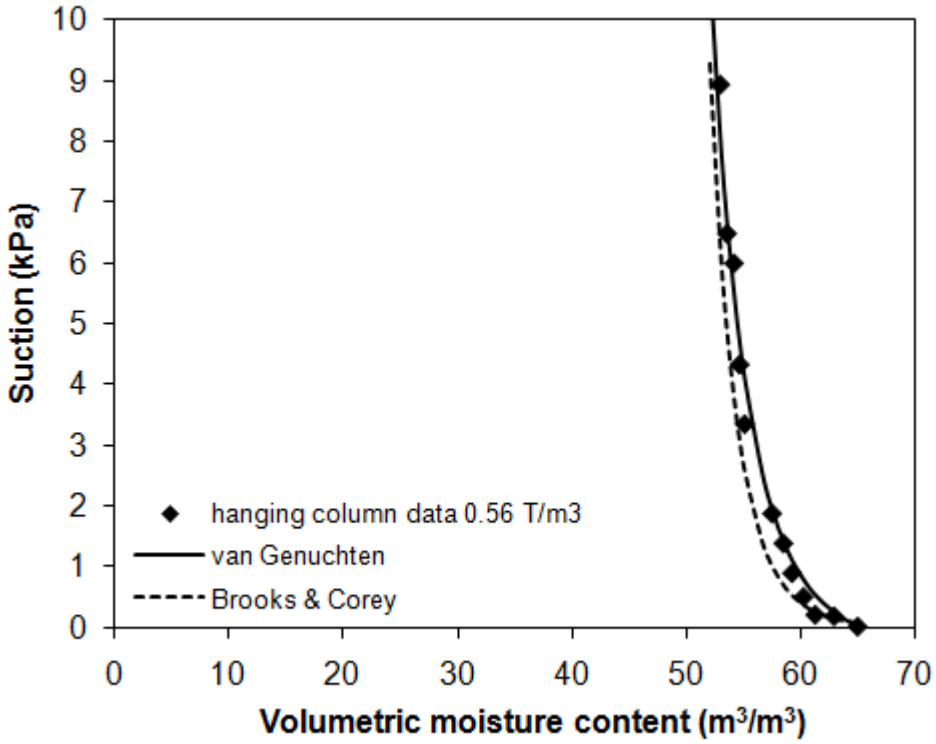

Table J.1 Fitted van Genuchten parameters to the data

Waste	θr	θs	α (kPa^{-1})	n	RSQ
MBT one-step drainage 0.516 T/m^3	0.15	0.69	0.8	2.5	0.83
MBT hanging column 0.35 T/m^3	0.27	0.7	1.57	2.32	0.962
MBT hanging column 0.50 T/m^3	0.15	0.69	3.55	1.26	0.996
MBT hanging column 0.56 T/m^3	0.2	0.65	3	1.10	0.985

Table J.2 Fitted Brooks & Corey parameters to the data

Waste	θr	θs	ψ_{aev}	λ	RSQ
MBT one-step drainage 0.516 T/m^3	0.15	0.69	1	1.43	0.76
MBT hanging column 0.35 T/m^3	0.27	0.7	0.47	1.159	0.961
MBT hanging column 0.50 T/m^3	0.15	0.69	0.23	0.24	0.996
MBT hanging column 0.56 T/m^3	0.2	0.65	0.077	0.071	0.985

Appendix K- Determination of the unsaturated permeability from the pressure plate test using Gardner method

Unsaturated hydraulic conductivity was computed using analytical method in Gardner (1956), which is based on an analytical solution to the 1-D Richards' equation:

$$ln\left(\frac{V_\infty - V_t}{V_\infty}\right) = ln\left(\frac{8}{\pi^2}\right) - D_\theta \frac{\pi^2 t}{4L^2} \quad (1)$$

where: V_∞ is the cumulative outflow volume at equilibrium for a given suction (ψ), V_t is the cumulative outflow volume at elapsed time (t) from the initial application of ψ (as shown in Figure K.1), L is the thickness of the specimen, and $D_\theta$is the water diffusivity of the porous material. The water diffusivity of the material is determined by graphing Eq. 1 as a function of time and computing the slope of the resulting linear relationship (Qn) (Figure K.2).

The unsaturated hydraulic conductivity is calculated from $D_\theta$using the relationship:

$$K_\theta = \gamma_w D_\theta \frac{\Delta\theta}{\Delta\psi} \quad (2)$$

where Δθ is the change in equilibrium water content over a suction increment Δψ and γ_w is the unit weight of water. Gardner's solution assumes that the hydraulic conductivity is constant over a small suction increment Δψ, water content is linearly variable with respect to suction, and hydraulic impedances from the experimental apparatus are negligible.

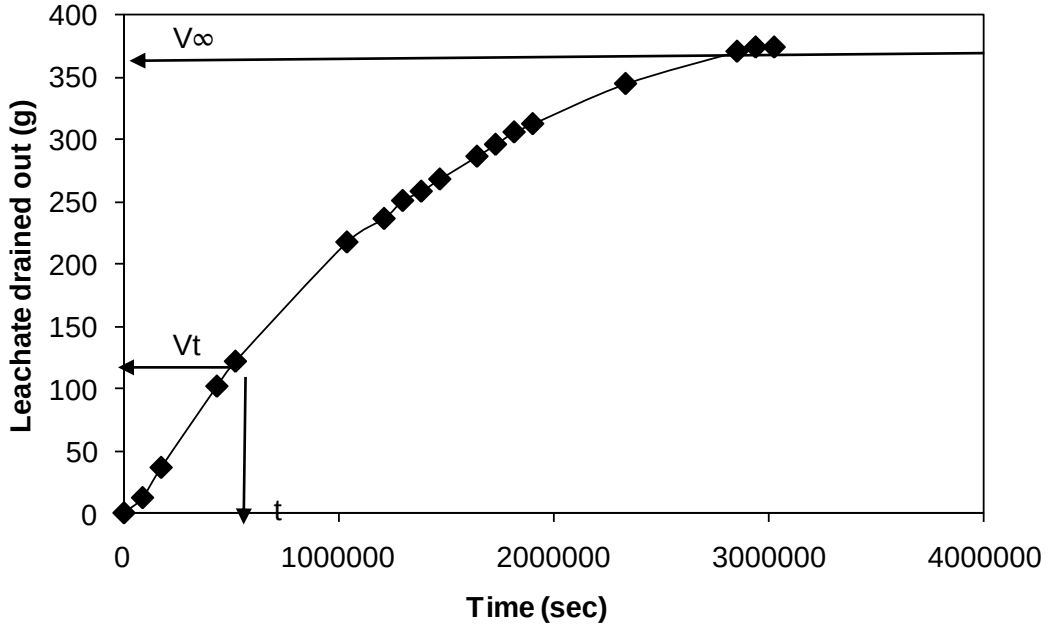

Figure K.1 Transient outflow data from the pressure plate plotted (at suction= 6kPa)

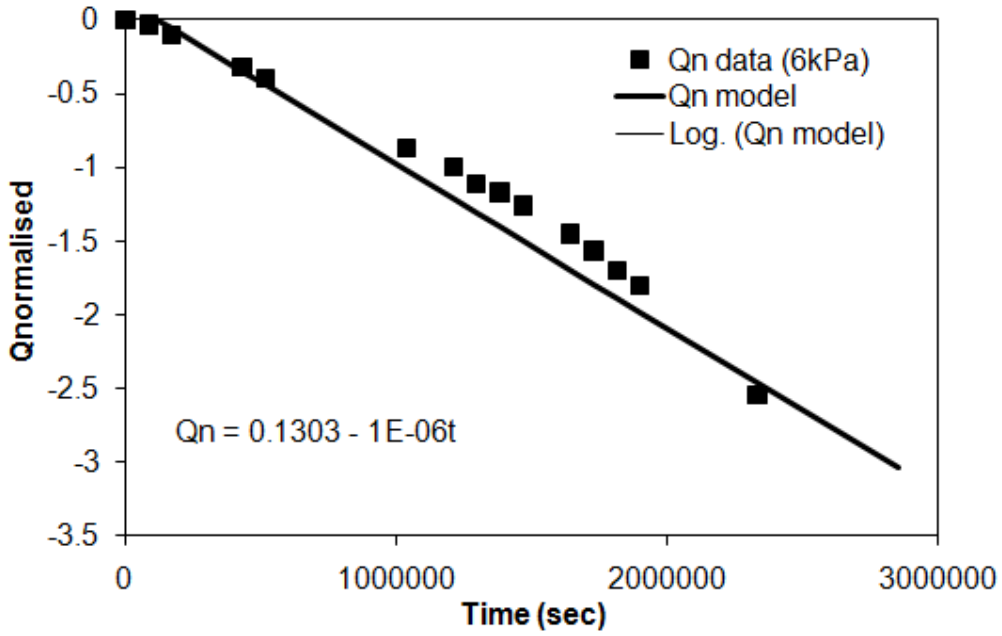

Figure K.2 Normalized outflow against time. The slope is used to calculate diffusivity D_θ (at suction= 6kPa).

Appendix L - Application of Passioura method to the pressure plate data

Passioura (1976) developed a method of calculating diffusivity, which is related to unsaturated permeability, from one-step outflow data from a pressure plate apparatus. In this method, an initially saturated specimen (θ_i) is subjected to an increment of gas pressure at the upper surface (x = L, where L is the height of the sample). The outflow is measured at the base (x = 0) until the moisture content reaches an equilibrium with the gas pressure. It is assumed that volumetric moisture content at x = 0 is reduced to the final moisture content (θ_f) instantly, i.e. at the onset of outflow.

The governing equation, derived from Richard's equation and neglecting gravity, is:

$$\frac{\partial \theta}{\partial t} = \frac{\partial}{\partial x}\left(D(\theta)\frac{\partial \theta}{\partial x} \right) \quad (1)$$

where D(θ) is liquid diffusivity which is the flux of water per unit gradient of moisture content and $K(\theta) = \frac{\partial \theta}{\partial \psi} D(\theta)$

The initial and boundary conditions of such a system are given as:

$\theta = \theta_i$, $0 \le x \le L$, $t=0$

$\theta = \theta_f$, $x=0$, $t>0$

$\partial\theta/\partial x = 0$, $x=L$, $t>0$

There are three stages of outflow (Figure L.2). The first stage is controlled by the ceramic plate and its resistance to flow; hence the cumulative outflow (Q) is proportional to time (t). During the second stage the flow rate decreases as the medium permeability controls the flow. The resistance of the ceramic plate becomes negligible and the moisture content at the bottom of the specimen reaches θ_f. The time origin for the analysis is at the beginning of the third stage. During this stage the cumulative outflow (Q) is a linear function of $\sqrt{t}$. The third stage starts when this linear relationship ceases and the top boundary condition, x=L, begins to influence the flow. This is the stage when the assumption of uniform moisture content over most of the specimen is used to determine D(θ).

Using the above assumption, Passioura (1976) found the following solution to Equation 1:

$$D(\theta_L) = \frac{dF}{dW}\frac{L^2}{2} \qquad (2)$$

where F is the rate of outflow, W is the moisture content remained in the specimen at any time and θ_L is the moisture content at x=L. Equation 2 is obtained by assuming $\theta_L >> \theta_f$.

Since $\partial\theta/\partial t$ is independent of x during the third stage of outflow, the difference between θ_L and the mean moisture content of the specimen, θ^* denoted by δ, is constant. To find a relation between θ_L and θ^*, the following relationships are used:

for $\theta_L >> \theta_f$, $\delta = \theta_L - \theta^* = 0.61/B$ (Passioura, 1976) (3)

where $B = d(\ln D(\theta_L)/d\theta^*$ at $\theta^* = (\theta_i + \theta_f)/2$

when θ_L approaches θ_f , $\frac{\theta_L - \theta_f}{\theta^* - \theta_f} = \frac{\pi}{2}$ (Gupta et al., 1974) (4)

K(θ) values corresponding to the calculated D(θ) values are then determined using the equation:

$$K(\theta) = \frac{\partial\theta}{\partial\psi} D(\theta) \qquad (5)$$

Since the pressure plate test described in Chapter 3 was a multistep outflow experiment, the outflow data were fitted to the exponential equation 6 in order to represent a one-step outflow curve (Figure L.1):

$Q = Q_f * (1 - \exp(At))$ (6)

where Q_f=635.86 cm^3 and the parameter A was calculated by the method of least squared errors and it was equal to -9.88E-04.

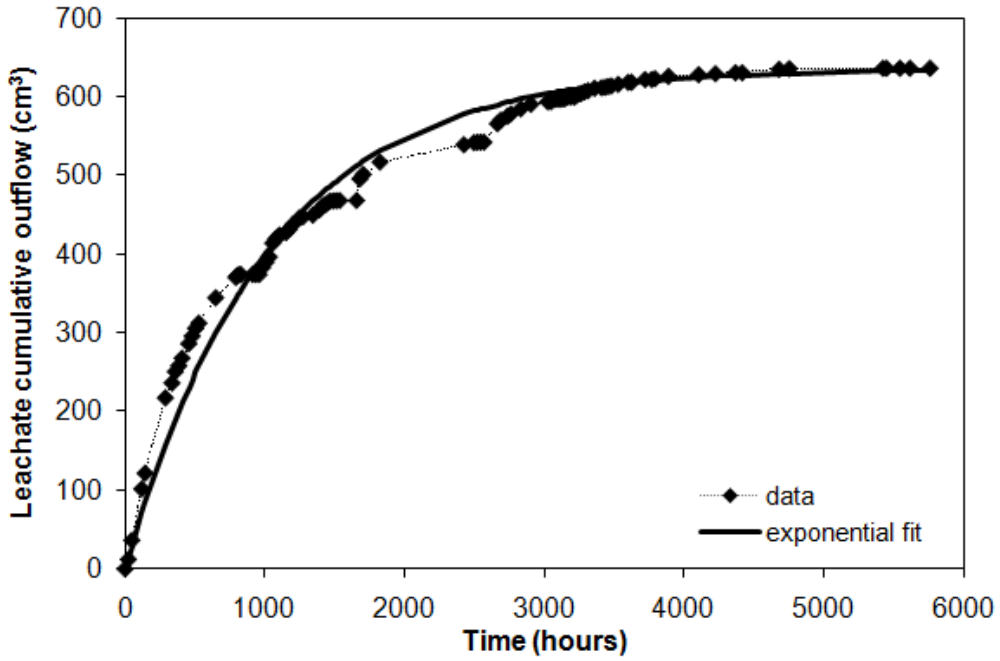

Figure L.1 Exponential fit to the multistep outflow data from the pressure plate experiment

The following steps were followed for the calculation of the diffusivity and unsaturated hydraulic conductivity from the pressure plate experiment data:

1. The leachate cumulative outflow data Q derived from the exponential fit were plotted against $\sqrt{t}$ and the three stages described earlier were identified (Figure L.2). Any measurement points where outflow change is zero are discarded.

2. The volume of moisture remaining in the material (W) at each time step was calculated from θ x V. Calculations start at equilibrium (last entry);

$$W = \theta_f \times V \quad (7)$$

At each time step (i) then working backwards,

$$W_i = W_{i+1} + \Delta Q_i \quad (8)$$

ΔQ was found by differencing the Q entries (e.g. $\Delta Q_2 = Q_3 - Q_2$)

3. The rate of outflow F ($cm^3\ h^{-1}$) was calculated by dividing the differences in Q by the differences in time (t), i.e.

$$F_2 = (Q_1 - Q_3) / (t_1 - t_3) \quad (9)$$

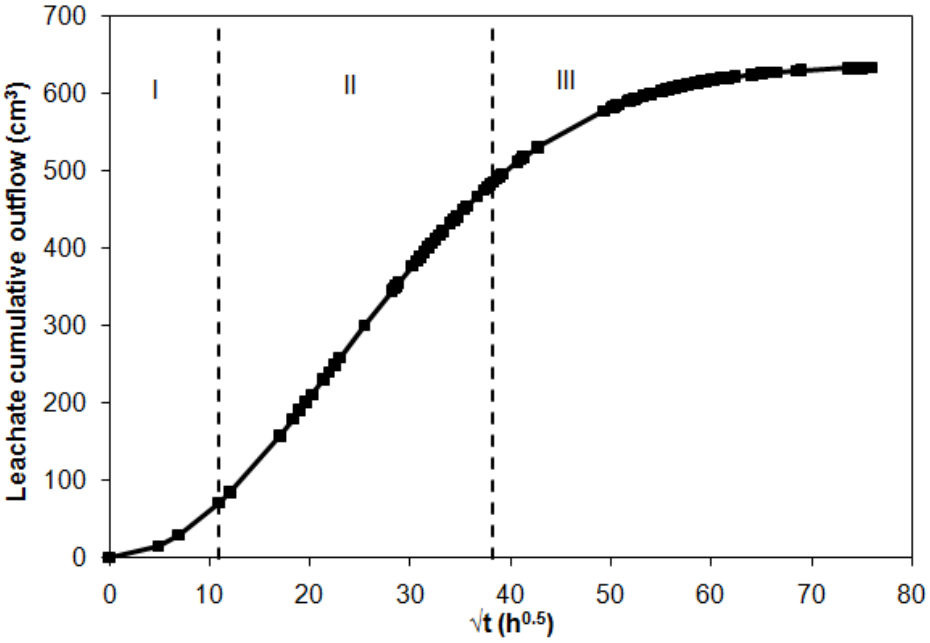

Figure L.2 Leachate cumulative outflow against √t, showing the three stages of outflow

4. From this point only the data from stage III were used. Different functions (polynomials, power law, or exponential) were fitted to F-W data. The fitted F values for each value of W were calculated using the best fitting exponential function.

5. dF/dW was calculated from fitted F values using central differencing,

$(dF/dW)_2 = (F_1 - F_3)/(W_1 - W_3)$ (10)

6. Diffusivity D was calculated from $D = dF/dW \times (L^2/2)$ (11)

7. The average moisture content for each entry was calculated from

$\theta^* = W/V$ (12)

8. lnD versus θ* was plotted and the slope (B) of this curve at the point $\theta^* = (\theta_i + \theta_f)/2$ was estimated. Then $\delta = 0.61/B$

9. θ_j values were calculated as $\theta_j = \theta^* + \delta$ (13)

and θ_k values as $\theta_k = (\theta_f + \pi/2) \times (\theta^* - \theta_f)$ (14)

Then θ_j and θ_k data were plotted against θ* on the same graph. The intersection point (θ^*_{m1} and θ^*_{m2}) of the two lines was identified and a line was drawn between the mid points of lines past the intersection point.

10. From the above graph we derived θ_L against θ^*. For each θ^*, θ_L was derived following the below rules:

If $\theta^* > \theta^*_{m1}$, $\theta_L = \theta^* + \delta = \theta_j$ (15)

If $\theta^* < \theta^*_{m1}$, $\theta_L = (\theta_f+\pi/2)x(\theta^*- \theta_f) = \theta_k$ (16)

If $\theta^*_{m2} < \theta^* < \theta^*_{m1}$, $\theta_L = \alpha\ \theta^* + b$ (17)

where α and b are the slope and intercept of the line calculated in step 9.

This step completes the $D(\theta_L)$ vs θ_L calculation

11. The natural log of suction and moisture content were taken from the retention characteristic data and the slope $d\ln\theta/d\ln\psi$ was calculated at each entry using forward differencing.

12. For each θ_L value the corresponding suction value was calculated by linear interpolation on the natural logarithmic scale using the values from step 11. The slope of the characteristic curve was determined using forward differencing.

13. The unsaturated hydraulic conductivity was calculated using Equation 5.

Appendix M - Derivation of the constitutive multicomponent-multiphase equation of flow used in LDAT model

The purpose of this Appendix is to explain how the LDAT constitutive equation, which is given as equation (6.2) in Chapter 6, may be derived from first principles.

The following derivation is based on the LDAT documentation which may be found using the link '**LDAT code and documentation pack'** in the page: http://www.wmrg.soton.ac.uk/LDAT.htm

The conservation of the mass of component (i) of phase F within the representative elementary volume V_E (Figure M.1) can be expressed by the following equation:

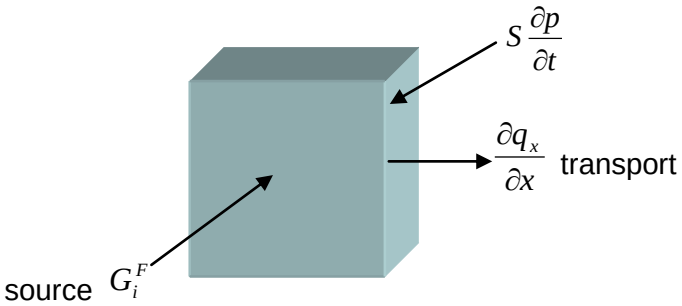

Figure M.1 Representative elementary volume diagram for Equation 1

$$\frac{\partial\left(\rho_i^F z_i^F V_E\right)}{\partial t} = \rho_i^F G_i^F V_E - \sum_{X,Y,Z} \rho_i^F A_i^F \frac{V_E}{A_X} \frac{\partial\left(q_i^F\right)_x}{\partial x} \qquad (1)$$

- The left hand side term is the rate of change of the mass of the component in the REV. z_i^F is the volumetric concentration of the component and ρ_i^F is the component density.

- The first term on the right hand side is the rate at which any type of source of the component is introducing mass into the representative elementary volume

where G_i^F is the concentration of the source flow expressed in the units $m^3/sec/m^3$.

- The second term on the right hand side is the net mass flow out of the representative elementary volume consisting itself of the sum of three similar terms one for each of the x, y and z directions. A_i^F is the area of flow of the component and q_i^F is its flow velocity. A_x is the total area of the representative elementary volume normal to the x direction.

Dividing the Equation 1 by $\rho_i^F V_E$ and differentiating with respect to time, gives:

$$\frac{z_i^F}{\rho_i^F}\frac{\partial \rho_i^F}{\partial t} + \frac{\partial z_i^F}{\partial t} = G_i^F - \sum_{x,y,z}\frac{A_i^F}{A_x}\frac{\partial\left(q_i^F\right)_x}{\partial x} \qquad (2)$$

According to the above equation, the rate of change of concentration of the component $\left(\frac{\partial z_i^F}{\partial t}\right)$ is expressed as the concentration of the source flow $\left(G_i^F\right)$ minus the changes due to flow, minus the changes due to changes in the density of the component $\left(\frac{z_i^F}{\rho_i^F}\frac{\partial \rho_i^F}{\partial t}\right)$. Since changes in density are related to compression or expansion, the term $\frac{z_i^F}{\rho_i^F}\frac{\partial \rho_i^F}{\partial t}$ is usually replaced by $z_i^F S_i^F \frac{\partial p^F}{\partial t}$ where p^F is the phase pressure and S_i^F is a storage coefficient with units $1/kN/m^2$.

For estimating the storage coefficient, S_i^F, the bulk modulus is used for a liquid or solid component and the ideal gas law for a gas component. Hence, for a liquid/solid phase component: $S_i^F = \frac{1}{K_i}$ and for a gas phase component: $S_i^G = \frac{1}{\left(p + p_A\right)}$, where p_A is the atmospheric pressure (assuming the gas obeys the ideal gas law p/ro = RT, where R is the universal gas constant and T is absolute temperature).

Hence Equation 2 becomes: $z_i^F S_i^F \frac{\partial p_i^F}{\partial t} + \frac{\partial z_i^F}{\partial t} = G_i^F - \sum_{x,y,z} \frac{A_i^F}{A_x} \frac{\partial \left(q_i^F\right)_x}{\partial x}$ (3)

The individual concentrations of the compounds z_i^F are related to the overall concentrations of the solid z^S, liquid z^L and gas z^G phases and to the porosity ϕ by the relationships:

$$z^S = \sum_i z_i^S \ , \ z^L = \sum_i z_i^L \ , \ z^G = \sum_i z_i^G \ , z^L + z^G + z^S = 1, \phi = z^L + z^G \ , \ 1 - \phi = z^S$$

Also, z^L is the moisture content (θ) so the degree of saturation is: $\zeta = \frac{z^L}{\phi}$

Adding Equation 3 for each phase and using these relationships the following constitutive equations for the components in each of the three phases (solid, liquid and gas) are obtained:

$$z^S S^S \frac{\partial p^S}{\partial t} + \frac{\partial z^S}{\partial t} = \sum G_i^S - \sum_i \sum_{x,y,z} \frac{A_i^S}{A_x} \frac{\partial \left(q_i^S\right)_x}{\partial x} \quad (4)$$

$$z^L S^L \frac{\partial p^L}{\partial t} + \frac{\partial z^L}{\partial t} = \sum G_i^L - \sum_i \sum_{x,y,z} \frac{A_i^L}{A_x} \frac{\partial \left(q_i^L\right)_x}{\partial x} \quad (5)$$

$$z^G S^G \frac{\partial p^G}{\partial t} + \frac{\partial z^G}{\partial t} = \sum G_i^G - \sum_i \sum_{x,y,z} \frac{A_i^G}{A_x} \frac{\partial \left(q_i^G\right)_x}{\partial x} \quad (6)$$

In the above equations the storage coefficients S^F are the weighted average values given by $\frac{\sum_i z_i^F S_i^F}{z^F}$

Note that the term $\sum G_i^F$ is the sum of four parts reflecting volumetric changes due to: recharge/abstraction flows in the element; bio-chemical-degradation ; phase changes through solid and gas solubility, chemical equilibrium and water vapour generation; and the diffusion and dispersion of components.

With the impact of diffusion and dispersion contained in the source term, the liquid and gas phase velocities may be estimated using Darcy's law,

$$\left(q_i^F\right)_x = -\left(k_i^F\right)_x \frac{\partial h^F}{\partial x} \tag{7}$$

The head (h^F) is related to the pressure (p^F) and density (ρ^F) in the x direction and to the effective gas/liquid density ro_dash in the z direction. Thus in the x and y directions: $h^F = \frac{p^F}{\rho^F g}$ and in the z direction: $h^F = \frac{1}{\rho^F g}\left(p^F + \rho' g z\right)$.

After calculating the source terms $\sum G_i^F$, the sum of the Equations 5 and 6 become the Fluid Equation 8 by having assumed that: $\frac{A_i^F}{A_x} = z_i^F$.

$$z^L S^L \frac{\partial p^L}{\partial t} + z^G S^G \frac{\partial p^G}{\partial t} + \frac{\partial \phi}{\partial t} = \sum\left(G_i^L + G_i^G\right) + \sum_i \sum_{x,y,z} z_i^F \left(k_i^F\right) \frac{\partial h^F}{\partial x^2} \tag{8}$$

Hence, for the x direction, equation 8 takes the form:

$$z^L S^L \frac{\partial p^L}{\partial t} + z^G S^G \frac{\partial p^G}{\partial t} + \frac{\partial \phi}{\partial t} = \sum\left(G_i^L + G_i^G\right) + z^L \frac{k^L}{\rho^L g} \frac{\partial^2 p^L}{\partial x^2} + z^G \frac{k^G}{\rho^G g} \frac{\partial^2 p^G}{\partial x^2} \tag{9}$$

An equation similar to Equation 9 may be used for the y direction, but for the vertical direction z, where the head gradient depends on the effective fluid density as well as pressure, additional terms are required.

For the case of a specific application such as vertical drainage appropriate boundary conditions and initial conditions need to be applied.

Equation 9 together with those for the y and z directions can be solved numerically if it is known how the liquid and gas pressure fields are related. This can be achieved by invoking a van Genuchten capillary pressure ($p_C = p^G - p^L$) type of

relationship or its equivalent. The compound concentrations (z_i^F) can then be obtained by a back calculation using Equations 5, 6 and 7 for each phase.

Adding Equations 5 and 6 results in a term $\frac{\partial z^L}{\partial t}+\frac{\partial z^G}{\partial t}=\frac{\partial \phi}{\partial t}$ (10)

and it is therefore necessary to evaluate this to solve for the pressure fields.

$\frac{\partial \phi}{\partial t}$ is the term that couples the liquid and gas phase equations to the solid phase equation because in equation (18) $\frac{\partial z^S}{\partial t}=\frac{\partial(1-\phi)}{\partial t}=-\frac{\partial \phi}{\partial t}$.

The coupling term $\frac{\partial \phi}{\partial t}$ may be calculated using the Powrie and Beaven (1999) relationship: $\rho_D = A(\sigma - p)^a$ (11)

where $\sigma - p$ is the local effective stress.

By differentiating with respect to time the equation $\phi = 1-\frac{\rho_D}{\rho_S}$, it is obtained:

$$\frac{\partial \phi}{\partial t}=-\frac{1}{\rho_S}\frac{\partial \rho_D}{\partial t}=\frac{1}{\rho_S}Aa(\sigma-p)^{a-1}\frac{\partial p}{\partial t}=\frac{\rho_D}{\rho_S}\frac{a}{(\sigma-p)}\frac{\partial p}{\partial t} \quad (12)$$

A further simplification of the solution of these equations for multi-component multi-phase flow is to decouple the liquid phase, equation (19), by assuming a relationship between the term $\frac{\partial z^L}{\partial t}$ and the pressure field p^L, and just solve for the liquid phase. Since $\frac{\partial z^L}{\partial t}=\frac{\partial \theta}{\partial t}$ this can be achieved by invoking a van Genuchten type of relationship and assuming that the gas pressure is constant. This leads to Richards' equation which is the constitutive equation for the Hydrus model.

Appendix N - HYDRUS-1D inverse (dual permeability) simulations of the outflow flux

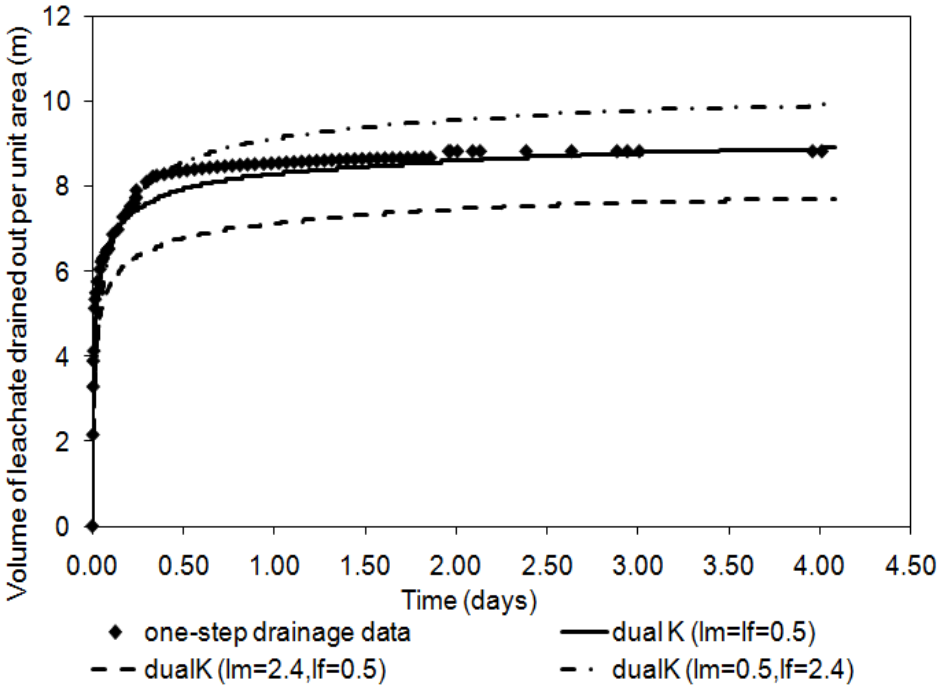

Figure N.1 Measured and Hydrus-1D inverse (dual permeability) simulated mass of leachate drained out (kg) against elapsed time (one-step drainage) fitting the α_m and k_s parameters for different values of l_f and l_m parameters

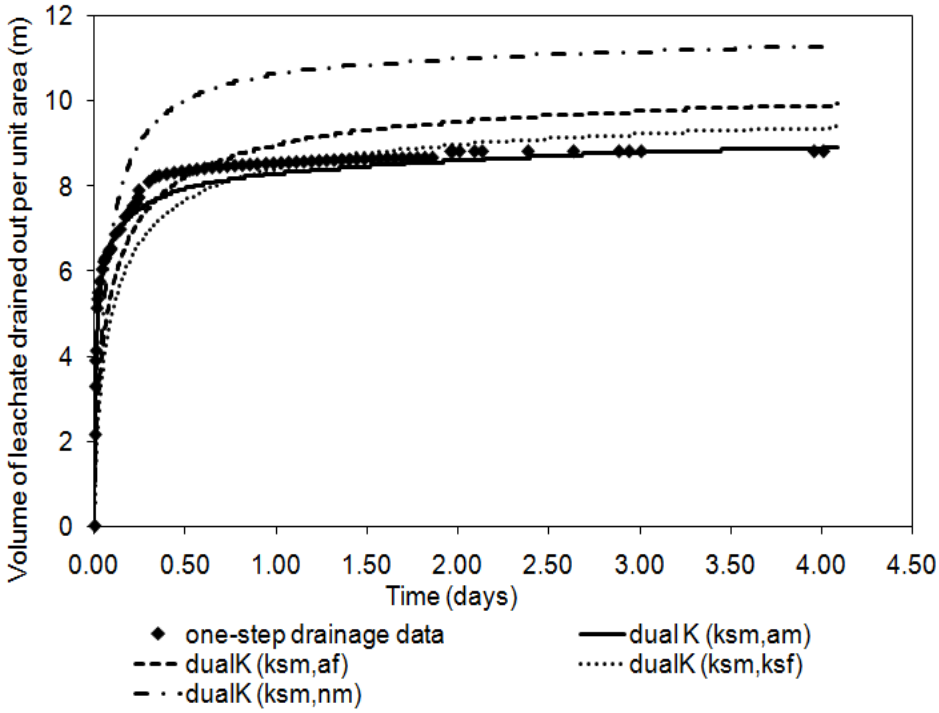

Figure N.2 Measured and Hydrus-1D inverse (dual permeability) simulated mass of leachate drained out (kg) against elapsed time (one-step drainage) fitting the parameters in parenthesis for l_f and l_m =0.5

APPENDIX O - HYDRUS-1D inverse dual porosity results

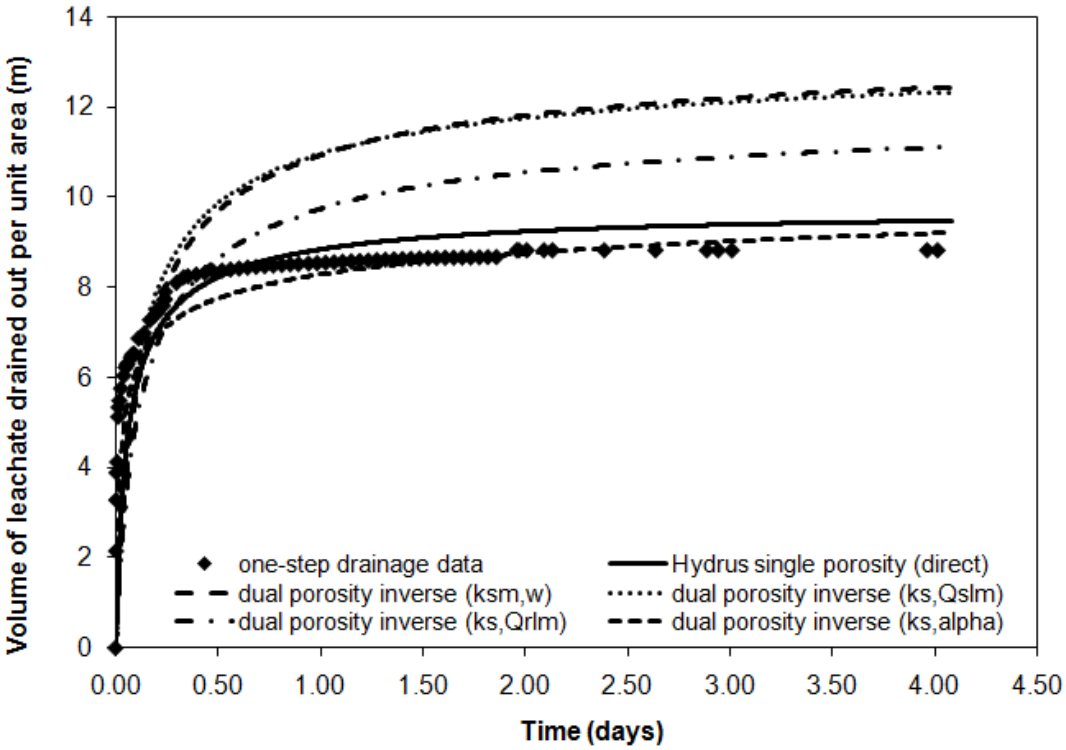

Figure O.1 Measured and Hydrus-1D inverse (dual porosity) simulated mass of leachate drained out (kg) against elapsed time (one-step drainage) with the optimised parameters in parenthesis

The best case was when the saturated hydraulic conductivity (ks) and the parameter α (alpha) were optimised (Table O.1). Figures O.2 and O.3 show the simulated pore liquid pressure and volumetric moisture content profiles using the single and dual porosity models. The other parameters used in Hydus-1D dual porosity model were: θ_r=0.15, θ_s=0.69, n=2.5, $l = 0.5$, θ_{rlm}=0.1, θ_{slm}=0.3 and w=1.

Table O.1 Saturated hydraulic conductivity (ks) and van Genuchten parameter α (alpha) optimised with Hydrus-1D dual porosity inverse model

Layer	Depth (m)	α	$k_{smatrix}$ (m/s)
1	0-0.078	4	4×10^{-6}
2	0.078-0.162	14.17	1.2×10^{-4}
3	0.162-0.246	4	2.2×10^{-4}
4	0.246-0.338	15.5	1.19×10^{-4}
5	0.336-0.437	4	5.8×10^{-4}
6	0.437-0.56	12.35	5.15×10^{-5}

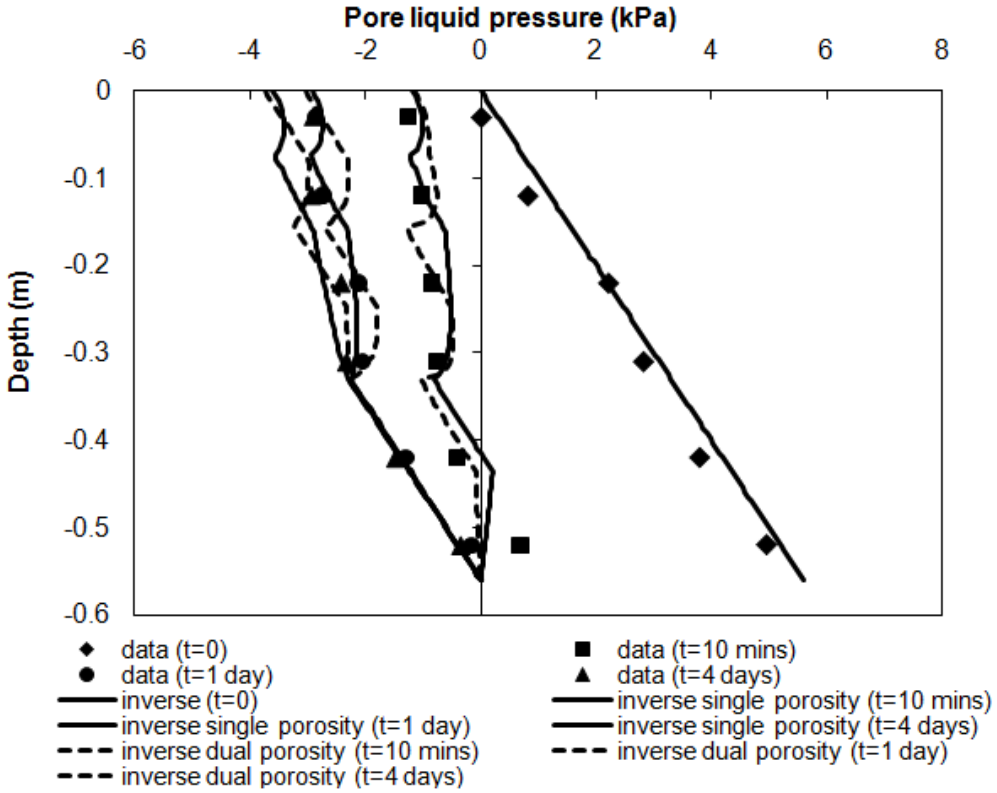

Figure O.2 Measured and Hydrus-1D inverse (single porosity with L=2.4 and dual porosity) simulated pore liquid pressure profiles (one-step drainage)

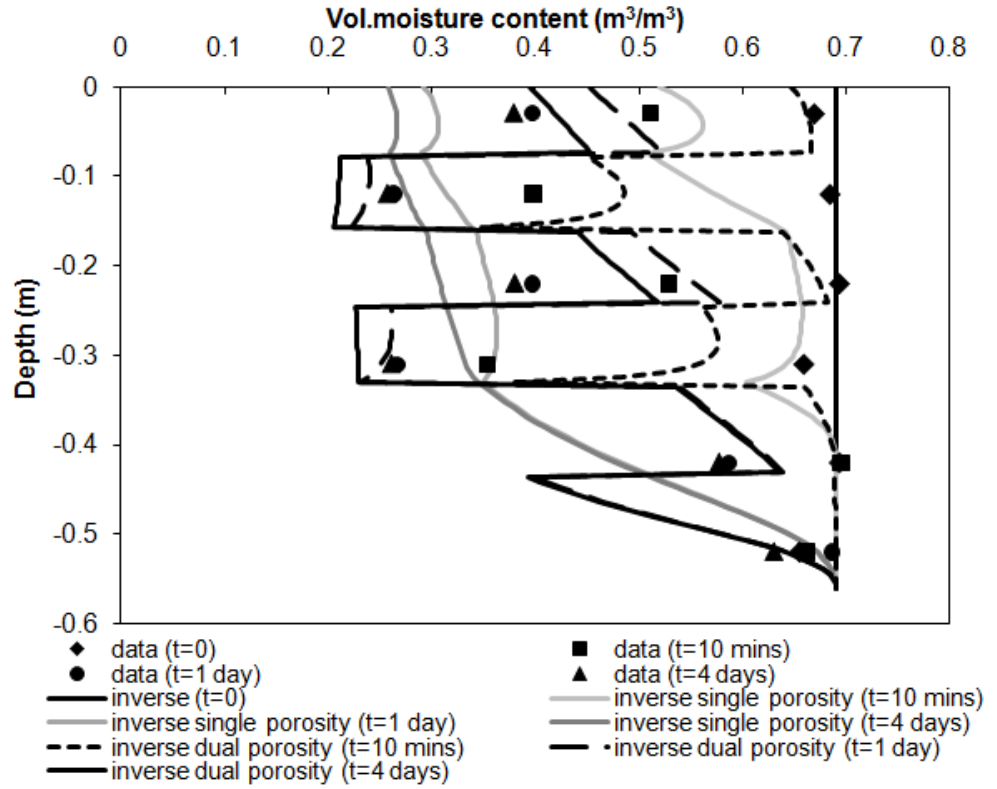

Figure O.3 Measured and Hydrus-1D inverse (single porosity with L=2.4 and dual porosity) simulated volumetric moisture profiles (one-step drainage)